CLEAN FILAMENT WINDING: INDUSTRIAL SITE TRIALS AND PRODUCT EVALUATION

by

CLAIRE FIONA WAIT

A thesis submitted to the University of Birmingham for the degree of

DOCTOR OF PHILOSOPHY

School of Metallurgy and Materials

College of Engineering and Physical Sciences

University of Birmingham, UK

September 2015

ABSTRACT

Wet-filament winding is an established manufacturing process that is used to produce composite components such as pipes and pressure vessels. In this manufacturing method, the fibre bundles or tows are impregnated using a drum-based resin bath. The impregnated fibre bundles are then directed to a traversing-arm prior to being over-wound onto a rotating mandrel. Once the required number of layers of the impregnated fibres has been deposited on the mandrel, the assembly is transferred to an oven to cross-link or cure the thermosetting resin. After this operation, the composite and the mandrel are cooled to ambient temperature. The composite is then extracted from the mandrel by mechanical means.

There are a number of issues with the conventional manufacturing method including the generation of waste resin, utilisation of significant volumes of solvent for cleaning the equipment at the end of each shift in the factory, contamination of the factory floor due to resin drips from the impregnated fibre bundles and the cost of waste disposal. This thesis reports on the integration of a modified wet-filament winding process, which is referred to as "clean filament winding", into an industrial filament winding manufacturing operation.

A number of site trials were carried out to assess the fit-for-purpose of the clean filament winding method. In the first phase of the research project, detailed observations were made to appreciate the various modes of impregnation of the fibre bundles, from the resin bath, to the over-wrapping stage at the mandrel. Due attention was also given to quantifying the volume of waste resin generated from the resin bath (residual volume at the end of production) and resin drips (resin loss from the

impregnated fibre bundles when they make contact with various fibre-guides). The data gathered on-site was used to design an impregnation unit to replace the resin bath. A second impregnation unit was also produced after assessing the on-site issues associated with the first prototype design. Two types of resin delivery systems were used to feed the resin impregnation unit: (i) a pressure-pot involving a pre-mixed resin system; and (ii) a precision gear pump-based resin delivery unit where the resin and hardener are stored separately and dispensed on-demand. Two classes of resin systems were evaluated: (i) polyester (pressure-pot-based delivery); and (ii) epoxy/amine (precision gear-pump-based delivery). The impregnation unit was retrofitted onto the traversing-arm of the filament winding machine.

It was demonstrated that the clean filament winding process can be utilised to address the above-mentioned issues associated with the conventional wet-filament winding. For example, an 88.1% and 87.5% reduction in solvent consumption and the generation of waste resin respectively was verified when compared to conventional wet-filament winding.

The resin impregnators along with the resin delivery systems were used on-site to manufacture filament wound tubes. The physical and mechanical properties of the conventional and clean filament wound tubes were evaluated. The average void contents for E-glass/polyester composites were 1.28 ± 0.22% and 0.72 ± 0.48% respectively (7 m/min winding speed). The corresponding void contents for the E-glass/epoxy/amine resin systems were 3.5 ± 0.7% and 3.5 ± 0.67% respectively. The average hoop tensile strengths for the conventional wet-filament wound composites tubes produced using the polyester and epoxy resin systems (7 m/min winding speed) were 12.89 MPa and 14.95 MPa respectively (normalised to 55% fibre volume

fraction). The average hoop tensile strength for the composites manufactured via the clean filament winging technique using the polyester and epoxy resin systems were 11.29 MPa and 14.95 MPa respectively. Hence, it can be concluded that the clean filament winding technique is capable of producing industrially relevant filament wound composites with equivalent properties when compared to conventional wet-filament winding. However, the environmental benefits of the clean filament winding technique are significant. Furthermore, it was shown that the clean filament winding technique could be retrofitted with minimal effort onto the industrial production equipment.

DEDICATIONS

This thesis is dedicated to

My fiancé and best friend Simon Phelan
(Without your support I don't think I would have made it to the end)

&

My Mother and Father
(For your advice and belief)

ACKNOWLEDGEMENTS

I would like to thank my supervisor Professor Gerard Fernando for giving me the opportunity to work on this project. His knowledge and guidance has helped me in the completion of this work.

I am very appreciative of the help received from my colleagues in the Sensors and Composites Group. Especially to Dr Muhammad Shafiq Irfan, Dr Ramani Mahendran, Dr Raj Machavaram, Dr Surya Pandita, Fran Nieves, Richard Murray and Samuel Ojo who all gave up their time to help when asked. I would also like to give thanks for the support given from members of the University of Birmingham Metallurgy and Materials school, in particular Mark Paget, Frank Biddlestone, Mick Cunningham, Mrs. Anne Cabezas, Mrs. Kay Jones and Sebastian Ballard, for helping me during my work in one way or another.

I am very grateful for the funding and support given by the Engineering and Physical Sciences Research Council (EPSRC), and Technology Strategy Board (TSB). Appreciation is also given to the industrial partners involved in the project.

I am also grateful to my friends who have been part of my time during my PhD at Birmingham, without them my time would have been filled with far less laughter.

Finally, I would like to thank my mother and father who have supported me continuously throughout all my studies, and my wonderful fiancé who has had to listen to all my troubles as well as complete his own PhD.

PUBLICATIONS

Wait, C. F., Shotton-Gale, N., Smith, C., Irfan, M., Pandita, S., Wang, L., Paget, M., Price, R., James, J. and Fernando, G.F. (2013) 'The recovery, reprocessing and reuse of waste glass fibre fabrics: "Closed-loop recycling" **The 19TH International Conference on Composite Materials,** Montreal, Canada.

Murray, R., Irfan, M., Machavaram, V., White, R., Kim, H., Wait, C., Bogonez, F., Ojo, S., Papaelias, M., Curtis, P. and Fernando, G.F. (2013) "Production and evaluation of intra-filament hybrids" **The 19th International Conference on Composite Materials,** Montreal, Canada.

Irfan, M., Shotton-Gale, N., Wait, C., Pandita, S., Machavaram, V., Mahendran, R., Paget, M., Harris, D., Leek, C., Wootton, S., Tait, M., and Fernando, G.F. (2012) 'Clean and environmentally friendly production of composites', **International Symposium on Advanced Polymeric Materials 2012 (ISAPM 2012) under the auspices of 8th International Materials Technology Conference and Exhibition (IMTCE 2012)** 7, Kuala Lumpur, Malaysia

Smith, C., Shotton-Gale, N., Wait, C., Paget, M., Harris, D., Machavaram, V., Wang, L., James, J., Price, R. and Fernando, G.F. (2010) 'Manufacture and evaluation of filament wound tubes from loom (weaving) waste', **SAMPE Europe**, Paris, France.

Irfan, M., Machavaram, V., Murray, R., Bogonez, F., Wait, C., Pandita, S., Paget, M., Hudson, M. and Fernando, G. (2013) "The design and optimisation of a rig to enable the lateral spreading of fibre bundles" **Journal of Composite Materials,** 48 (15): 1813-1831.

Pandita, S., Irfan, M., Machavaram, V., Shotton-Gale, N., Paget, M., Mahendran, R., Wait, C., Harris, D. and Fernando, G. (2012). Clean wet-filament winding – Part 1: Design concept and simulations. **Journal of Composite Materials**, 47 (3): 379-390.

Irfan, M., Machavaram, V., Mahendran, R., Shotton-Gale, N., Wait, C., Paget, M., Hudson, M. and Fernando, G., (2011) "Lateral spreading of a fibre roving via mechanical means" **Journal of Composite Materials**, 46(3): 311-330.

CONTENTS

LIST OF FIGURES

LIST OF TABLES

1. INTRODUCTION

1.1 BACKGROUND

The global market value and the volume of production for glass fibres in 2012 were estimated to be in the region of US$ 22.2 billion and 9.9 million metric tonnes respectively (Industry Experts, 2012). The global glass fibre industry is predicted to reach approximately US$ 45.12 billion between 2014 and 2019 with a significant 67% of the global market being dominated by Asia-Pacific and North America (Market and Markets, 2014). The total global market value for composites is expected to reach around US$90 billion by 2020, growing at an annual growth rate of 7% to 9% from 2015 to 2020 (Market and Markets, 2014). The maximum growth in the industry is expected to be generated by the construction and wind energy industries (Market and Markets, 2014).

Conventional wet-filament winding (referred to as conventional filament winding from here on) is a process where continuous fibre bundles are impregnated with a resin system and then wound around a rotating mandrel (Morley, 1987). Figure 1.1 illustrates the conventional wet-filament winding process.

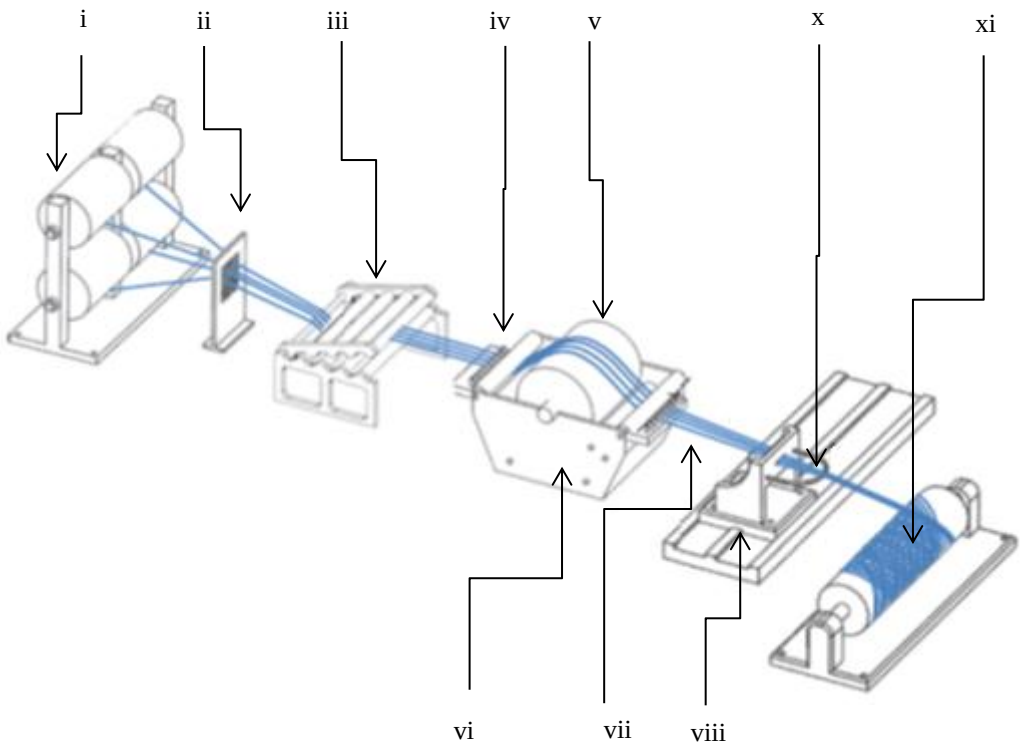

Figure 1.1 Schematic illustration of the conventional wet-filament winding process. The key components are labelled as follows: (i) fibre creels; (ii) fibre guide; (iii) tensioning systems; (iv) guide pins; (v) drum-impregnator with a doctor-blade; (vi) resin bath; (vii) impregnated fibre bundles; (viii) traversing carriage; (x) D-eye; and (xi) rotating mandrel (Pandita *et al.*, 2012).

During filament winding, the reinforcing fibres are hauled-off from fibre creels and directed into a resin bath. Resin and hardener of correct stoichiometric ratio are measured and mixed manually before they are poured into the resin bath. The resin bath contains an impregnation drum, over which, the fibre bundles are directed. As the fibres are hauled off, the drum rotates due to friction between the fibres and the surface of the drum. The "thickness" of the resin that is picked up onto the surface of the rotating drum is controlled by a doctor-blade. The resin that is picked upon the surface of the rotating drum is transferred to the fibres; this represents the start of the impregnation process. The impregnated fibres leave the resin bath ~~a~~nd with the use of guide plates and pins, are directed onto a traversing carriage. As the carriage traverses along the mandrel, the fibres are hauled onto a rotating mandrel at a defined angle

which is a result of the winding speed and traversing carriage speed (Shotton-Gale *et al.*, 2010).

In general, components made via this technique are easily reproduced due to the process being computerised. For example winding angles, the traverse rate can be set as well as the speed of the winding and the number of layers (Koussios *et al.*, 2004). Filament winding is used for the production of components such as pipes, pressure vessels, missile launch tubes and motor cases, automotive leaf springs and fuse holders (Kliger and Wilson, 1990). They are being used increasingly in oil, gas, water, sewage, offshore, ducts and chemical sectors (Rafiee, 2012).

However, there are some issues involved with using the filament winding technique to manufacture composites. At the end of a production shift, the resin bath must be emptied of leftover waste resin and this needs to be cured and disposed of. It is also necessary for solvent to be used to clean all parts of the equipment that has come into contact with the mixed resin system. The resin contaminated solvent is generally recovered by distillation and the sludge is disposed of. Appropriate local extraction and ventilation need to be operational to comply with REACH regulations (Corrigendum to Regulation (EC) No 1907/2006 REACH).

Although composites have been produced via filament winding for the last 60 years, a number of issues still need to be addressed in order for the process to meet the ever increasing demands of the composite industry and legislation. The primary EU legislations of relevance to composites are: (i) Directive 1999/31/EC on Landfill of Waste, (ii) Directive 2000/76/EC for Incineration of Waste; and (iii) Council Directive

2000/53/EC on End of Life Vehicles. The following four points prevent the process from being more efficient, cost effective and environmentally friendly.

(i) Pot-life of the pre-mixed resin system.

(ii) Resin bath.

(iii) Solvents.

(iv) Waste resin.

Clean filament winding was developed in the laboratory to overcome some of the above-mentioned limitations (Shotton-Gale *et al.*, 2010). Figure 1.2 illustrates the clean filament winding process.

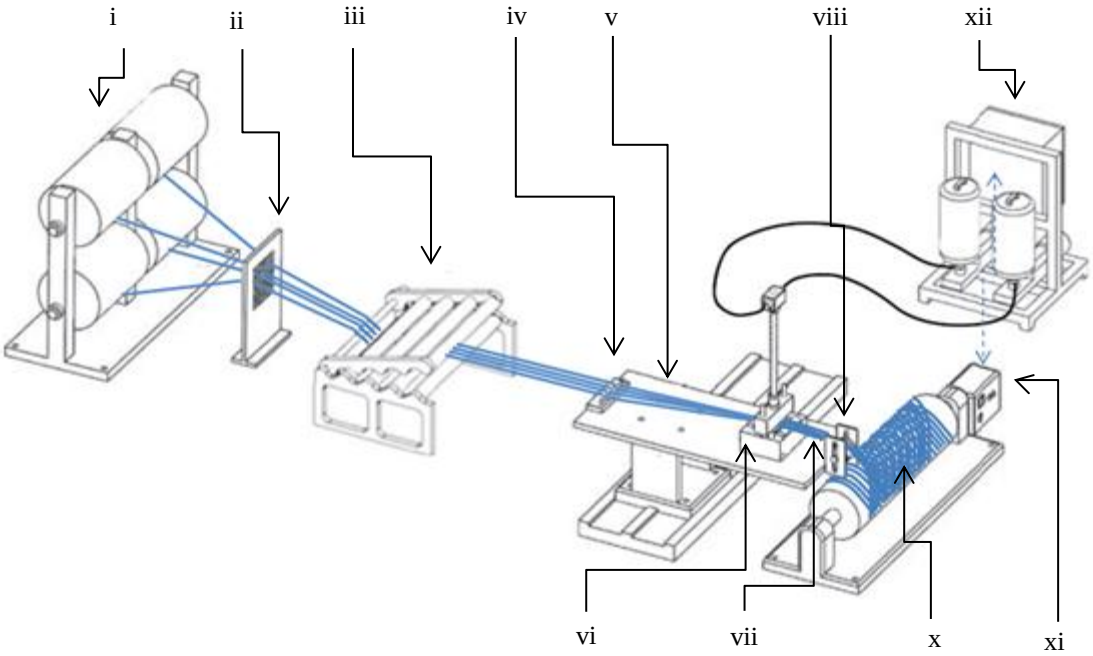

Figure 1.2 A Schematic illustration of the clean filament winding process. The key components are coded as follows. (i) Fibre creels (ii) Fibre guide (iii) Tensioning system (iv) Guide pins (v) Traversing carriage with a platform/adaptor to house the integrated fibre spreading unit and resin impregnator (vi) Resin Impregnator unit (vii) Resin-impregnated fibre bundles (viii) 'Collector' roller or D-Ring (x) Rotating mandrel (xi) Feedback control unit to synchronise the resin dispensing unit to the fibre haul-off rate or rotation speed of the mandrel (xii) Resin dispenser (Pandita *et al.*, 2012).

As with conventional filament winding, the process begins by fibres being hauled off creels. The fibres then pass through a series of tensioning rollers which are mounted on the traverse arm and into an injector system where the fibre bundles are impregnated. From here, they are wound around a rotating mandrel. The injector system consists of a resin impregnator unit and static mixer. The static mixer is used to enable intimate mixing of the resin and hardener. Unlike conventional filament winding where a resin bath is used to impregnate fibres, in clean filament winding, a custom-designed resin impregnator unit is used. Clean filament winding is designed so that the fibres are impregnated directly as they are hauled through the resin impregnation unit. This allows the resin and hardener to be stored separately, thus minimising airborne contamination (as is the case with the resin bath). The hardener component of the polyester resin system used by the industrial partner had a viscosity of approximately 24 Pa.s, sourcing a gear-pump that was capable of dispensing the small quantities of the hardener to meet the stoichiometric ratios required was not achievable and meant that the investment cost in the gear-pumps was too prohibitive. Hence, a resin delivery system based on a pressure-pot was implemented for polyester resin. Here, pre-mixed resin and hardener were introduced into a pneumatically-powered pressure-pot.

Issues related to solvent use and the volume of waste resin generated at the end of each production cycle is a function of the volume of the resin bath, the distance between the impregnated fibres to the mandrel, and the number of contact points and mode of delivery of impregnated fibres onto the mandrel (pins, D-eye). In the case of clean filament winding, these issues are minimised because of the relatively low volume of the impregnator compared to the resin bath, and the fact that the impregnator is in relatively close proximity to the mandrel. It has also been reported that a significant

reduction of the cleaning time was achieved with clean filament winding on site (Pandita *et al.,* 2007). Moreover, it was stated that the generation of waste and solvent usage can be reduced significantly when compared with conventional filament winding production; up to 80% less solvent consumption has been achieved, along with an equivalent reduction of resin waste (www.netcomposites.com).

This current study investigated the development of two prototype resin impregnators for the clean filament winding process. These devices were retrofitted and used during industrial site trials. The primary focus of this thesis was to investigate the feasibility of using clean filament winding instead of conventional filament winding to manufacture composite tubes with comparable properties and production rates, in an industrial environment.

1.2 AIMS OF THE STUDY

The aims of this project were as follows:

(i) To design a resin impregnator unit with a view to replacing the resin bath used in wet-filament winding.

(ii) To demonstrate the clean filament winding concept, using the resin impregnator, in an industrial environment.

(iii) To compare the relative mechanical and physical properties of filament wound tubes manufactured using the conventional and clean filament winding techniques.

(iv) To investigate the impregnation characteristics of E-glass fibres from two manufacturers.

(v) To assess the "green credentials" of the conventional and clean wet-filament winding techniques using life cycle analysis.

1.3 STRUCTURE OF THESIS

The subsequent sections of this thesis are structured as follows:

Chapter 2 presents a critical literature review which firstly reviews the glass fibre manufacturing process with emphasis on the role of the binder. This is followed by a detailed review of the literature, focusing on the impregnation of glass fibres with reference to filament winding. Finally, the review addresses the available literature on clean filament winding.

Chapter 3 details the experimental procedures that were used in the research programme to undertake conventional and clean filament winding trials on an industrial filament winding machine in industry. This section also gives details of the relevant standards used in assessing the composites produced. The second section of this chapter provides details of the experimental procedures used to characterise the impregnation of glass fibres supplied by two manufactures.

Chapter 4 presents the results and discussion of conventional and clean filament winding trials undertaken in an industrial environment. The physical and mechanical properties are discussed in detail. The subsequent section of the chapter reports on the impregnation characteristics of two fibre types, with a focus on the effect of the binder content.

Chapter 5 presents the conclusions from the study along with recommendations for future work.

2. LITERATURE REVIEW

This chapter presents a detailed review of the fibres, matrices and in particular aspects that are related to filament winding. The first section of this chapter addresses glass fibre reinforcements, including the production and the effect of binders used and their effect during production of glass fibre composite materials. The second section of this chapter explores the different models for impregnating fibre bundles, noting different theories and the associated outcome of each. Thereafter, the chapter examines the filament winding process and discusses literature in relation to the production of filament wound tubes.

2.1 GLASS FIBRES

The main focus of this study was on glass fibre composites and therefore, the following section describes the different types of glass fibres with a particular focus on the manufacture and characteristics of E-glass fibres.

Reinforcing glass fibres can be categorised into the following classes: electrical-grade glass (E-glass), high-strength glass (S-2 glass), corrosion glass (C-glass), electro-corrosion resistant glass (ECR-glass) and reinforcement glass (R-glass also referred to as S and TE-glass): as defined by ASTM D578/D578M - 05(2011). The main components and quantities used in the manufacture of conventional types of glass fibre are summarised in Table 2.1.

	Composition, wt%											
Fibre	SiO_2	B_2O_3	Al_2O_3	CaO	MgO	ZnO	TiO_2	Zr_2O_3	Na_2O	K_2O	Li_2O	Fe_2O_3
General-purpose fibres												
Boron-containing E-glass	52 - 56	4 - 6	12 - 15	21 - 23	0.4 - 4	...	0.2 - 0.5	...	0 - 1	Trace	...	0.2 - 0.4
Boron-free E-glass	59	...	12.1	22.6	3.4	...	1.5	...	0.9	...	...	0.2
	60.1	...	13.2	22.1	3.1	...	0.5	...	0.6	0.2	...	0.2
Special-purpose fibres												
ECR-glass	58.2	...	11.6	21.7	2	2.9	2.5	...	1	0.2	...	0.1
D-glass	74.5	22	0.3	0.5	...	...	...	...	1	< 1.3	...	...
S-,R-, and TE-glass	60 - 65.5	...	23 - 25	0 - 9	6 - 11	...	...	0 - 1	0 - 0.1	...	...	0 - 0.1
C-Glass	65	6	4	14	3	...	...	...	8	...	...	0.2

Table 2.1 A summary of the composition of different types of commercial glass fibres (Wallenberger *et al.*, 2001 and Milewski and Katz, 1987).

E-glass fibres are formed from an alumina borosilicate glass which is extruded into small diameter fibres (Parratt, 1972). The primary composition is of oxides of sodium, calcium, aluminium and silicon (ASTM D578/D578M). Depending on the manufacturer and the desired properties, smaller concentrations of oxides of magnesium, sodium, potassium, titanium, iron and fluorine are also added (Pantano *et al.*, 1992). S-glass is a formulation based on oxides of silicon, aluminium and magnesium (SiO_2-AL_2O_3-MgO) but contain higher percentages of SiO_2 for applications in which tensile strength is an important requirement (www.compositesworld.com). C-glass describes glass fibres composed primarily of the oxides of sodium, calcium, boron, aluminium, and silicon which demonstrates good acid resistance (ASTM D578/D578M). C-glass fibres are sometimes used to replace E-glass fibres because they demonstrate better corrosion resistance properties. Selected mechanical properties of some of these fibres are characterised in Table 2.2. Finally, E-CR-glass is used for

boron-free modified E-Glass compositions for improved resistance to corrosion by most acids (ASTM D578/D578M).

Fibre	E-glass	S-glass	C-glass	ECR-glass	Reference
Density	2600	2480	2490		Campbell (1994)
(kg/m^3)	2620	2500	-		www.rapra.net
	2550	2490	-		www.azom.com
	2600	-	-		glassproperties.com
	2540-2550	2480-2490	-	2660-2680	Wallenberger et al., (2001)
	2600	-	-		Hull & Clyne (1996)
Young's Modulus, E	76	85.5	69		Campbell (1994)
(GPa)	81	89			www.rapra.net
	80	89			www.azom.com
	73				glassproperties.com
	76-78	88-91		80-81	Wallenberger et al., (2001)
	80-81*				Wallenberger et al., (2001)
	76				Hull & Clyne (1996)
Tensile Strength	3.45	4.60	3.3		Campbell (1994)
(GPa)	3.45	4.59			www.rapra.net
	2.0	4.75			www.azom.com
	3.40				glassproperties.com
	3.1-3.8	4.38-4.59		3.1-3.8	Wallenberger et al., (2001)
	2.0				Hull & Clyne (1996)
Thermal Expansivity	4.9	5.6	7.2		Campbell (1994)
($10^{-1} K^{-1}$)	4.9				Hull & Clyne (1996)
Thermal Conductivity	13	13	13		Campbell (1994)
($W m^{-1} K^{-1}$)	13				Hull & Clyne (1996)
Maximum Operating Temperature (°C)	550	650	600		Campbell (1994)

*Boron-free E-glass

Table 2.2 Typical selected properties obtained from different types of glass fibres.

The type of fibre reinforcement used in this current study was E-glass fibre. This was because the collaborating industrial partner used E-glass fibres exclusively for filament winding. In general, E-glass fibres are used commonly in filament winding applications

due to their low cost: ~£1-2/kg (Cripps, 2015). Reinforcements such as R or S-fibres have better properties but the price of fibres is ~£12-20/kg (Cripps, 2015).

2.1.1 E-Glass Fibre Production

Figure 2.1 shows a schematic illustration of the glass fibre production process (Irfan *et al.*, 2014).

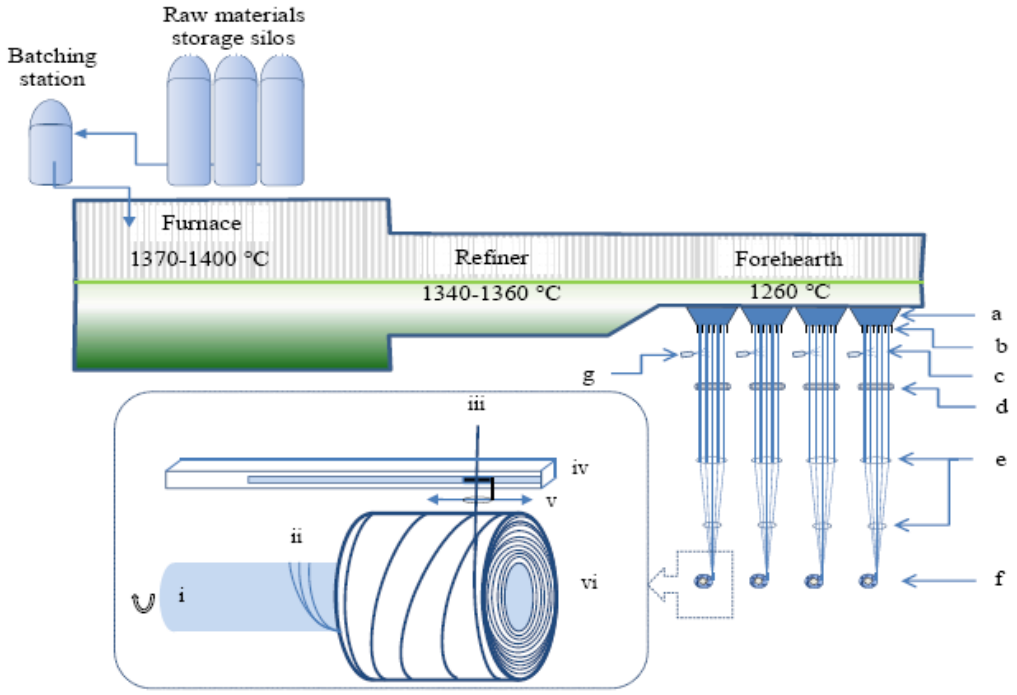

Figure 2.1 Schematic illustrating the production process of glass fibres (Irfan *et al.*, 2014).

The process begins by the storage of oxides in silos. The oxides are delivered and mixed at the batching station where they are then fed into the furnace. Furnaces used in the operation are generally split into three areas with different temperature ranges. In the initial part of the furnace, the temperature is at its hottest at around 1370 - 1400 °C. It is at this point where the inorganic oxides are melted (Irfan *et al.*, 2014). The next section of the furnace is termed the refiner. The temperature is slightly lower at around

1340 - 1360 °C and it is at this stage that absorbed gases, moisture and decomposition products are removed. The third and final area of the furnaces, known as the forehearth is held at the lowest temperature at 1260 °C. It is at this stage the molten liquid is fed into temperature controlled bushings. Bushings are generally made of a platinum/rhodium alloy and consist of multiple orifices (400 - 8000) ranging from 0.75 – 2.00 mm in diameter (Thomason and Adzima, 2001, Shelby, 2005, Kinsella, 2001). The molten glass is drawn though the bushings in a process called fiberizing. The molten glass flows through the bushings at approximately 55 - 60 m/s (Campbell, 2004, Kinsella, 2001). The bushings are heated electrically to maintain the glass at the correct melt viscosity (Wallenberger *et al.,* 2001). Once the fibres are extruded through the bushings, they are quenched with water or an air spray to solidify the molten glass in its amorphous structure (Campbell, 2004, Kinsella, 2001). This rapid quenching prevents crystallisation of the glass (Thomason and Adzima, 2001 and Morley 1987). The properties of the glass fibres are affected by their subsequent thermal history during processing (Loewenstein, 1983, Thomason, 1999, Campbell, 2004 and Yue *et al.*, (2004)).

Aside from the diameter of the bushings, there are a few other factors which influence the diameter of the filaments. Thomason, (1999) stated that the diameter (D) of individual glass filaments is a function of the instantaneous production conditions and is given by Equation 2.1:

$$D = D_0\sqrt{(V_0|V)}$$

Equation 2.1

Where:

D_0 is the internal diameter (mm) of the bushing tip;

V_0 is the velocity (m/s) that the molten glass flows through the bushing; and

V is the velocity (m/s) the fibre is being drawn.

Therefore, the winding speed and the pressure exerted on the molten glass to push it through the bushings both affect the fibre diameter. Other factors which also contribute to the diameter of the glass fibres are the viscosity of the liquid which needs to be controlled accurately by adjusting the temperature within the furnace and the point at which the glass is cooled to a solid.

After rapid cooling has taken place, the glass filaments are coated by an aqueous emulsion which contains a lubricant and other additives. This helps to minimise abrasive damage that the fibres may be subjected to. This emulsion is generally called the binder or "size" and its function is discussed in more detail in the following section. After the application of the binder, the glass filaments from each bushing are drawn together into individual bundles. As the individual filaments are combined they are wound onto spindles with a cardboard sleeve at velocities of between 15 to 90 m/s (Wallenberger *et al.*, 2001, Xiong, 2002). The term "tex" is used to describe the unit of linear density, equal to the mass in grams of 1000 meters of fibre, (ASTM D123). Once the glass fibre creels are produced, they are transferred to an oven and heated to approximately 140-150 °C for 10-hours. This drying process is used to remove water from the creels (Dell'Anno and Lees, 2012).

2.1.2 Binders

2.1.2.1 Binder Application

The binder is typically an aqueous solution that is applied by either passing the filaments over a roller or spraying the filaments (Kinsella, 2001). The application of the binder occurs over a contact distance of less than 10 mm when using a roller-based application method and occurs in less than 0.5 milli-seconds (Thomason and Dwight, 1999).

The typically amount of binder added to each filament is approximately 15% of the weight of the filaments (Thomason 2012). As mentioned previously, the filaments are then subjected to a drying process which removes the liquid in the binder and provides a new set of properties to the fibre surface which can optimise composite processing and performance (Thomason and Adzima, 2001). Therefore, of that 15% there is approximately 2-10% weight of solids so at the upper level 0.2-2% fibre weight of binder could potentially make it onto dry glass fibre (Fraser *et al.*, 1983, Britcher *et al.*, 1999 and Thomason, 2012). The binder content can be lost due to subsequent processing such as weaving and braiding (Thomason and Dwight, 1999). Some weavers remove the original binding agent and apply their own for the weaving operation for specific end-users.

Thomason and Kalinka, (2001) used a single-fibre pull out test designed by Meretz *et al.,* (1993) to measure the tensile strength of E and S-glass fibres (3 mm – 20 µm) gauge length. They found that for a given fibre type and length from the same manufacturer there was a varying distribution in the tensile strength results. These were thought to be due to a number of different reasons including processing of the glass fibres. Due to the

fact that these fibres were 4 mm chopped fibres it was assumed that the time between the application of the binder and the chopping of fibres had a significant effect on the strength of the interface due to removal of the binder. They also showed there was a significant difference in the impact test on notched and un-notched samples. However, these values were not stated in the study.

The distribution of the binder content on the glass fibres has been shown to be uneven which is demonstrated in Figure 2.2 (i) by Thomason and Dwight, (1999) and (ii) by Mallarino *et al.,* (2005).

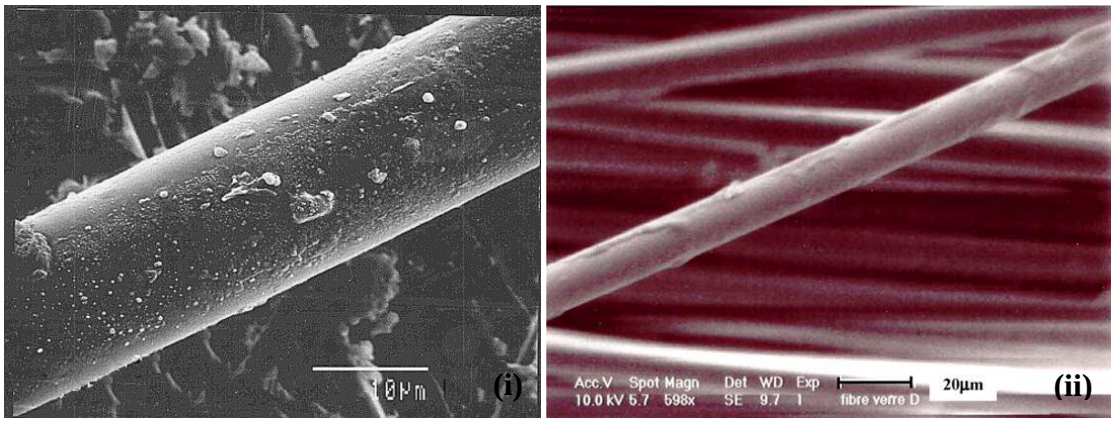

Figure 2.2 SEM micrographs showing inhomogeneous distribution of binder on glass fibres reported by (i) Thomason and Dwight, (1999), and (ii) the non-uniformity of the binder layer around the fibres reported by Mallarino *et al.,* (2005).

2.1.2.2 Composition of the Binder

Along with the chemical composition of the glass fibres, the components of the binder impart strand integrity, processability, resin compatibility, and adhesion properties to the final product and therefore tailor the fibre properties to the specific end-use requirements (Wallenberger *et al*., 2001).

The binder is made up of a mixture of coupling agents, lubricants, antistatic agents, emulsified polymers, film formers and other additives. The formulation of the binder is closely guarded secret by glass fibre manufacturers and also varies from manufacturer to manufacturer as this is the main commercial advantage they have over their competitors. Table 2.3 shows the common ingredients used in conventional binders (Kinsella *et al*., 2001).

Ingredient Category	Typical Chemistry	Role
Film formers	Epoxies, polyesters, polyvinyl acetate, polyvinyl alcohol, polyolefins, polyurethanes, starch.	Fibre protection, strand integrity, strand wetting and solubility.
Lubricants	Imidazolines, mineral oil, polyethylene glycol fatty acid esters, vegetable oil.	Fibre protection, strand integrity, lower surface friction, improving fibre bundle forming and processability.
Emulsifiers	Ethoxylated fatty acids, ethoxylated alkylphenols, other ethylene oxide derivatives, etc.	Make film formers and lubricants water compatible.
Coupling agents	Silanes, titanates, zirconates.	Provide glass to resin and film former bonding .
Other additives	Metal halides, quaternary ammonium compounds, acids and bases.	Antistatic agents, pH control, nucleating agents- to control crystallinity (for thermoplastics).
Water (~90%)	Relatively high purity	Cooling, carrier for binder, aids distribution

Table 2.3 A summary of the common ingredients used in conventional binders (Kinsella *et al.,* 2001).

The optimisation of the binder layer is complex and often is a compromise between manufacturing, marketing, technical and economic factors (Thomason and Adzima, 2001). A "good" binding agent applied to reinforcing fibres should deliver: high strand integrity, low levels of fuzz, low degree of friction, good wettability, and good dispersion (Thomason, 2012). The role of the emulsified polymer and aqueous coating

is principally to displace water from the fibre surface and provide appropriate hydrophobicity for compatibility with relatively non-polar polymers (Jones, 2007).

The lubricant is added to promote stand integrity and reduce the friction caused by fibres as they slide over one another or move over post-processing equipment (weaving, filament winding etc.). Film formers as stated in Table 2.3 promote wettability. Feuillade *et al.*, (2006) found increasing the thickness or concentration of the film former was shown to decrease the polar component of the surface energy of the glass fibre. The nature of the film former and especially the type of polyester used was seen to have a major influence on the surface properties of the glass fibres. They investigated the influence of the binder composition on the wetting characteristics of fibres and an unsaturated polyester matrix during the manufacture of sheet moulding compounds. The parameters studied were: (i) the concentration of binder; (ii) the nature of the antistatic agent; (iii) the nature and concentration of the film former (highly unsaturated, bisphenolic aromatic or no bisphenolic aromatic); and (iv) the method of depositing the antistatic agent (quaternary ammonium chloride and quaternary ammonium sulphate with or without a fluorinated component). One other finding from the experiment was that the surface free-energy increases when an antistatic agent is added to the binder which was subsequently applied to the fibre surface.

A coupling agent is also present in the binder. The main function of the coupling agent is to increase the adhesion between the reinforcing fibre and the matrix. The chemical composition of the coupling agent is specific to the matrix being used. An example of a common coupling agent used with epoxy or polyester resin systems is silane. Hatsuo

and Koenig (1979) stated that the number of silane monolayers (vinyltrimethoxysilane) deposited on the glass surface is typically around 100 monolayers. A silane coupling agent can be represented by the formula $(RO)_3$ -Si – R' (Wang *et al.*, 2009). The R' group reacts with a specific functional group in the resin and the RO_3 (alkoxy) hydrolyses to from a silanol group and which then reacts with the hydroxyl groups on the glass surface (Sever *et al.*, 2008).

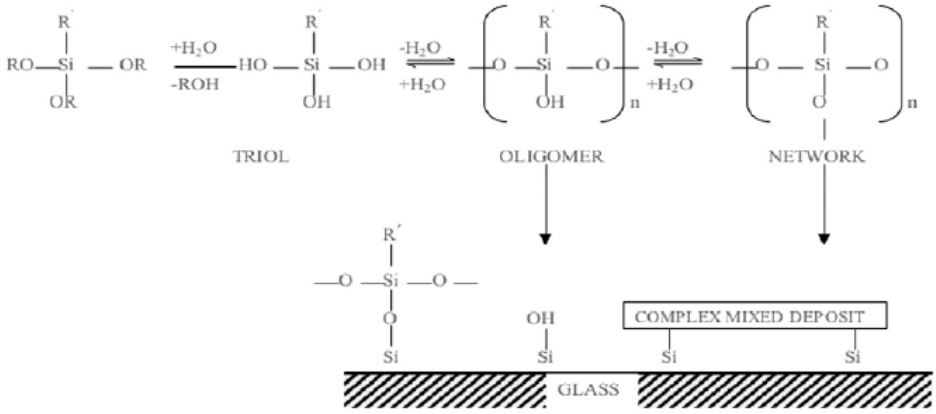

Figure 2.3 A schematic showing the hydrolysed silane deposited on the surface of silane-treated glass fibre (Jones, 2007).

The pH of the emulsion is adjusted to promote the hydrolysis of the alkoxy groups. These silanol groups can then condense into oligomers and polymers. Therefore, coating on the glass fibre is a complex mixture of polymers and oligomers which is seen in Figure 2.3 (Jones, 2007). Amino silane used on epoxy resins is known to deposit a mixture of oligomers and polymers. The migration of the soluble oligomeric component into the matrix was said to leave molecular pores in the silane deposit into which the resin can permeate (Jones, 2007).

2.1.2.3 Formation of the Interphase

Although the properties of the composite depend on the properties of the individual components (reinforcing fibre and matrix), they also depend on the interface region between the fibre and the matrix. There are 6 key interfacial adhesion categories defined by Hull and Clyne, (1996) that are used to describe the resin-to-fibre adhesion. Figure 2.4 demonstrates each category.

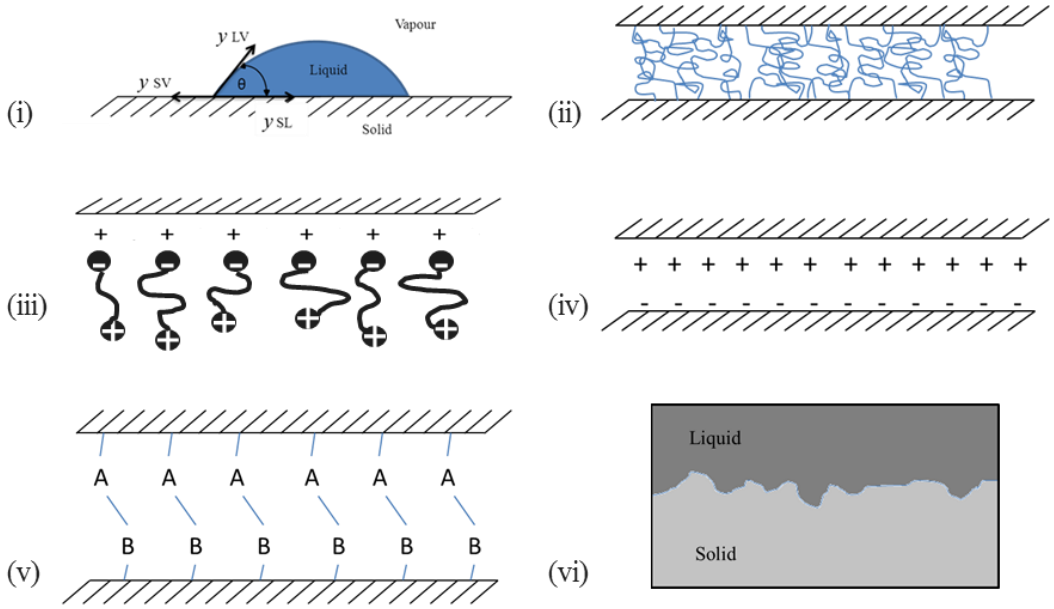

Figure 2.4 A schematic showing the (i) wetting and absorption - Contact angle (θ) and surface tension (*y*) for a liquid drop on a solid surface. SV (solid-vapour), SL (solid-liquid) and LV (liquid-vapour) interfaces, (ii) molecular entanglement following inter-diffusion, (iii) cationic groups at the end of molecules attracted to an anionic surface, resulting in polymer orientation at the surface, (iv) electrostatic interaction, (v) Chemical reaction and (vi) Mechanical adhesion (Hull and Clyne, 1996).

With these categories in mind, a critical component to be considered in the manufacture of glass fibres and their composite is the binder that is applied to the surface of the fibres during the extrusion part of the glass fibre production process (Kinsella, 2001). The interphase has chemical and mechanical properties which are different from the bulk matrix (Jones, 2007).

Gao and Mäder, (2002) used nano-indentation tests based on atomic force microscopy (AFM) techniques to study the interphase properties of glass fibres treated with γ-aminopropyltriethoxy silane coupling agent, either polyurethane (PU) or polypropylene (PP) film formers and combined with polypropylene (PP) and epoxy matrixes. They found the interphase thickness to vary between less than 100 nm and ≈300 nm depending on the type of binder and matrix material. They also observed variations in the Young's moduli across the interphase region. This view was supported by Jones, (2007) who found the interphase to be in the order of 20-200 nm when the binder polymer and added lubricating agents migrate into the matrix. Figure 2.5 shows the typical silanes used on glass fibres for different resin systems.

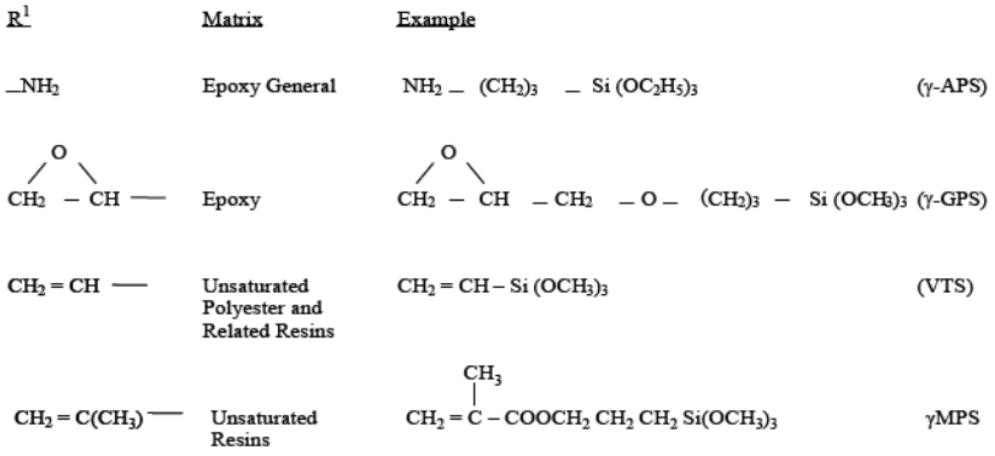

Figure 2.5 Typical silanes showing the choice of R' for compatibility with different resin systems (Jones, 2007).

2.1.2.4 The Effect of the Binder on the Properties of Composite

As mentioned previously, the surface energy of the fibre with the surface tension of the matrix has an impact on the degree of adhesion. Nishioka, (1990) used heat-cleaned E-glass fibre fabrics which were subjected to dip-coating a varying number of times (exact

values not specified) into one of three different mono-functional organosilanes (trimethylethoxysilane, butyldimethylethoxysilane and phenyldimethylethoxysilane) controlled at a pH of 5. A dynamic contact angle machine was then used to investigate the interaction of organosilanes with E-glass fibres. The advancing and receding contact angles of different liquids on silane-treated glass fibres were measured. It was shown that with increasing levels of silane coupling agents, there was a subsequent decrease in the polarity of the E-glass fibres. This was due to the gradual reaction of the polar surface hydroxyl groups with the organosilane which resulted in increased wettability of the fibres. After ten surface treatments with the organosilane solutions, the surface of the glass was fully saturated and therefore wettability plateaued.

A similar finding was observed by Park and Jin, (2001). They investigated the effect of the varying concentrations of amino-silane coupling agents (0.1-0.5 wt.%), on the degree of adhesion on resulting inter-laminar shear strength properties of glass fibre fabric/unsaturated polyester composites. They found that the fibre surface free-energy increased up to around 0.2% concentration increasing the hydrophilic properties of the treated fibres. These results were attributed to an increase in the hydroxyl groups resulting in an increase in hydrogen bonding. This demonstrated the important role coupling agents play on improving the degree of adhesion at the interphases in a composite system. These results correlated with the mechanical interfacial properties of composite samples produced with unsaturated polyester matrixes demonstrating an increase in inter-laminar shear strength up to 0.2% concentration (~26 MPa) followed by a decrease is strength thereafter up to 0.5% concentration (~24 MPa), this was attributed to the increased concentration of silane at the interphase resulting in a

lubrication effect. The type of glass fibre was not specified in this experiment by the authors.

Olmos *et al.*, (2006) studied the influence of amino-silane fibre coatings on the water absorption characteristics of E-glass reinforced epoxy composites. The authors used a binder burn-off technique (1-hour at 500 °C) to remove the original organic matter from the surface of the fibres, regenerated the hydroxyl groups using an activation treatment (10 wt.% hydrochloric acid aqueous solution) and then applied the silane solution. They also washed and dried fibres after application of the silane solution. The samples were tested using gravimetry, near-FTIR spectroscopy and steady-state florescence spectroscopy. They found that the presence of the silanised fibres appeared to induce changes in the water absorption process of the epoxy resin by decreasing the relative gain of mass at equilibrium. This was also demonstrated in the FTIR spectroscopy, gravimetry and fluorescence spectroscopy results.

Gomez and Kilgour (1993) suggested that experiments undertaken to study the sizing of glass fibres should be carried out by reproducing the application of sizing during the glass fibre production process. They conducted experiments to observe the difference between water-sized glass fibres which were subsequently sized with a silane, and fibres sized during production with a silane solution during the drawing stage in the glass fibre production. They found that fibres coated during the production process contained much fewer flaws in the surface of the fibres compare to those treated with a sizing after the processing

Thomason (1995) used E, ECR and S-glass fibres with a range of commercial sizing agents which were then subsequently used on three resin systems which were all based on EPIKOTE 828 EL to produced pultruded rods. The material details are summarised in Table 2.4.

Fibre	Glass	Tex	Comment
A	E	2009	Epoxy-compatible
B	E	2400	Polyester/epoxy compatible
C	E	2400	Polyester/epoxy compatible
E	E	4600	Epoxy-compatible
F	E	2400	Multi-compatible
G	E	2170	Polyester- compatible
H	ECR	2400	Polyester/epoxy compatible
I	E	2400	Epoxy-compatible
J	E	2400	Epoxy-compatible containing *y* - aminopropylsilane
K	E	2400	Epoxy-compatible containing y – (aminoethyl) aminopropylsilane
L	E	2400	Epoxy-compatible containing chloro-substituted aminosilane
M	E	2400	Epoxy-compatible containing y – glycidoxypropylsilane
N	E	2400	Epoxy-compatible
O	S	2000	Epoxy-compatible
P	S	2000	Epoxy-compatible

Table 2.4 A Summary of the different fibre and resin systems used in the experiment by Thomason (1995).

Fibres were subjected to washing in acetone, heating to 200 °C and 500 °C to investigate the effect of different stages of binder removal. It was shown that the interfacial strength of the composites was dependant on the nature of the glass coating. It was reported that there was no influence on the inter-laminar shear strength (ILSS) values of the 200 °C heat-treated fibres and only a 3-4 MPa decrease for acetone extracted fibres. However, heating the fibres to 500 °C for 24-hours reduced the ILSS from 89 MPa to 56 MPa. The reduction in strength in this case was thought to be due to the increased void contact seen in these samples as the surface treatments were removed. The loss of tensile properties after heat treatment was also shown by Feih *et al.*, (2008) who demonstrated that heat-cleaned fibres for 15 minutes at 450 °C exhibited a 50% reduction in single-fibre tensile strength and 60% reduction in fibre

bundle strength. This reduced by a further 18% when fibres were heat treated at 450 °C for 30 minutes for the fibre bundle test. This was also attributed to the removal of the lubricant within the protective binder layer which resulted in a greater frictional force between filaments. When an energy dispersive X-ray (EDX) analysis was completed on the chemical composition of the fibres pre and post-heat-treatment, there was no significant difference in the results. Therefore, the decrease strength in the single-fibre tensile strength was attributed to the growth of pre-exiting surface flaws or the creation of new flaws during the heat treatment process and was not caused by the physical changes in the glass network or metallic ions leaching.

Iglesias *et al.,* (2002) reported that the removal of the binder via solvent extraction could also cause a decrease in availability of functional groups of the coupling layer as the level of binder reduced leading to the decrease in properties. Iglesias *et al.,* (2002) completed experiments observing the influence of different silane coupling agents (3-aminopropyldimethylethoxysilane, 3-aminopropylmethyldiethoxysilane and 3-aminopropyltriethoxysilane) on the mechanical strength and resistance to hydrolysis of an E-glass fibre/epoxy composite. Using scanning electron microscopy (SEM) fractographic analysis and tensile testing, they demonstrated that the cross-linking density and rigidity increased as the accessibility of the functional groups of the coupling layer increased.

Wang *et al.,* (1999) reported similar finding to the previous studies when they used mechanical testing and surface fractography to characterise the fracture of E-glass fibre fabric reinforced epoxy composites as a function of the silane coupling agent used. The two silanes used were: aminopropyltriethoxysilane (APS) and δ-

aminobutyltriethoxysilane (ABS). The flexural strengths of untreated, ABS, and APS-treated E-glass-fibre reinforced composites were 449 ± 40, 510 ± 19, and 566 ± 9 MPa (dry state); and 389 ± 23, 459 ± 7, and 510 ± 54 MPa (wet state), respectively. They also, observed that a larger fibre de-bonding area was formed in the crack tip region for the untreated glass composites. They suggested this was due to a lower degree of bonding compared to those treated with coupling agents. These findings support the work by DiBenedetto and Lex (1989) who also found that using silane coatings improve the tensile strength of E-glass filaments when used in an epoxy composite compared to unsized fibres. The fibre matrix interface was evaluated as a function of temperature and after exposure to boiling water. Single-fibre pull-out tests (ASTM D3379-75) were used to measure the interfacial shear strength. Phenyl-amino silane and an amino-silane were reported to be effective at increasing the interfacial shear stress with all surface treatments investigated demonstrating higher values than fibres with no coatings for all gauge lengths. They also demonstrated that as the gauge length of the sample increased from 0.51 cm to 2.54 cm, the silane treated fibres were able to retain a higher strength value (3.160-1.409 MPa for uncoated fibres and 3.312-1.616 MPa for silane treated fibre).

Mallarino *et al.*, (2005) found that the relaxation behaviour of a composite tested using dynamic mechanical analysis (DMA) varied when a D-glass fibre fabric was subjected to different binder modifications (binder burn-off, solvent extraction and as-received). They showed that the interface was a combination of the thermosetting cyanate ester resin matrix used and the binder used on the fibres when studied using micro Fourier transform infrared (FTIR) spectroscopy to obtain depth profiles. They also demonstrated that samples with binder resulted in a cohesive failure as opposed to

samples with no binder treatment which resulted in adhesive failure demonstrating the increased adhesion with the effect of the correct binder. The method in which the fracture profiles were obtained was not described.

Findings by Järneteg and Berglund (1992) into the effect of surface treatments on glass fibres used for the production of filament wound tube differs to the previously mentioned results. The two treatments used were: aminosilane coupling agent (AS) and no aminosilane coupling agent (No AS). They found that the treatment had little effect on the fracture toughness and ILSS of the composite in the dry state. However, there was a significant reduction in the mechanical properties of the samples after they were subjected to a saturation test (to attain an equilibrium moisture content) at 70 °C and 70% relative humidity for three months. During this saturation test, the amino-silane was reported to be advantageous due to the chemical bonds fromed between the glass/aminosilane and the epoxy matrix. The fracture toughness dropped from 1.88 to 1.78 MPa√m for the AS sized composite and 1.87 to 1.23 MPa√m for No AS binder. A similar finding was found for tensile strengths and ILSS which drop from 42 to 39 MPa for AS and 41 to 30 MPa for No AS. However, the samples with the AS binder did have a 3% higher fibre volume fraction and the void content was only reported as low for both composites. Therefore, the effect of void content within the samples was not taken into account in these findings. In the experiment by Thomason (1995) described previously it was found that using different coatings on reinforcing glass fibres can increase the ILSS but has little effect on the water absorption properties. However, these findings were in agreement with Ahlstrom and Gerard (1995) who attributed the

higher single-fibre tensile strength of the silane-treated glass fibres compared to the untreated fibres due to the silane binding agent protecting against water intrusion.

A flaw-healing mechanism was invoked by Gao *et al.,* (2003) to explain the observed differences between two types of silane treated E-glass fibres. Fibres were subjected to the following post-binder treatments: (i) distilled water at room temperature, (ii) mixed NaOH/KOH/ $Ca(OH)_2$, (iii) hexane/ethanol, (iv) distilled water at 100 °C, (v) NaOH and (iv) 600 °C pyrolysis to remove the binder. Individual post treated filaments were then tensile tested in accordance with EN ISO 5079. For both fibre types, the decrease in strength was in the order: as-received; hexane/ethanol extraction; distilled water at 100 °C; NaOH aqueous solution and pyrolysis. Both room temperature water and mixed NaOH/KOH/$Ca(OH)_2$ aqueous solution did not influence the tensile strength. Fibre failure strength was shown to be surface-flaw-dependent based on results obtained from atomic force microscopy (AFM). The influence of the binder was shown to affect both the population and size of flaws on the fibre surface by 'healing effects'.

Briard *et al.,* (2005) also invoked flaw healing as the primary reason for strength retention in silane treated E-glass fibres. They proposed a crack bridging mechanism for the strengthening of a soda-lime-silicate glass. A Vicker's micro-indenter was used to create defects on the surface of a 2.9 mm thick glass slide/plate. A load of 10 N was held constant for 5 seconds. The plates were treated using a dipping technique in an aqueous solution of amino-silane or epoxy-silanes or blends of the two. Dipping was followed by drying at 10 to 30 minutes in air and curing at 200 °C for 20 minutes. Failure strengths of coated and uncoated samples were measured using four-point bending on a Zwick mechanical test machine. The indented side was in tension and an

adhesive tape was placed on the other side of the samples for retention of the broken fragments after failure. The loading rate was 10 mm/min. Although the use of just the epoxy or amino-silane coatings had no effect on the tensile strength, the indented glass coated with a mixture of the epoxy-silane/amino-silane film of 100 nm thickness exhibits a significant 75% increase in the flexural strength. This was thought to be mainly due to healing of the crack by bridging the crack-point resulting in channelling the load through the face of the glass rather than at the crack-point.

The previous section demonstrates the effect of binder treatment on the mechanical performance of the final composite. It can be seen from the literature that it is essential to tailor the composition of the binder used to ensure good fibre to matrix adhesion. The following section describes the thermosetting resin systems used in this study and the cross-linking mechanisms.

2.2 RESINS SYSTEMS

Resins used as matrixes within fibre reinforced polymers can be divided into two groups: thermosets; and thermoplastics. The focus of this study was on thermosetting resins, as such, the following sections provide more details on this class of resins. Thermosetting resins undergo a chemical reaction known as curing in order to convert the liquid resin into a solid cross-linked polymer. Curing involves a cross-linking process and is achieved by a series of chemical reactions. These generalised reactions are discussed briefly.

The curing of thermosetting resins can be achieved using a variety of activation methods, for example, microwaves (Azzarri *et al*., 2003) and light (Koran and

Kürschner, 2001). Table 2.5 shows typical selected properties for epoxy and polyester thermosetting resins.

Matrix	Density ($Mg\ m^{-3}$)	Young's Modulus, E (GPa)	Poisson's Ratio	Tensile Strength (GPa)	Failure Strain (%)	Thermal Expansivity ($10^{-1}\ K^{-1}$)	Thermal Conductivity ($W\ m^{-1}\ K^{-1}$)
Epoxy	1.1 – 1.4	3 -6	0.38 – 0.4	0.035 – 0.1	1 – 6	60	0.1
Polyester	1.2 – 1.5	2.0 – 4.5	0.37 – 0.39	0.04 – 0.09	2	100 – 200	0.2

Table 2.5 Properties of epoxy and polyester resin (Hull and Clyne, 1996).

2.2.1 Epoxy Resin and Amine Hardener

Epoxy resins are used widely as the matrix component of high-performance fibre reinforced composites (Morgan, 1977 and Jones, 1994). The term epoxy resin is used to describe the pre-polymer state made up of reactive epoxy rings (oxirane rings) as shown in Figure 2.6.

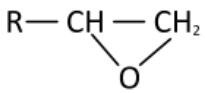

Figure 2.6 The epoxy (oxirane) ring structure (Tomlin, 2010).

A hardener is a curing agent that is used to cross-link the epoxy resin. Hardeners react with the epoxy functional groups to provide the linkages in the cross-linked structure (Tomlin, 2010). There are a variety of different hardeners that can be used to cure epoxy resins. In the current study, an amine hardener was used.

The amine hardener contains hydrogen atoms which react with the epoxy ring to form a covalent bond along with the formation of a hydroxyl group (Nair *et al.*, 2015). During

the cross-linking of epoxy-amine resins, there are two main reactions which occur, primary epoxy–amine addition and secondary epoxy-amine addition.

During the primary epoxy-amine addition, a nitrogen atom from the primary amine, couples with a carbon atom on the epoxy group (Smith, 1961). This can be seen in Figure 2.7

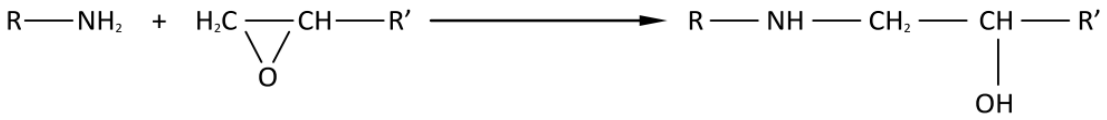

Figure 2.7 A generalised reaction showing the primary epoxy/amine reaction (Nair *et al.,* 2015).

The outcome of this reaction is the carbon-oxygen bond being broken, resulting in the formation of two further functional groups: a secondary amine group; and a hydroxyl group (OH). The secondary amine group can now react with a further epoxy ring, resulting in the production of a tertiary amine group. This reaction can be seen in Figure 2.8.

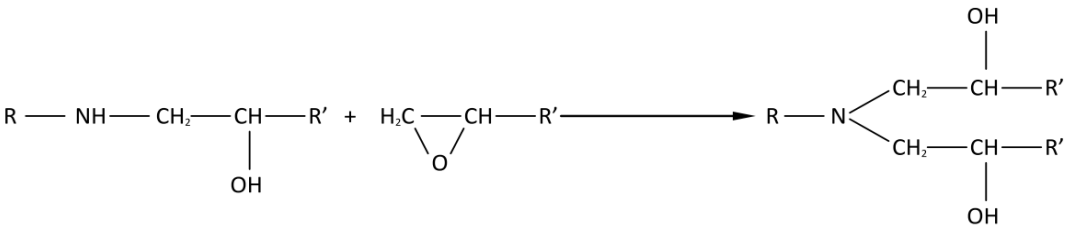

Figure 2.8 A generalised reaction showing the secondary amine group addition reaction (Nair *et al.,* 2015).

2.2.2 Polyester Resin

Figure 2.9 demonstrates a generalised reaction of an unsaturated polyester resin. An ester functional group is represented by the structure shown in Figure 2.9 (i). Esters are

formed by reacting a diol and a diacid as illustrated via a generalised reaction scheme shown in Figure 2.9 (ii).

In general, commercial polyester resins contain reactive unsaturation or double bonds (see Figure 2.9 (iii)) where the reaction between maleic anhydride (with a double bond or unsaturation) and ethylene glycol is shown. The polyester that is formed is indicated along with a short-form representation. The unsaturated acid provides a site for subsequent cross-linking whilst the introduction of a saturated acid reduces the number of sites for cross-linking and hence reduces the cross-link density and brittleness of the end-product (Brydson, 1999). The mechanical properties of the polyester resin are dependent on the density of cross-links and on the rigidity of the molecules cross-linked (Brydson, 1999).

Styrene is frequently used as a diluent and as a cross-linking agent in conjunction with an initiator. Prior to illustrating this, a generalised reaction scheme to demonstrate the creation of reactive free-radical via the use of benzoyl peroxide (initiator) is shown in Figure 2.9 (iv)

The free-radical species, coded as FR* (the * indicate that it is a free-radical or a species with an unpaired electron), readily reacts with double bonds as shown in Figure 2.9 (v). The propagating polystyrene free-radical can react with the double bonds present on the polyester as shown in Figure 2.9 (vi). Thus, the polyester is cross-linked via the polystyrene.

(i) 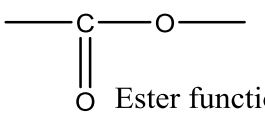

Ester functional group

(ii)

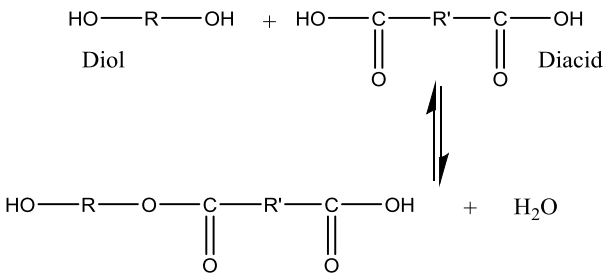

(iii)

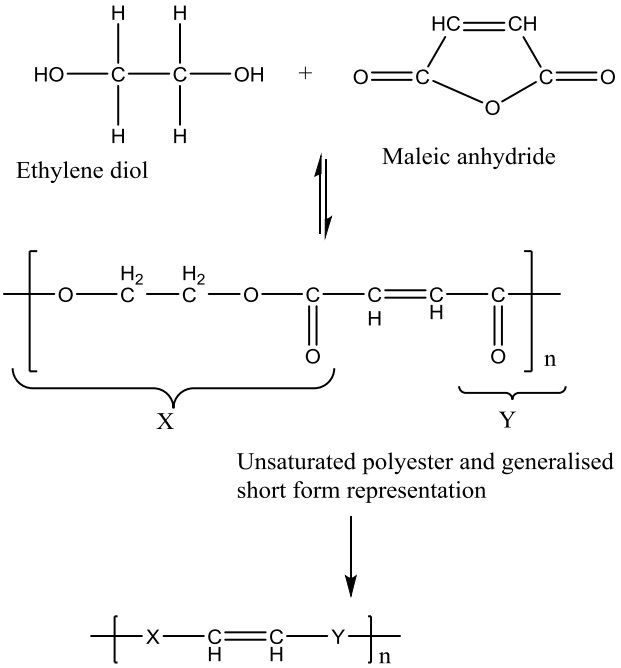

Unsaturated polyester and generalised short form representation

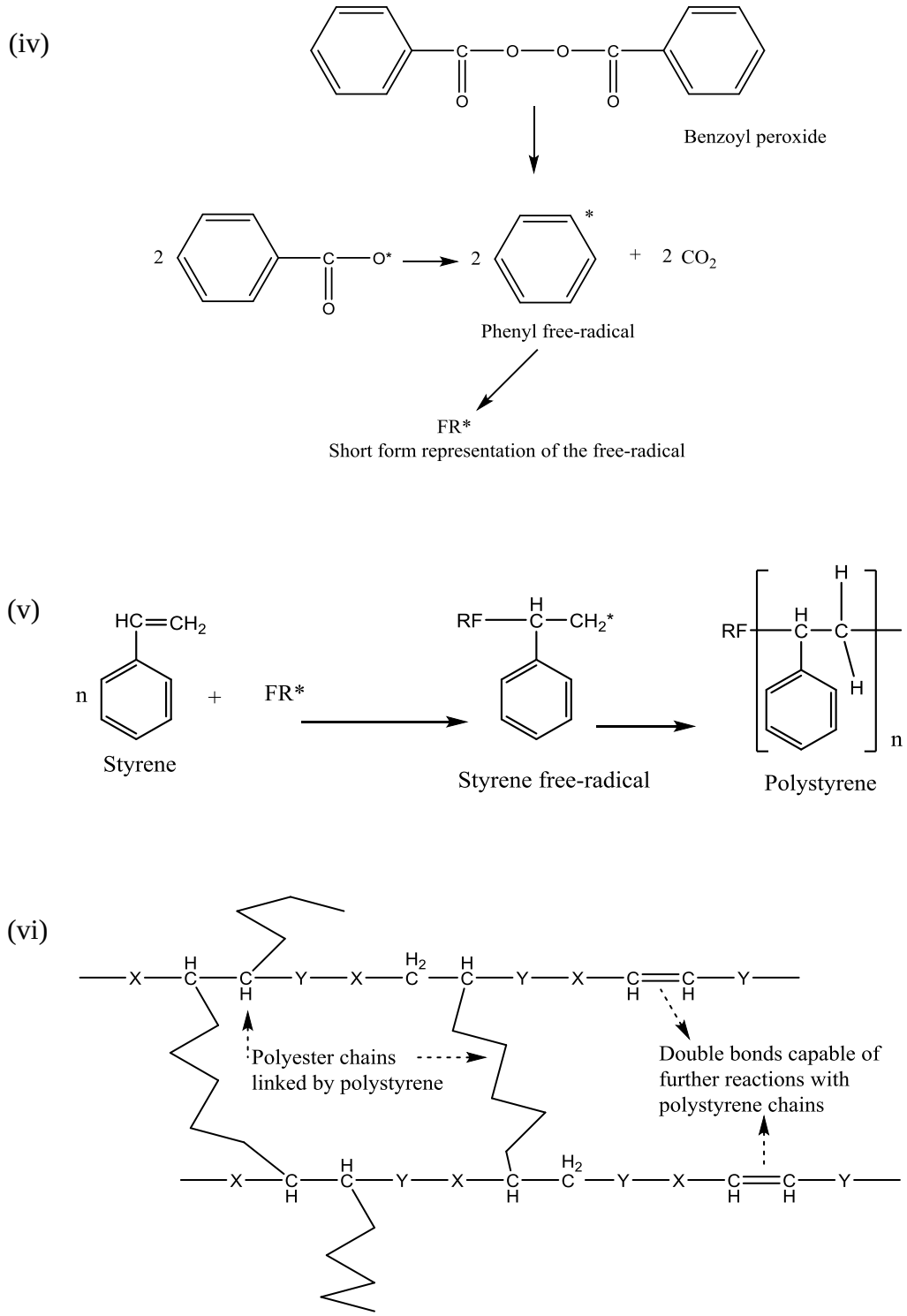

Figure 2.9 A generalised reaction showing stages (i) to (vi) for unsaturated polyester resin.

2.3 FILAMENT WINDING

2.3.1 Conventional Filament Winding

As mentioned previously, during the filament winding process, the fibres are hauled off fibre creels and directed into a resin bath. Resin and hardener are weighted in the correct stoichiometric ratio and mixed manually before they are poured into the resin bath. The resin bath has a impregnation drum around which fibres are directed. The movement of the fibres over the drum causes it to rotate and transfer a thin layer of resin to partially coat the fibre bundles. The "thickness" of this layer of resin is adjusted using a doctor blade, which is controlled manually by the operator depending on the visually-assessed degree of impregnation of the fibres. The impregnated fibres leave the resin bath and pass through a series of guide plates and pins onto a traversing carriage. The fibres are then pulled through a D-eye, a concave shaped device that draws the fibre bundles together to form a ribbon. These are then wound onto a rotating mandrel (Shotton-Gale *et al.,* 2009). As the traversing carriage reciprocates left-and-right, the impregnated fibres are wrapped onto the mandrel in a predetermined pattern.

Winding angles can be varied by altering the speed at which the mandrel rotates and, the rate of traverse of the carriage. Typical winding patterns used during filament winding include polar, helical, and hoop winding. These are shown in Figure 2.10 as (i), (ii) and (iii) respectively (Shen, 1995).

Once the required pattern and number of layers has been laid down with the corresponding desired winding angle on the mandrel, the impregnated fibres can be cured on the mandrel via a variety of techniques. These include, infra-red heating, electro-thermal curing, volume heating by high frequency irradiation, and conductive heating through the inside surface of the mandrel via a heated mandrel (Korotkov *et al.*,

1993, Xu *et al.,* 2014). More commonly, the filament wound preform is transferred to an oven to be cured. Once the resin is cured, the assembly is removed from the oven and allowed to cool to room temperature. The mandrel is then extracted using mechanical, hydraulic or pneumatic methods (Shotton-Gale, 2013, Wait, 2011).

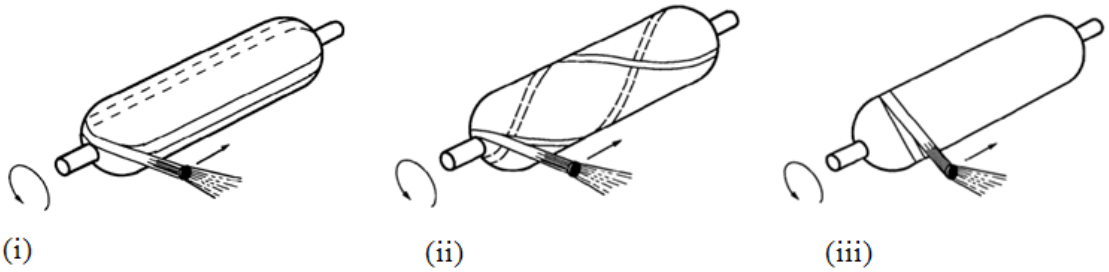

Figure 2.10 A schematic to demonstrate the three different common winding patterns: (i) Polar-winding pattern, (ii) Helical-winding Pattern; and (iii) Hoop-winding Pattern (Shen, 1995).

There are two types of mandrels in general use, permanent and removable. Permanent mandrels are used for products such as pressure vessels, where the mandrel is integral to the final structure and contributes to the strength and stiffness of the component. Removable mandrels are used to shape the filament wound part, and after the composite is cured/solidified the mandrel is extracted. In general, chrome-plated steel mandrels are used as removable devices. Other types of removable mandrels include, sand with a binder or soluble plaster that breakdown/dissolve in water, eutectic metals or salts that can be melted, inflatable elastomeric devices and segmented mandrels that can be disassembled (Munro, 1988). More recently, shape memory polymers (Everhart *et al.,* 2006) have also been used as removable mandrels.

2.3.1.1 Conventional Filament Winding: Issues

As stated previously, wet-filament winding has been used for the past six decades. The following section addresses five areas that have the potential for process improvement.

(i) **Pot-life of the pre-mixed resin system:** The resin and hardener need to be mixed manually and added to the resin bath prior to the winding commencing. In the current work the term 'resin system' is defined as the situation where the resin and hardener have been mixed. In other words, the resin system will cross-link as a function of temperature and time. Once the resin has been mixed, there is a then a limited time before the resin starts to cross-link to the point where it is no longer usable, this is referred to as the "pot life" (Pandita *et al.*, 2012). Another consideration is that ambient temperature can influence the viscosity and cross-linking rate of thermosetting resins. If the resin system that comes into contact with the processing equipment cross-links fully during manufacturing, the removal of the cross-linked resin can be a tedious, time-consuming and a costly operation (Shotton-Gale, 2013).

(ii) **Manual weighing, mixing and pouring:** Manual mixing can lead to a number of problems such as, incorrect stoichiometric ratio and the work force being exposed to emissions from the resin and hardener as they are mixed. The degassing stage of the mixed resin system is generally not carried out during the production process on site. The lack of degassing can lead to air bubbles in the resin system which can in turn result in poor impregnation of the fibres and potentially increase the void content in the composite.

(iii) **Aeration:** Aeration of the resin is also caused by the rotation of the impregnation drum in the resin bath. This can lead to the accumulation of bubbles which tend to

migrate to the surface of the resin and are subsequently picked up by fibres and transported onto the mandrel. One consequence of this is poor impregnation of the fibres and an increase in the void content (Pandita *et al*, 2012).

(iv) **Waste resin:** Due to the construction of conventional resin baths and the presence of the impregnation drum, a proportion of the resin is retained in the resin bath at the end of production. This excess resin has to be cross-linked and disposed of (Shotton-Gale *et al*., 2009). As well as the cost incurred as a consequence, there is also safety issues associated with curing large volumes of resin. Precautions need to be taken to ensure that the resin system does not exotherm. When there is a large volume of mixed resin, excessive heat can be generated during cross-linking. This can lead to an auto-acceleration of the reactions leading to the thermo-oxidative degradation (Pandita *et al.*, 2012).

(v) **Solvents:** Due to the dimensions of conventional resin baths (5-10 litres), as well as the equipment required for mixing the resin and hardener and guiding the impregnated reinforcing fibre to the mandrel, there is a large surface area that will require cleaning, at the end of production. Cleaning the equipment whilst the resin is in a liquid form is much easier and can be achieved with solvents such as acetone, isopropanol and methylethylketone. Adequate solvent recovery systems are required prior to disposal of the contaminated resin system (sludge).

The above mentioned issues have been addressed via the clean filament winding process which is described in the following section.

2.3.2 Clean Filament Winding

The clean filament winding technique was developed in the laboratory to overcome some of the afore-mentioned limitations commonly found in traditional filament winding (Shotton-Gale *et al.*, 2009). Figure 2.11 illustrates the clean filament winding process. Unlike conventional filament winding where a resin bath is used to impregnate fibres, in clean filament winding, a custom-designed resin impregnator unit is used. Initial laboratory work undertaken by Pandita, *et al.*, (2007) demonstrated that the resin and hardener could be stored separately and injected on demand, to impregnate the fibres. They showed that the volumes of waste generated and solvent usage was reduced significantly when compared with traditional wet-filament winding. They reported an 80% reduction in solvent consumption for cleaning, along with an equivalent reduction of mixed resin waste. The authors also stated that the time required for cleaning was approximately 5 minutes as opposed to 60 minutes for the conventional filament winding process (5 litre resin bath).

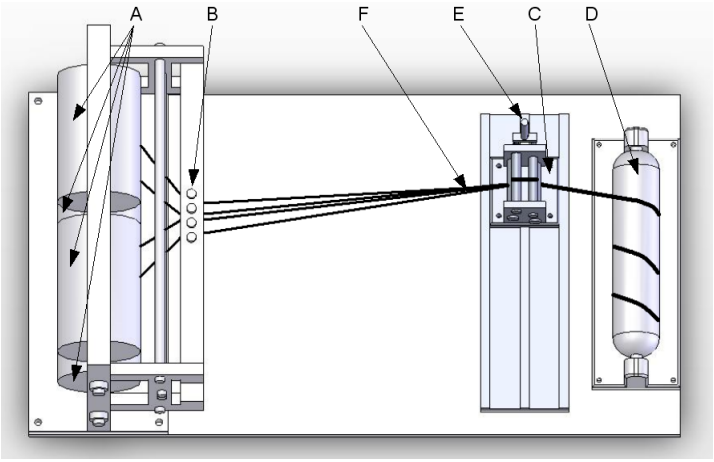

Figure 2.11 Schematic illustration of the Clean Filament Winding process; note that the resin-bath has been eliminated from the manufacturing process. The key components are coded as follows. (A) Fibre creels, (B) Fibre spreading station, (C) Traversing platform, (D) Mandrel, (E) A static mixer attached to a resin impregnator unit and (F) Fibre bundles (Pandita *et al.*, 2007).

With reference to Figure 2.11, the fibres are hauled off creels (A), then enter a series of tensioning rollers and/or fibre spreading devices (B), before being directed to a resin injection system (E) that is located on the traverse carriage (C). The fibres are impregnated by the resin impregnator unit. The impregnated fibres are then wound around a rotating mandrel (D) to obtain the required thickness with the corresponding winding-angles. The impregnator is composed of a static mixer and a custom-designed resin impregnator unit. The static mixer enables intimate mixing of the resin and hardener before it is delivered to the resin impregnator unit to impregnate the fibres as they are hauled through the resin impregnator unit.

With reference to Figure 2.12, the static mixer contains a series of helical elements which are fixed within a tubular housing. The consecutive elements are positioned opposite to each other so that the adjacent edges are perpendicular. As a consequence of this, the fluid is split every time it leaves one element and enters another. This process continues along the length of the static mixer and results in a mixed resin system at the end of the tubular housing.

Figure 2.12 A photograph showing (A) a static mixer and (B) the helical inner element (Shotton-Gale, 2013)

The details of the resin delivery system are discussed in Chapter 3. In summary in the case of epoxy/amine resin system, a custom-designed resin delivery system was used.

As mentioned previously the two components are stored separately and pumped on demand to a static mixer. This could not be completed using the polyester resin system. Therefore, a pressure-pot was used. Hence, the resin impregnator unit was designed to accommodate the static mixer or a delivery pipe from the pressure-pot unit.

The following section reports on aspects of impregnation of relevance to the current project.

2.4 IMPREGNATION

A key feature to be considered during the filament winding process is to ensure that the fibres are impregnated fully. Under-impregnation will result in dry areas that can lead to composites with lower mechanical properties (Peltonen and Järvelä, 1992 and Binetruy *et al.,* 1998).

2.4.1 Pin Impregnation

In conventional filament winding, the use of rollers and pins is a common method to ensure effective impregnation of the fibres. These devices operate by spreading the fibre bundle and thus allowing the resin to penetrate. In addition, another mechanism which contributes to the impregnation is a "squeezing action" (wedge impregnation) of the resin between the surfaces of the pin/roller and the fibres. However, the addition of pins can lead to increases in tension. During the pin impregnation process, there are many parameters that can influence the rate and degree of impregnation.

Pin impregnation was discussed by Blok, (1953) who demonstrated that a flexible impermeable tape in contact with a rotating cylinder lubricated with oil, will produce a wedged shaped region between the tape and the rotating cylinder. This is generated due to an increase in oil pressure between the tape and cylinder. This is followed by a constant oil film thickness resulting in a thin layer between the tape and cylinder. Chandler *et al.*, (1992) progressed this work by completing a study to investigate the tension generated as glass fibres were pulled over a pin located within a pool of molten polyamide-66. They divided the contact area of the fibre and pin into four regions based on the thickness of the resin film on the pin at a given time. These regions are defined and illustrated in Figure 2.13:

(i) *The entry zone.* Here the fibre approaches the pin at a given angle determined by the trajectory of the inlet/outlet bundle. As the angle between the fibre and pin decreases, there is a pressure build up on the resin film which keeps the fibre and the pin separated.

(ii) *The impregnation zone*. The pressure build-up causes the resin to be squeezed into the fibre bundle.

(iii) *The contact zone.* Once the resin has been squeezed into the fibre bundle, there is now contact between the fibre and the surface of the pin (minimal resin layer). This region contributes the greatest with regards to the increase in tension due to the friction between the pin and fibre.

(iv) *The exit zone.* This represents the zone where the fibre bundle is not in contact with the pin.

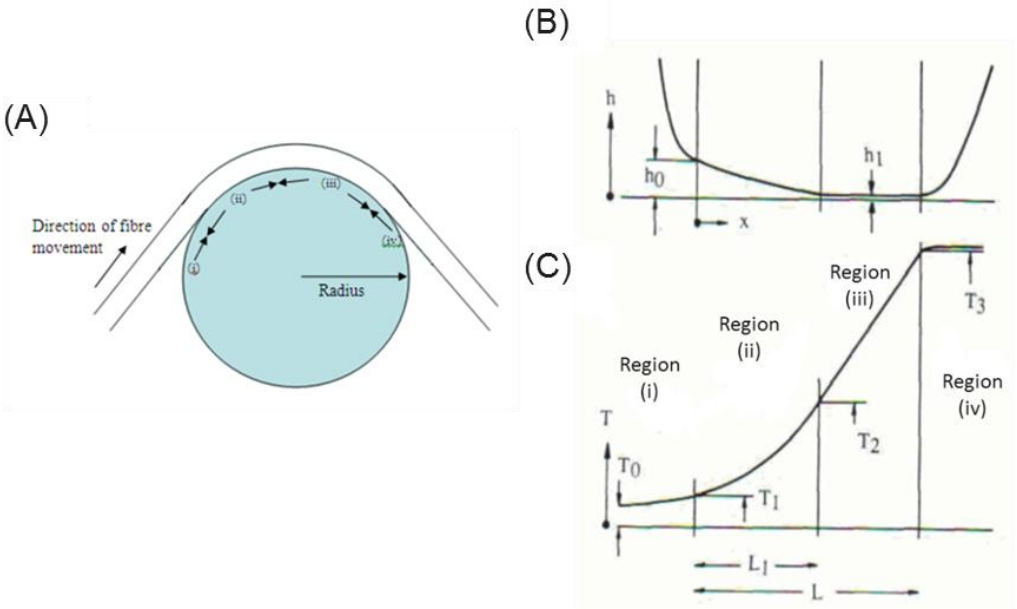

Figure 2.13 (A) A schematic of a bundle passing over a pin and the four regions of impregnation (B) A graph showing resin film thickness at these four regions and (C) A graph showing the tension build up at the four impregnation regions (Chandler *et al.,* 1992).

They concluded that the tension build up was due to viscous shear stresses in the gaps between the fibres and the pin. This observation has been supported by Ripert *et al*., (1992). They traversed a glass fibre bundle over a single pin which was in contact with silicon oil. They found the pulling force was a function of oil viscosity. At higher viscosities, the pull-force increases rapidly with the viscosity as shown in Figure 2.14.

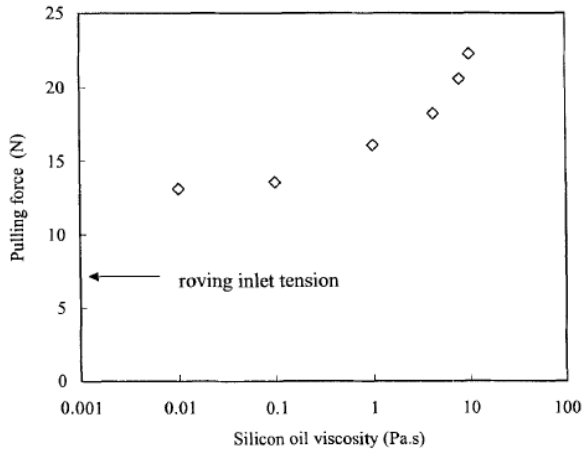

Figure 2.14 A graph showing the force required to pull a glass fibre bundle under 6.6 N of tension at a speed of 18 m/min over a single pin in silicon oil with changing viscosity (Ripert *et al.,* 1992).

Bates and Charrier (2000) also reported a similar finding when they pulled a 2400 tex glass fibre bundle through a series of pins located in a pool of polyamide-66.

Gaymans and Wevers (1998) studied the pin-assisted polypropylene (PP) melt-impregnation of glass fibre bundles during pultrusion. The impregnation rate was studied as a function of the diameter of the pin, the line-speed, the forces on the fibre, and the effect of multiple pins. The fibre tension was maintained at 7 N throughout the experiments. The pultruded rods were polished and examined. Darcy's equation (Equation 2.2 on page 52) was used to calculate the penetration, and the Kozeny-Carman equation (Equation 2.4 on page 54), was used to determine the permeability coefficient. They found that without the use of a pin, the image analysis showed that only low degrees of impregnation (~15%) were obtained. Moreover, only the outer filaments of the fibre bundle were wetted. Whereas, when pin-assisted impregnation was used, a significant increase in the impregnation was observed (~60%). The contact time of the fibre on the pin was taken to be the impregnation time. This was found to be dependent on the contact angle of the fibre with the pin, the pin diameter and line speed of the fibre.

Gayman and Wevers (1998) found Darcy's equation to fit with the first stage of the impregnation over a pin, which had a linear correlation to the square root of contact time. This however is not the case with the second stage which showed that at longer contact times impregnation began to flatten off. This lower than predicted value of impregnation was attributed to the dry contact region between the pin and fibres. Increasing the pin diameter was found by the authors to lower the impregnation rate due to the earlier onset of the dry friction. They also demonstrated that by increasing the

number of pins to five, the degree of impregnation could be increased by a factor of 3.2 as shown in Figure 2.15.

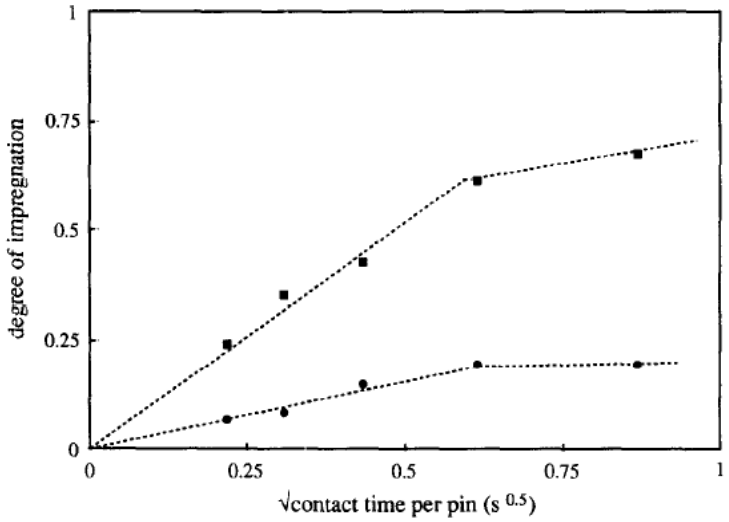

Figure 2.15 Graph showing impregnation data as a function of contact time for either one pin (circles) or five pins (squares) on a 2400 tex fibre bundle (Gayman and Wevers, 1998).

Bijsterbosch and Gaymans (1993) presented a paper on the impregnation of E-glass bundles with a polyamide-6 melt through an impregnation bath. They reported that the fibre bundles had a width of one hundred fibres and a thickness of six fibres. Fibre bundles contacted zero, one, three or five pins; in addition they also designed a convex pin to study impregnation. The authors found a clear influence of pins on the degree of impregnation. Without a pin, more than 90% of the fibres remain unwetted, even at the lower speeds (~40 µm/s); impregnation only occurred where the fibre bundle was one or two fibres thick. This was thought to be because the capillary-based impregnation (discussed in Section 2.4.4) was limited due to the high viscosity of the thermoplastic melt. The impregnation was found to improve when the fibre bundle was pulled around a pin due to the wedge-based impregnation process mentioned previously. The extent of impregnation was reported to increase dramatically when the number of pins was

increased to five. The use of the convex shaped pins to spread the fibres was shown to increase the degree of impregnation. It was calculated (assuming fibre spreading to 5 mm with two to three layers of fibres and each bundle containing 600 x 20 µm diameter fibres) that around 75% of the impregnation achieved occurred around the convex pin used in the impregnation process. This was said to be due to the faster impregnation when the fibre bundle thickness is reduced to a few filaments as a consequence of spreading. Marissen *et al.*, (2000) stated that improved impregnation could be obtained by using concave bars, whereas the use of convex bars could achieve better spreading. As such, the authors developed a device to impregnate fibres using powered rotating spreader-bars which were conical/convex in shape. This combination was thought to achieve better spreading and impregnation. Figure 2.16 shows a photograph of the impregnation device, powered by conical convex bars, as developed by Marissen *et al.*, (2000).

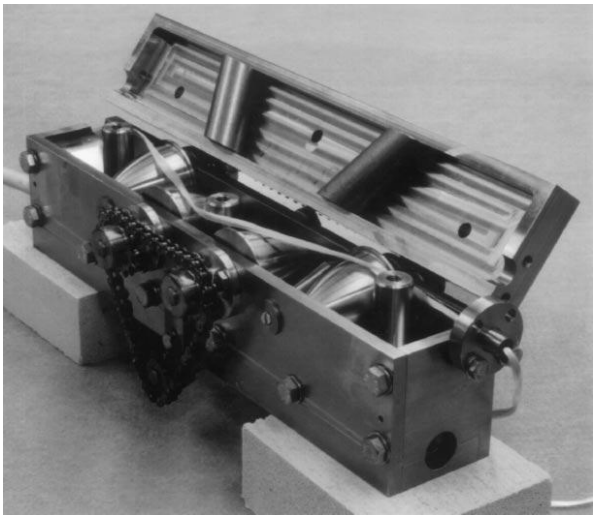

Figure 2.16 A photograph showing the impregnation device powered by conical/convex bars (Marissen *et al.*, 2000).

2.4.2 Dimensions of the Fibre Bundle

The dimensions of the fibre bundles are thought to have a significant influence on the impregnation rates that can be attained. As mentioned previously, spreading a fibre bundle decreases it's thickness and subsequently increases the impregnation according to Darcy's equation (Equation 2.2). Some of the factors that influence spreading during filament winding are: the tension applied to the fibres, the fibre tex, and the speed of winding (Irfan *et al.*, 2011). Foley and Gillespie, (2005) used a model based on Darcy's equation and found the number of fibre bundles and the diameter of the fibres could significantly affect the impregnation time. It was found that if the fibre diameter was decreased by 100 times, the capillary pressure would increase by the same magnitude and therefore, impregnation time would increase by 100 times for a given fibre bundle diameter. Figure 2.17 demonstrates the relationship where, $\propto$ is used to indicate proportional to.

$$\downarrow Fibre\ diameter \propto \uparrow capillary\ pressure \propto \uparrow Impregnation\ time$$

Figure 2.17 A schematic showing the interaction between fibre diameter, capillary pressure and impregnation time.

Bates and Charrier (2000) measured the spread width of a single 2400 tex glass fibre bundle as it was pulled over 3, 5 or 7 pins. The increase in the number of pins in contact with the fibres increases the tension due to the friction between the glass fibres and the pin. Their results are shown in Figure 2.18 where it is seen that increasing the number of pins to leads to an increase in spreading. However, this was found to be dependent upon the relative positions of the pins in their rig.

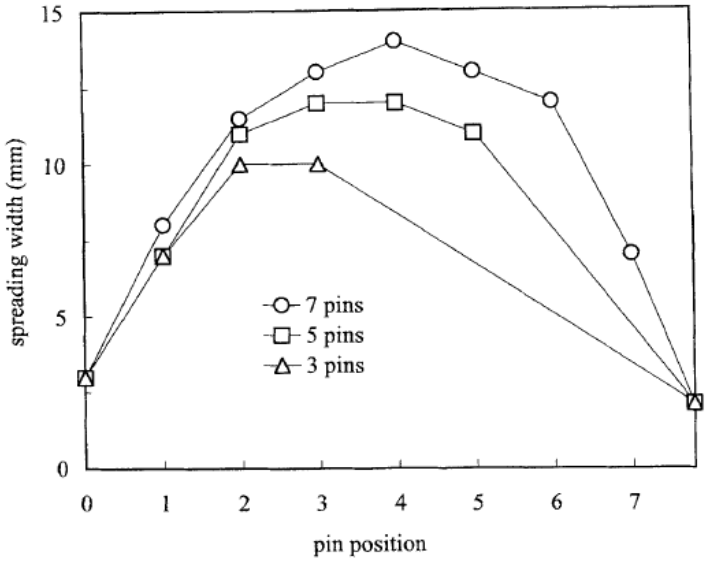

Figure 2.18 Graph showing the spreading with of a single 2400 tex glass fibre bundle as it was pulled over 3, 5 or 7 pins (Bates and Charrier, 2000).

Irfan, (2013) reanalysed the simulation presented by Pandita *et al*., (2012) to include the relationships between the impregnation time and the thickness of the fibre bundles using Darcy's equation.

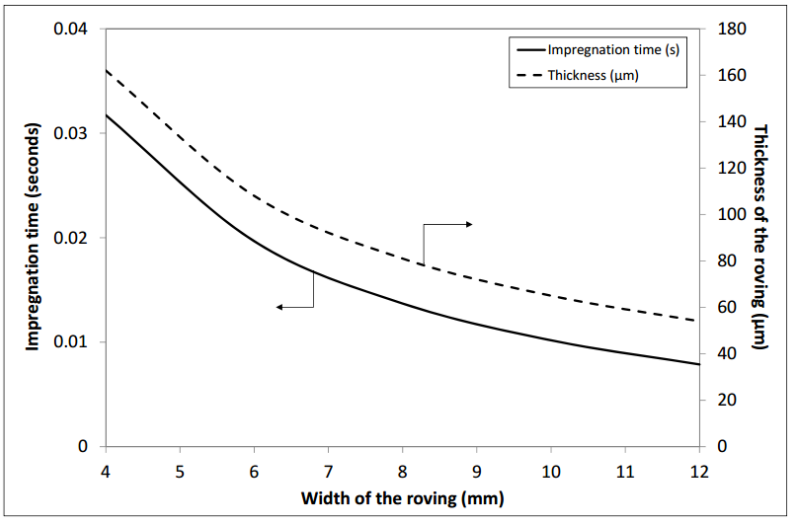

Figure 2.19 Simulation of the effect of fibre spreading on the impregnation time and fibre bundle thickness (Irfan, 2013).

On inspecting Figure 2.19, it can be seen there is a decrease in the impregnation time with a reduction in the fibre bundle thickness. However, both the authors emphasised that a balance must be made between achieving a high level of spreading to increase impregnation, and fibre damage and segmentation. Fibre damage can be detrimental effects to mechanical properties while segmentation could lead to air entrapment.

2.4.3 Fibre Tension during Filament Winding

Some factors that influence the tensioning on the fibres during filament winding include pre-set fibre tension, number of contact points, fibre trajectory, winding angle, winding speed, viscosity of liquid resin and the resin volume fraction. Winding tension is an important parameter to be controlled because it directly influences the compaction (fibre volume fraction) and the alignment of the fibres (Polini and Sorrentino, 2005). Fibre separation via spreading and disruption of the cohesion of the binder was deemed to be a prerequisite in achieving homogeneous impregnation (Henninger *et al*., 2002).

Cohen, (1997) manufactured filament wound tubes to investigate the effect of processing conditions where the fibre tension was one of the variables. The authors showed that a high winding tension of 9 lb./fibre bundle (4.1 kg per fibre bundle) produced higher fibre volumes, 56.8% , than lower tension tubes of 3 lb./fibre bundle (1.4 kg per fibre bundle) with a fibre volume of 53.2%. This was thought to be due to higher fibre compaction.

Mertiny and Ellyin, (2002) investigated the influence of winding tension on the performance of pressurised tubular components produced using filament winding. Two different fibre bundle tensions were used (24.7 and 44.5 N) during the production of ±

60° glass fibre composite tubes. It was found that the fibre volume fraction increased by 3% at the higher winding tension.

Aleong and Munro (1991) studied the effect of winding tension and cure schedule on residual stresses in thick fibre composite rings. They found there was an increase of 5.8% in the fibre volume fraction where the tension was increase from 37.2 MPa to 87.1 MPa. This increase in winding tension was said to increase the transverse tensile modulus. However, only one value was derived experimentally for an applied tension of 62.2 MPa; the other values cited were calculated. They also showed that decreasing winding tension resulted in an increase in radial residual stress, whilst increasing the tension had the opposite effect.

Bates *et al.*, (2001) found that when there were tension-induced compressive stresses caused by hanging a fibre bundle over a pin. The distribution of compressive stresses across the fibre bundle cross-section was thought to be greatest at the pin surface, decreasing to zero further away from the pin. This was said to result in a distribution of voids by squeezing the trapped air out of the fibre bundle, thus changes the permeability within the bundle.

As expected, Henninger *et al*., (2002) reported that the tension on the fibre bundles would increase with increasing winding speed. In their study, glass fibre bundles and either polypropylene (PP) or polyamide-12 (PA12) were used to produce filament wound tubes. Their results demonstrated there was an optimum tension with regard to obtaining the desired properties from the composite tubes. Above this optimum tension, there was a decrease in tensile and shear strength which was thought to be due to fibre

damage. They also showed that the degree of impregnation was ‘acceptable’ up to speeds of 15 m/min but above this fibre fracture was observed. This fibre damage was attributed to the increase in the pulling force caused by the increased winding speed. It was thought by Henninger *et al.,* (2002) that the broken filaments were no longer available for load transfer in the tensile mode, and in the case of shear loads, the broken filaments resulted in discontinuities in the shear plane thus reducing mechanical properties.

Haupert and Friedrich (1995) stated fibre bundle tension was necessary for guidance of the reinforcement on a predetermined fibre path, and that when winding glass fibres, recommended minimising the tension, so that the magnitude of the residual stresses introduced in the rings are lower. The authors did recognise the need for increasing compaction pressure as they believed this would allow better matrix flow through the fibres and give a lower void content. However, a higher consolidation force was thought to damage the fibres and cause squeezing of the molten polymer out of the ring rather than aid impregnation.

Chen and Chiao (1996) modelled fibre consolidation using undulating channel systems and found that winding tension had an effect on the fibre consolidation. They showed that a lower winding tension and closer fibre packing within a fibre layer resulted in an increase in the consolidation time.

2.4.4 Viscosity of Resin

Viscosity of the resin matrix has a significant effect on the rate of impregnation of fibre bundles. This can be seen when increasing or decreasing the value of viscosity in

Darcy's equation (Equation 2.2). Ahmadi *et al.*, (2000) showed that by elevating the matrix temperature from 190 to 240 °C and thus decreasing the viscosity of the molten polypropylene, there was a resulting 16% increase in the impregnation rate. Pandita *et al.*, (2012) adapted an equation proposed by Foley and Gillespie, (2005), which is shown in Figure 2.20, to demonstrate how decreasing the viscosity of the resin reduces the impregnation time of a stationary fibre bundle.

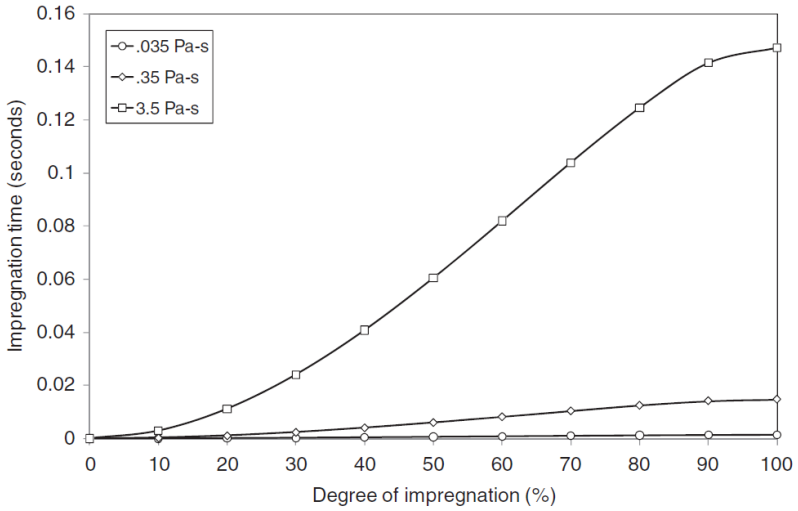

Figure 2.20 A graph showing the effect of resin viscosity on the time and degree of impregnation. Here the width of the bundle was 8 mm and tension in the bundle was 10 N (Pandita *et al.,* 2012).

2.4.5 Permeability

The following section is a review of studies and models focusing on fibre impregnation. This information was used subsequently in the experimental chapter to aid with the design of a new clean filament winding resin impregnator unit.

Contemporary literature begins with Darcy's equation shown in Equation 2.2 (Shotton-Gale *et al.,* 2009), which explores fibre permeability within the impregnation process. Previous literature (Chen and Chiao, 1996) has described Darcy's equation as being inadequate in the simulation of resin flow because the difficulty of modifying position

dependant permeability and porosity along with the varying fibre bed structure. Instead, they simulated the fibre/resin system using an asymptotic analysis with lubrication theory in their study of the motion of continuous fibres through a Newtonian resin.

Darcy's equation describes the flow of Newtonian fluid through a porous medium. There are four key components to Darcy's equation: permeability, dimensions of the reinforcement, viscosity and pressure.

$$v = \frac{K}{\mu \phi} \frac{\Delta P}{L} \qquad \textbf{Equation 2.2}$$

Where:

v is the superficial velocity (m/s);

K is the permeability of the porous medium (mm^2);

ϕ is the porosity (%);

μ is the viscosity of the fluid (Pa.s); and

$\Delta P/L$ is the pressure gradient (Pa) over a characteristic dimension L (mm).

With reference to Equation 2.2, the first term considered is permeability (K). Permeability can be divided into two components: axial, in which the fluid flows in the direction parallel to the fibres and, transverse (through-thickness), in which the fluid flows perpendicular to the direction of the fibres. Figure 2.21 shows the terminology used to describe the directions of impregnation in a fibre bundle.

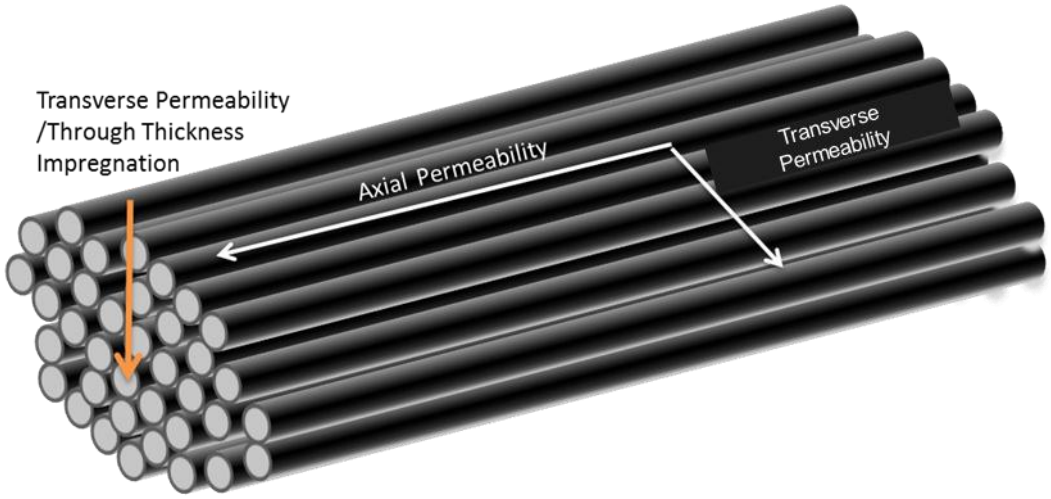

Figure 2.21 A schematic showing the terminology used to describe directions of impregnation of a resin into a fibre bundle.

During a study by Gebart (1992) into predicting resin flow in resin transfer moulding, they introduced a friction factor or resistance co-efficient, λ, to predict the axial permeability of a fibre bundle. Frictional factors are used to describe the flow characteristics of the laminar flow through the channels and ducts (space between the fibres in a bundle) in the fibre bundle. Equation 2.3 is used to calculate the friction factor which in turn is used to derive the permeability.

$$\lambda = \frac{\Delta P}{L}\frac{2D_h}{\rho v^2}$$

Equation 2.3

Where:

$\Delta P/L$ is the pressure gradient (Pa/mm);

D_h is hydraulic diameter (mm) (duct cross-sectional area divided by the impregnated perimeter);

ρ is the density of the fluid (kg/m^3); and

v is mean resin velocity (m/s) over the fibre cross-section (m^2).

The Kozeny-Carmen equation shown in Equation 2.4 was further utilised by Shotton-Gale *et al*., (2009) and was used to relate the permeability of a fibre bundle to the void fraction V_f, characteristic fibre radius r_f and a combined parameter called the Kozeny constant:

$$K = \frac{{r_f}^2}{c} \frac{(1 - V_f)^3}{{V_f}^2}$$

Equation 2.4

Where:

V_f is the void fraction (%);

r_f is the characteristic fibre radius (mm); and

c is equal to either 57 or 53 for quadratic or hexagonal arrays of fibres.

Values of the Kozeny constant are different for flows parallel and transverse to the fibres during impregnation. Bates *et al.*, (2002) studied the compaction and traverse permeability of glass fibre bundles. They found that the flow of silicon oils through the glass fibre bundles could be modelled using Darcy's equation.

Bayramli and Powell (1991) measured axial impregnation via capillary action of silicon oil and epoxy resin into a carbon fibre bundle. They showed the kinetics of axial impregnation followed the following relationship:

$$h \propto At^{1/2}$$

Equation 2.5

In Equation 2.5, h is the average displacement (mm) of the advancing flow front, t is the time (s) of impregnation and A is a constant that depends on the detailed pore geometry as shown in Equation 2.6:

$$A = A'\left(\frac{\gamma cos\theta}{\mu}\right)^{\frac{1}{2}}$$

Equation 2.6

Where:

A' is a constant which depends on the geometry of the medium;

γ is the surface tension (N/m);

θ is the apparent contact angle of the contact line on the solid wall; and

μ is the viscosity (Pa.s).

The findings from their study showed that the impregnation rates were higher than those predicted by theoretical models based upon single geometries. This was attributed to the heterogeneity of pore sizes in the fibre bundles. Bayramli and Powell (1991) also found that theoretically, the axial impregnation could be between 10 and 100 times faster than transverse (perpendicular to the fibre direction) impregnation in carbon fibre bundles.

Amico and Lekakou (2002) used a similar method to study the axial impregnation of an E-glass fibre bundle. They used single fibre bundles with one end attached to a weight

and the other to a support connected to an analytical weighing balance. The end with the attached weight was hung in either a silicon oil or epoxy resin. Impregnation was observed visually and the mass increase was recorded over time and plotted. They used this information to determine the capillary pressure, Pc, and permeability. The equation (Equation 2.7) used to calculate capillary pressure using visual data measuring the height of the liquid level in the fibre bundle was:

$$Pc = \rho g\left(\frac{a_h}{b_h}\right)$$

Equation 2.7

Where:

ρ is the liquid density (kg/m^3);

g is the gravitational acceleration (m/s^2);

a_h is the straight line slope of velocity of the rising liquid front against 1/height; and

b_h is the intercept.

Equation 2.8 that was used to calculate capillary pressure using the mass-gained that was measured during the experiment.

$$Pc = \frac{\mu\phi}{K\rho^2}\left(\frac{a_w}{A_{TV}^2}\right)$$

Equation 2.8

Where:

μ is the viscosity of the liquid (Pa.s);

ρ is the liquid density (kg/m^3);

ϕ is the porosity of the fibre bundle (%);

K is the permeability;

a_w is the slope; and

A_{TV} is the total pore area in the fibre bundle.

Most of the impregnation experiments carried out by Amico and Lekakou (2002) were completed using epoxy resin but without the hardener to minimise the effect of viscosity changes due to curing during the experiment. They found that the long-term capillary experiment lasting 23 days using an epoxy resin without the hardener yielded a capillary pressure value of 9600 Pa. They concluded that this was comparable to the theoretically predicted value of 10,290 Pa. However, experiments conducted for two hours did not match with the theoretical results for capillary pressure and permeability. Zhu *et al.*, (2004) repeated the experiment developed by Amico and Lekakou (2002) and also showed that the experimental data gathered for short-term capillary experiments did not fit the theoretical model. This was thought to be due to the effect of gravity which was not taken into account in the short-term experiments. However, the data obtained from experiments carried out for seven days correlated with the curves that were produced from the theoretical model. In this instance the effect of gravity was accounted for in the model.

2.5 SUMMARY

It is acknowledged that the production of the constituent materials (fibres and resin systems) and the manufacturing processes associated with the fabrication of composites (high-volume and high-performance) is well developed. However, there are differences in the constituent materials supplied by different manufacturers. An area of interest in the current work is the variation in the binder system that is applied to the fibres at the production stage. The literature review has established that the binder can have a significant effect on the performance of the composite. However, it is also apparent from the literature that the composition of the binder is proprietary information. This makes it difficult to reach definitive conclusions about the presence/absence of the binder on the surface properties of the fibre, the interphase and the composite. The review has revealed that standardised procedures are not used to remove the binder and common protocols are not applied universally for the reapplication of appropriate coupling agents. It is also apparent from the literature that it may not be appropriate for conclusions drawn in the laboratory to be applicable for processes such as the application of binders at the production stage. There is a significant volume of literature on the effect of the coupling agent on the mechanical properties of composites. However, little work has been reported on the relative distribution of the binder within the creel (bore, middle and surface regions) and their effect on the rate of impregnation.

A brief review was carried out to summarise the general properties of the two resin systems used within this study (epoxy and polyester). The importance of the resin viscosity, surface tension and contact angle was discussed in the context of

impregnation. Some of the key models with regard to impregnation were discussed and the information gained was applied subsequently in the design of the resin impregnator.

The degree of impregnation can be modelled using several well documented theories. There is a wide range of variables which can contribute towards the impregnation occurring within the fibre bundles. These issues need to be considered carefully to avoid wrong conclusions being reached about the impregnation mechanisms and efficiency. A few studies have therefore tried to demonstrate experimental techniques used to measure the rate of impregnation with some success. However, there are limitations in the experimental techniques discussed in this review with only few of them being applicable to composite production in an industrial environment.

Filament winding is a well-established technique and it has been reviewed extensively in the literature with a focus on conventional filament winding. Considerable attention has been paid to parameters such as tension, viscosity, winding speed and winding angle, and the mechanical properties. However, little attention has been paid to the effect of these parameters to the void content. Moreover, there are some major concerns associated with conventional filament winding. For example: (i) the need for a copious volume of solvent to clean every component that the impregnated fibres come into contact with the production equipment; (ii) the need for excess resin in the resin bath has to be transferred to a container and cross-linked; and (iii) the limited options that are available to influence the impregnation process.

The information reviewed in the literature along with the issues identified with conventional filament winding was used in the development of the clean filament winding process. Prior work in this area has been limited to the author's research

group. However, this has been limited predominantly to laboratory trials. These authors have shown that clean filament winding has environmental benefits when compared to conventional filament winding. The current work reported here represents the first full-scale implementation of clean filament winding in an industrial environment.

3. EXPERIMENTAL

The experimental chapter is divided into two sections. The first section details the processes and procedures used to manufacture and evaluate E-glass filament wound tubes. The filament wound tubes were manufactured using the conventional and clean filament winding processes at an industrial site. The second section characterises E-glass fibres supplied by two manufacturers where the focus was on their respective binder concentrations and impregnation characteristics. These fibres were used during the industrial filament winding trials.

3.1 FILAMENT WINDING

3.1.1 Materials

3.1.1.1 Reinforcing Fibres

The fibre reinforcement used to produce the filament wound tubes was 2400 tex E-glass fibres with a binder containing a silane coupling agent. E-glass fibres of the same tex were acquired from two different manufactures and were coded as Type-I and Type-II. Type-I fibres were used to produce conventionally wound tubes and this was the fibre type used by the industrial partner. Type-II fibres were supplied by another project partner and these were used to produce clean filament wound tubes. Both fibre types were designed for filament winding and were epoxy and polyester compatible. The mechanical properties of the fibres and their composites reported by the manufactures are shown in Table 3.1.

Test Procedure		Resin Matrix	Fibre Type-I	Fibre Type-II
Impregnated Strand Tensile Test (ASTM 2343)	Tensile Strength (ksi/MPa)	Epoxy (Anhydide/DER 331)	390/2710	405/2790 57.9% glass fibre content by weight Resin not specified
		Polyester F201	415/2860	-
Interlaminar Shear Strength (ASTM D2344)	Horizontal Shear Dry (ksi/MPa)	Epoxy (Anhydide)	63 MPa	10.4/71.7
		Polyester	62.8 MPa	9.96/68.7
	Horizontal Shear Wet (ksi/MPa)	Epoxy (Anhydide)	-	10.2/70.3**
		Polyester	-	8.79/60.6**
	Strength Retention	Epoxy (Anhydide)	94%*	72.6%
		Polyester	83 %*	72.2%

*72-hour boil conditioning **6-hour water boil conditioning

Table 3.1 A comparison of the mechanical properties of Type-I and Type-II E-glass fibres as reported by the manufactures.

3.1.1.2 Resin Systems

Two resin systems were used in the filament winding trails: epoxy; and polyester. The epoxy resin used in this study was an LY3505 epoxy and the hardener was XB3403 (Huntsman Advanced Materials, UK). This recommended mix ratio for epoxy resin and hardener was 100:35 respectively. In subsequent sections, the term epoxy is used to describe the cured state. The cure schedule for the epoxy resin system was 80 °C for 6 hours (Huntsman Advanced Materials, UK). The polyester resin was Crystic 397PA (Scott Bader, UK). This was a pre-accelerated, isophthalic/neopentyl glycol polyester resin. 2 ml of grey or blue Crystic Pigment Paste (Scott Bader, UK) was added to every 1 kg of the Crystic 397PA. An antifoaming agent (unspecified) was also added with an

inhibitor. The mix ratio for the anti-foaming agent was 1 ml per kg of Crystic 397PA. Finally, 8 ml per kg of hardener was added and the constituents were manually mixed. The polyester formulation described was cured in an air-circulated oven at 80 °C for 3 hours (Scott Bader, UK).

3.1.2 Conventional Filament Winding

A schematic of the conventional filament winding process used for the industrial site trials is shown in Figure 3.1. The process was previously described in Chapter 2. This section describes the key components of the conventional filament winding machine used during the site trial in detail.

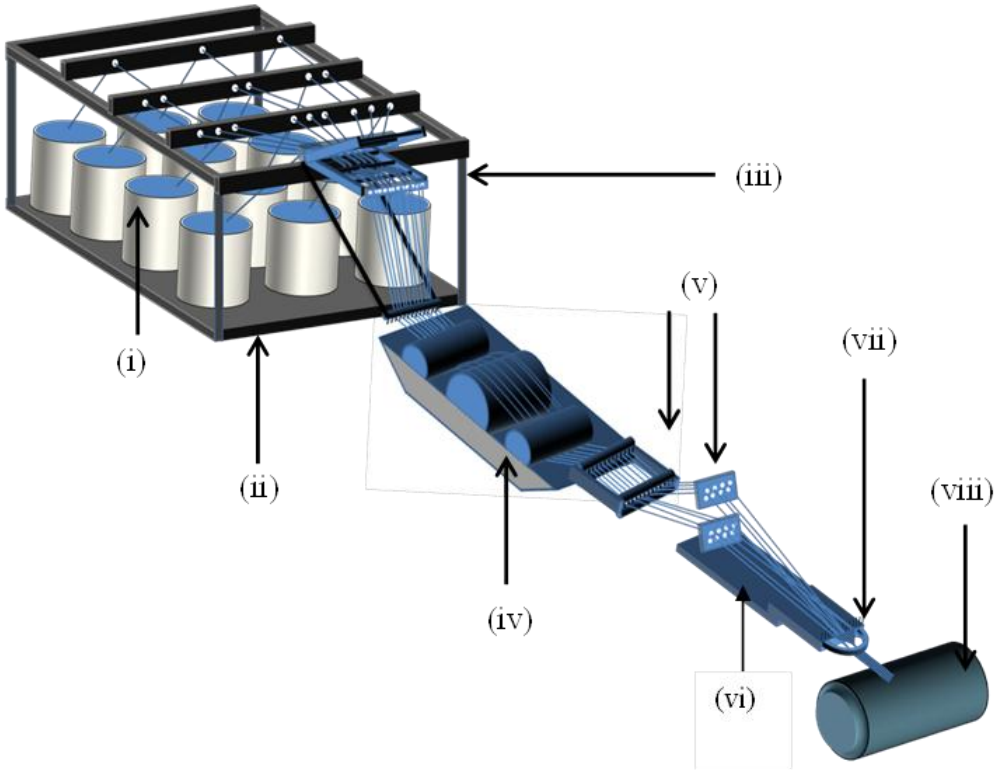

Figure 3.1 A schematic illustration of specified section of the conventional filament winding process used to manufacture the conventional filament wound tubes. The key items labelled are (i) Centre-pull creels of glass fibres, (ii) Creel stand, (iii) Pre-tension device, (iv) Resin bath, (v) Guide pins, (vi) Traversing platform, (vii) Guide pins and D-eye and (viii) Rotating mandrel.

Figure 3.2 shows photographs of the key components used in the conventional filament winding process. Details of each item are described in the text below.

(i) *Pre-tension:* Figure 3.2 (i) shows the pre-tensioning device. The fibre bundles are directed into the back of the pre-tensioning device through an acetal guide plate. The top-arm of the pre-tensioning device can be lowered and raised, as required, to adjust the extent of contact between the fibre bundles and the metal pins. In this manner, the desired tension is imposed on the fibre bundles.

(ii) *Conventional Resin Bath:* Figure 3.2 (ii) shows the resin bath system used for the conventional filament winding trials. Within the resin bath there are three rollers: the impregnation drum and two acetal rollers (black rollers seen in Figure 3.2 (ii)). The fibres are directed under the 1st black roller, over the top of the impregnation drum, and then under the 2nd black roller. Due to the friction between the fibres and the surface of the impregnation drum, a frictional force is generated resulting in the rotation of the drum. The rotation of the impregnation drum causes it to pick up resin from the filled resin bath. A doctor blade is used to remove excess resin from the drum, leaving a thin layer of resin on the surface (the position of the doctor blade is set manually). As the fibres are traversed over the surface of the drum, they become partially impregnated with resin as a result of pin impregnation as described in Chapter 2.

(iii) *Traversing Platform:* Figure 3.2 (iii) shows the traversing platform where the fibres are passed through a set of guide plates and pins. The traversing platform

reciprocates along the mandrel at a specified rate depending on the wind-angle required.

(iv) *D-eye:* Figure 3.2 (iv) shows the D-eye where the impregnated fibres converge into a ribbon. This ribbon, without gaps between the fibre bundles, is wound around the rotating mandrel.

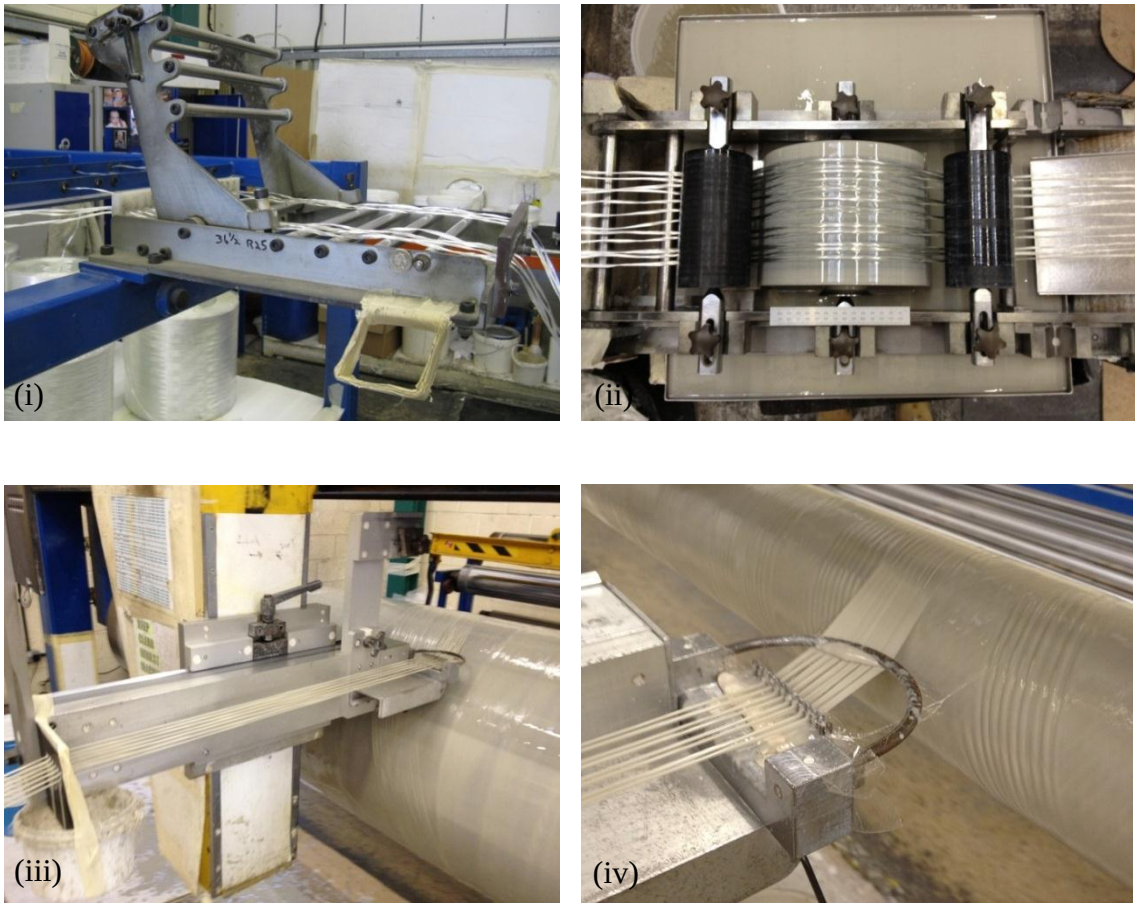

Figure 3.2 Photographs showing: (i) Pre-tension device; (ii) Resin bath; (iii) Traversing platform; and (iv) D-eye.

The filament winding machine used during the industrial site trial was used to manufacture composite tubes that ranged from 2 inches (50.8 mm) to 26 inches (660.4 mm). Depending on the size of the tube produced the operating conditions were varied

to achieve maximum impregnation at the highest production speed. The winding speed used as mentioned varied on the tubes being produced. For the tubes wound in this study (4.5 inch mandrel) the industrial winding speeds were 21 m/min. Winding speeds were maximum for 10 inch mandrels at 52 m/min. 52 m/min is the maximum speed of this machine with increases above this resulting in resin flicking off the mandrel as it rotates. The industrial filament winding machine was capable of winding up to 12 fibre bundles. This again was dependant on the tube diameter or if two smaller tubes are wound at once. The filament winding machine was also capable of winding both hoop and helical winding (< 45 degrees). However helical winding was limited due to a fixed location D-eye.

3.1.2.1. Conventional Filament Winding: Optimising Winding Tension

Eight fibre bundles were used to manufacture a set of four tubes to investigate the optimum tension required for the filament winding trials. Four specified fibre winding tensions were used: 5; 10; 15; and 18 kg. The required tension was achieved by lowering the upper arm of the pre-tensioning device (see Figure 3.2 (i)) by one level each time. At each setting, the tension was measured six times using a tensometer (RSFG-5000, RS Force Measurement Indicator). The tubes produced using polyester resin were hoop wound at 7 m/min onto a steel mandrel with an outer diameter of 106 mm and 3 m long. The details of the tubes manufactured, as a function of applied tension, are summarised in Table 3.2.

Winding	Resin System	Fibre (Type-I)	No. of Layers	Mandrel Diameter (mm)	Winding Speed (m/min)	Winding Angle	Fibre Tension (kg)
Conventional Filament Winding	CRYSTIC 397 PA Polyester	8 x 2400 tex	4	106	7	Hoop	5
Conventional Filament Winding	CRYSTIC 397 PA Polyester	8 x 2400 tex	4	106	7	Hoop	10
Conventional Filament Winding	CRYSTIC 397 PA Polyester	8 x 2400 tex	4	106	7	Hoop	15
Conventional Filament Winding	CRYSTIC 397 PA Polyester	8 x 2400 tex	4	106	7	Hoop	18

Table 3.2 The tubes produced during the winding tension trials where the effect of the applied tension was investigated.

The density, fibre volume fraction, void content and hoop tensile strengths were determined using the relevant test methods detailed in Section 3.1.6.

The criteria used to define the optimum tension were as follows:

(i) To enable the formation of a coherent and consistent ribbon at the D-eye.

(ii) To produce filament wound tubes with the visually observed 'best' combination of fibre compaction and degree of impregnation.

(iii) To obtain the 'best' mechanical properties as determined by hoop tensile strength.

(iv) To minimise fibre damage as assessed visually.

As will be discussed in Section 4.1, a tension of 15 kg was deemed to fulfil the above mentioned criteria. Thus, a tension of 15 kg was used for manufacturing the subsequent tubes in this study.

3.1.2.2. Conventional Filament Winding: Winding Speed

Following the experiments to determine the optimal winding tension, four tubes were manufactured using conventional winding. These tubes served as the benchmark and will be referred to as the reference tubes from here on. A summary of tubes manufactured is presented in Table 3.3. Two tubes each were manufactured using the epoxy or polyester resin systems. Two winding speeds were used for both resin types: 7 and 21 m/min linear haul-off. Eight 2400 tex E-glass fibre bundles were used to produce four-layer hoop wound tubes.

Winding	Resin System	Fibre (Type-I)	No. of Layers	Mandrel Diameter (mm)	Winding Speed (m/min)	Winding Angle	Fibre Tension (kg)
Conventional Filament Winding	LY3505/XB3403 epoxy/amine	8 x 2400 tex	4	106	7	Hoop	15
Conventional Filament Winding	LY3505/XB3403 epoxy/amine	8 x 2400 tex	4	106	21	Hoop	15
Conventional Filament Winding	CRYSTIC 397 PA Polyester	8 x 2400 tex	4	106	7	Hoop	15
Conventional Filament Winding	CRYSTIC 397 PA Polyester	8 x 2400 tex	4	106	21	Hoop	15

Table 3.3 Summary of the coding, resin system, reinforcement, ply thickness, mandrel diameter, winding speed and angle for the tubes produced via conventional filament winding.

3.1.3. Clean Filament Winding

As described in the Chapter 2, in the clean filament winding process, the resin bath and impregnation drum used in conventional winding are replaced with a resin impregnator unit that spreads and impregnates the fibres. The options considered for the location of

the resin impregnator unit was to retrofit it on the resin bath or the traversing platform. The latter option was chosen because it avoided the prospect of the impregnated fibres dripping resin between the resin impregnator unit and the traversing platform. However, the distance that the impregnated fibres travel before reaching the rotating mandrel is reduced significantly. Therefore, it was necessary to ensure efficient impregnation with in this shorter distance. Furthermore, as will be seen in Chapter 4, the number of contact point between the partially impregnated fibre bundles and the processing equipment is also reduced in the clean filament winding technique.

As discussed previously, the methods of resin delivery used in the clean filament winding process ensures that the correct stoichiometric ratios of resin and hardener are delivered to the impregnator unit on demand. The reasons for the difference in required dispenser was also mentioned previously. Figure 3.3 (i) is a photograph of the resin dispenser used to deliver the epoxy resin (LY3505) and hardener (XB4303) to the injector head. The rate of resin delivery can be adjusted via the manual controls on the machine which can calculate the ratios required for a given filament winding speed. Figure 3.3 (ii) shows the pressure-pot equipment used to deliver the pre-mixed polyester resin system to the injector head. The pressure-pot can also be controlled via the manual controls on the machine and again can be set to dispense the required quantity of resin required for different winding speeds (calculation estimates volume resin required for 100% impregnation).

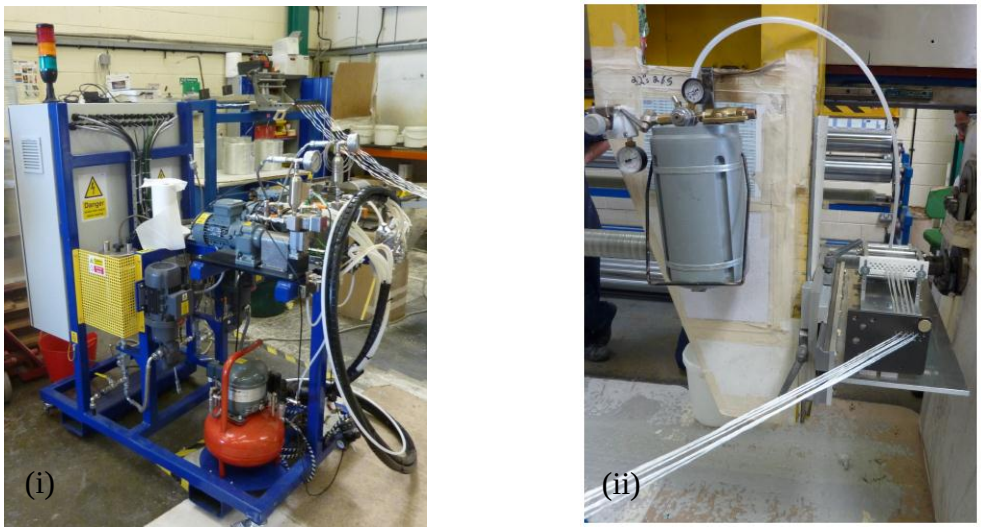

Figure 3.3 Photographs showing: (i) the resin dispenser unit used for epoxy resin; and (ii) the pressure-pot used for the delivery of the polyester system.

The following section outlines the design criteria used in the design and development of resin impregnators Prototypes-1 and 2 for clean filament winding.

3.1.3.1 Clean Filament Winding: Design Criteria

The following section outlines the design criteria for clean filament winding. Calculations used to validate the designs are shown in Appendix A. The design criterion was further developed after the analysis of tubes produced with Prototype-1 during site trials in designing Prototype-2. The criteria were as follows:

(i) **Retrofitting** – The clean filament winding prototype impregnators must be able to be retrofitted onto the existing conventional filament winding machine without any significant alteration to the existing machinery.

(ii) **Assembly and Disassembly** - The introduction of the clean filament winding prototype impregnators to the industrial machine must be completed with ease and in a time scale which is less or equal to the conventional winding set up (10 minutes). In addition to this, it was also important to consider the ease with which the prototype could be removed, dismantled, and cleaned. *During Prototype-1 trials it was found that this was not achieved to the level required within industry and therefore was addressed in the design of Prototype-2.*

(iii) **Reduce waste resin** – By impregnating the fibres as close to the mandrel as possible, there is the potential to reduce resin drippage. The impregnation methods used in clean filament winding negate the use of a resin bath and therefore the waste associated with the remaining resin left in the bath (~2.5 litres) after production; this also reduces cross-linking occurring in regions where there is less resin flow (i.e. the corners of the resin bath).

(iv) **Multiple resin systems** - The clean filament winding prototype rig design had to be capable of winding tubes with comparable properties to conventional wound tubes for epoxy and polyester resin systems. The industrial manufacturer involved in this project used epoxy and polyester resins to produce composite tubes. Therefore, it was deemed necessary that the clean filament winding resin impregnator unit match these processing requirements.

(v) **High winding speeds** - The clean filament winding prototype impregnator had to be able to produce composite tubes with comparable properties to conventionally wound tubes when winding at speeds up to 21 m/min. Previous site trials involving

clean filament winding have only wound at speeds of 7 m/min in an industrial setting. 21 m/min is the speed used for the majority of tubes wound by the manufacture involved in this study**.**

(vi) **Impregnation efficiency** - The resin impregnator unit had to deliver a mixed resin system evenly to every fibre bundle in the winding process. Each and every fibre bundle must receive a uniform and consistent quantity of resin to enable a uniform degree of impregnation. Uneven impregnation levels could result in inconsistencies in physical and mechanical properties of the final composite. Key impregnation parameters, considered when designing the prototypes were: (i) resin viscosity, (ii) porosity of the fibre bundle, (iii) resin injection pressure, (iv) fibre tension, and (v) the fibre architecture within the fibre bundle**.** *For Prototype-2 the contact/manipulation points were increased to assist impregnation for higher winding speeds.*

(vii) **Fibre Spreading** - The use of a spreading station to increase the width of the fibre bundle, with a subsequent reduction in the fibre bundle thickness, was incorporated into both designs. This facilitates the breaking up of the binder and enhances the transverse impregnation of the mixed resin system through the fibre bundle.

(viii) **Ribbon formation at D-eye** – It was considered important to ensure that a D-eye was used that sufficiently brought the fibre bundles into a ribbon of fibre. This meant that after the fibres were spread to increase the impregnation rate, they then converged together to form a ribbon at the D-eye before moving onto the mandrel.

This ensured there were no fibreless areas in the first layer of fibres wound onto the mandrel.

(ix) **Reduced fibre damage** – Both prototypes were designed to ensure that the fibre path through the resin impregnator unit did not result in any filament fractures or micro flaws, as this could reduce the strength of the composite tube. This was achieved by reducing the amount of sharp angles and edges the fibres pass through prior to the addition of the resin.

From the criteria mentioned above, Prototypes-1 and 2 were designed, produced, and used in clean filament winding trials at the industrial filament winding site.

3.1.3.2 Clean Filament Winding: Winding Trails

The next section describes each prototype, how it was mounted to the industrial winding machine, the key features of each prototype, and the set up for each of the tubes produced.

3.1.3.2.1 Prototype-1

A schematic illustration of Prototype-1 is shown in Figure 3.4 (B) and the manufactured device is shown in Figure 3.4 (A) where the key components have been labelled and are described in the subsequent section. Prototype-1 was both designed and manufactured at the University of Birmingham.

(A)

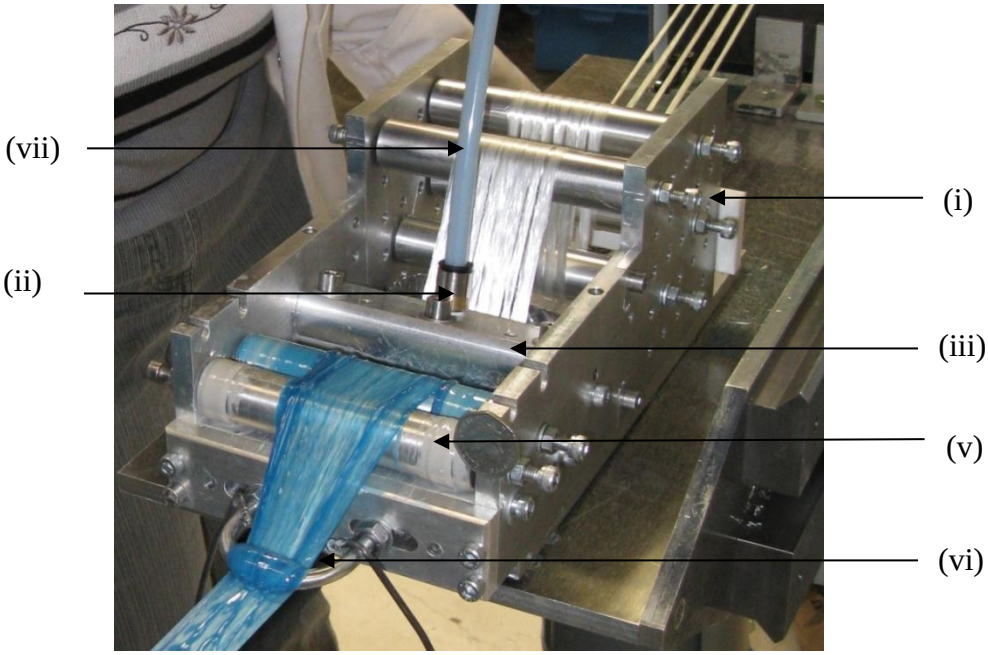

(B)

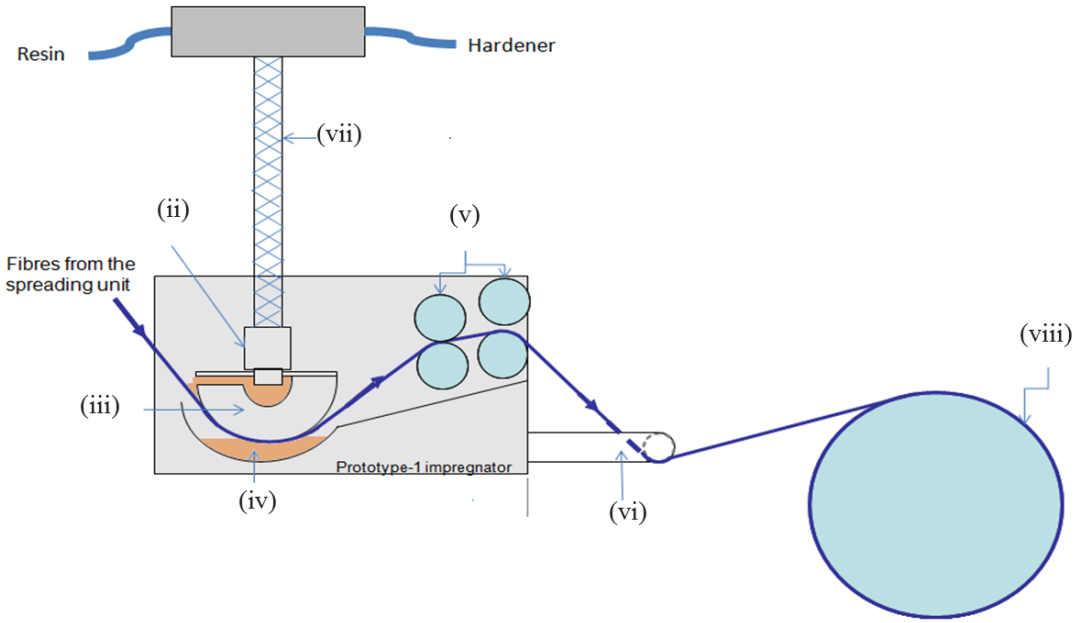

Figure 3.4 (A) A photograph of the Prototype-1 and (B) a schematic of the manufacture d Prototype-1 with the key components labelled: (i) configurable spreading station, (ii) Resin injector housing, (iii) Curtain flow injector, (iv) Miniature resin reservoir, (v) Manipulation pins, (vi) D-eye, (vii) Static mixer/pressure-pot pipe and (viii) Mandrel.

(i) **Configurable spreading station:** The spreading station was used to increase the spreading of up to eight 2400 tex E- glass fibre bundles.

(ii) **Resin injector housing:** This was designed to allow the static mixer to be directly attached to supply resin to the fibres and miniature reservoir. This allowed the resin injector to be more adjustable and fibres could be plunged into the reservoir to the required height. The resin injector housing was developed: (a) to minimise the dead-volume of resin and (b) to make sure that the fibre bundle did touch the surface of the metal.

(iii) **Curtain flow injector:** Resin was pumped into the resin impregnator unit where it then filled up a cavity, within the head. Once this cavity was filled, the resin then flowed along the gap and over the edge of the curved face. This then flowed down the curved section until contact is made with the fibres. Figure 3.5 shows how the curtain flow produces a wedge region between the fibres and the Prototype-1 resin impregnator unit. This was again designed to minimise the dead volume. The angle of the injector could also be adjusted to serve as a direct injector (as opposed to curtain flow).

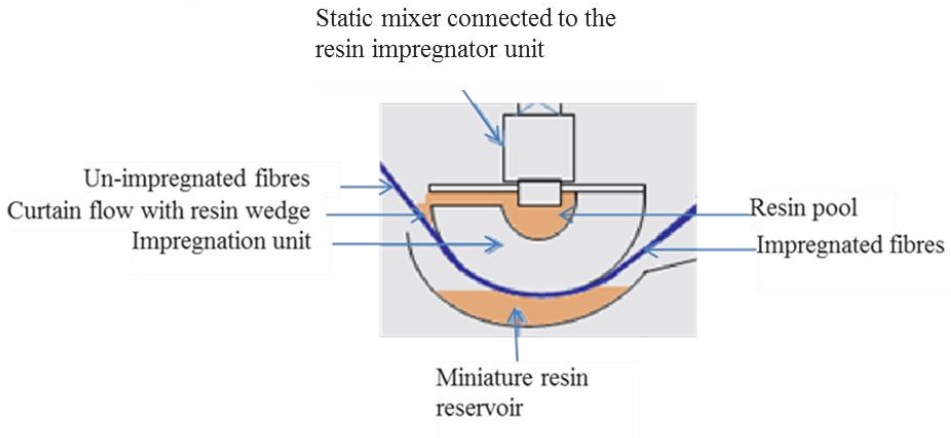

Figure 3.5 A schematic showing how the curtain flow produces a wedge of resin in impregnator Prototype-1.

(iv) **Miniature resin reservoir:** This captures excess resin removed at the manipulation pins and also aids with capillary impregnation at the underside of the fibres increasing the overall degree of impregnation. Figure 3.5 shows the miniature resin reservoir and how it was used to accumulate excess resin. This was designed to capture waste resin which was removed by the rollers. The excess resin then flows back down the angled platform to enable the back surface of the fibre bundles to be impregnated.

(v) **Manipulation pins/rollers:** These could be adjusted to serve as pins or rollers in order to aid the manipulation of resin into the fibre bundles via the force generated by the fibres tension/friction against the pin surface. This subsequently squeezes the resin through the thickness of the fibre bundle.

(vi) **D-eye:** This was a 45 mm D-eye which was used to converge the fibres bundles into a ribbon. The ribbon was then wound onto the rotating mandrel.

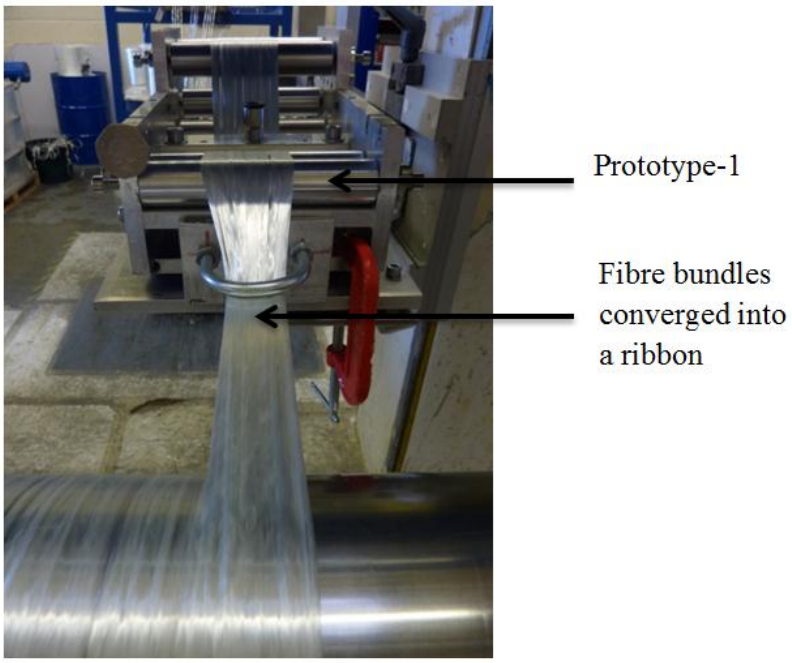

Figure 3.6 A photograph showing how the D-eye of Prototype-1 converged the fibre bundles and optimised (without segmentation or gaps) the placement of the ribbon onto the mandrel.

As can be seen in Figure 3.6, the resin impregnator unit is mounted on the traversing platform of the industrial filament winding machine thus bringing the resin impregnator unit into closer proximity to the mandrel.

Three tubes were produced using Prototype-1. One tube was manufactured using epoxy resin at 7 m/min and two tubes were manufactured using polyester resin at 7 and 21 m/min. For all the tubes produced, a 106 mm outer diameter mandrel was used which required eight x 2400 tex E-glass fibre bundles. Each tube was hoop wound and was four layers thick. The details of the tubes and parameters used to produce them using Prototype-1 are summarised in Table 3.4.

Winding	Resin System	Fibre (Type-II)	No. of Layers	Mandrel Diameter (mm)	Winding Speed (m/min)	Winding Angle	Fibre Tension (kg)
CFW_Prototype-1	LY3505/XB3403 epoxy/amine	8 x 2400 tex	4	106	7	Hoop	15
CFW_Prototype-1	CRYSTIC 397 PA Polyester	8 x 2400 tex	4	106	7	Hoop	15
CFW_Prototype-1	CRYSTIC 397 PA Polyester	8 x 2400 tex	4	106	21	Hoop	15

Table 3.4 Summary of the coding, resin system, reinforcement, ply thickness, mandrel diameter, winding speed and angle for the tubes produced via clean filament winding with Prototype-1.

3.1.3.2.2 Prototype-2

A schematic illustration of Prototype-2 is shown in Figure 3.7 (B) and a photograph of this device is shown in Figure 3.7 (A). The design was based on observations made whilst using Prototype-1. Further requirements were added to the design criteria by the industrial manufacturer as a result of the winding undertaken with Prototype-1. Prototype-2 was manufactured to be retrofitted easily on the filament winding machine

used on site. It was also designed to enable fast disassembly and cleaning at the end of production. The following section gives details of components used in Prototype-2.

(A)

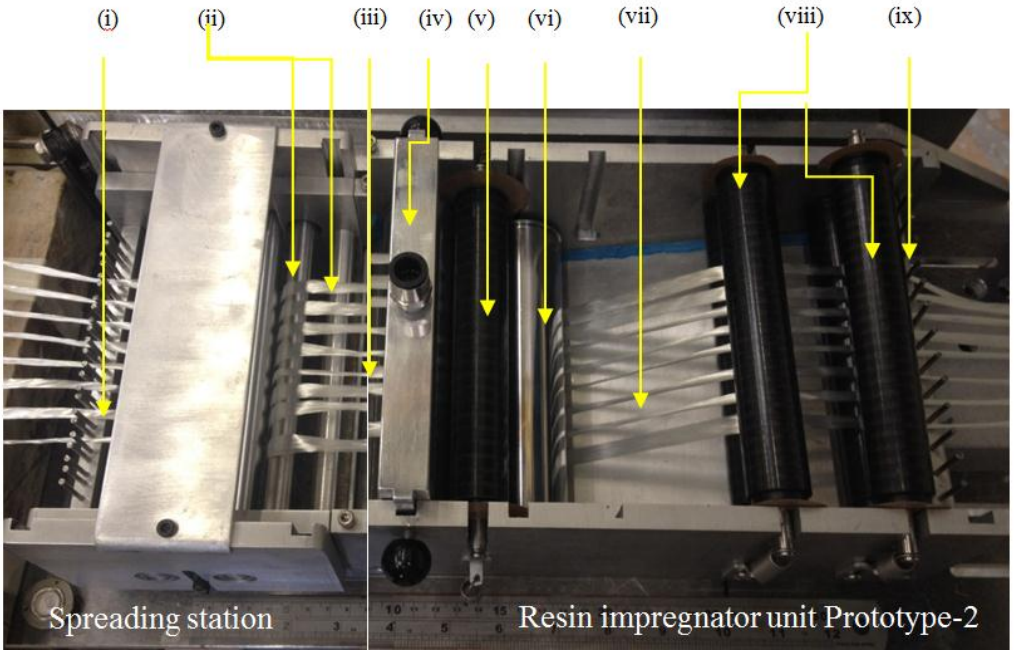

(B)

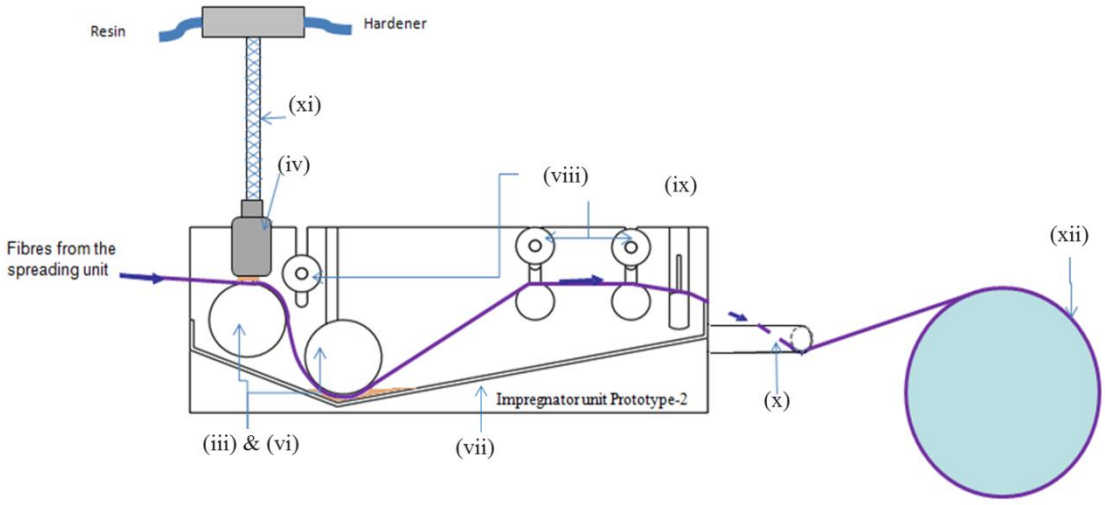

Figure 3.7 (A) A photograph of the manufactured Prototype-2 and (B) A schematic image of Prototype-2 with key components labelled (i) Guide pins, (ii) 5 spreading rollers, (iii) 1st roller, (iv) Injector head, (v) Acetyl roller, (vi) Pin, (vii) Angled base plate, (viii) Pinch pins, (ix) Second guide pins, (x) D-eye, (xi) Static mixer/pressure-pot pipe and (xii) Mandrel.

(i) **Guide pins:** These were used to maintain the fibres in position as they were hauled through the spreading rollers and under the resin impregnator unit.

(ii) **5 spreading rollers:** The lower three rollers were secured in place and the top two being adjustable in the vertical direction. This in effect increased or decreased the contact of the fibres with the rollers and thus the desired tension could be achieved.

(iii) **1st roller:** The first roller was placed under the injector head, rotating as the fibres were pulled through. This aided the manipulation of resin into the fibres.

(iv) **Injector head:** Resin system was supplied via the resin delivery system into the injector head. The resin filled the cavity in the resin impregnator unit similar to that seen for Prototype-1, overflowing down the slot and delivering a constant quantity of resin to all the fibres (seen in Figure 3.8). This impregnator coated the surface of the bundles in resin. This was then manipulated into the bundle as it progressed under the resin impregnator unit.

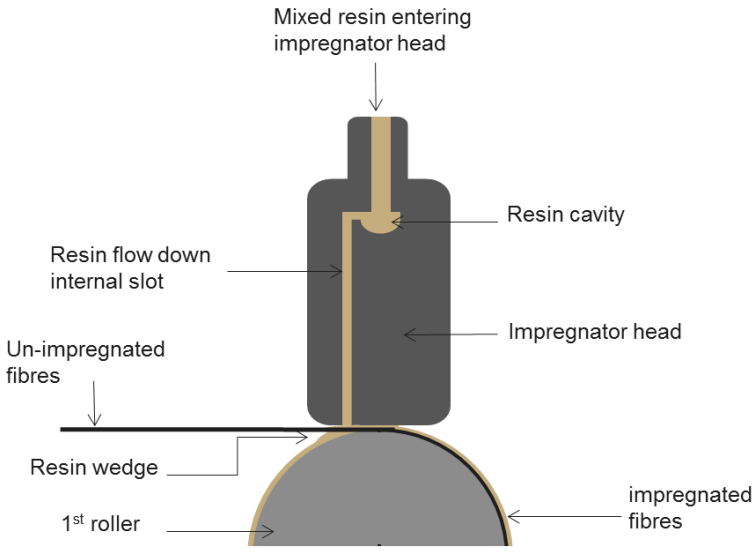

Figure 3.8 A schematic showing the internal feature of the resin impregnator unit for Prototype-2.

(v) **Acetal roller:** This was used to generate a resin-wedge as described previously to aid impregnation by squeezing the resin into the fibre bundles.

(vi) **Pin:** Fibres were pulled under the partially submerged pins. This coated the bottom side of the fibres with resin and helped to manipulate the resin into the fibres.

(vii) **Angled base plate**: The angled plate ensured the excess resin scraped off the fibres flowed back to the small reservoir beneath the pin (at point (vi)).

(viii) **Pinch pins**: These had adjustable tension settings, in other words, they could be altered depending on the volume of resin that required to be removed. The adjustments were made by varying the length of the spring attached to the roller. By increasing the length, more tension is applied to the pin, and conversely, decreasing the length, the applied tension reduced. The two sets of pinch pins helped to manipulate the resin into the fibre bundles. This differs to Prototype-1 where there was no adjustment in tension of the manipulation pins.

(ix) Second guide pins: These were used in conjunction with the first set of guide pins to maintain the fibre bundles in the correct trajectory as they were hauled under the injector head. They also aid in maintaining the required trajectory as the impregnated fibre bundle exits the resin impregnator unit prior to be directed to the D-eye**.**

(x) **D-eye:** This converges the fibres and generates a single flat ribbon, without segmentation, that was then wound onto the mandrel.

Prototype-2, like Prototype-1, was mounted directly on the traversing platform of the conventional winding machine. Prototype-2 was used to manufacture the tubes summarised in Table 3.5.

Winding	Resin System	Fibre (Type-II)	No. of Layers	Mandrel Diameter (mm)	Winding Speed (m/min)	Winding Angle	Fibre Tension (kg)
CFW_Prototype-2	CRYSTIC 397 PA Polyester	8 x 2400 tex	4	106	7	Hoop	15
CFW_Prototype-2	CRYSTIC 397 PA Polyester	8 x 2400 tex	4	106	21	Hoop	15

Table 3.5 Summary of the coding, resin system, reinforcement, ply thickness, mandrel diameter, winding speed and angle for the tubes produced via clean filament winding with Prototype-2.

3.1.4 Curing

After the required number of layers of the impregnated fibre bundles were overwound onto the mandrel, the fibre bundles were cut in close proximity to the mandrel and the ends were secured in position. A layer of peel-ply, in the form of a 75 mm wide ribbon, was overwrapped on the impregnated mandrel assembly. The 75 mm width peel-ply was used to: (i) retain the resin on the mandrel during its transportation to the oven; (ii) impart the desired surface texture on the post-cured composite; and (iii) ensure safe handling during and after extraction of composite from the mandrel. The mandrel assembly was then transported via an overhead crane system to the oven. The mandrel assembly was placed in the oven and was secured onto a motorised cog system to enable rotation of the mandrel for the duration of the cure schedule. The cure schedules for the epoxy and polyester resin were described previously in Section 3.1.

3.1.5 Mandrel Extraction

After the tubes had been cured and cooled to ambient temperature, they were removed from the oven and placed in a hydraulic mandrel extractor. An electrically-controlled

hydraulic ram was used to extract the mandrel from the filament wound tube. Figure 3.9 shows the industrial hydraulic mandrel extractor that was used.

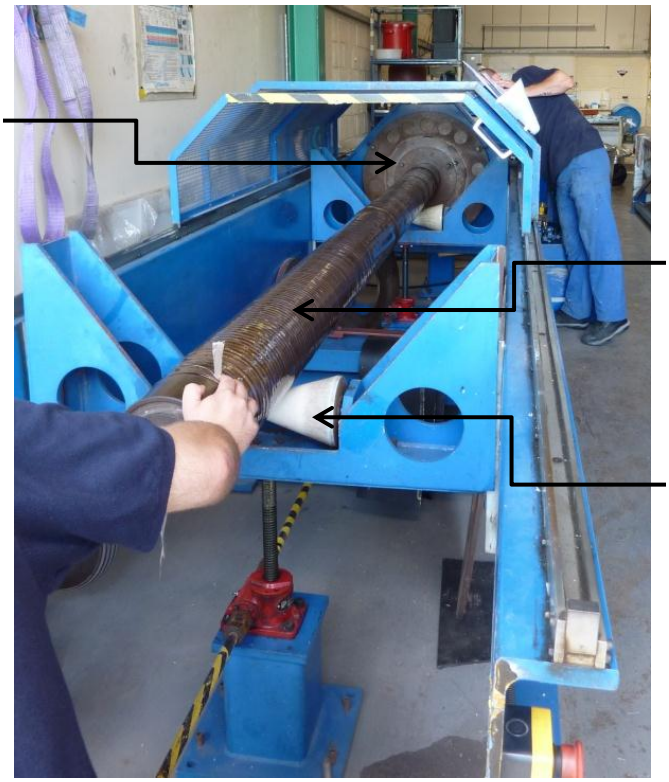

Figure 3.9 A photograph showing the hydraulic ram used for mandrel extraction.

3.1.6 Evaluation of Composite Tubes

Figure 3.10 shows the experimental plan for each of the tubes manufactured during the filament winding trial.

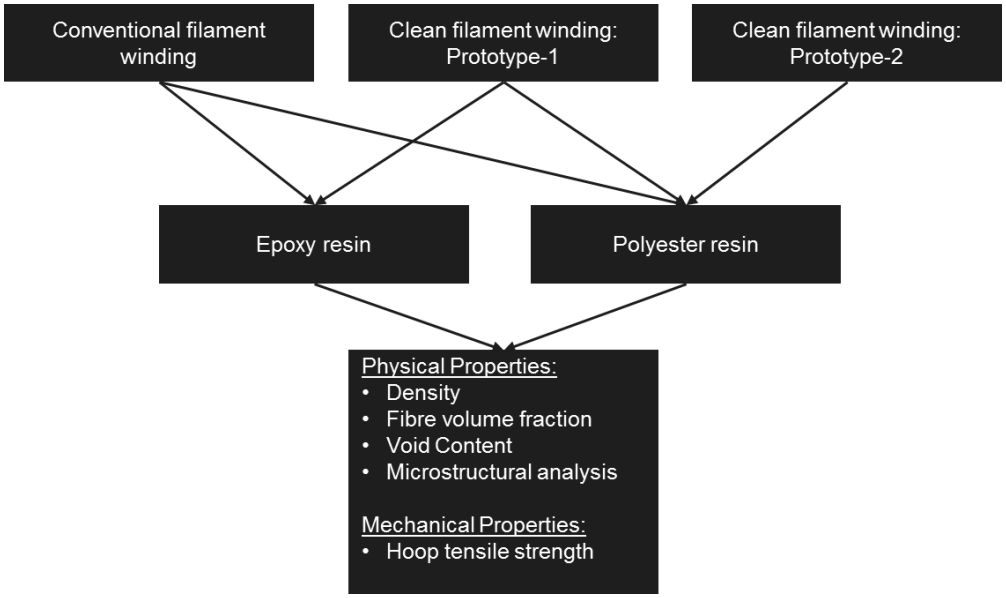

Figure 3.10 A schematic showing the experimental plan for each of the tubes manufactured during this study.

3.1.6.1. Visual Inspection of the Tubes

After the tubes were cured and extracted from the mandrel, a visual inspection of each tube was undertaken. A visual assessment was made of the degree of impregnation to identify the presence of dry patches and air bubbles on the surface. Each tube was then photographed, measured and marked for sectioning in order to produce the relevant test specimens. Once the tube was marked, it was photographed allowing each sample to be referenced against its original position in the tube. A photograph of a marked tube is shown in Figure 3.11. The marked specimens were cut using a diamond-coated cutting wheel. The cut-edges were abraded using 1200-grit abrasive paper.

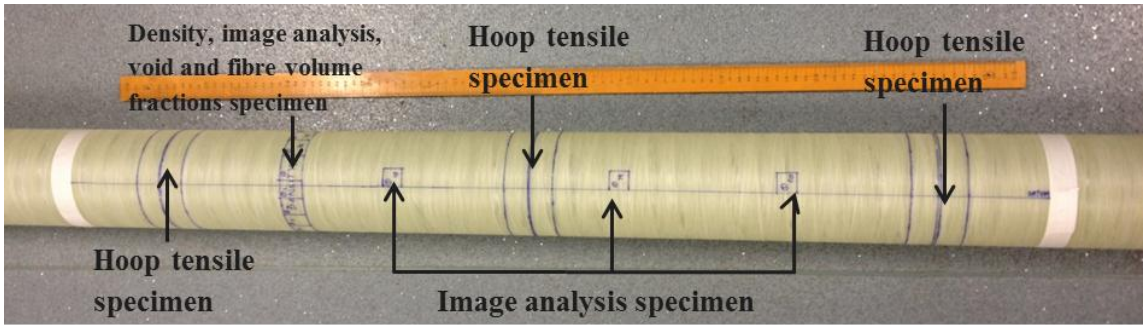

Figure 3.11 A photograph showing the tube marked up to complete the programme of analysis.

3.1.6.2 Density Measurements

The density of 10 samples from each of tubes produced was measured using a density determination kit AP250D (Ohaus). These tests were carried out in accordance with ASTM D792-00. The mass of the composite was first determined in air by placing the crucible on the balance and measuring it to the nearest 0.1 mg. The balance was tared and the composite sample was placed inside the crucible with the mass noted to the nearest 0.1 mg. The balance was then tared again before the sample was removed from the crucible and immersed in distilled water. The mass was recorded and termed sample buoyancy. The temperature of the distilled water was used to acquire a liquid density via a conversion table (Ohaus). The test was carried out in standard laboratory atmospheric conditions of 23 ± 2 °C and 50 ± 5% relative humidity. Equation 3.1 was used to calculate the density of the samples.

$$Sample\ Density = \frac{Sample\ Weight}{Sample\ Bouyancy} \times Density\ of\ Test\ Liquid$$

Equation 3.1

3.1.6.3 Fibre Volume Fraction Measurements

The fibre volume fraction of the filament wound tube was determined via the resin burn-off technique as described in ASTM D2584. Six individual samples per tube produced were used to determine fibre volume fraction. Each sample tested weighed approximately 5 g and the minimum area corresponded to 25 mm^2. The samples were weighed, placed in a crucible and re-weighed to the nearest 1.0 mg. The crucibles containing the samples were placed in a muffle furnace that was set at 565 ˚C for 6-hours to burn off the matrix. After 6-hours, the crucible containing the samples was allowed to cool to room temperature in a desiccator. Once cooled to room temperature, the crucibles with the reinforcements were weighed. The fibre volume fraction was determined using Equation 3.2.

$$V_f\% = \left(\frac{W_{Glass}}{\rho_{Glass}}\right) / \left(\frac{W_{Comp}}{\rho_{Comp}}\right) \times 100$$

Equation 3.2

Where:

W_{Glass} is the weight (kg) of glass (after heat treatment in the furnace);

W_{Comp} is the weight of composite (kg) (before heat treatment in the furnace);

ρ_{Comp} is the density of composite (kg/m^3);

ρ_{Glass} is the density of glass fibre (kg/m^3); and

V_f% is the percent volume fraction.

3.1.6.4 Void Content Calculations

The void content was calculated using Equation 3.4 in accordance with ASTM D2734:

$$V = 100 - M_d\left(\frac{r}{d_r} + \frac{g}{d_g}\right)$$

Equation 3.4

Where:

V is the void content (volume %);

M_d is the measured density of composite;

r is the resin (weight %);

g is the glass (weight %);

d_r is the density of resin (measurement taken of epoxy and polyester were 1180 kg/m^3); and

d_g is the density of glass (2620 kg/m^3 for Type-I and Type-II 2400 tex E-glass fibres).

3.1.6.5 Microstructural Analysis

With reference to Figure 3.11, six sections from each tube (specimens for image analysis) were placed into plastic pots and filled with a mounting resin (Epofix resin and hardener, Struers, UK). The ratio of the resin and the hardener was 25:3 respectively. The curing of the mounting resin was carried out at ambient temperature for 24-hours. The samples were removed from the pot and ground/polished using the following grades of SiC abrasive paper: 400; 800; 1200; 2500; and 4000 (MetPrep,

UK). Water was used as the lubricant during grinding/polishing. The final polishing stage involved the use of 0.05 μm alumina suspension (Aqueous Suspension Gamma micron size 0.05, MetPrep, UK) in conjunction with a Chemicloth polishing disk. This final polishing stage was repeated twice. Samples were cleaned, rinsed with tap water and then placed in a beaker containing distilled water, and transferred to an ultrasonic bath for 6 minutes between each polishing stages. The polished samples were dried using lint-free tissue and placed in the oven at 40 °C for 1-hour. Microstructural analysis was carried out using a Zeiss Axioskop 2 optical microscope.

3.1.6.6 Hoop Tensile Strength

Hoop tensile tests were carried out in accordance with ASTM D2290. Six rings were taken from each of the filament wound tubes (the locations were shown previously in Figure 3.11). Each ring was cut using a diamond-coated cutting wheel and then polished using 800 grit abrasive paper to produce with widths of 25 mm. Each sample was notched at a specified datum point marked on the tube. The relative positions and the dimensions of the notches are shown in Figure 3.12 (i). The notches were introduced using a 7 mm diameter diamond-coated milling-cutter on a milling machine. The profile of the notches was semi-circular with a radius of 3.5 mm. The notched surface was abraded using 1200 grit abrasive paper. The ring was loaded on to a test fixture, as illustrated in Figure 3.12 (ii), and the hoop tensile tests were carried out using a Zwick 1484 at a cross-head displacement rate of 2 mm/min.

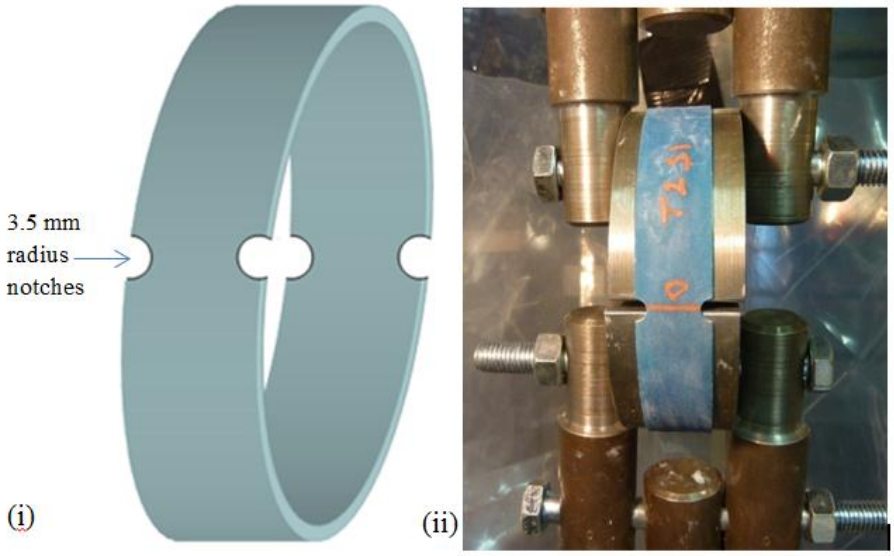

Figure 3.12 (i) A schematic showing the relevant notch locations on each of the hoop tensile specimen. (ii) A photograph showing a hoop tensile specimen loaded in the tensile rig on the Zwick 1484 mechanical test machine.

3.1.6.7 Data Acquisition for Life Cycle Analysis

A life cycle analysis (LCA) was carried out for tubes produced using the conventional and clean filament winding production techniques. The LCA was based on tubes that were wound with eight 2400 tex E-glass fibre bundles at 7 m/min onto 106 mm outer diameter mandrels. Each tube consisted of four layers of hoop wound fibres with a length of 1500 mm. The LCA data collected for each production method were as follows:

(i) mass of fibres required per tube;

(ii) mass of resin required per tube;

(iii) electrical power requirements;

(iv) mass of waste resin generated;

(v) mass of solvent used; and

(vi) cleaning time.

Mass of fibres used: The fibre mass used was calculated for the 106 mm tubes by dry-winding two hoop layers to produce a tube length of 1500 mm. The quantity of fibres was then weighed and multiplied by 2 to estimate the fibre mass for the four-layer tube.

Mass of resin used: For the conventionally wound tubes, the mass of the resin used was estimated by winding a single layer of impregnated fibres and then removing and weighing them. This value was multiplied by 4 to estimate the content of the resin for a four layer tube to be produced.

Electrical power requirements: These were acquired for the filament winding machine, the oven and in the case of the clean filament winding production method, the resin dispenser.

Waste resin: This was collected and weighed from all the visible points where the resin dripped as illustrated in Figure 3.13 and Table 3.6. Included in this category was the waste resin generated by the removal of excess resin present on the tube during conventional winding. For the resin bath, this was the waste left in the resin bath after the tube production. This was added into the calculations as 2.5 litres to amount remaining in the resin bath after production.

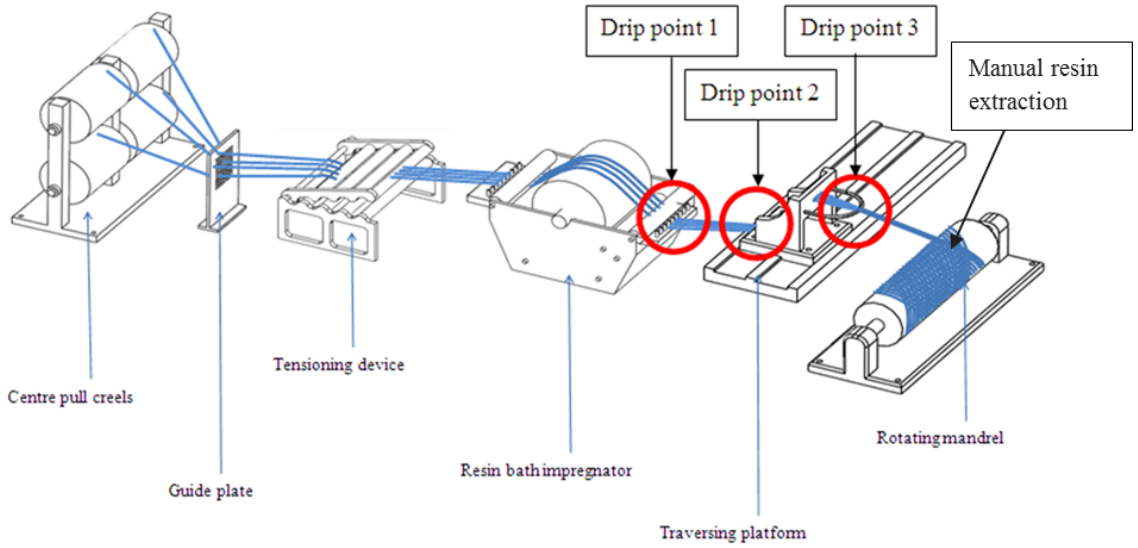

Figure 3.13 A schematic showing the drip points where the resin was collected from for the LCA calculations. The waste resin was also generated at the mandrel, where the excess resin was removed periodically during conventional filament winding.

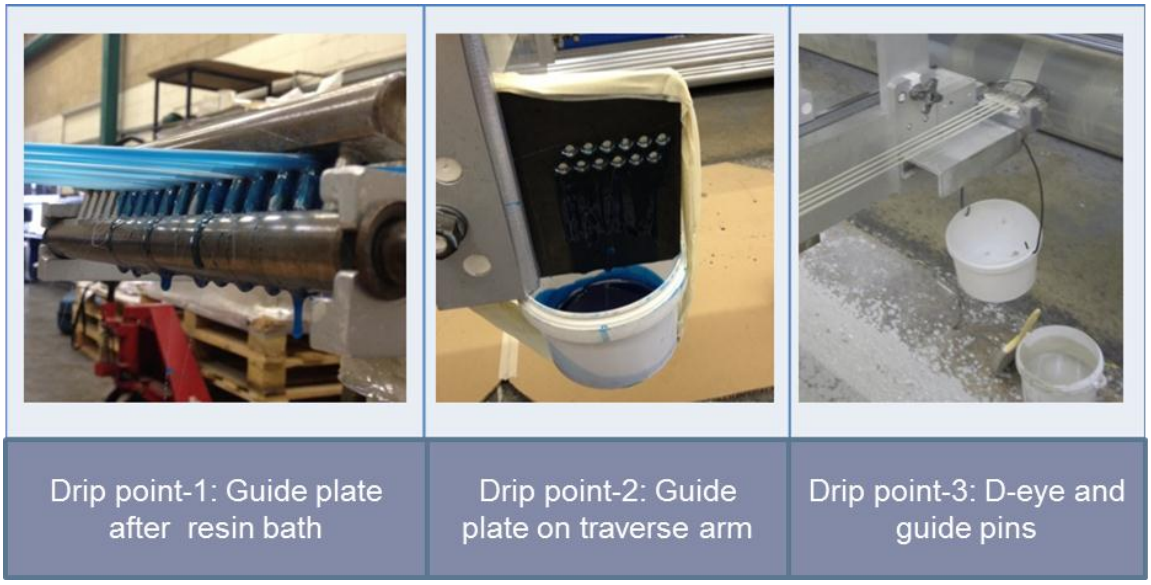

Table 3.6 The drip points where resin was collected for LCA measurements.

3.1.6.8 Cleaning Filament Winding Equipment

During production, the equipment was wiped regularly with an acetone-soaked rag to stop build-up of the polyester at drip points labelled in Figure 3.13. This operation was

not found to interfere with the conventional winding process. This was not an issue with clean filament winding. The volume of solvent used for this operation is small and therefore it was difficult to quantify.

For conventional winding, the cleaning time required on average for two persons was approximately 20 minutes. However, this could increase up to 45 minutes during the summer months because the resin cures more rapidly and more effort is required to remove it from some of the items. In the clean filament winding process, the time required for three persons to complete the cleaning was approximately 20 minutes. The onsite team from the University always included three persons. Prototype-2 was designed for the site trials to be as versatile and adjustable as possible, thus adding to its complexity and increases cleaning time. This could be reduced by the industrial winding team once optimal parameters were known. The total mass of acetone used was approximately 2800 g per production day to clean the conventional equipment. Whereas, approximately 250 g was required to clean Prototype-2.

3.2 FIBRE CHARACTERISATION

3.2.1 Reinforcing Fibres

The reinforcing fibres used for the fibre characterisation experiments were Type-I and Type-II fibre detailed in Section 3.1.1. These fibres were used in the subsequent experiment to study the effect of binder content and how this can affect fibre bundle impregnation rate.

3.2.2 Examination of the Binder

3.2.2.1 Scanning Electron Microscopy

Samples of as-received, acetone extracted and heat-treated (loss-on-ignition - LOI) Type-I and Type-II were examined using a Jeol 6060 scanning electron microscopy (SEM). The fibre bundles were prepared in such a way to minimise changes to the architecture of the bundle. This was achieved in the following manner.

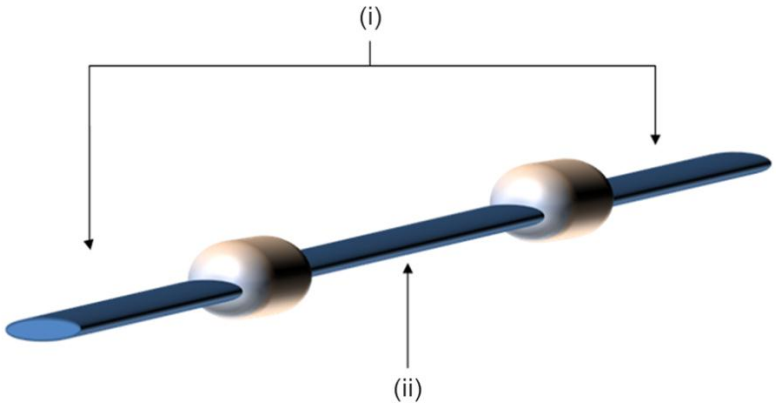

Figure 3.14 Schematic showing the location of the NOA63 UV resin beads applied to the fibre bundle to maintain the architecture of the fibre bundle for SEM inspection.

With reference to Figure 3.14, two drops of NOA63 photo-curable resin (Norland Co., USA), were placed on the fibre bundle approximately 15 mm apart and cured using a UV light source (UV75 light, Thorlabs UK) with a wavelength in the range of 350-500 nm, to freeze and capture the impregnation area after 3 minutes. A scalpel blade was used to cut the fibre bundle at points (i) at the distal ends of the cured resin. The area of fibre bundle labelled (ii) was mounted on a SEM stub with a carbon-coated adhesive pad. Agar silver paint G302 (Agar Scientific, UK) was used to provide additional bonding and a conducting path. The sample was gold sputter coated in an Emscope SC

500 for 3 minutes using conventional procedures. Samples were examined using the Jeol 6060 SEM.

3.2.2.2 Extraction of the Binder using Acetone

Acetone extraction of the binder was carried out in a fume cupboard using a custom-designed glass vessel. A photograph of this vessel is shown in Figure 3.15. With reference to Figure 3.15, the procedure used in the extraction of the binder was as follows. A silicone tray (i) was used as the "moat" and the glass vessel was placed on top of it. This assembly was placed on a magnetic stirrer (ii) and secured using a retort stand (iii). A PTFE-coated magnetic stirring element was dropped into the bottom of the glass vessel (iv). Thirty individual samples of 450 mm long glass fibre bundles were cut from the centre of Type-I and Type-II fibre creels (v). Each fibre bundle was initially weighed and then an aluminium foil identification tab was crimped to the top of the each bundle; each bundle was re-weighed. The fibre bundles were mounted one at a time on a support-fixture (vi) allowing them to hang freely. The cylinder was then quarter-filled with acetone using a funnel (vii). The E-glass fibres that were mounted on the support-fixture were then lowered into the glass cylinder and rested on a ledge within the top section of the cylinder (viii).

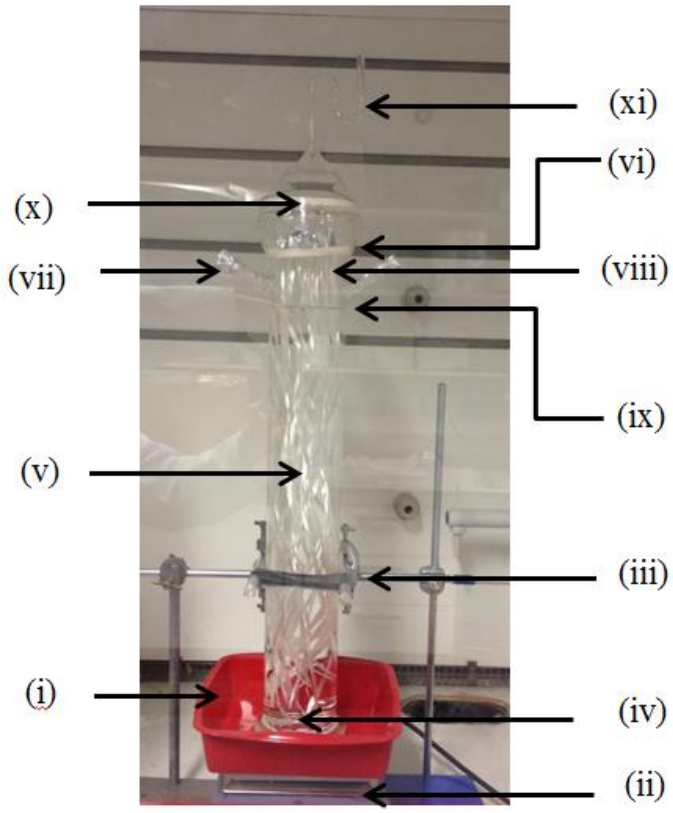

Figure 3.15 A photograph showing the experimental set up used for the acetone extraction experiment. Key features labelled include: (i) silicon tray, (ii) magnetic stirrer plate, (iii) retort stand, (iv) PTFE coated magnetic stirring element, (v) glass fibre bundles, (vi) fibre bundle support-fixture, (vii) side funnel, (viii) resting ledge, (ix) liquid level, (x) Parafilm®, (xi) U- bend filled with water.

More acetone was added slowly to the inner surface of the glassware until the final liquid level was attained as shown at point (ix). Due care and attention was paid not to disturb the fibre bundles. Stoppers were placed in the two flutes (vii) and Parafilm® was wrapped around the top of the glass vessel to secure the lid (x). The lid contained a U-bend filled with distilled water (xi). This was used to visualise if any significant evaporation had occurred. Once the assembly with the glass fibres was secured, the magnetic stirrer was turned on. The experiment was conducted for either 24 or 48-hours after which the magnetic stirrer was turned off and the lid was removed. The support-fixture with the glass fibre bundles was removed from the glass vessel and left suspended in air for 1-hour to evaporate the bulk of the solvent. This assembly was

then transferred to an air circulated oven at 50 °C for a further hour to remove any residual solvent. After an hour, the fibres were re-weighed and the percentage weight loss was calculated.

A further experiment was also carried out where the binder was extracted for 24-hours in the acetone as described above. This procedure was repeated and fibre bundles re-weighed. The fibre bundles were then placed in a furnace for 30 minutes at 625 °C, after which they were cooled to ambient temperature and re-weighed. This experiment was carried out to estimate the weight loss at each stage of the de-binding process.

3.2.2.3 Extraction of Binder using Loss-on-Ignition

The loss-on-ignition method as specified in ASTM D4963/D4963M was used on fibre Type-I and II as a method to remove the binder. The organic content on the glass fibre bundle was determined by weighing specimen before and after heat treatment (30 mins at 625 °C). The weight loss was the reported as a percentage of the total mass before heat treatment. Six individual samples each of Type-I and II fibres were taken from five locations from the creels as show in Figures 3.16 (i) and (ii) respectively. ASTM D4963/D4963M standard required that the mass of each sample had to be greater than 6 g.

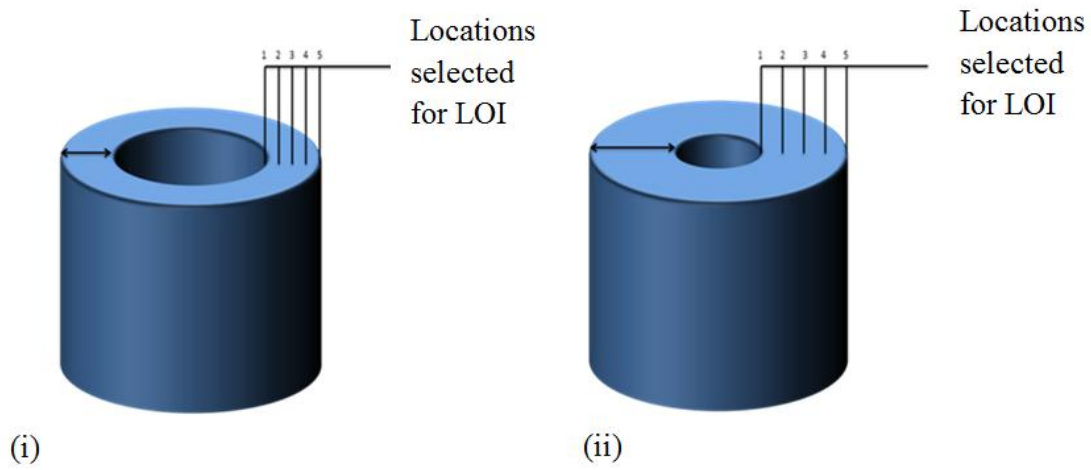

Figure 3.16 Schematic showing the locations of fibre bundle taken for LOI taken from (i) Type-I fibre and (ii) Type-II fibre. Points 1 and 5 represent the bore and surface of the creel respectively; the other three points were equidistant from the bore.

The samples were firstly preconditioned in an oven at 105 °C for 1-hour. Samples were weighted before and after the preconditioning to measure any weight loss due to absorbed moisture. The containers were fashioned from steel foil and these were preconditioned in a muffle furnace at 625 °C for 30 minutes, removed and then cooled to room temperature for 30 minutes, prior to use. The weight of the empty container was weighed to nearest 0.001 g and the balance was tared (T). Each glass fibre bundle was placed in a container and re-weighed. This was termed the initial mass (A). The container with the specimen was placed in the furnace at 625 °C for 30 minutes. After which it was removed from the furnace and allowed to cool to room temperature in a desiccator for 30 minutes. The container and specimen were then removed and weighed; coded as the ignited mass (B). The ignition loss was calculated using Equation 3.5:

$$Ignition\ Loss, (\%) = \ 100\ x\ \frac{(A - B)}{(A/T)}$$

Equation 3.5

Where:

A is the initial mass (kg) of container and specimen prior to heat treatment;

B is the mass (kg) of container and glass residue after heat treatment; and

T is the mass (kg) of the container.

3.2.3 Impregnation Monitoring

3.2.3.1 Fibre Bundle Impregnation Experiment

The axial and through-thickness impregnation of the fibre bundle was monitored using equipment developed by Bogonez (2013). The experimental set up is shown schematically in Figure Figure 3.17.

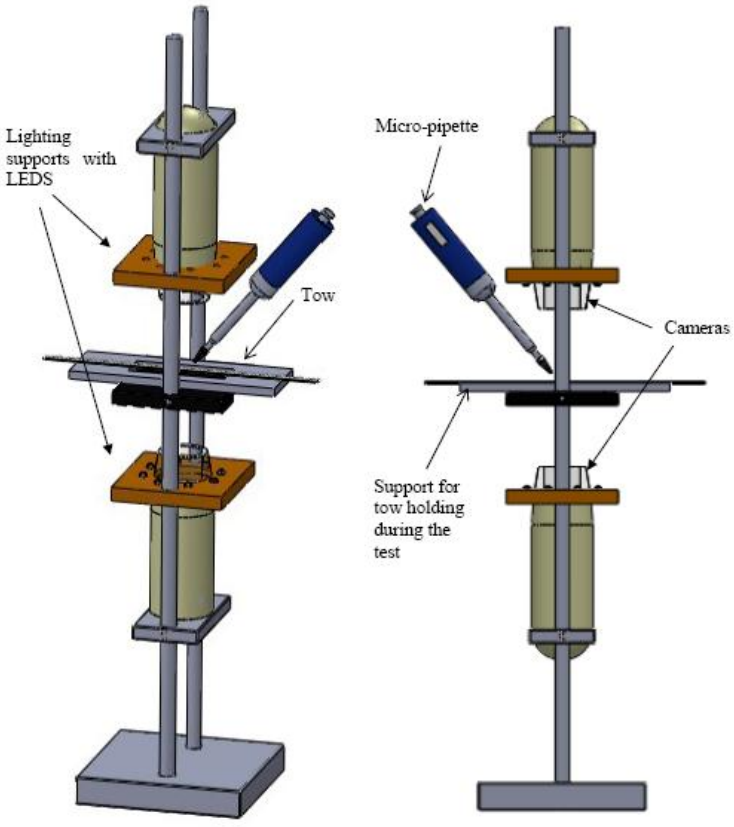

Figure 3.17 Schematic illustration of the experimental set up used during the impregnation monitoring experiments. Reproduced from Bogonez (2013).

Two USB cameras with a 2 Mega Pixel CMOS lens were used to track the flow-front and through-thickness impregnation area of resin on the fibre surface. An aluminium frame was built to secure the USB cameras, one above and one below a fibre bundle viewing area. Each support incorporated an LED lighting system as shown in Figure 3.18.

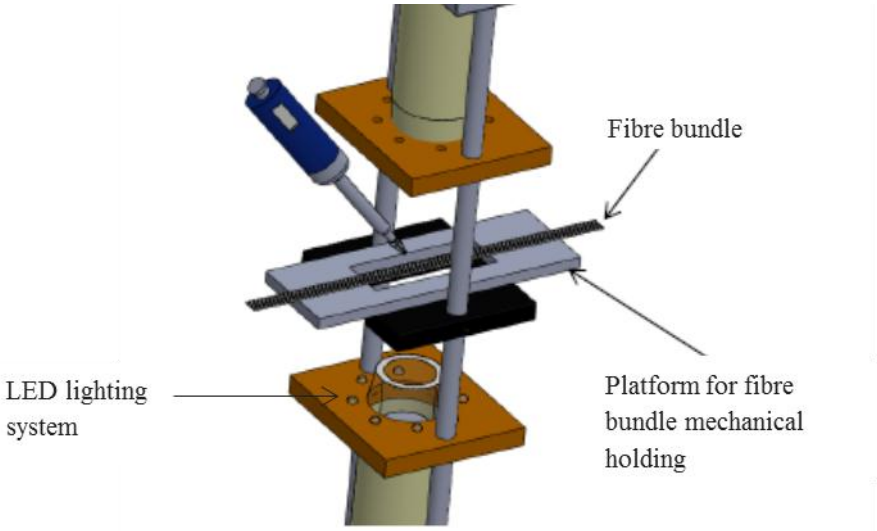

Figure 3.18 Schematic showing a magnified view of the fibre bundle viewing area. Reproduced from Bogonez (2013).

Eight white LEDs were spaced around the circumference of the camera and were controlled independently using custom-made circuit boards and adjusted using a potentiometer. Bogonez, (2013) completed several trials to determine the optimum light intensity to illuminate the surfaces of the fibre bundle. The aluminium support rig was encased in a blacked-out enclosure to remove stray light The resin used for this experiment was a photo-curable resin NOA63 (Norland Co., USA). This resin had a viscosity that was similar to the epoxy LY3505/XB3403 and therefore, was deemed a suitable replacement in this experiment. The NOA63 resin could be cross-linked using a UV light source (UV75 light, Thorlabs UK) with a wavelength in the range of 350-

500 nm, to freeze and capture the impregnation area after 3 minutes. Due to the optical transparency of the NOA63 photo-curable resin, a red pigment (Araldite colouring paste, Huntsman, UK) was used to enhance the contrast between the resin and the fibre bundle. It was found that a 0.5 weight % gave the best contrast without any significant effect on the resin viscosity as reported by Bogonez (2013).

An orifice was positioned on the side of the enclosure to enable a micropipette (Mline, Biohit, UK) to be introduced and positioned directly above the centre of the fibre bundle. The fixture permitted the tip of the micro-pipette to be positioned 20 mm above the fibre bundle at 30° in a repeatable manner. It was found that 40 ml of resin was the optimum volume. Each fibre bundle tested was secured on an aluminium platform with the centre section removed to enable imaging, as shown in Figure 3.18. The resin droplet was monitored, via the pair of CCD cameras, as it penetrated through and along the fibre bundle for 200 seconds with custom-written Labview based software (Bogonez, 2013). The impregnated area, length, width, and through-thickness profiles were calculated. However, in the current study only the through-thickness data are presented. Figure 3.19 show images attained from the top (i) and bottom (ii) camera during an impregnation experiment using Type-II fibres. Bogonez, (2013) performed extensive calibrations to ensure that area measured by the Labview software correlated to the results obtained manually from the images. The author repeated these calibrations and arrived at the same conclusions. The outcome of this calibration study can be seen in Appendix B.

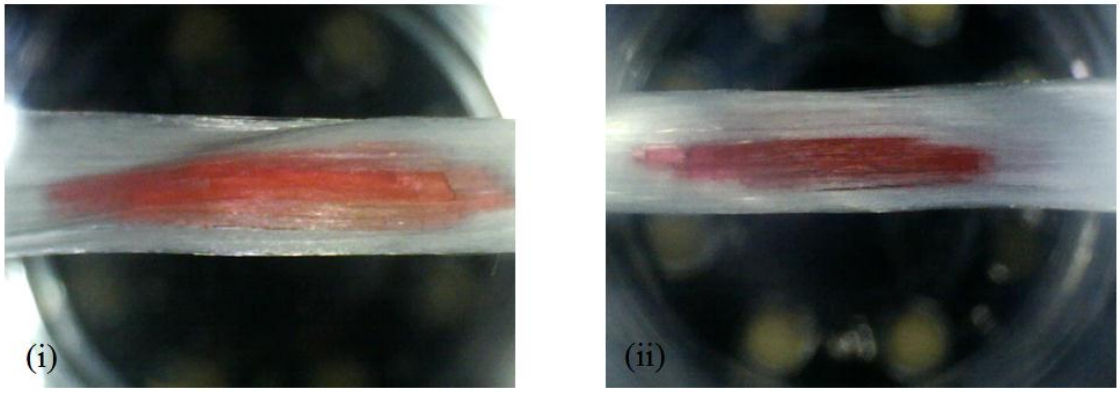

Figure 3.19 A photograph of the images taken from a Type-II fibre demonstration the examples of: (i) top; and (ii) bottom, recording during as-received impregnation.

3.2.3.2. Image Analysis of Fibre Architecture

Samples were produced using the effect of capillary wicking to ensure that the fibre bundle architecture remained unchanged. Sections of as-received Type-I and II were cut using a scalpel. One end was connected to a supporting beam while the opposite end was allowed to hang freely in a small sample mounting pot which was filled with potting resin (Epofix resin and hardener, Struers, UK). The samples were left for 24-hours to cure. The samples were then removed from the supporting beam and the remaining loose fibres were cut from the sample. The potted samples then were subjected to a series of grinding and polishing steps to expose an area of the fibre which was representative of the as-received fibre bundle architecture. These were then imaged using an optical microscope (Zeiss Axioskop 2).

3.2.3.3 Impregnation Blocks

This experiment was carried out to study the architecture of the as-received fibre bundles. A silicone mould with the dimensions 80 mm x 40 mm x 40 mm was used to impregnate and cast Types-I and II fibres. 2400 tex E-glass fibres were removed from

the inner bore of the creels. Fibre lengths of 60 mm were cut using a razor blade and placed in a silicon mould. LY3505/XB4303 mixed epoxy resin was used as the casting medium. The mould was filled carefully to the top to immerse the glass fibres. This assembly was then degassed for 15 minutes and then cured for 24-hours at room temperature followed by post-curing at 80 °C for 6-hours. Once cured, the epoxy/glass fibre composite was removed from the silicone mould and sectioned for examination of the as-received architecture and the degree of impregnation achieved. Image analysis was carried out on all samples produced using an optical microscope (Zeiss Axioskop 2). Figure 3.20 shows how the sections were selected for image analysis.

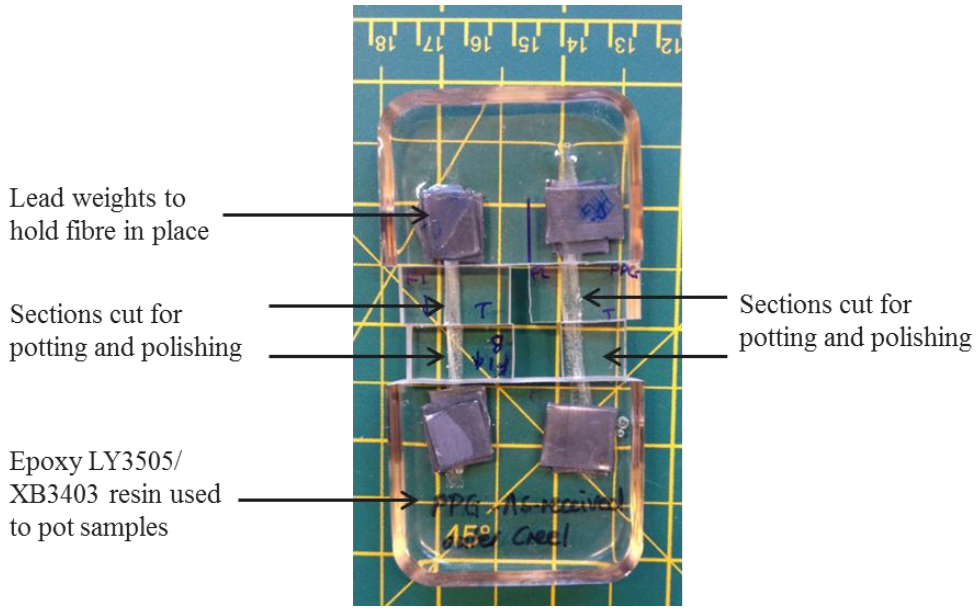

Figure 3.20 A Photograph showing the casting of as-received fibre bundles. The sections that were designated for potting and polishing (for optical microscopy) are indicated.

3.2.4 Fibre Bundle Tensile Test

Fibre bundle tensile tests were carried out in accordance with BS ISO 3341:2000. 2 mm thick aluminium sheets were guillotined to produce end-tabs of dimensions of 50 mm x 25 mm. The edges of the end-tabs were abraded using 400 grade abrasive paper.

This was performed to minimise the possibility of the fibres being damaged during end-tabbing and tensile testing. The surface of the end-tabs was sandblasted and degreased in acetone for 15 minutes using an ultrasonic bath. The abraded face of the end-tabs were coated with a thin layer of Scotchweld 9323-2 B/A structural adhesive (3M, UK) and then placed in an oven at 65 °C for 2-hours to cure the resin.

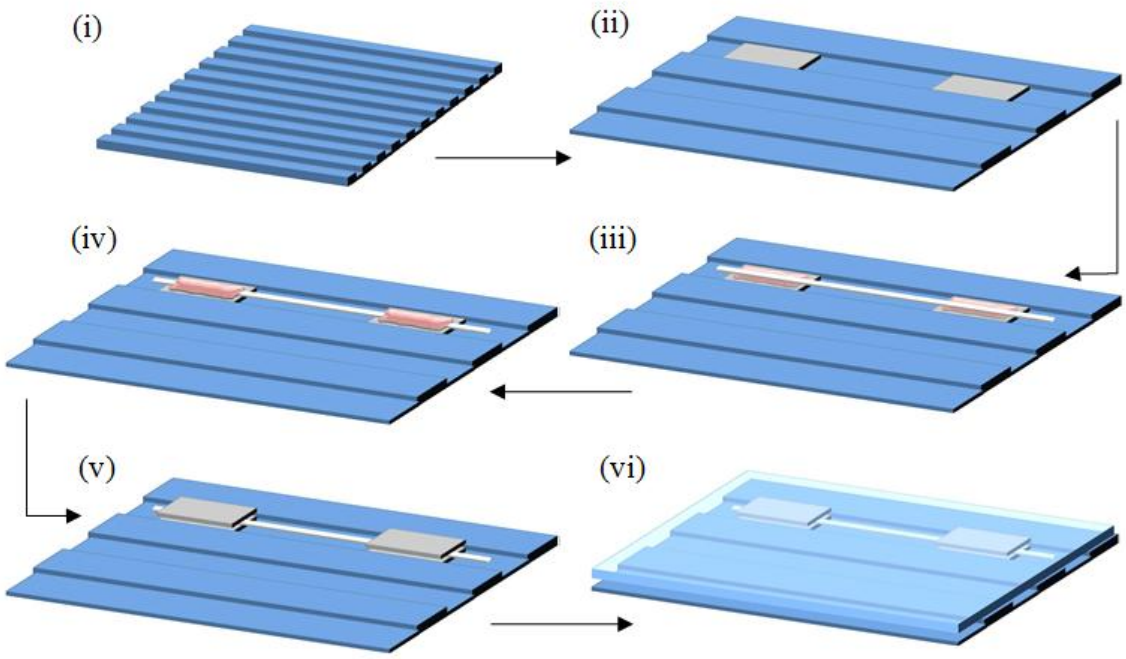

Figure 3.21 Schematic illustrations demonstrating the procedure used to produce tensile testing fibre bundle samples with end-tabs.

Figure 3.21 shows the procedure for producing the single-bundle tensile samples using a simple rig. The rig was made from medium density fibre board (MDF) and recesses of dimensions 25 mm in width were machined to enable the end-tabs to be located securely. The positioning of the end-tabs within the recesses are indicated in Figure 3.21 (i). The end-tabs were placed 100 mm apart in the rig to obtain a gauge length of 100 mm. A layer of resin was applied to the previously coated end-tabs. 400 mm length of the fibre bundle was removed from the creel and secured in place over the

end-tabs this is indicated in Figure 3.21 (iii). The ends of the fibre were secured to the edges of the rig using bulldog clips. The clips enable the fibres to be held under tension. Once the fibre was secured in place, another layer of resin was added to the end-tab, this time ensuring that the fibre was impregnated fully with the resin shown in Figure 3.21 (iv). A second end-tab was then placed on top of the resin impregnated fibre. After ten samples had been end-tabbed, a flat top-plate was placed on the top of the rig. Five 2 kg weights were positioned on the top plate. The resin was cured for 24-hours. This procedure was used to produce thirty as-received samples of Types-I and II fibres. Thirty samples each of the other pre-treated Type-I and II fibres were also produced. Table 3.7 summarises the samples produced for the fibre bundle tensile tests.

Fibre Type	Fibre Treatment	Number of samples
Type-I	As-received fibres	30
	Acetone Extracted – 24 hours	30
	Acetone Extracted – 48 hours	30
Type-II	As-received fibres	30
	Acetone Extracted – 24 hours	30
	Acetone Extracted – 48 hours	30

Table 3.7 A summary of the samples produced for Type-I and Type-II fibre bundle tensile experiment.

4. RESULTS AND DISCUSSION

4.1 FILAMENT WINDING

4.1.1 Conventional Filament Winding

4.1.1.1 Observations of Impregnation Points during Filament Winding

As stated in the literature review, filament winding is a process by which continuous fibre bundles are impregnated with a resin system and then wound around a rotating mandrel in conjunction with a traversing platform. Figure 3.1 shows a schematic illustration of the industrial filament winding set up that was used by the author for the conventional and clean winding site trials. The key components associated with the filament winding process were described previously in the Chapter 3, Section 3.1.2.

With reference to the site trials undertaken by the author and the observations made, the following section reports on the impregnation process at different stages during conventional filament winding. The impregnation process begins at the resin bath and continues all the way through to the D-eye and the mandrel. Visual observations made with regard to the general impregnation process at each of the contact points between the fibre bundle and an item of the filament winding equipment is presented in Figure 4.1.

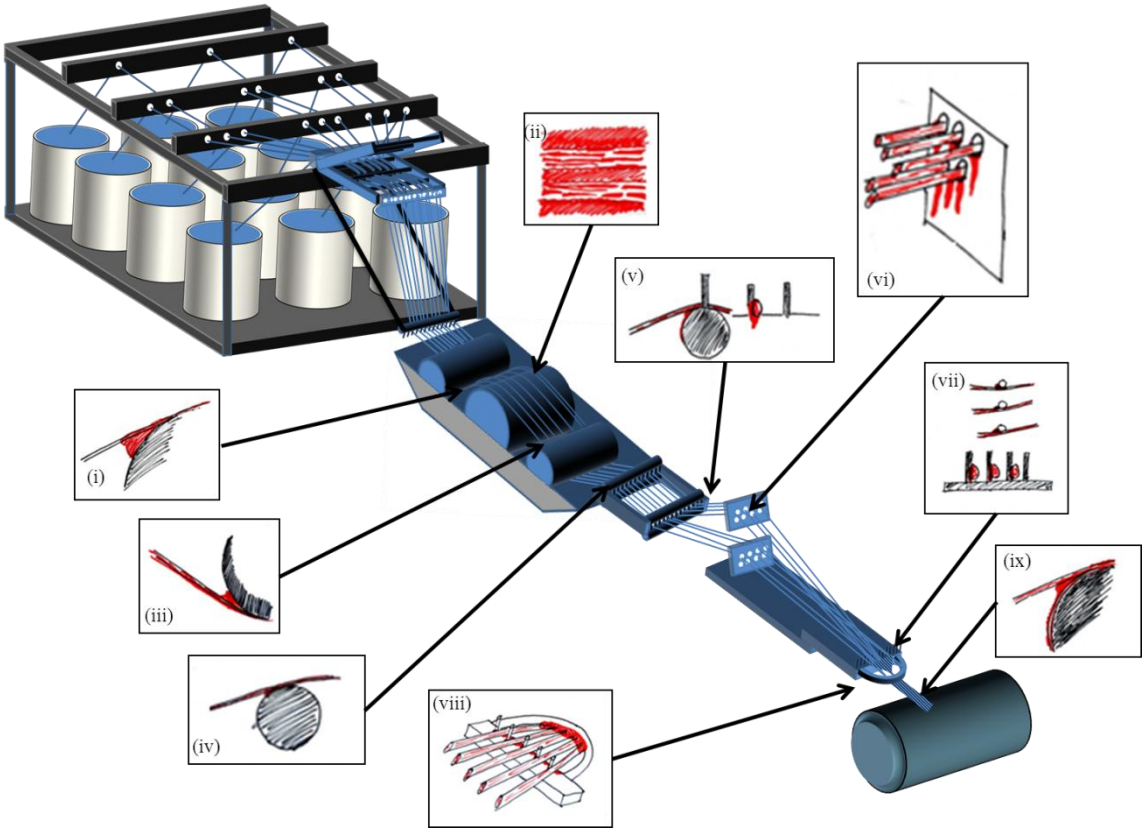

Figure 4.1 A numbered set of schematic illustrations showing the different impregnation processes occurring at different contact points during conventional filament winding; these observations were made during the production of tubes at an industrial concern in industry. The numbered items are discussed in the text.

(i) **Drum wedge impregnation** – this is the first point at which the resin contacts the fibres. Resin is picked up onto the partially submerged impregnation drum. A doctor blade is used to control the volume or "thickness" of the resin that is present on the impregnation drum. At the point where the fibres contact the resin-covered drum, a wedge of the resin is formed, as shown in Figure 4.1 (i). This wedge of resin is forced into the fibres in the axial, transverse and through-thickness directions. Resin is also squeezed to the edges of the fibre bundle. A general profile of the resin within the bundle at the initial contact point between the bundle and the drum is shown in Figure 4.2.

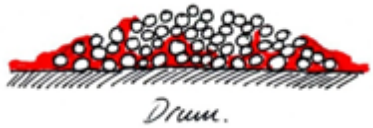

Figure 4.2 A schematic of the impregnation occurring at contact point-(i) in Figure 4.1; this represents the initial contact between the bundle and the impregnation drum. The coloured regions indicate the visually observed profile of the impregnation zone.

(ii) **Maximum contact** – At this point along the impregnation drum, the fibres are in complete contact with the top of the drum. Resin from underneath the fibres begins to penetrate through the bundle due to the pressure exerted on the fluid layer remaining on the impregnation drum (shown in Figure 4.3). The momentary loss in tension as the traverse-carriage reaches the end of its travel tends to create a pulsating action and this too may assist in the through-thickness impregnation of the bundle. However, further research is needed to verify this speculation. If slippage occurs between the impregnation drum and the fibre bundle, additional resin pick-up will be possible. If the movement of the fibres and drum are synchronised, the resin-depleted region will be replenished only when that portion of the impregnation drum is immersed in the resin system. In instances where excess resin is picked up by the impregnation drum, for example, if too large a doctor blade setting is used, the resin that is squeezed out from the sides of the fibre bundle will be re-deposited along the edges of the bundle. The consequence of this is dependent on the number of contact points the impregnated bundle makes with the processing equipment prior to being deposited on the mandrel. In some instances, as the fibres are hauled-off from the creel, they tended to split into two or more strands as they reached the impregnation drum. The net effect of this was the accumulation of resin in between the split bundle.

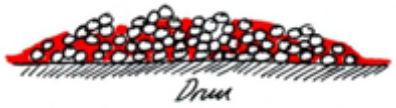

Figure 4.3 A schematic illustration of the observed impregnation at contact point-(ii) in Figure 4.1.

(iii) **Impregnation at the roller** – After leaving the impregnation drum, the fibres contact the second guide-roller (the first guide-roller does not come into contact with the resin system). As the fibres traverse under the roller, the resin that has penetrated through the thickness of the fibre bundle, or in a region where the bundle has split, combined with the resin collected on the sides of the bundle, generates another smaller resin wedge region (illustrated in Figure 4.1 (iii)). This second roller is above the liquid level in the resin bath. Therefore, the formation of the wedge of resin was gradually built up after a few rotations or subsequent to a few metres of the impregnated fibre bundle being hauled-off under it. The pressure created by the contact between the fibres, resin and the surface of the roller squeezes the resin into the bundle; this form of manipulation of the fibres (apart from splitting of the bundle) will aid with the through-thickness impregnation. Figure 4.4 shows a schematic illustration of the impregnation at the second roller.

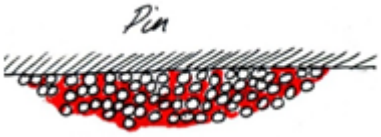

Figure 4.4 Schematic illustration of the impregnation occurring at contact point-(iii) in Figure 4.1.

(iv) and (v) **Pin and wedge-based impregnation** – These are used to control the trajectory of the impregnated fibres as they exit the resin bath on route to the mandrel. In general, pins are used in conjunction with a removable top-cap or bar with holes to

accommodate the pins; this allows easy access by the operator to rethread the fibres in the event of an entanglement or fracture of the bundle. With reference to items (iv) and (v) in Figure 4.1, and the magnified illustration shown in Figure 4.5, at this contact point the fibre bundle not only contacts the top of the pin but also the sides of vertical separation pins. This causes the fibre bundle to change its profile as the sidewalls cause the bundle to bunch up into a semi-triangular shape. This change in bundle shape aids with the re-distribution of the resin within the fibre bundle. Also a small wedge region is created as the impregnated fibres contact the pin.

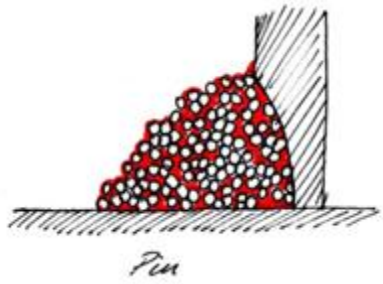

Figure 4.5 Schematic of the impregnation occurring at contact points-(iv) and (v) in Figure 4.1.

(vi) **Eyelet** – At this contact point, the fibre bundles pass through individual eyelets acting as guides. Between contact points (v) and (vi) the fibres travel approximately 2.5 meters without any contact with the processing equipment. This allows time for capillary flow of the resin through the fibre bundles. As the fibres enter the eyelet, they make contact with the base and side, this can be the left or right side depending on the position of the traversing arm. The contact with the surface of the eyelet aids resin redistribution. This can be seen in Figure 4.6.

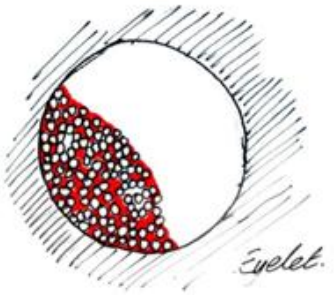

Figure 4.6 Schematic of the impregnation at the eyelet when the traverse arm is at the extreme left of the mandrel. This represents contact point (vi) in Figure 4.1.

(vii) **Pin** – This is similar to points (iv) and (v) discussed previously.

(viii) **D-eye** - The D-eye is the penultimate point of contact. At this point the impregnated fibre bundles converge together to form a ribbon. Due to the applied tension, a resin wedge region is formed. This can result in: (a) resin being squeezed into the fibre bundle; or (b) cause drips at the D-eye.

(ix) **Mandrel Impregnation** – Before winding the first layer of fibres the mandrel is coated manually with a layer of the resin system. Therefore, when the first layer of fibre is wound, they come into contact with the mandrel and generate another resin wedge which squeezes more resin into the fibre bundles. As further layers are wound, the pressure generated causes the resin within the fibres to be squeezed to the surface. However, this can lead to lower resin content in the inner (bore) layers of the composite.

4.1.1.2 Observations during the Production of Filament Wound Tubes

The following section summarises some of the observations made by the author during filament winding. It is emphasised that the processing conditions used for manufacturing the pipes are specific for a particular product. For example, the fibre

angle (hoop or specified angle), the thickness, the fibre tension and the fibre haul-off rate can be different per product type. Hence, it is difficult to attribute "cause and effect" without reference to the particular product. In practice, the uniformity of reinforcement (binder content, as-received fibre damage, etc.) is outside the control of the operator. However, experienced operators generally have the ability to make real-time modification to the processing conditions to obtain an acceptable product quality.

(i) **Fibre damage:** Figure 3.1 presented a schematic illustration of the overall layout of the filament winding station. The creels are stacked on a creel stand and guided through ceramic eyelets (see Figures 4.7 (i) and (ii)) prior to being presented to a linear array of eyelets.

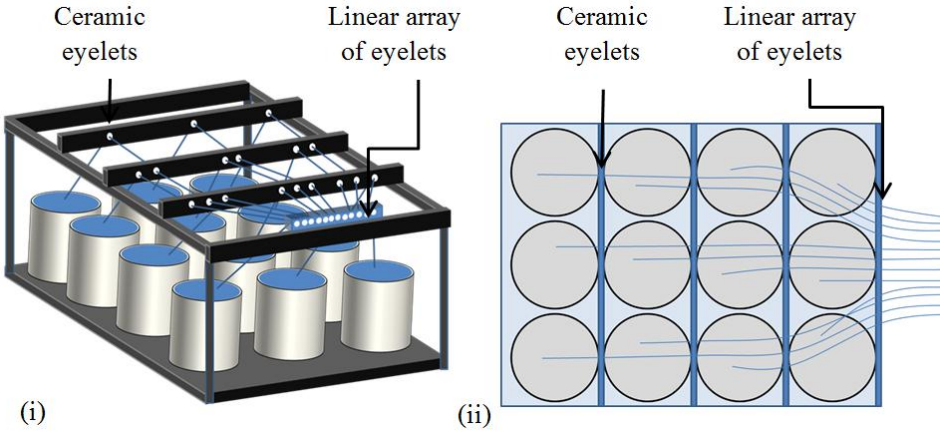

Figure 4.7 A Schematic showing the relative positions of glass fibre creels and the ceramic eyelets that guide the fibres from the creels: (i) an isometric perspective; and (ii) an aerial perspective.

As illustrated in Figure 4.7 (ii), the relative position of a creel within the stand dictates the number of the ceramic eyelets that the bundle is threaded through. In this region, the fibres are not under any significant tension as they are hauled from the centre of the creel (centre-pull). However, evidence of accumulated fibre damage was observed on the creel stand and this was probably due to damage in the as-received creels. The

function of the linear array of polymeric fibre guides is to present a parallel (see Figure 4.8 (ii)) array of fibre bundles to the tensioning device.

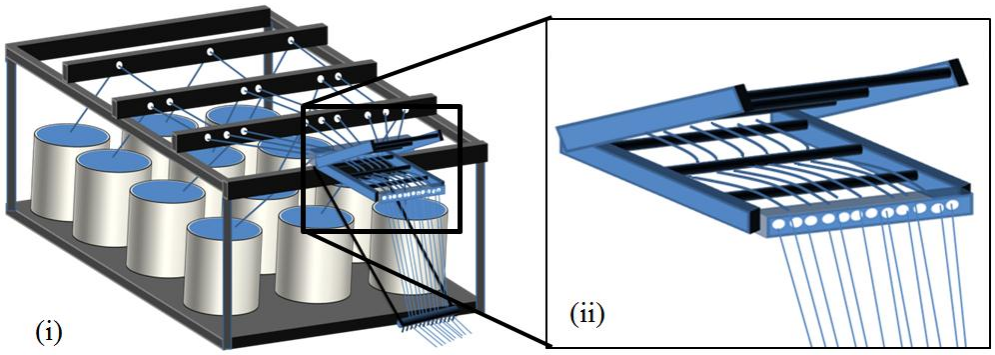

Figure 4.8 A schematic showing the pre-tensioning system. (i) The relative position of the pre-tensioning device to the creel stand, (ii) An enlarged view of the pre-tension device.

The tensioning device is shown in Figure 4.8 (i) and (ii) is the point at which any significant tension is applied to the fibres. This was a mechanically adjustable device where lowering the top-section increased the contact of the fibres with pins increasing the friction and thus the tension on the fibres; the lower the top-platform, the higher the tension experienced by the fibres.

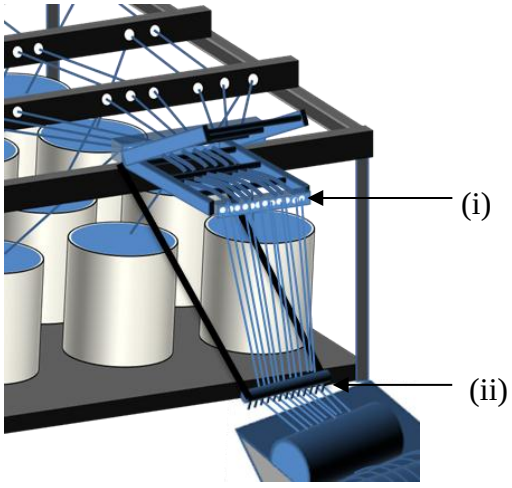

Figure 4.9 A schematic showing the change in fibre direction from the pre-tension device to the resin bath. (i) Metallic eyelet at the front of the pre-tension device directing fibres at a near 90 degrees. (ii) Guide pins are used to direct fibres to the resin bath at the required height and angle.

A metal plate with an array of metallic eyelets is positioned in front of the tensioning device. Due to the relative positions of the metallic eyelets and the resin bath (see Figure 4.9 at point (i)), the fibres are forced to take a near-ninety degree change in direction. A further change in the fibre trajectory is created (as illustrated in Figure 4.9 at point (ii)) in order to present the fibres at the required angle to the resin bath. In practice, it can be difficult to arrange the creels at the same level of the resin bath due to space constraints or because of the number of creels involved in the production process.

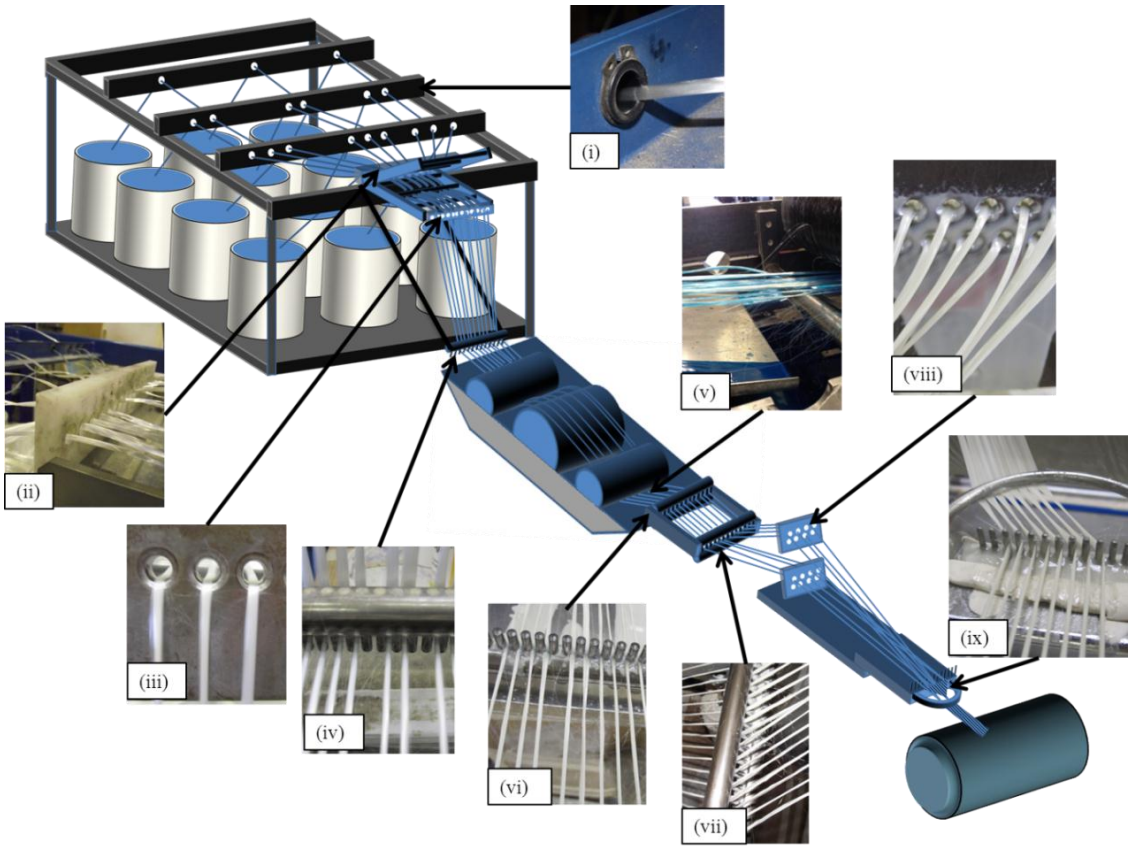

Figure 4.10 A schematic with photographs to highlight the observed areas of fibre damage during filament winding.

With regard to visually observed fibre damage, Figures 4.10 and Table 4.1 show the areas where fibre damage was observed. The highest concentration was found after the fibres exited the metallic eyelets, item (iii) in Table 4.1.

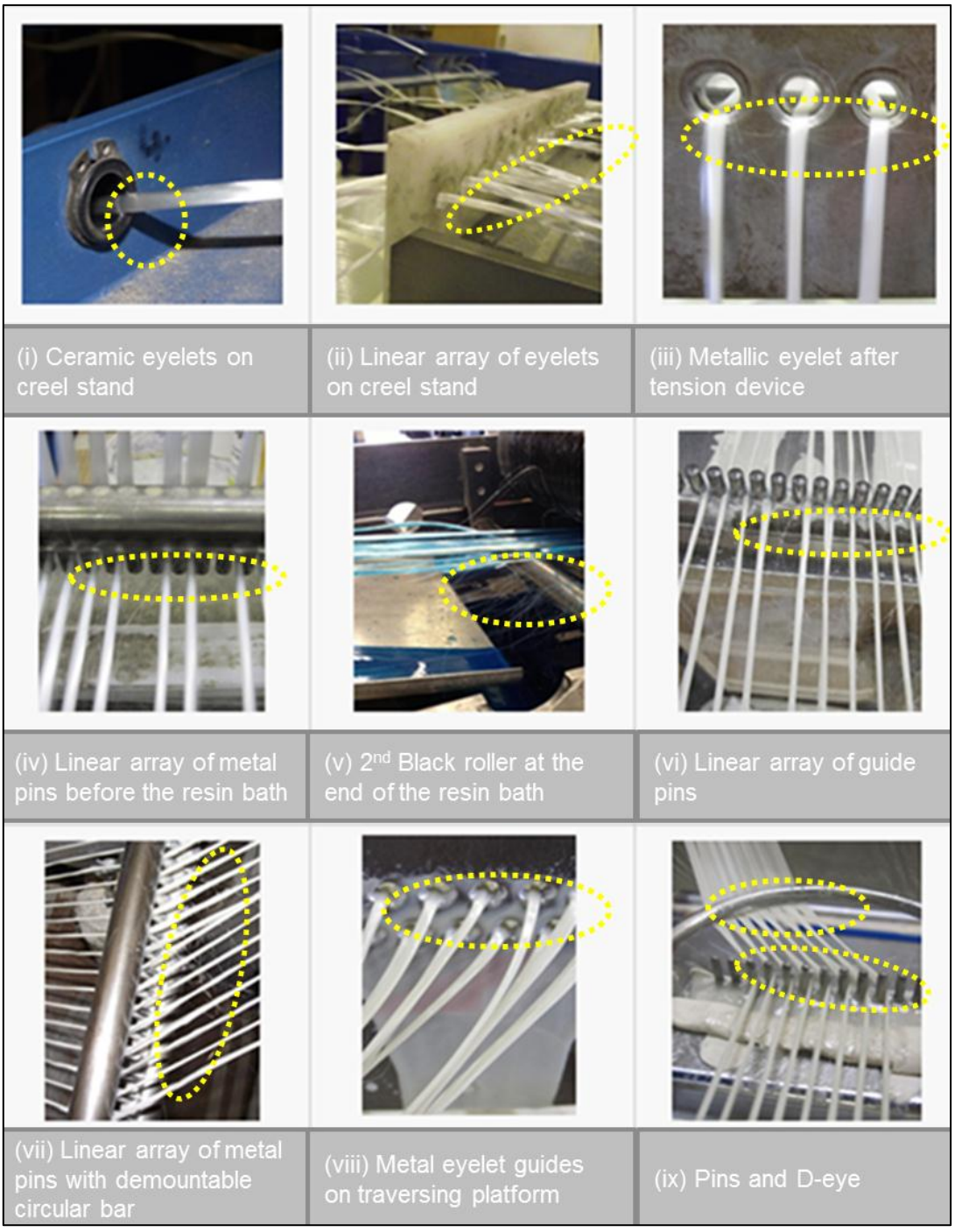

Table 4.1 Magnified photographs taken from Figure 4.10 showing areas of fibre damage occurring during conventional filament winding. The dotted circles highlight the areas where the fibre fractures were detected.

In instances where the level of fibre damage was observed to be high, this was found to be translated to the subsequent regions within the resin bath. It was initially envisaged

that any evidence for damaged fibres would "vanish" upon impregnation as the loose ends are held together by the resin. However, this was not observed to be the case for three reasons. Firstly, as the fibres reach the impregnation drum, the fibres are not impregnated evenly. Therefore, in instances where the presence of surface-based fibre fractures coincides with the un-impregnated regions, they adhere to subsequent processing equipment that have come into contact with the resin – this is illustrated in Figure 4.10 (v). Secondly, although no direct evidence was obtained or measured, it is possible that the fractured fibres on the surface of the bundle were subjected to electrostatic attraction over the metal surfaces that they were drawn over. Finally, it was observed that when a broken filament adhered to the drum or the components downstream with a coating of the resin; they tended to be separated from the bundle and accumulated as "fuzz". In some instances, these were transferred to the mandrel. The variability in the consistency of the as-received fibre bundles is discussed in Section 4.2.

In the context of the mechanical properties of filament wound composites, it is known that significant fibre fractures will lead to a reduction in the mechanical properties. Ahmadi and Oskouei, (2009) attributed the strength of glass fibres bundles to their surface condition. They speculated that damage can be induced during the manufacturing process and handling of the fibres. They stated there was a general trend towards lower strength with increasing surface damage.

(ii) **Visually observed impregnation:** The filament winding trials were carried out at 7 m/min and 21 m/min (measured as the linear fibre haul-off rates). It was observed visually that the apparent degree of impregnation decreased as the winding speed was increased. This can be inferred from Figure 4.11 (i) and (ii) where the under impregnated fibres have been circled and indicated with arrows. It was difficult to infer

the degree of impregnation of the fibre bundles on the top of the drum because at this point, some fibre spreading takes places and as the fibres are impregnated, they appear translucent. The reflection from the surface of the steel drum also tended to reduce the contrast between the impregnated and un-impregnated regions. However, these artefacts are not present within the circled regions where the areas of under impregnation are clearer.

Figures 4.11 (i) and (ii) and 4.12 (i) and (ii) show the observed level of impregnation for the tubes that were manufactured at linear fibre haul-off rates, corresponding to 21 and 52 m/min respectively. In both figures, the under impregnated areas are indicated by arrows. It is possible to see the limited impregnation that occurred for a 10 inch mandrel winding at ~21 m/min. This image shows the lack of impregnation of the fibres at the resin bath. This can also be seen in Figure 4.12, which is for a 10 inch mandrel winding at ~52 m/min. The residence time of the bundle on the impregnation drum plays an important role on the volume of resin transferred to the fibres. At the higher winding speeds a lack of impregnation at the impregnation drum can result in poorly impregnated fibres at the mandrel.

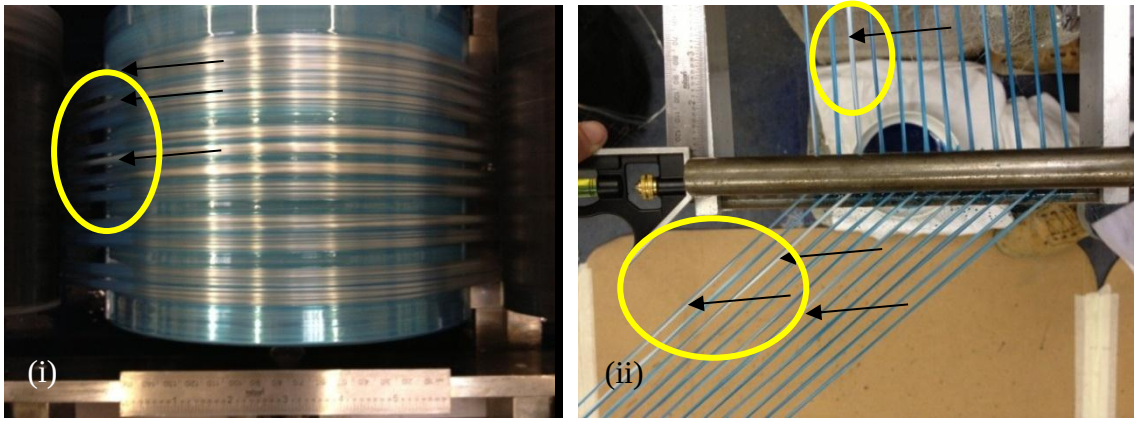

Figures 4.11 Photographs (i) and (ii) show the under-impregnation at specified regions within the fibre bundles. Here, a 10 inch mandrel was used along with a linear fibre haul-off rate of 21 m/min during conventional winding.

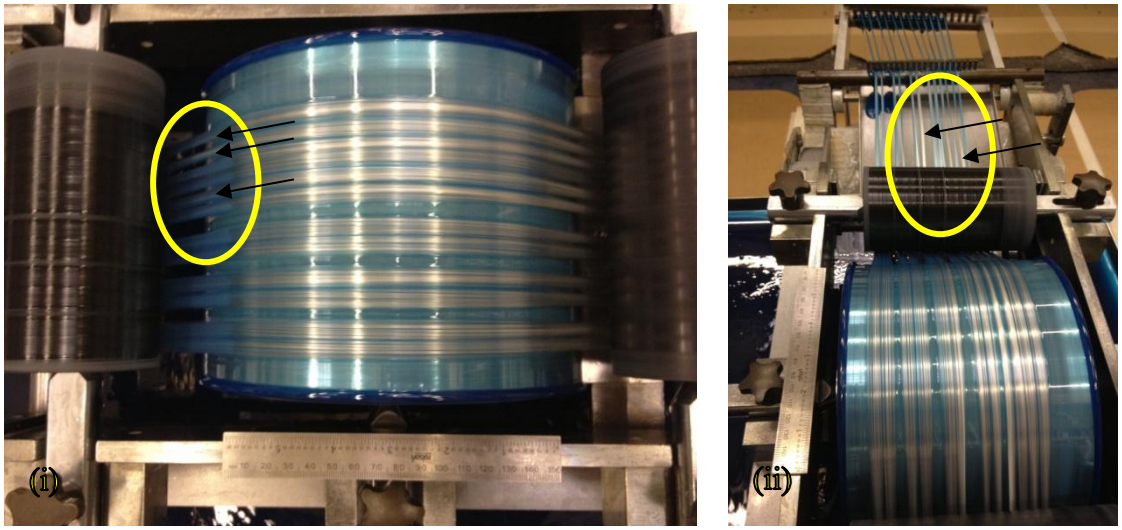

Figures 4.12 Photographs (i) and (ii) show limited impregnation occurring for a 10 inch mandrel winding at 52 m/min over a conventional impregnation drum.

It was difficult to generalise if these under-impregnated regions are transferred to the mandrel because: (i) Additional pickup or further resin depletion (via scraping when in contact with the processing equipment) is possible as the partially impregnated fibre bundles are hauled through to the mandrel. However, it was observed that when a bead of resin was present on the D-eye, whilst the majority of the under-impregnated areas were re-impregnated; this was not always the case. This variability may be attributed to the binder content (discussed in Section 4.2), the extent of fibre spreading experienced at each of the contact points, and the volume of the resin that has accumulated on the processing equipment at these points before they drip. (ii) The intrinsic twisting of the fibre bundle during centre-pull is likely to be another plausible reason for the observed variations.

(iii) **Controlling the resin volume fraction**: In general, this was controlled by the doctor-blade setting, the affinity of the fibre bundle to be wetted and impregnated by the resin, and distance between the impregnation drum and the mandrel. However, as

discussed previously, the extent to which the resin is scraped off the fibre bundle is also a contributing factor. Accepting that manufacturing procedures and protocols will differ, in some circumstances it may be more productive to over-impregnate the fibres, collect the drips and then reintroduce it to the resin bath. In addition the excess resin at the mandrel was removed manually as illustrated in Figure 4.13. When un-impregnated fibre bundles are observed on the mandrel, manual intervention was used to rectify the problem. The excess resin was sometimes returned to the resin bath or used to coat the mandrel before the first layer of the impregnated fibres were wound.

Figure 4.13 A photograph showing the manual intervention carried out on a 10 inch diameter mandrel during conventional filament winding to remove the excess resin and/or to impregnate the under-impregnated areas.

In circumstance where the doctor-blade does not extend to cover the length of the drum, excess resin was seen to be picked up at the edge regions during the stationary period of the traversing platform. This excess resin subsequently meanders to the impregnation region of the drum leading to a higher resin fraction than desired.

(iv) **Aeration of the resin bath:** At the higher winding speeds, it was observed that aeration of the resin bath was significant. As the impregnation drum rotates, a vortex was seen to form between the drum and the resin surface of the liquid level. This had

the effect of drawing and trapping air in the resin. The aeration of the resin bath is shown in Figure 4.14 (i), (ii) and (iii). However, there was no obvious evidence to indicate if these bubbles were transferred to the mandrel. When the under impregnated fibres reach the mandrel, manual resin application was used to ensure there was adequate resin on the tube to impregnate the dry fibres (Figure 4.13).

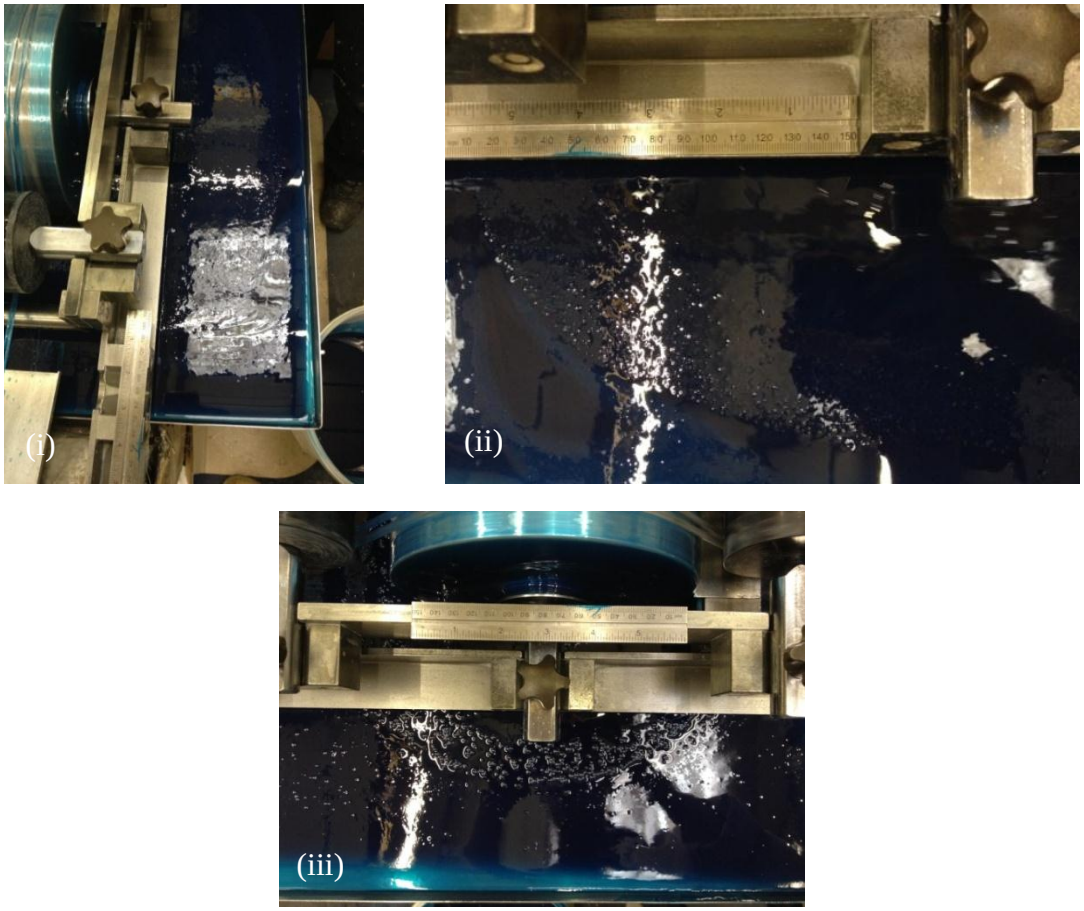

Figure 4.14 Photographs (i), (ii) and (iii) show the aeration occurring in the conventional resin bath during filament winding at higher speeds.

(v) **Peel-ply:** A peel-ply was used to overwrap the composite tubes to make them safe to handle, this was found to contribute to the impregnation process by retaining the resin on the mandrel. As the mandrel is heated to progress the cross-linking of the resin, the

viscosity of the resin is initially lowered. Since the resin was contained in this instance, it aids further impregnation.

In summary:

(i) The degree of impregnation, as observed visually, was variable and it was progressively poorer at winding speeds corresponding to 52 m/min.

(ii) Several different factors have been found to account for the variability in the volume of resin that was picked up at the impregnation drum including, the intrinsic twist on the fibre bundles.

(iii) Manual intervention was used in some instances to control the resin volume fraction and the extent of impregnation at the mandrel.

(iv) Each of the contact points between the impregnated fibre bundle and the processing equipment requires a container to collect the drips.

The clean filament winding process was designed to eliminate some of the issues associated with conventional filament winding. As mentioned in the design criteria (Section 3.1.3.1) of the Experimental, the clean filament winding impregnator Prototypes-1 and 2 aimed to address these issues.

The following section discusses the parameters required for, and used in, the clean filament winding industrial site trials.

4.1.1.3 Conventional Filament Winding: Winding Parameters

4.1.1.3.1 Fibre Bundle Tension

The first series of conventional filament winding trials were undertaken to establish the optimum processing parameters. A summary of the tubes that were manufactured on an industrial machine on-site is shown in Table 4.2. This also presents a summary of the physical and mechanical properties of the tubes wound at 7 m/min as a function of the applied fibre bundle tension. Each of the tubes produced was tested to ascertain the density, fibre volume fraction, void content, hoop tensile strength testing and microstructural makeup of the tubes.

Winding	Resin System	Fibre (Type-I)	No. of Layers	Mandrel Diameter (mm)	Winding Speed (m/min)	Winding Angle	Fibre Tension (kg)	Density (kg/m^3)	Fibre Volume Fraction (FVF) (%)	Void Content (%)	Hoop Tensile Strength (MPa)	Hoop Tensile Strength Normalised to 55% FVF
Conventional Filament Winding	CRYSTIC 397 PA Polyester	8 x 2400 tex	4	106	7	Hoop	5	1914.35 (±7.57)	52.07 (±0.37)	1.31 (±0.35)	1013.63 (±59.15)	1070.74
Conventional Filament Winding	CRYSTIC 397 PA Polyester	8 x 2400 tex	4	106	7	Hoop	10	1933.26 (±14.51)	53.71 (±0.66)	1.7 (±0.77)	940.27 (±56.63)	962.92
Conventional Filament Winding	CRYSTIC 397 PA Polyester	8 x 2400 tex	4	106	7	Hoop	15	1956.31 (±6.4)	54.85 (±0.43)	1.15 (±0.16)	968.56 (±55.04)	971.13
Conventional Filament Winding	CRYSTIC 397 PA Polyester	8 x 2400 tex	4	106	7	Hoop	18	1984.84 (±10.99)	56.76 (±0.73)	1.07 (±0.12)	881.04 (±52.28)	853.64

Table 4.2 A summary of the mechanical and physical properties of conventionally would filament wound tubes as a function of applied tension.

Figure 4.15 shows average fibre volume fraction measurements for the composites manufactured on site using the fibre bundle tension rates of 5, 10, 15 and 18 kg, at a linear fibre haul-off rate of 7 m/min. A linear trend was seen for the fibre volume fraction as a function of the applied fibre bundle tension. An explanation for the

apparent linearity was the increased compaction of the fibre bundles with increasing applied tension as they are wound over the mandrel. Since the fibres have a higher density when compared to the resin, in the absence of significant voiding, the density of the composite will show an increase with the applied fibre bundle tension (illustrated in Figure 4.16). This observed increase in the density as a function of the fibre bundle tension is due to an increase in the degree of fibre compaction (Mertiny and Ellyin, 2002). The scatter of data for the 10 kg tension tube was higher when compared to the other three datasets. The findings regarding void content are also represented in Figure 4.17. It can be seen that the scatter for the 5 and 10 kg fibre bundle tension is significantly higher 0.35 and 0.31% when compared to the 15 and 18 kg fibre bundle tensions of 0.16 and 0.12%, respectively. A possible reason for this is the expulsion of trapped air and voids with greater compaction at the higher applied fibre bundle tension.

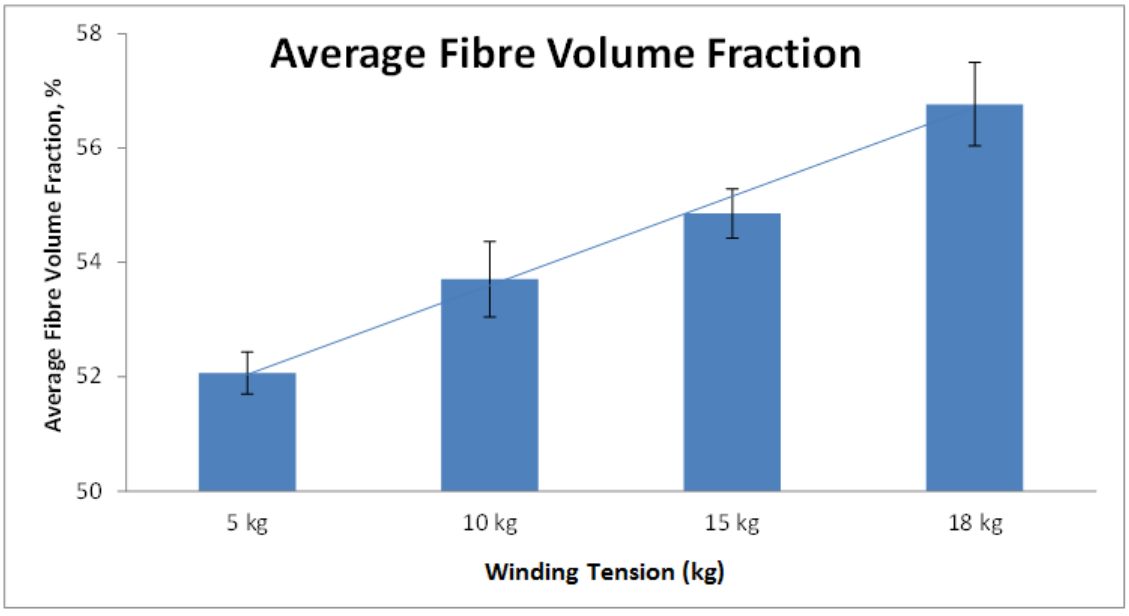

Figure 4.15 A graph showing the average fibre volume fraction measurements for the composite tubes wound at 5, 10, 15 and 18 kg fibre bundle winding tensions.

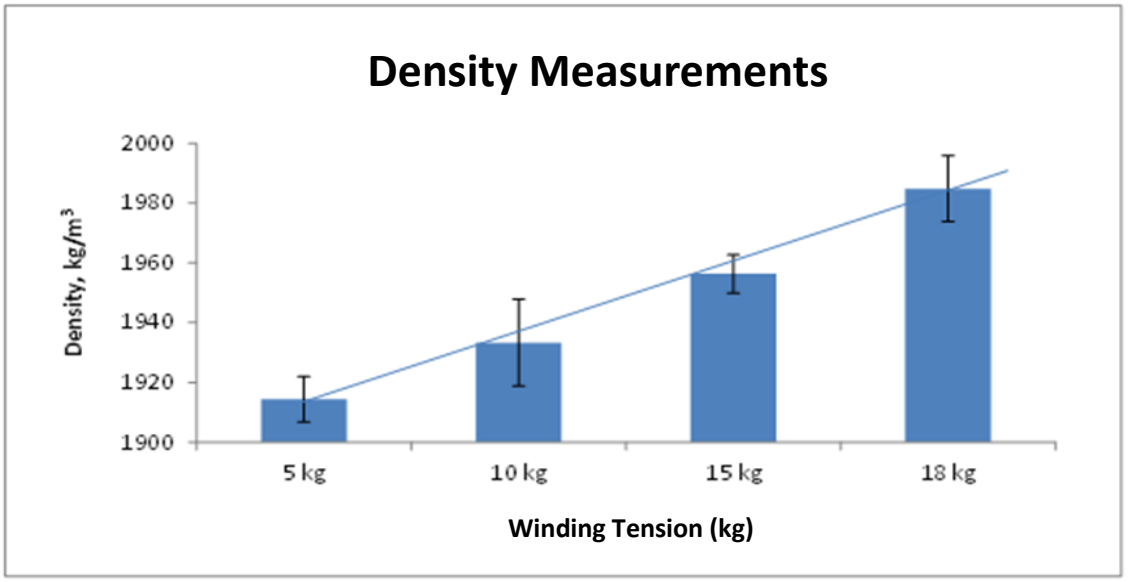

Figure 4.16 A graph showing the density measurements for the composite tubes wound at 5, 10, 15 and 18 kg fibre bundle tensions.

The density of the filament wound composites correlate with the data presented in Figure 4.16 where a small increase in the fibre volume fraction is observed with the applied tension. This observation is in agreement with Aleong and Munro (1991), who suggested that during filament winding the problems with packing efficiency was due to a low tension of 300 MPa, which would result in a lower fibre volume fraction. However, Haupert and Friedrich (1995) demonstrated that minimising the fibre bundle tension (20 N) to allow resin flow into the fibre bundles lowered the void content. They believed the higher fibre bundle tension and the resulting consolidation would lead to fibre damage. This is not in agreement with the findings of the current study which demonstrate slightly higher void contents at the lower comparable tensions (see Figure 4.17).

With reference to the binder that is present on the fibre bundle (discussed in Section 4.2), increasing the tension does not directly aid the de-cohesion of the binder. Instead, it was the path taken by the fibre bundle with regard to its trajectory from the creel to

the impregnator. In the current case, a schematic of the tensioning device is illustrated in Figure 4.8. As the tension is increased, the degree of undulation and lateral forces experienced by the fibre bundle increases. It is proposed that this, and the other fibre guiding devices (pins, bars, rollers), can aid in the de-cohesion of the binder thus enhancing the impregnation efficiency.

The void content in relation to the manufacturing tensions of the fibre bundles is shown in Figure 4.17. It can be seen that there is a significantly larger standard deviation in the void content for the composites that were manufactured using lower winding tension (5 and 10 kg).

The formation of voids in filament wound tubes can be caused by a number of factors including the tension on the fibre bundle. Mertiny and Ellyin, (2002) demonstrated that increasing fibre tension increases the consolidation of the fibres, which governs the physical properties, as well as reducing the voids within the part. This is in agreement with Cohen, (1997) demonstrated the average void content in the composite was significantly affected by winding tension. Higher winding tension of 72 lb (33 kg) was found to result in a composite with a 23% lower void content by volume.

With reference to Figures 4.15 and 4.17, in the current study, the composites manufactured with a tension of 18 kg produced the highest average fibre volume fraction and the lowest average void content, followed by the 15 kg fibre tension. Although the composites manufactured using a tension of 10 kg displayed a significantly higher average void content when compared to samples produced using tensions of 15 and 18 kg, this trend was not observed for the 5 kg dataset. The scatter in the 10 kg samples was the highest when compared to the other three composites.

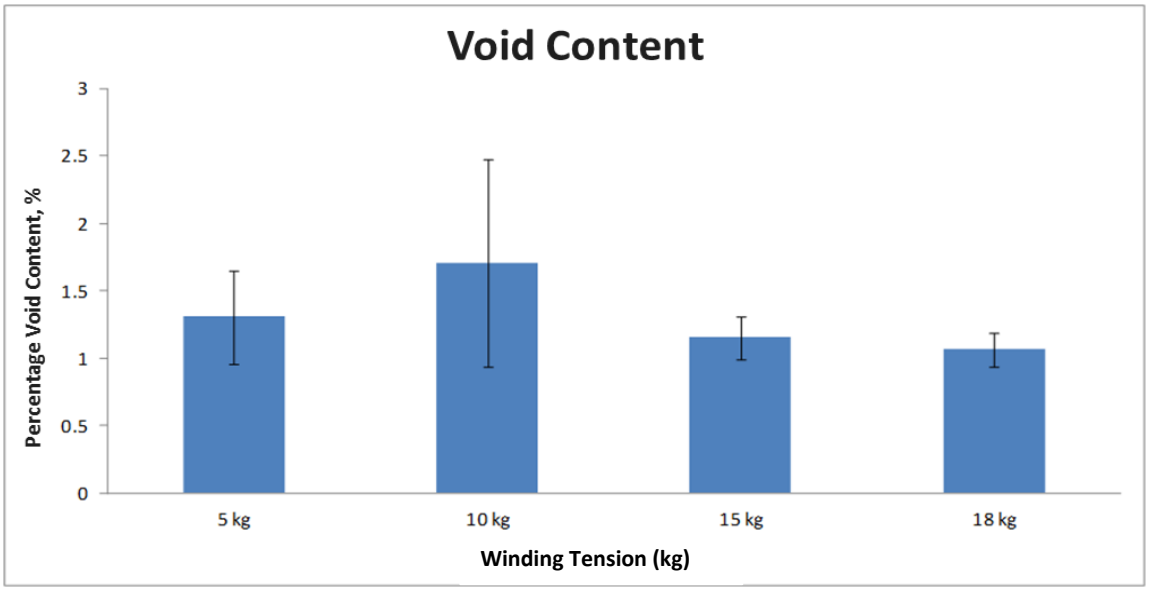

Figure 4.17 A graph showing the void content measurements for the composite tubes wound at 5, 10, 15 and 18 kg fibre bundle tensions.

The determination of the void content was carried out in accordance with ASTM D2734. As seen in Figure 4.17, larger standard deviations were observed in the void content for composites produced at tensions corresponding to 5 and 10 kg. On inspecting the void content datasets presented in Appendix C, it was seen that for one each of the six samples for the 5 and 10 kg fibre tensions have a significantly higher average void content than the other samples. If these outliers are removed from the 5 kg and 10 kg samples, there is a much better correlation with findings reported previously in the literature. It is generally known that voids can have a detrimental effect on the mechanical properties of composites (Mertiny and Ellyin, 2002).

In addition to the void content reported in the previous section (in Figure 4.17), image analysis of polished samples was carried out and these are presented in Figures 4.18, 4.19, 4.20 and 4.21 for the 5, 10, 15 and 18 kg tubes respectively. On inspecting these micrographs, it was readily apparent that the macroscopic void content indicates an

increase in the void content as the tension was increased from 5 kg to 18 kg. However, a surprising feature was that the voids seem to be clustered. This may be in-part, due to variability in the binder content in the fibre bundle, the intermittent poor impregnation discussed in Section 4.2 and the transfer of fractured fibre debris to the mandrel at the higher applied fibre bundle tensions.

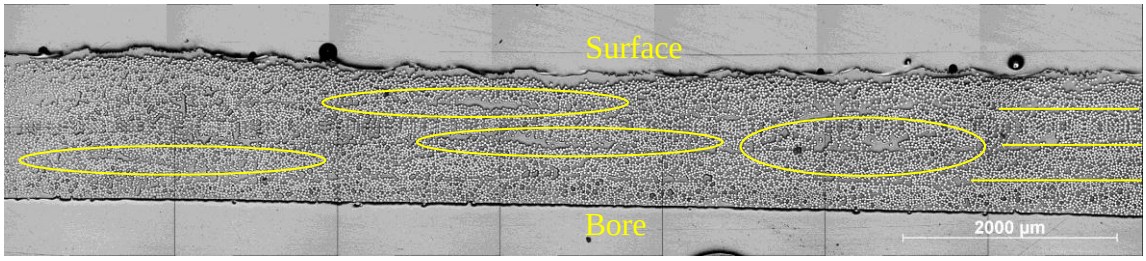

Figure 4.18 A collage of micrographs for a conventionally wound composite tube with an applied tension of 5 kg. The dashed horizontal lines represent the layers of the composite tube.

The following features are apparent in Figure 4.18:

(i) The bore of the tube (bottom) appears smooth when compared to the surface (top).

(ii) The boundaries between the four layers, or plys, are indicated by the dotted lines. With reference to the circled areas, the extent of bundle-to-bundle-nesting was not apparent in the 4-layers as distinct resin-rich boundaries can be observed. The extent of the resin-rich regions was seen to be more prominent in progressing from the bore to the surface.

(iii) The void content was negligible in these micrographs but it does highlight the fact that inferring the void fraction based on image analysis can be misleading. However, the collage of micrographs presented here does correlate with the trend observed previously in Figure 4.17 for the void content.

The macroscopic appearance of a collage of transverse section for tubes manufactured with tensions corresponding to 10 kg, 15 kg and 18 kg are presented in Figures 4.19, 4.20 and 4.21 respectively.

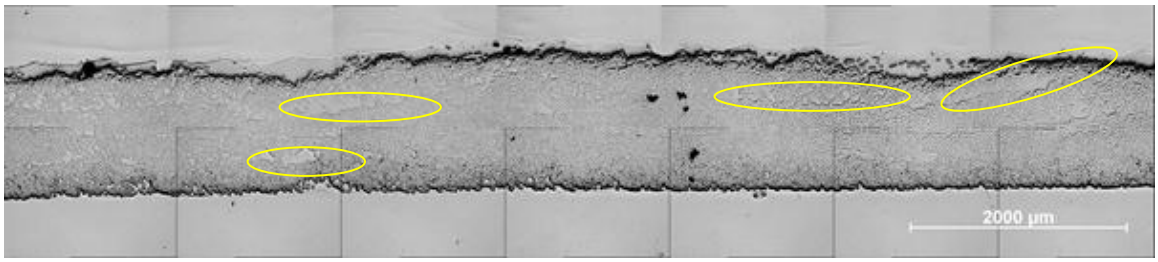

Figure 4.19 A collage of micrographs representing transverse sections of a tube that was manufactured using a fibre bundle tension of 10 kg.

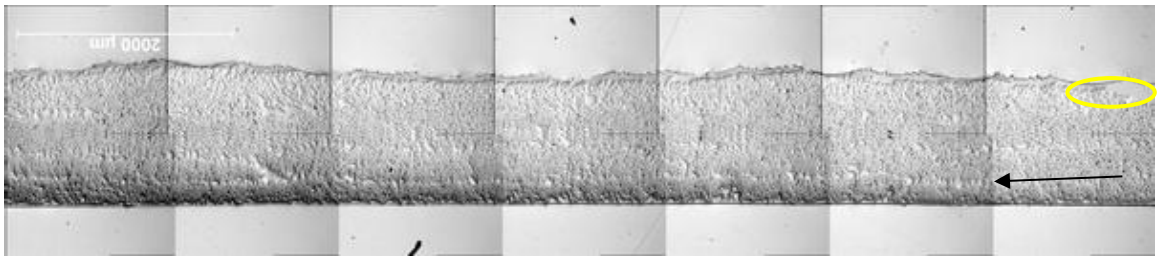

Figure 4.20 A collage of micrographs representing transverse sections of a tube that was manufactured using a fibre bundle tension of 15 kg. Scale bar is upside down for comparison purposes.

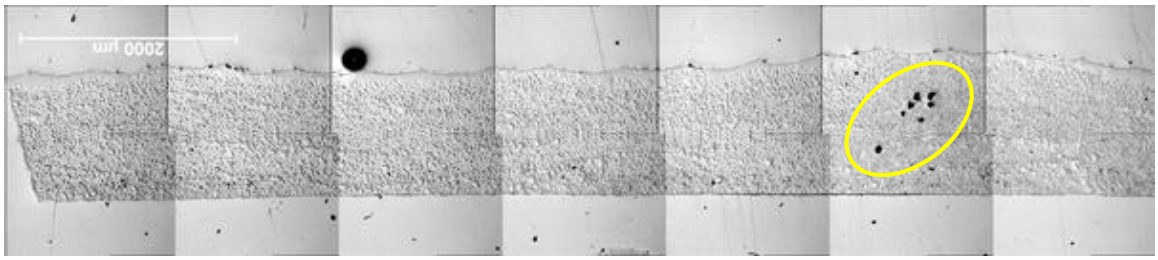

Figure 4.21 A collage of micrographs representing transverse sections of a tube that was manufactured using a fibre bundle tension of 18 kg. Scale bar is upside down for comparison purposes.

On comparing the micrographs for the 4 levels of applied tension, the following conclusions can be reached:

(i) The distribution of resin-rich regions along the ply interface is seen to decrease as the tension is increased.

(ii) The uniformity of the bore was most variable for the 10 kg fibre bundle tension. Moreover, significant undulations are observed in the surface regions along with large pockets of resin-rich regions on the surface.

(iii) The bore region in Figure 4.20 indicates a resin-rich region. A distinct resin-rich region was also observed between the bore-ply and the second ply; this is indicated by the arrow. It was disclosed previously that a layer of the resin system was applied manually to the mandrel surface prior to the filament winding operation. It was speculated that the resin-rich border between plies 1-2 may be due to a consequence of this where the resin from the mandrel and the impregnated fibre bundles are squeezed to the surface as the first ply is wrapped on the mandrel.

(iv) A resin-rich region, of a variable volume fraction was observed on the surface of the filament wound tube. As discussed previously, the manual intervention of the operator during the winding operation in this instance was based on visual observations and the experience of the operator. The production criterion was predominately driven by the visual assessments of the degree of impregnation, and the volume of resin that was present on the surface. Furthermore, after the excess resin on the surface was removed manually (see Figure 4.13), a peel-ply was wrapped over the surface manually; the tension in this instance was a variable.

The above-mentioned issues are likely to have contributed to the observed variability in the physical properties.

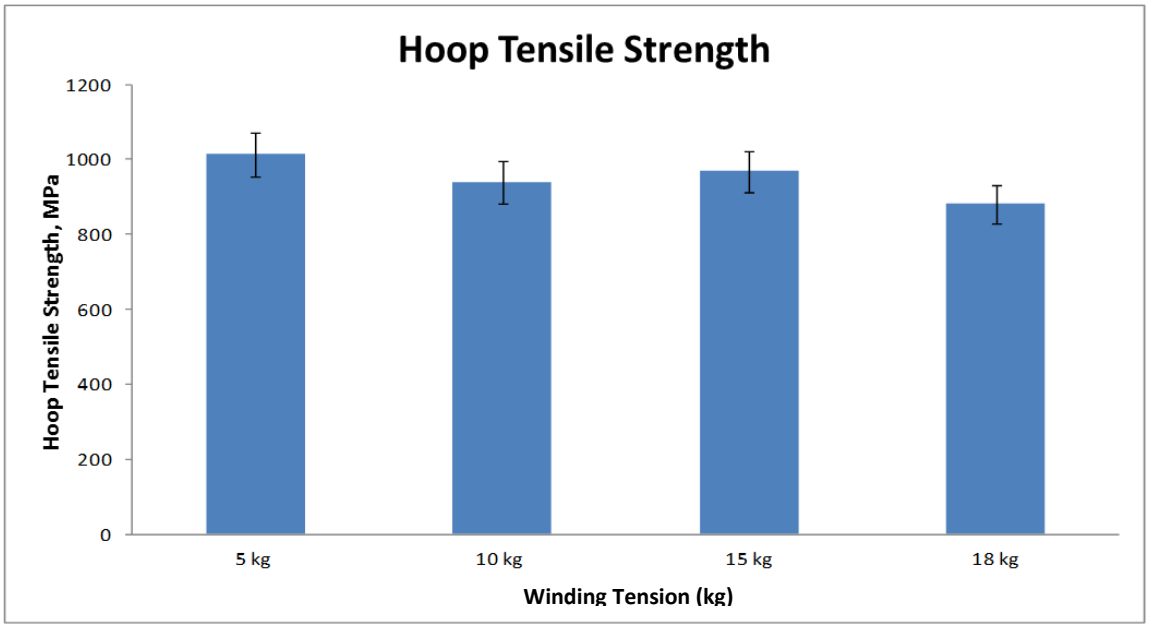

Figure 4.22 A graph showing the hoop tensile strength of composite tubes wound at 5, 10, 15 and 18 kg fibre bundle tension.

The hoop tensile strength data for the tubes wound at specified levels of fibre tension are shown in Figure 4.22. With the exception of the 15 kg fibre tension dataset, the general trend seen was a decrease in the hoop tensile strength with increasing tension. This could potentially be due to increased fibre damage. Aleong and Munro, (1991) found that excessive fibre damage occurred when winding tension was greater than approximately 45 MPa. The hoop tensile tests were carried out using the procedures specified in ASTM D2290 where a minimum of five sample rings was recommended. In the current work, six individual samples were used and these were obtained from the central region of the tube. On comparing the hoop tensile strengths for the tubes manufactured at 5 and 18 kg of fibre tension, a noticeable reduction is observed. However, the hoop tensile strength of filament wound tubes can be influenced by a number of factors including the following.

(i) Filament winding machine: Due to the age of the machine that was used in the site trials, the traverse rate was not constant across the length of the 3 m mandrel. This meant that the deposition of the impregnated fibre bundle was not consistent. In other words, random gaps were introduced between the fibre bundles during the winding process. However, it was observed that the centre region of the mandrel showed the lowest variability in terms of wind angle, speed of traversing arm and spacing between the fibre bundles.

(ii) Manual intervention: As mentioned previously, it was customary for the operator to deposit additional resin on the surface of the tube during the winding operation. This manual intervention was based on the significant experience of the operator where additional resin was introduced to compensate for patches of poorly impregnated areas. Although the doctor-blade on the drum-impregnator was pre-set, adjustments were made sometimes to ensure the presence of a constant resin film on the surface of the drum. As stated previously, on occasions, towards the end of the winding operation, excess resin was removed manually.

(iii) The hoop tensile specimen: In the current programme, a custom-made jig was used to ensure that the notches were positioned diametrically opposite. The notch was introduced using a 7 mm diameter diamond coated milling piece and the surface was abraded using 1200 grit abrading paper. Although these procedures were implemented to ensure consistency in the notch profile and surface, the variations in the fibre volume fractions or degree of compaction in the vicinity of notches may have contributed to scatter in the datasets.

As a result of the data presented in Section 4.1.1.3.1, the winding tension of 15 kg was deemed the optimum. It was therefore decided that for all subsequent experiments, combined fibre bundle tension of 15 kg would be used to ensure that a comparison between the results could be achieved.

4.1.1.3.2 Filament Winding Speeds

The following section reviews the results of tubes that were manufactured via conventional filament winding using epoxy/amine and polyester resins at 7 and 21 m/min. The length and the inner bore diameter of the mandrel were 150 mm and 106 mm respectively. From here on, these tubes will be referred to as the "reference" tubes to enable comparison with the clean filament winding production process. The tubes parameters and their properties are displayed in Table 4.3.

Winding	Resin System	Fibre (Type-I)	No. of Layers	Mandrel Diameter (mm)	Winding Speed (m/min)	Winding Angle	Fibre Tension (kg)	Density (kg/m^3)	Fibre Volume Fraction (FVF) (%)	Void Content (%)	Hoop Tensile Strength (MPa)	Hoop Tensile Strength Normalised to 55% FVF
Conventional Filament Winding	LY3505/XB3403 epoxy/amine	8 x 2400 tex	4	106	7	Hoop	15	1967.36 (± 11)	56.7 (± 2.1)	3.5 (± 0.7)	847.35 (± 29.92)	822
Conventional Filament Winding	LY3505/XB3403 epoxy/amine	8 x 2400 tex	4	106	21	Hoop	15	1942.47 (± 49.2)	55.37 (± 1.38)	4.2 (± 0.3)	812.61 (± 31.01)	807.24
Conventional Filament Winding	CRYSTIC 397 PA Polyester	8 x 2400 tex	4	106	7	Hoop	15	1952.64 (± 7.96)	54.86 (± 0.34)	1.28 (± 0.22)	707.16 (± 26.62)	709.01
Conventional Filament Winding	CRYSTIC 397 PA Polyester	8 x 2400 tex	4	106	21	Hoop	15	1953.1 (± 10.05)	54.45 (± 0.43)	1.47 (± 0.39)	686.2 (± 14.64)	693.18

Table 4.3 A summary of the physical and mechanical properties of the tubes manufactured using the conventional filament winding process with tubes manufactured at different winding speeds and with specified resin systems.

The physical properties for the conventional filament wound samples manufactured at different winding speeds on-site are presented in Figures 4.23-4.25. Figure 4.23 shows the average fibre volume fractions, measured using the procedure outlined in Section 3.1.6.3. The samples were manufactured by the author with assistance from the operators in the factory for the two resin systems along with the linear fibre haul-off rates of 7 m/min and 21 m/min. Both winding speeds are used on a regular basis by the industrial winding company to manufacture composite tubes for customers.

In Figure 4.23, the degree of scatter in the epoxy resin-based tubes is higher than that observed for the polyester resin. The average fibre volume fractions for the polyester-based tubes are between 54.86% and 54.45% whereas those for the epoxy resin are 56.7% and 55.37% respectively. The small variations within the results of each tube may be attributed to localised variations in the fibre distribution.

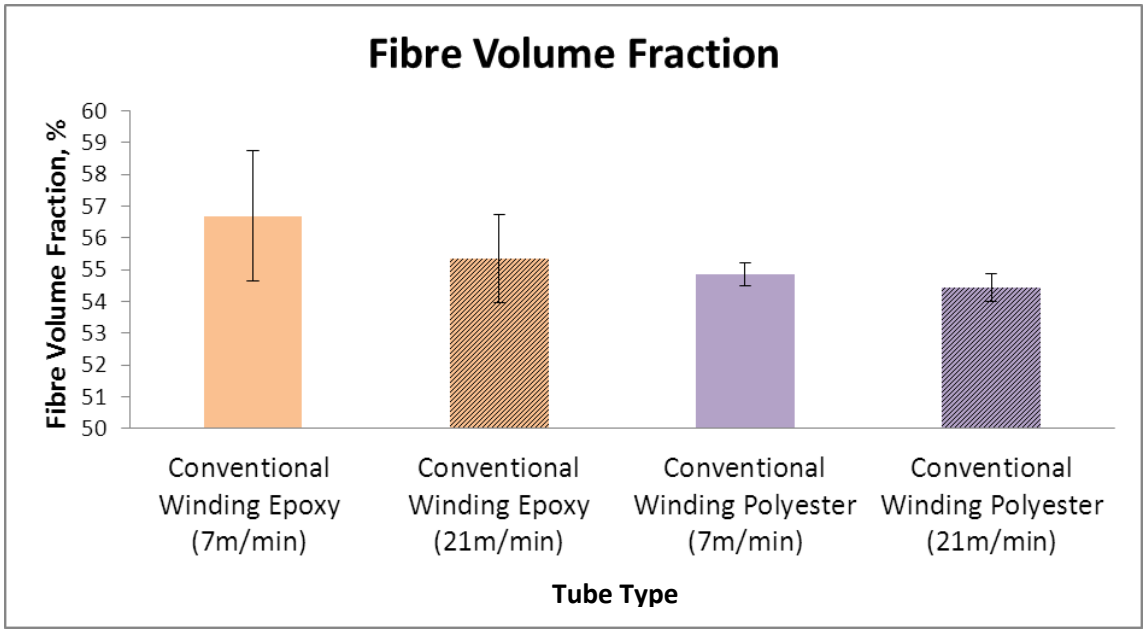

Figure 4.23 A graph showing the average fibre volume fractions for the reference tubes wound at 15kg produced using the polyester and epoxy resin systems, wound at 7 m/min and 21 m/min. The Y-axis has been expanded to help view the degree of scatter for each of the datasets.

The fibre volume fraction values seen in Figure 4.23 show the conventionally wound tubes to have approximately 50-60% for a glass fibre/epoxy filament wound tube. Cohen, (1997) found that having a higher fibre volume (around 68%) in the first hoop ply would tend to give higher composite strength. Cohen related the higher fibre volume fraction to the fibre motion through the resin and commented on the tension and resin viscosity being two of the key factors. It was said that both high-tension and low-viscosity result in higher fibre motion through the resin and therefore larger fibre compaction resulting in a higher fibre volume.

The viscosity of the epoxy differs from that of the polyester. For the epoxy resin used in this study the viscosity is stated as being between 300-400 mPa.s (Huntsman Advanced Materials, UK) whereas the viscosity of the polyester resin without the hardener component or other additives is stated as 240 mPa.s (Scott Bader, UK). Viscosity can also affect the void content in composites as seen in Figure 4.25. Park *et al.,* (2011) stated that if resin viscosity is low, capillary wicking in the compact sections of the fibre bundle leads the resin flow front. This is opposed to a high resin viscosity, in which the flow into the larger spaces within the fibre bundle leads the resin flow front. An imbalance in either can result in the formation of voids which can be seen in Figure 4.25. Epoxy has a higher viscosity than polyester and therefore the wicking or capillary impregnation occurring between the filaments is much slower than the rate of impregnation occurring at other areas of the composite. This can result in the formation of voids.

Park *et al.,* (2011) described two mechanisms for the formation of voids. The first is nucleation and growth of voids during cure. The second is mechanical air entrapment during impregnation of fibre bundles. As described by Bayramli and Powell (1991)

mechanical air entrapment is a result of non-uniform flow caused by random packing of fibre filaments within a fibre bundle. This gives the fibre bundle a heterogeneous microstructure. Void formation is caused by faster impregnation in large gaps, and slower impregnation in the closely packed fibres with smaller gaps. Voids of this nature can be characterised by two different types, micro-pores (inside the fibre bundle), and macro-pores (open gap between fibre bundles) (Park *et al.*, 2011). In macro-pores, viscous flow is more dominant whereas capillary wicking is more dominant in micro-pores.

Figure 4.24 presents a summary of the densities for the two classes of resins and filament winding speeds corresponding to 7 m/min and 21 m/min. The measured densities for the polyester resins were 1952.64 kg/m^3 (7 m/min) and 1953.1 kg/m^3 (21 m/min) and for epoxy resins were 1967.36 kg/m^3 (7 m/min) and 1942.47 kg/m^3 (21 m/min). The scatter in this case is seen to be largest at 49.2 kg/m^3 for the tube manufactured using epoxy resin at 21 m/min.

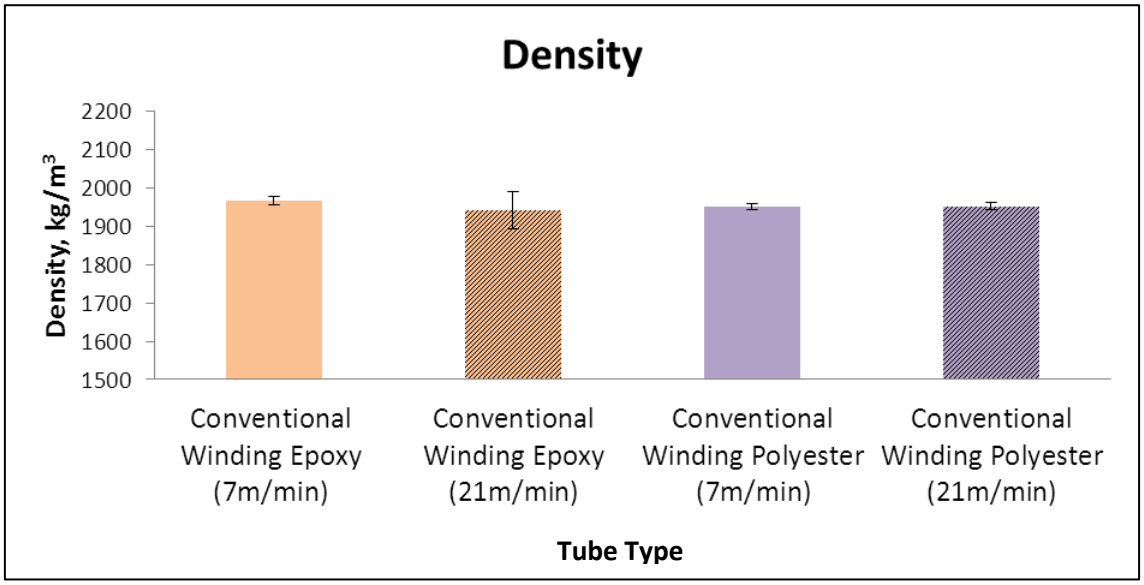

Figure 4.24 A graph showing a summary of the densities for the reference tubes wound at 15kg produced using polyester and epoxy resin systems at liner haul-off speeds corresponding to 7 m/min and 21 m/min.

From Figure 4.25 it can be seen that at higher winding speeds there is an increase in the average void content measured. This could be due to a reduced contact time in the wedge regions that promote impregnation. Thus, the fibres rely on the capillary impregnation to impregnate which is significantly slower than pin impregnation. This can be seen to a greater extent in the epoxy samples due to the increased viscosity of the resin. Pandita *et al.*, (2012) demonstrated how decreasing the viscosity of the resin reduces the impregnation time through-the-thickness of a stationary fibre bundle.

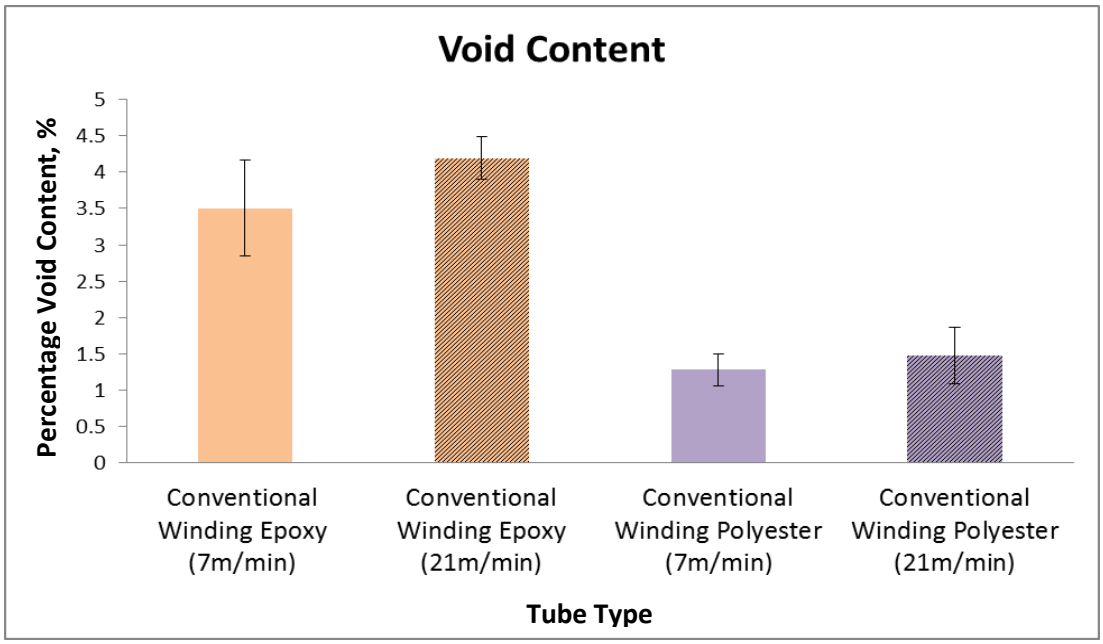

Figure 4.25 A graph showing the measured void contents for the reference tubes wound at 15kg produced using polyester and epoxy resin systems at linear fibre haul-off rates of 7 m/min and 21 m/min.

The epoxy reference samples, generate over twice the volume of voiding (3.5 and 4.2%) when compared to their polyester counterpart (1.28 and 1.47%). Therefore, the high level of voids is not likely to be caused by the manufacturing process. Instead, the cause could be attributed to either the difference in the resin viscosity, which is known

to generate voids, or this could be an effect of the fibres and in particular, the binder on the fibre surface (Park *et al.*, 2011).

Inspecting the micrographs for the epoxy samples shown in Figures 4.26 (i), (ii) and (iii) for 7 m/min and Figures 4.27 (i), (ii) and (iii) for 21 m/min, it can be seen there is a large void content, this is in agreement with the measured void contents (3.5 and 4.2% respectively) shown in Figure 4.25. There does appear to be a slight increase in the degree of voiding seen at the 21 m/min, which again matches the previous findings. The failure of a sample can be influenced by higher the void content and the spread of the voids. Varna *et al.*, (1995) demonstrated how cracks propagating through samples, connecting large voids together, resulted in failure.

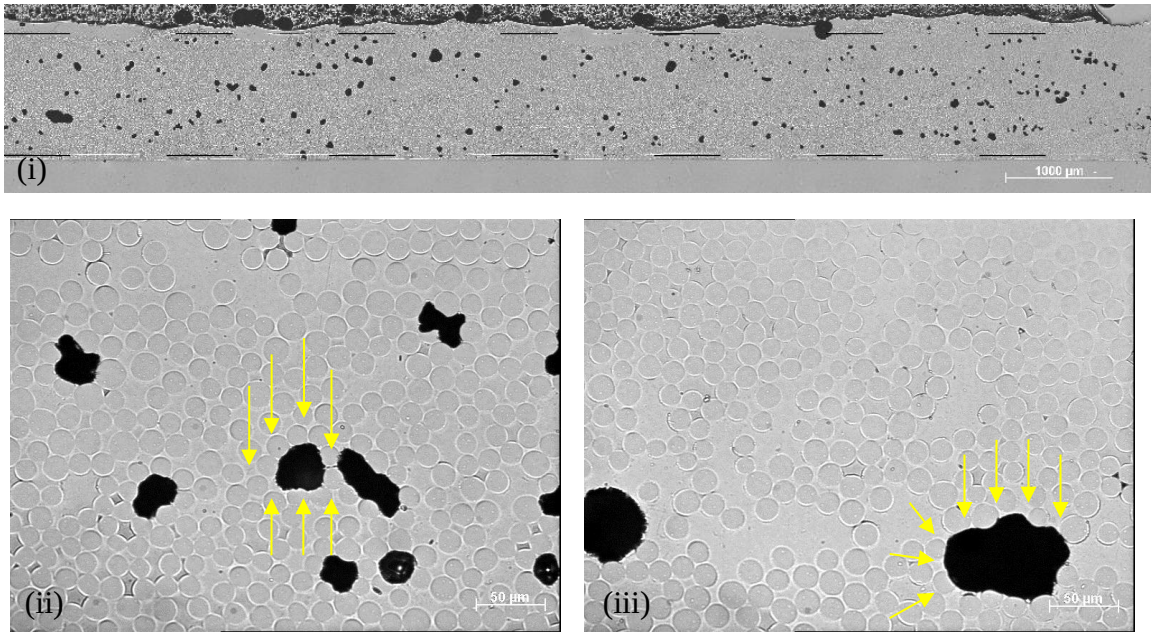

Figure 4.26 Micrographs (i), (ii) and (iii) showing a conventionally wound epoxy tube produced at 7 m/min.

Figure 4.26 (ii) and (iii) and Figure 4.27 (ii) and (iii) show magnified images of areas with voids. From these images, it can be seen that the perimeter of the voids tend to be populated with fibres. This suggests that these voids have been caused by air entrapment due the uneven resin flow through the fibre bundle.

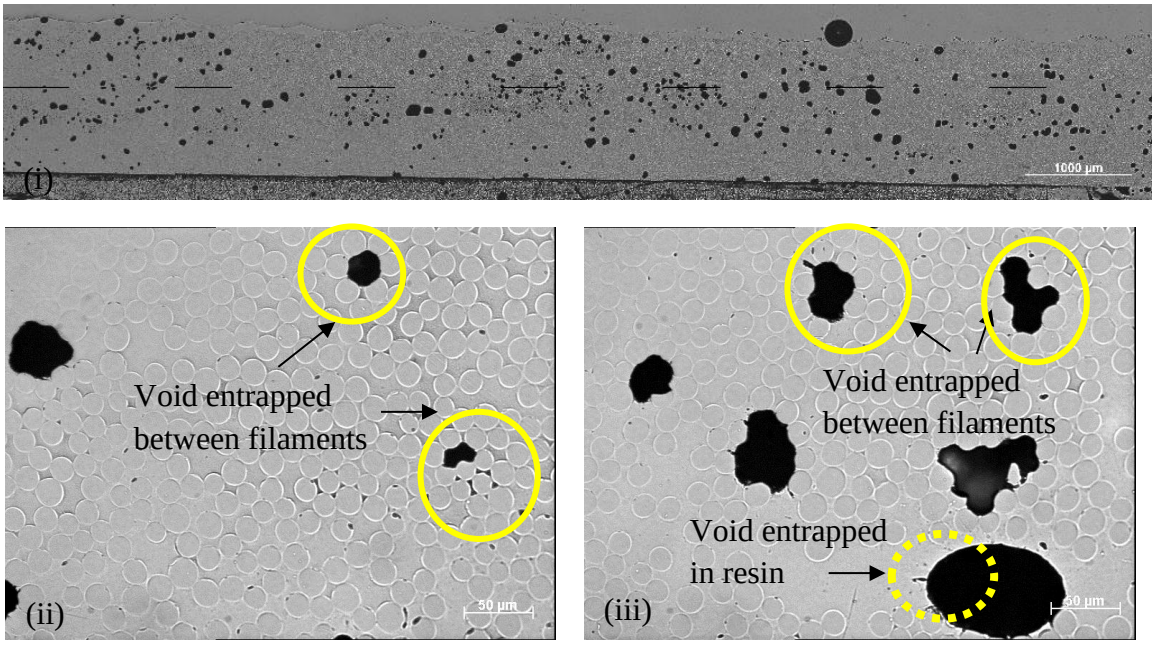

Figure 4.27 Micrograph (i), (ii) and (iii) showing a conventionally wound epoxy tube produced at 21 m/min.

Figure 4.27 (iii) shows a void within a resin rich region. This void could be produced by one of two mechanisms: (i) a void migrating from between fibres into the resin rich region; or (ii) aeration of the resin within the resin bath leading to air bubbles being transferred to the mandrel on the fibre bundles and becoming entrapped within the composite. The void is highlighted in Figure 4.27 (iii) with a dashed circle.

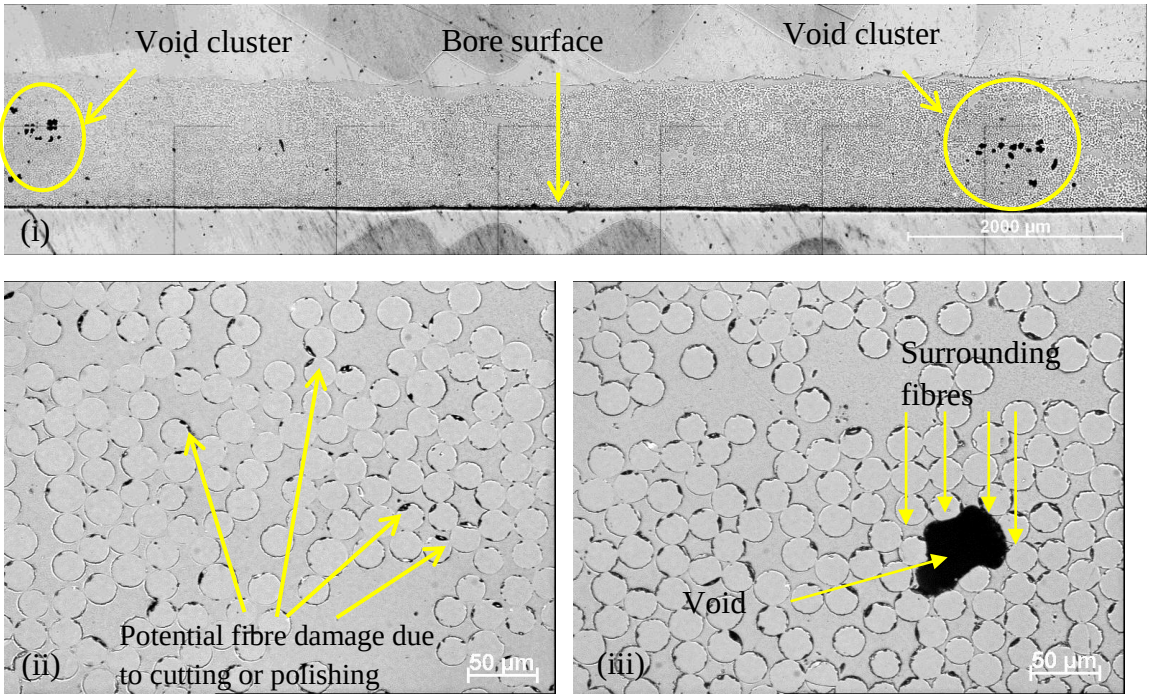

Figure 4.28 Micrographs (i), (ii) and (iii) showing a conventionally wound polyester tube produced at 7 m/min.

When looking at the micrographs of the polyester samples there is a much lower void content seen at 7 m/min (Figure 4.28 (i), (ii) and (iii)) and 21 m/min (Figure 4.29 (i), (ii) and (iii)) which are 1.28 and 1.47% respectively. As mentioned previously this could be due to a lower resin viscosity, 240 mPa.s as opposed to over 300 mPa.s, for the polyester resin compared to the epoxy. Therefore, the capillary wicking is more in line with the main flow of resin through the sample. From Figure 4.28 (i) it is possible to see there are areas within the sample, of void clusters. Due to the nature of these void formations it is possible that they are entrapped within a particular fibre bundle which is heavily bonded together. This is discussed in Section 4.2. Another notable feature includes the smooth inner bore region at 7 and 21 m/min which, as mentioned in the previous section, was due to a resin layer at the mandrel fibre contact.

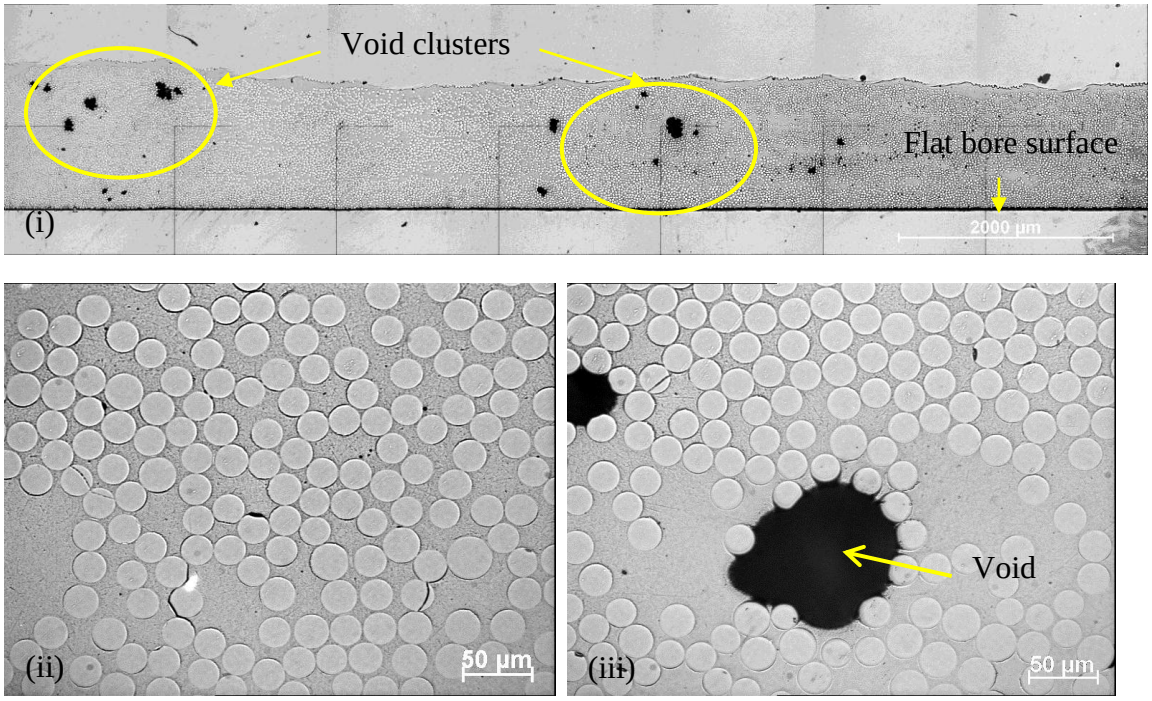

Figure 4.29 Three micrograph (i), (ii) and (iii) showing a conventionally wound polyester tube produced at 21 m/min.

Figure 4.30 shows the hoop tensile results for the conventionally wound reference samples produced using epoxy and polyester resin systems and wound at 7 and 21 m/min. It can be seen that in increasing the winding speed there is a subsequent decrease in hoop tensile strength. This is in agreement with results found by Haupert and Friedrich (1995). They showed higher winding speeds (30 m/min) decrease the time available for the matrix material to flow between the fibres. As a result the composites produced at higher winding speeds resulted in lower inter-laminar shear strength, and a decrease in the modulus.

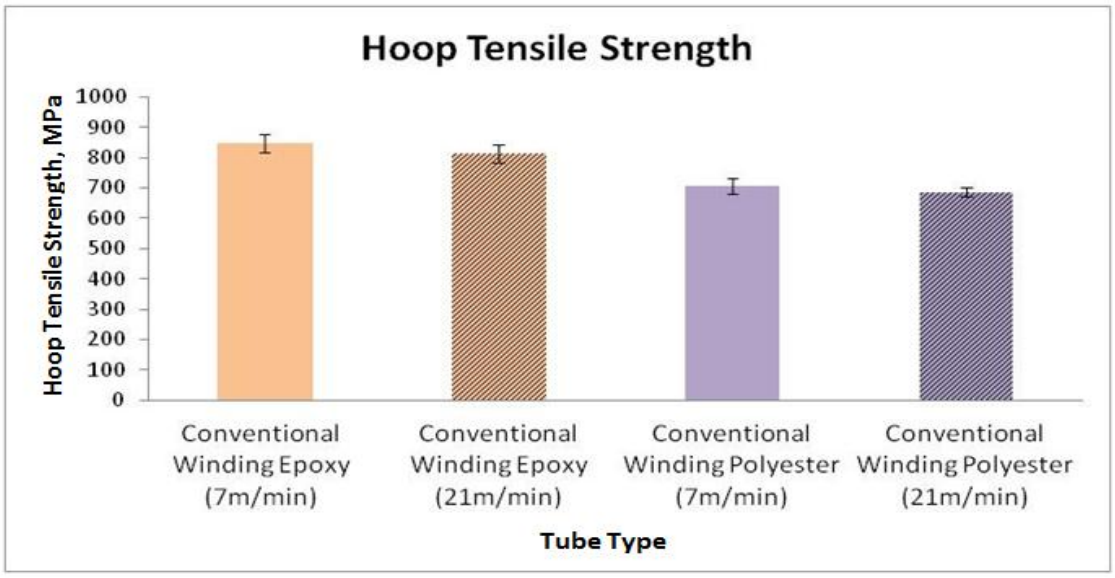

Figure 4.30 A graph showing hoop tensile strength of the reference tubes wound at 15kg produced using polyester and epoxy resin systems at 7 m/min and 21 m/min.

To make the results more comparable, the hoop tensile strength was normalised to 55% fibre volume fraction for each samples. Therefore, the strength values take into account the varying fibre volume fraction seen between samples. The results are shown in Figure 4.31.

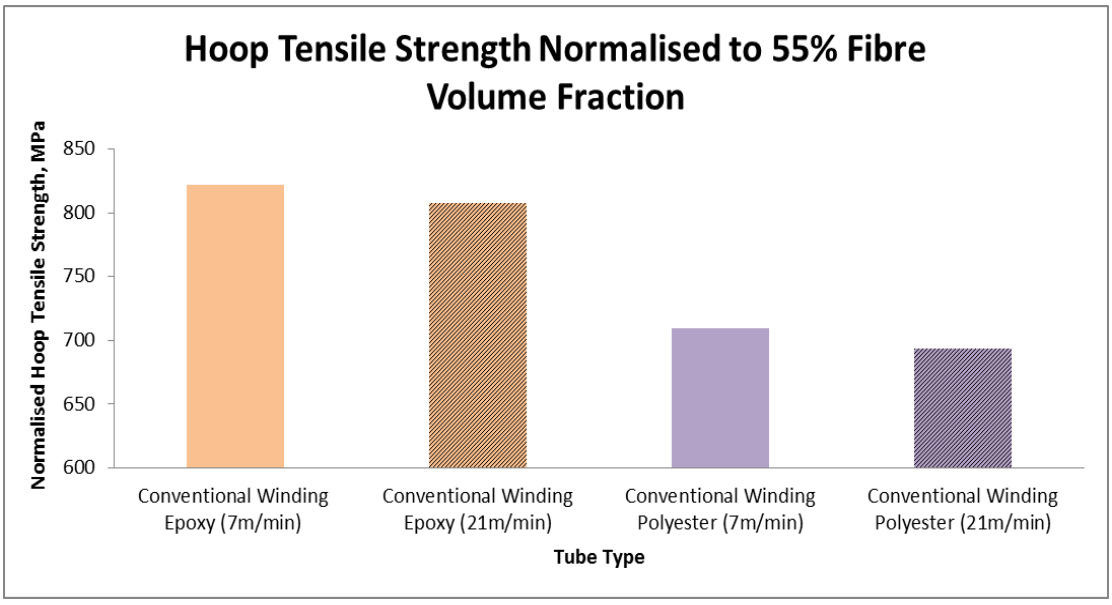

Figure 4.31 A graph showing the results of normalising the hoop tensile strength to 55% fibre volume fraction for reference tubes produced using polyester and epoxy resin systems at 7 m/min and 21 m/min.

From Figure 4.31, it can still be seen there was decrease in the strength of the tubes when the winding speed was increased.

This can be attributed to a number of factors.

(i) Reduced impregnation time: As discussed previously, increasing winding speed decreases the time the resin has to penetrate through the fibre bundles via impregnation on the resin drum. Therefore, capillary action becomes the main impregnation mode, which is slower and can lead to voids in the sample. However, as mentioned previously there are a large number of contact points in the conventional winding system, which should ensure the resin is squeezed into the fibre and thus reduce this as an influencing factor.

(ii) Increased void content: The reduction of composite strength could be due to the void content which is greater at higher winding speeds. Varna *et al.*, (1995) found there was a decrease in the transverse modulus from 20.6 to 17.6 GPa in a unidirectional fabric composite when the void content was increased from 0.4 to 4-5% respectively. They also showed similar finding in the tensile strength with a decrease from 55.6 MPa to 52.9 MPa.

(iii) Increased fibre tension: Although no evidence for this it was observed during the experiments. There could be a corresponding increase in fibre tension caused by increasing winding speed.

4.1.1.3.3 Summary

During the comparison between different winding parameters for conventional filament winding it was shown that the winding tension could have a significant effect on the

properties of the tubes produced both physically and mechanically. The major findings demonstrated in Section 4.1.1.3 are as follows:

(i) Optimum tension was required in order to manufacture tubes with a low void content, high fibre compaction (high fibre volume fraction), and low levels of fibre damage. From the experiments it was found that 15 kg gave the tension required to maximise the tube properties and therefore this was used for the all the subsequent winding experiments.

(ii) Results demonstrated that polyester resin could achieve a lower degree of voiding within the samples generated than the epoxy. This was believed to be due to either the viscosity of the resin, or compatibility issues between the epoxy resin and the binder used on the fibre.

(iii) It was found that in both the case of the epoxy and polyester resins that there was a subsequent increase in void content with increasing winding speed. Although this was less significant in the polyester tubes. The following section used the reference tubes produced using conventional winding to assess the quality of the tubes produced using clean filament winding.

4.1.2 Clean Filament Winding

4.1.2.1. Retrofitting

In order to mount clean filament winding prototypes on the industrial filament winding machine, an interface plate had to be constructed. This was designed to be attached to the traverse arm and allowed the necessary adjustments to be carried out during the winding i.e. adjusting the height so the fibres converging at the D-eye produced a tight

ribbon for winding. The interface used to mount clean filament winding rigs is shown in Figure 4.32 (A) and (B).

(A)

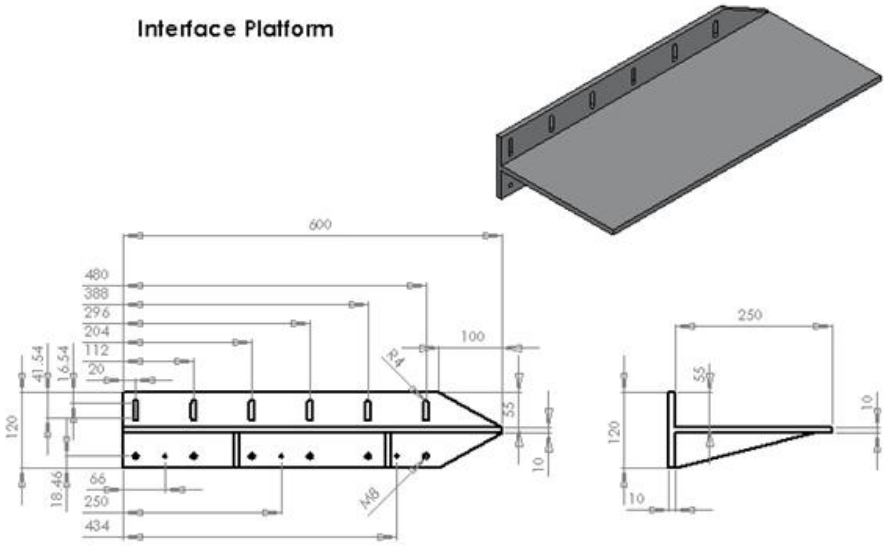

(B)

Figure 4.32 The interface platform that was used to mount Prototype-1 and Prototype-2 to the industrial filament winding machine (A) A detailed schematic of the interface platform. (B) A photograph showing the interface platform mounted on the filament winding machine.

With the new mounting platform the clean filament winding, Prototype-1 and 2 could be positioned close to the mandrel, and therefore reduce any resin wastage at drip points which were seen previously in conventional filament winding at the guide plates.

The interface platform slotted easily onto the traversing arm of the industrial filament winding machine replacing the normal platform. This took approximately 5 minutes. The interface platform had pre-drilled holes in the surface so that Prototype-1 and Prototype-2 could be mounted with the use of four screws. This made removal of Prototype-1 and 2 much easier for cleaning as the whole unit could be demounted from the platform and cleaned away from the winding machine.

4.1.2.2 Prototype-1

A site trial was arranged to investigate the feasibility of integrating and using the Prototype-1 impregnator design. Figure 4.33 shows Prototype-1 mounted on the industrial filament winding machine used to manufacture the reference tubes. Prototype-1 was easily mounted and demounted from the interface platform on the traverse arm.

From Figure 4.33, it can be seen that the fibres now bypass the resin bath and go straight through the guide plate. The fibres then pass through one further guide plate before entering the fibre spreading unit mounted to the back of Prototype-1 shown in Figure 4.34.

Figure 4.33 A photograph showing Prototype-1 fitted onto the interface platform which was mounted onto the traverse arm of the industrial filament winding.

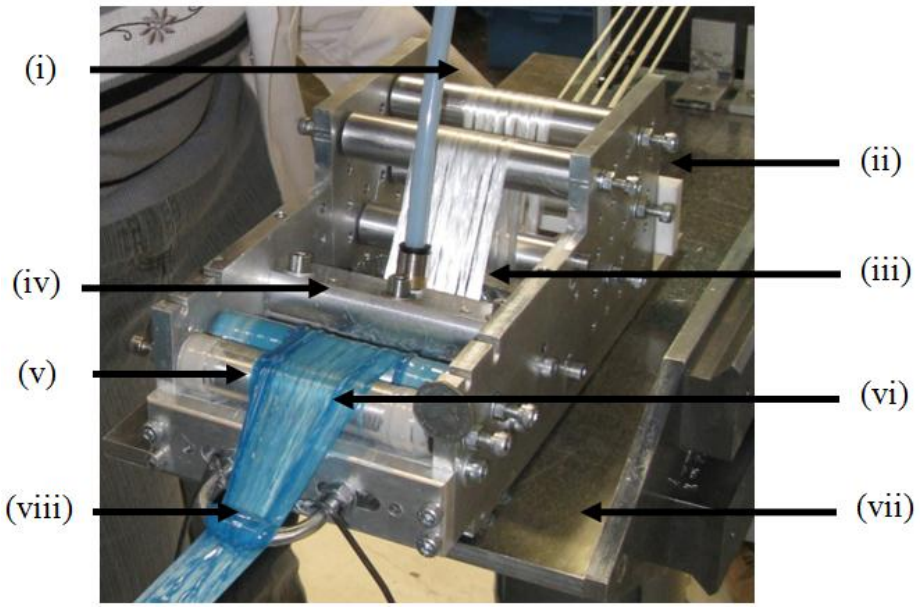

Figure 4.34 A photograph showing the components of impregnator Prototype-1. (i) Resin delivery pipe, (ii) Spreading station, (iii) Un-impregnated fibres, (iv) Resin impregnator unit, (v) Manipulation pins, (vi) Impregnated fibre ribbon, (vii) Interface platform and (viii) D-eye.

A spreading unit was added to spread the fibres and thus increase the rate of impregnation. As commented on by Shotton-Gale *et al.*, (2009), the spreading unit

helps to manipulate the fibres which in turn break the binder up as well as spreading the fibres to decrease the bundle thickness. Due to the close proximity of the impregnator unit to the mandrel fibre spreading is needed to increase the through-thickness impregnation rate, allowing filament winding at higher speeds. Figure 4.35 shows the increase width in the fibre after the spreading station used in Prototype-1. As mentioned previously decreasing the fibre bundle thickness can increased the impregnation rate (Pandita *et al.*, 2011). After the spreading station the fibres then enter the resin impregnator unit which uses curtain flow to attain a small wedge region. The fibres then pass through two sets of manipulation pins (point (v) in Figure 4.34 with the top two pins removed) used to squeeze and redistribute resin along the fibre bundle.

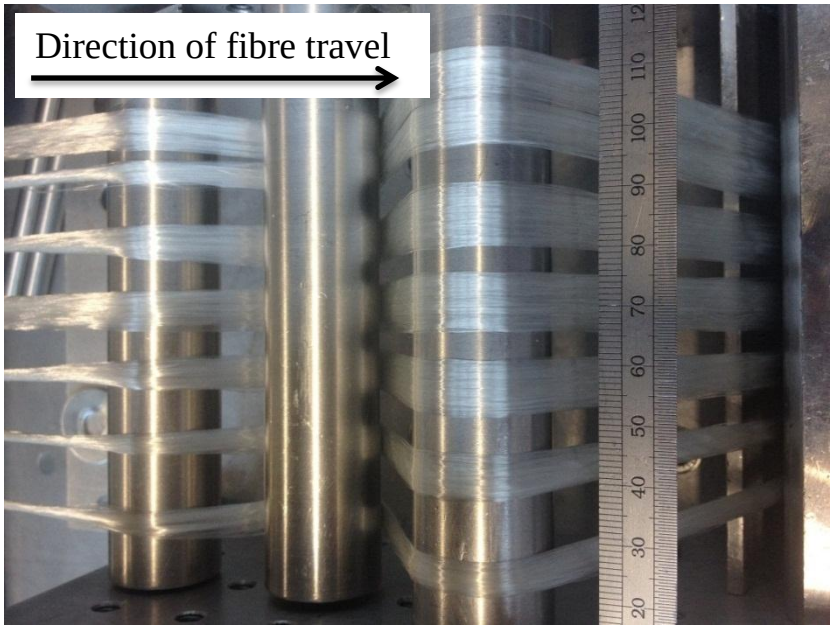

Figure 4.35 A photograph showing the as-received fibres entering Prototype-1 at the spreading station and then as they leave the spreading station as spread fibres.

Once the fibres have left the resin impregnator unit, they enter a D-eye, which draws the fibre bundles together to form an impregnated fibre ribbon. This is then wound onto the mandrel. The width of the ribbon measures and the value is used to acquire the winding

angle so that the ribbon lies side by side as its wound around the mandrel. This is important because gaps between the ribbon sections can cause air entrapment between layers as well as undulations in the final composite. Undulations can form due to uneven compaction levels and an uneven thickness of ribbon which cause concentrated fibre regions. Figures 4.36 and 4.37 show simplistic schematics of the position of Prototype-1 in respect to the mandrel.

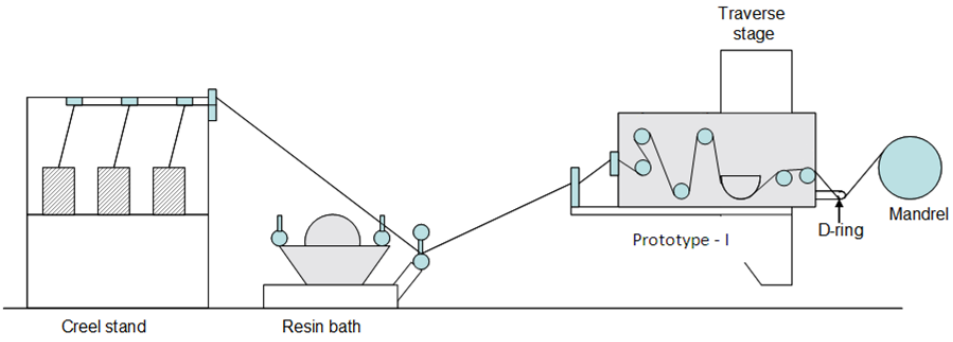

Figure 4.36 A schematic showing Prototype-1 mounted on the industrial filament winding machine. The Prototype-1 impregnator unit has been enlarged to highlight the key components.

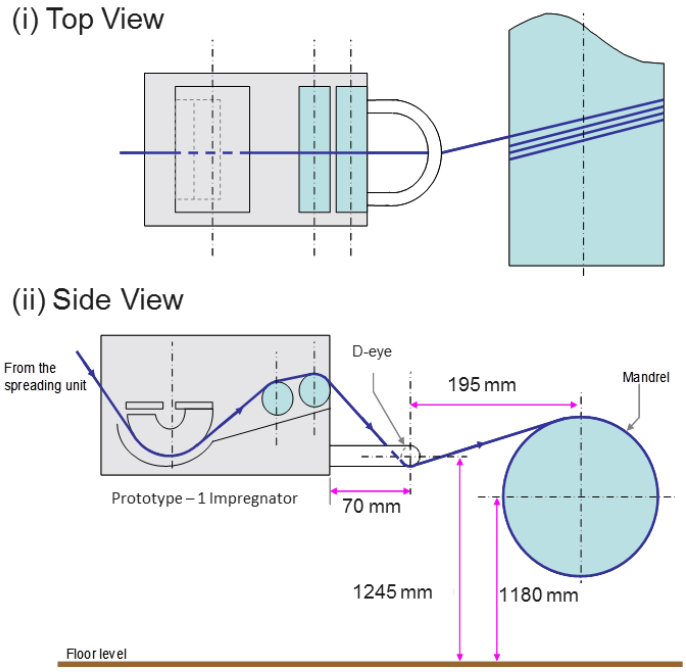

Figure 4.37 A schematic of Prototype-1 with the relative positions in relation to the mandrel. (i) Top view and (ii) side view. Both images are displayed with the top rollers removed.

As mentioned, it is important to achieve a ribbon of fibre bundles as they leave the D-eye. The aim of the ribbon is to have an even thickness with no gaps between bundles. Roisum, (1993) developed a method to determine the amount of web spreading (divergence of the fibre ribbon from the D-eye to the mandrel) as a function of the radius of curvature, and the diameter of the bowed pin. The same principle can be applied to converge the spread fibres in filament winding as shown in Figure 4.38. In this case spread fibre bundles pass through a bowed pin/D-eye in the reverse direction to reduce the overall width of the fibre bundles before winding on to the mandrel.

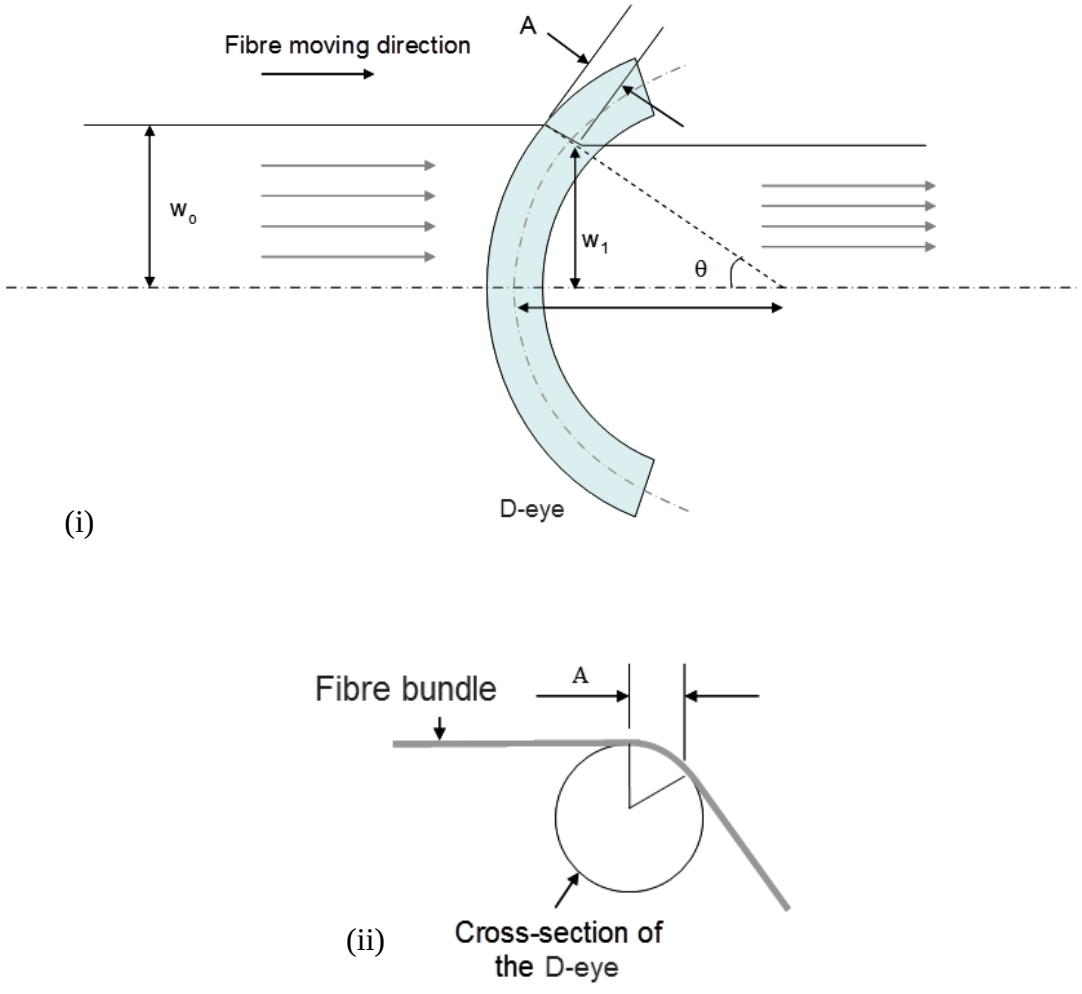

Figure 4.38 A schematic diagram showing the effect of using a D-eye to converge a fibre web. Image (i) shows a view from above and (ii) shows the cross-sectional view of the D-eye.

Due to the symmetry around the neutral axis of the fibre bundles, which is parallel to the fibre direction, half of the fibre bundle width is used to derive the equations. Based on the geometry of the D-eye and the dimensions of the fibre ribbon, the width of the converged fibre bundle at the exit of the D-eye can be defined in Equation 4.1 (Roisum, 1993):

$$W_1 = \frac{W_o\left[\left(R+r\right)-A\right]}{R+r}$$

Equation 4.1

Where:

W_o is the width of the original fibre bundles (mm);

R is the radius of curvature of the D-eye (mm);

r is the radius of the cross-section of the D-eye (mm);

W_1 is the width of the converged bundles (mm); and

A is the contact area (mm^2).

Based on Equation 4.1, and using the width of the fibre bundle measured at the location before the D-eye, expected fibre bundle width after the D-eye can be estimated. The estimated width using Roisum's equation and the measured width after the D-eye are shown in Table 4.4.

Method	Number of Fibre Bundles	Fibre Tension (kg)	Winding Speed (m/min)	Estimated Width (mm)	Measured Width (mm)
Width of the tow at the exit of the D-ring (D = 63 mm/ d = 8 mm)	6	5	7	35.49	27.53 (±0.84)

Table 4.4 A comparison of the estimated width of the fibre bundle using D-eye when using Roisum's equation (Equation 4.1) against the measured values.

It can be seen that the experimentally measured width is smaller compared with that estimated using Equation 4.1. This could be due to the fact that, Roisum's method does not consider the effect of tension of the ribbon on the change in width at the D-ring. Tension can converge the fibre ribbon further by increasing the inter-filament packing, and therefore reducing the width.

Roisum (1993) discussed the trajectory of the ribbon required to retain the width of the web that is achieved at the bowed pin. It was stated that the entering/exiting span length ratio on either side of the D-eye need to be 2:1 to retain the spread width of the fibre bundle (as shown in Figure 4.39). Therefore, this ratio was used to determine the distance the D-eye was positioned away from the mandrel during clean filament winding trials.

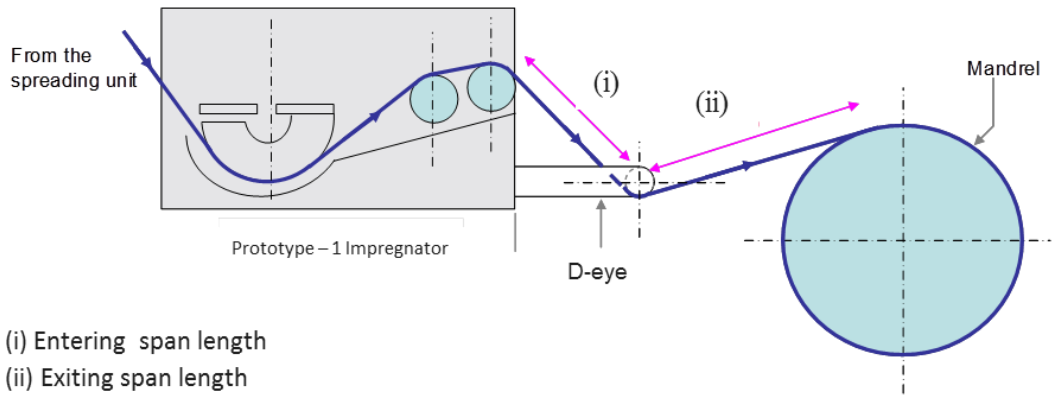

Figure 4.39 A schematic diagram showing (i) the entering and (ii) exiting span length of the fibre around the D-eye.

Creating the winding programme on the filament winding machine to hoop wind on a 106 mm mandrel was relatively straight forward, but required changing the D-eye used during conventional winding to a specially selected 45 mm diameter D-eye. Changing

the D-eye meant a ribbon of fibres could be created without gaps between the fibre bundles. Once the programs had been adjusted to accommodate the 45 mm diameter D-eye and dry winding trials demonstrated the improved ribbon, the wet winding trails commenced.

For tubes wound using the epoxy resin system, a static mixer was attached to the resin injector unit which was in turn attached to a manifold which contained two pipes attached to the resin dispenser. The resin dispenser supplied a given rate of resin and hardener based on the fibre haul-off speed. The dispenser was set to dispense resin at a rate that corresponded to the winding speed being used. For tubes wound using polyester a pressure-pot was used (reasons for this were discussed previously). Ideally the polyester too would be dispensed via a resin dispenser. This being said, the aim of these experiments were to validate the clean filament winding resin impregnator prototypes as the resin dispenser has been used previously by Shotton-Gale (2013) to demonstrate the process. Tubes were produced at either 7 m/min or 21 m/min, so a comparison could be made against the reference tubes manufactured previously (Table 4.3). Table 4.5 shows the variables used to manufacture each of the tubes using Prototype-1. During the winding trials, it was only possible to produce an epoxy tube wound at 7 m/min. It was observed when winding with the epoxy resin system, that at 21 m/min the fibres were under impregnated. Therefore, only one epoxy tube was wound at 7 m/min whereas both speeds could be used to produce the polyester resin composite tubes.

The physical and mechanical properties measured from Prototype-1 samples are shown in Table 4.5. The results from the reference tubes are also included for comparison.

Winding	Resin System	Fibre	No. of Layers	Mandrel Diameter (mm)	Winding Speed (m/min)	Winding Angle	Fibre Tension (kg)	Density (kg/m^3)	Fibre Volume Fraction (FVF) (%)	Void Content (%)	Hoop Tensile Strength (MPa)	Hoop Tensile Strength Normalised to 55% FVF
Conventional Filament Winding	LY3505/XB3403 epoxy/amine	8 x 2400 tex (Type-I)	4	106	7	Hoop	15	1967.36 (± 11)	56.7 (± 2.1)	3.5 (± 0.7)	847.35 (± 29.92)	822
CFW_Prototype-1	LY3505/XB3403 epoxy/amine	8 x 2400 tex (Type-II)	4	106	7	Hoop	15	1950.12 (± 12.18)	54.65 (± 0.51)	1.77 (± 0.08)	773.15 (± 78.82)	778.04
Conventional Filament Winding	CRYSTIC 397 PA Polyester	8 x 2400 tex (Type-I)	4	106	7	Hoop	15	1952.64 (± 7.96)	54.86 (± 0.34)	1.28 (± 0.22)	707.16 (± 26.62)	709.01
CFW_Prototype-1	CRYSTIC 397 PA Polyester	8 x 2400 tex (Type-II)	4	106	7	Hoop	15	1971.39 (± 23.65)	55.1 (± 1.09)	0.72 (± 0.49)	622.19 (± 22.01)	621.09
Conventional Filament Winding	CRYSTIC 397 PA Polyester	8 x 2400 tex (Type-I)	4	106	21	Hoop	15	1953.1 (± 10.05)	54.45 (± 0.43)	1.47 (± 0.39)	686.2 (± 14.64)	693.18
CFW_Prototype-1	CRYSTIC 397 PA Polyester	8 x 2400 tex (Type-II)	4	106	21	Hoop	15	1876.57 (± 13.39)	49 (± 0.58)	0.74 (± 0.58)	600.56 (± 25.3)	674.11

Table 4.5 Summary of the physical and mechanical properties of samples produced using Prototype-1 with epoxy and polyester resin systems.

Density measurements of Prototype-1 and reference tubes are shown in Figure 4.40. From the results it can be seen that the density of all the tubes, Prototype-1 and reference tubes, have a similar density value. A slight decrease in the density is observed for the polyester tubes that were wound at 21 m/min using Prototype-I.

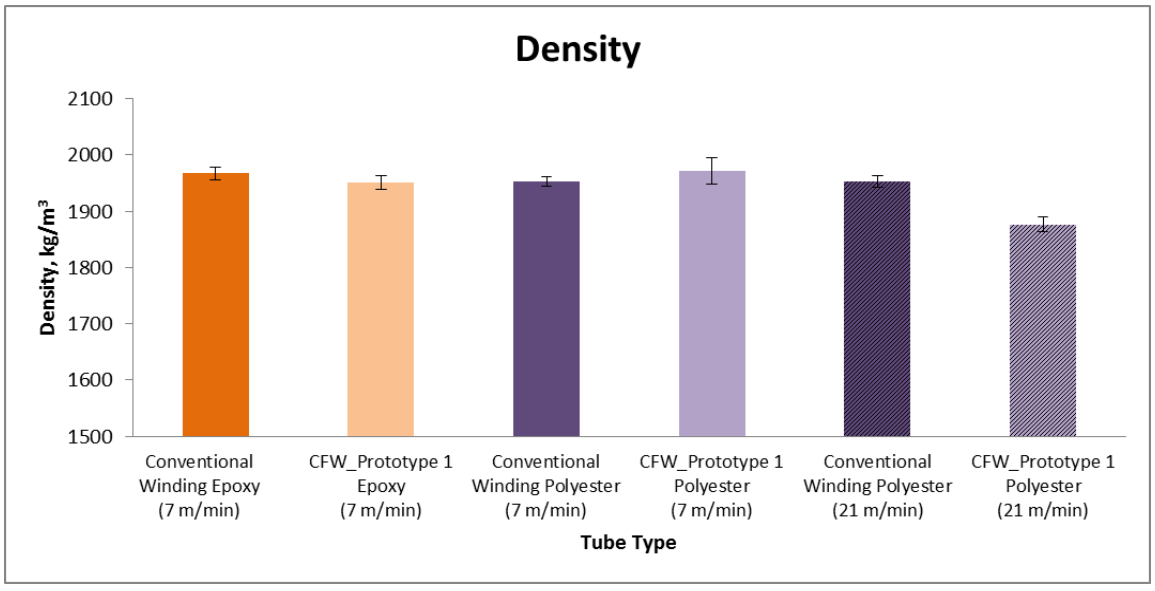

Figure 4.40 A graph showing the density results for the reference tubes produced and the Prototype-1 tubes produced.

Haupert and Friedrich, (1995) found the density of filament wound composite tubes decreases with winding speed which was attributed to an increase in voiding due to decreased impregnation. The decrease in density is in agreement with the samples produced using Prototype-1 but not the conventional samples. The void content measurements in Figure 4.42 show no change in void content which disagrees with these previous findings. Another possible reason for this decrease in density at higher speeds could be due to an increase in the quantity of damage sustained by the fibres using Prototype-1 at higher speeds.

Henninger *et al.*, (2002) attributed fibre damage to the subsequent increase in the pulling force caused by the increased winding speed. The fibre spreading station in Prototype-1 spreads the fibre bundles in a dry state before they enter the impregnator unit. Due to the fact the fibres have no liquid matrix to help lubricate the process at higher speeds there is an increase in tension, caused by the frictional force between the surface of the metal roller and the glass fibre bundle (Henninger *et al.*, 2002). This can result in fibre damage which can lead to premature failure of glass fibre filaments. The fibre bundles are also subjected to a very torturous path in both the spreading station and the resin impregnator unit.

The small diameter of the pins used in the spreading station can result in the fibres being subjected to more severe bending angles and therefore, lead to an increase in filament fractures. This was considered in the design of Prototype-2 because although it is important to spread the fibres to break up the binder and increase through-thickness impregnation, it is also important not to damage the fibre bundles as this will decrease load bearing capability of the filaments within the bundle and therefore decrease the composite strength (Henninger *et al.*, 2002).

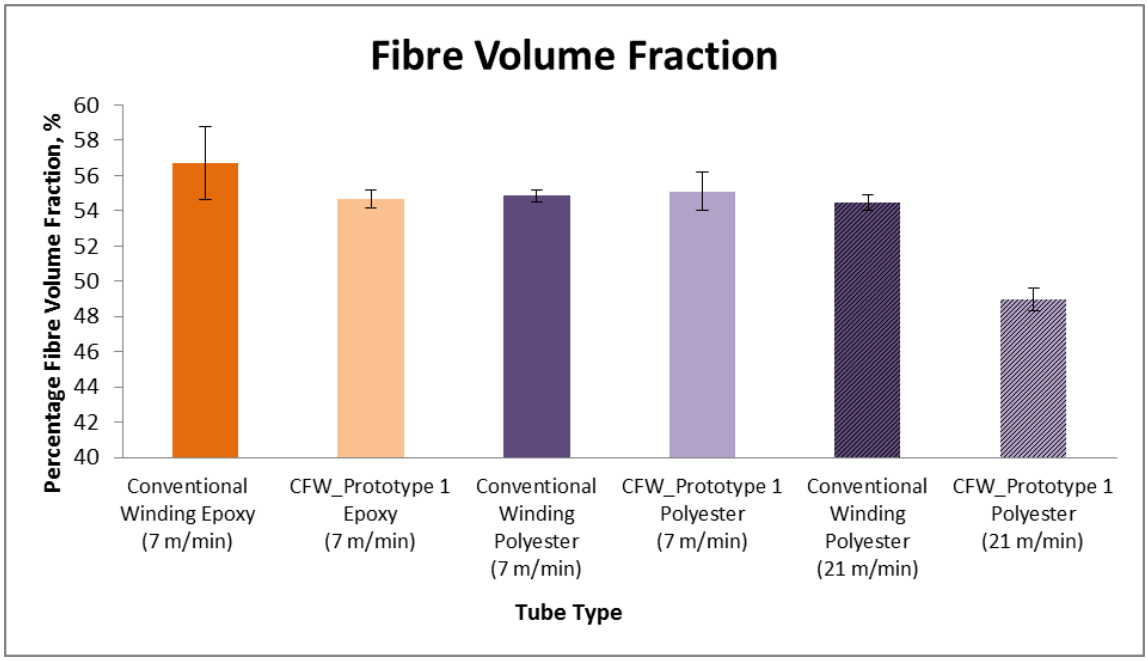

Figure 4.41 Fibre volume fraction results comparing the reference tubes produced against the Prototype-1 tubes.

Figure 4.41 shows the fibre volume fraction of the tubes manufactured display roughly the same percentage, between 50-56%, with the difference between the Protoype-1 samples compared to the conventional tubes negligible. The exception to this is the 21 m/min sample wound using polyester with Prototype-1, in which the clean filament wound tube is much lower (49% ± 0.58) than the conventionally wound tube (54.45% ± 0.43). There are three factors which could have contributed to this; (i) an increased resin layer on the surface of the fibres caused a higher degree of fibre compaction cause by the different D-eye used. (ii) Fibre damage could result in a small reduction in fibre volume. During the spreading section dry fibres can fracture easily, and thus reduce the percentage of filaments in the final composite. (iii) An increase in the void content due to lowered impregnation. This however, does not appear to be the case, as Figure 4.42 demonstrates the void content for both the Prototype-1 polyester and epoxy samples are lower than their reference counterparts.

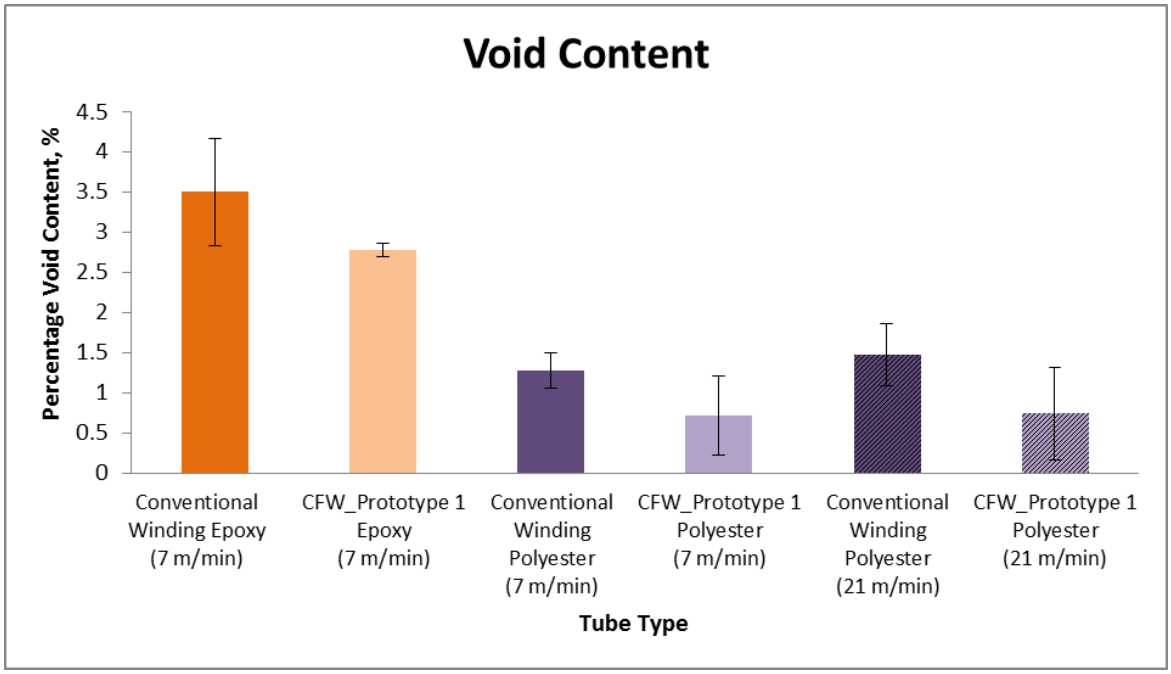

Figure 4.42 A graph showing void content results comparing the reference tubes produced against the Prototype-1 tubes.

Figure 4.42 shows the measured average void content found in Prototype-1 tubes compared to the references tubes produced. It can be seen that the Prototype-1 polyester tubes have a reduced average void content of below 1%, compared to the reference samples, which are both above 1%. Due to the low viscosity of polyester resin, the pin impregnation is much more effective here than in the case of the epoxy resin.

The void content in the micrographs (Figure 4.43 (i), (ii) and (iii)) of the Prototype-1 epoxy tube appear to be lower than the conventionally wound reference epoxy tube (Figure 4.26 (i), (ii) and (iii)) and does not show a significant difference also seen between the two tubes in the measured void content. Figure 4.44 (i), (ii) and (iii) and Figure 4.45 (i), (ii) and (iii) show the microstructure of the polyester tubes wound using Prototype-1 at 7 m/min and 21 m/min respectively.

Figure 4.43 (i) shows the microstructure of the epoxy tube wound at 7 m/min using Prototype-1, which appears to have a lower population of voids when compared to the reference sample seen in Figure 4.26 (i). This being said, a 21 m/min tube could not be wound successfully using Prototype-1 because there was not enough resin penetrating the fibres to produce a composite that could be removed from the mandrel. This differs to conventional winding in that at 21 m/min a tube could be easily produced. However, there is a subsequent rise in the void content seen in the reference tubes at higher winding speeds. This is where the capillary action and manipulation seen in the wetted fibres during conventional winding becomes more advantageous.

In conventional winding the fibres are almost immediately immersed in the resin and then undergo a series of manipulations caused by multiple contacts with guide plates and pins. This manipulation can aid the capillary impregnation by squeezing the resin through the thickness of the fibre bundle. In Prototype-1 there was only two manipulation points within a short distance of the mandrel, which does not appear to be sufficient in aiding the capillary process at higher speeds (21 m/min).

Due to the fact Prototype-1 is mounted on the traverse platform directly before the mandrel there does not appear to be enough time for capillary impregnation to take place at 21 m/min before un-impregnated fibre bundles are trapped within the layers of the composite and the air entrapped cannot escape. This factor was taken into consideration when establishing the design criteria for Prototype-2.

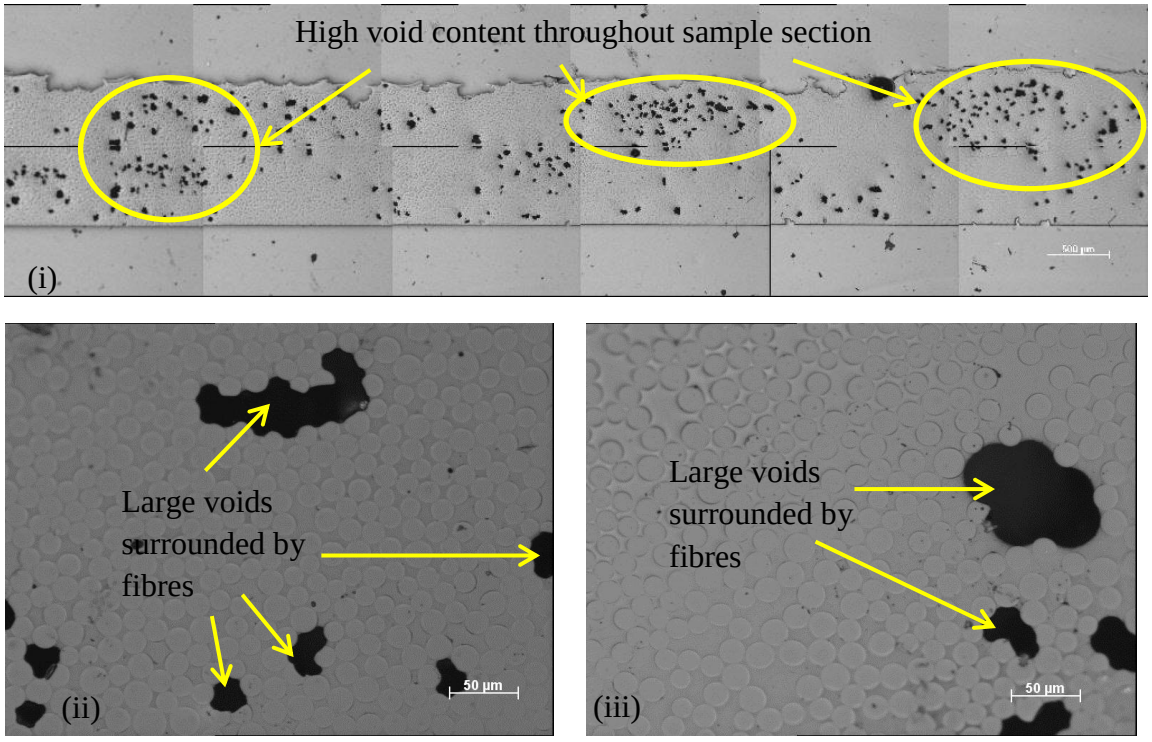

Figure 4.43 Micrographs (i), (ii) and (iii) showing tubes produced using Prototype-1 with an epoxy resin matrix at a 7 m/min winding speed.

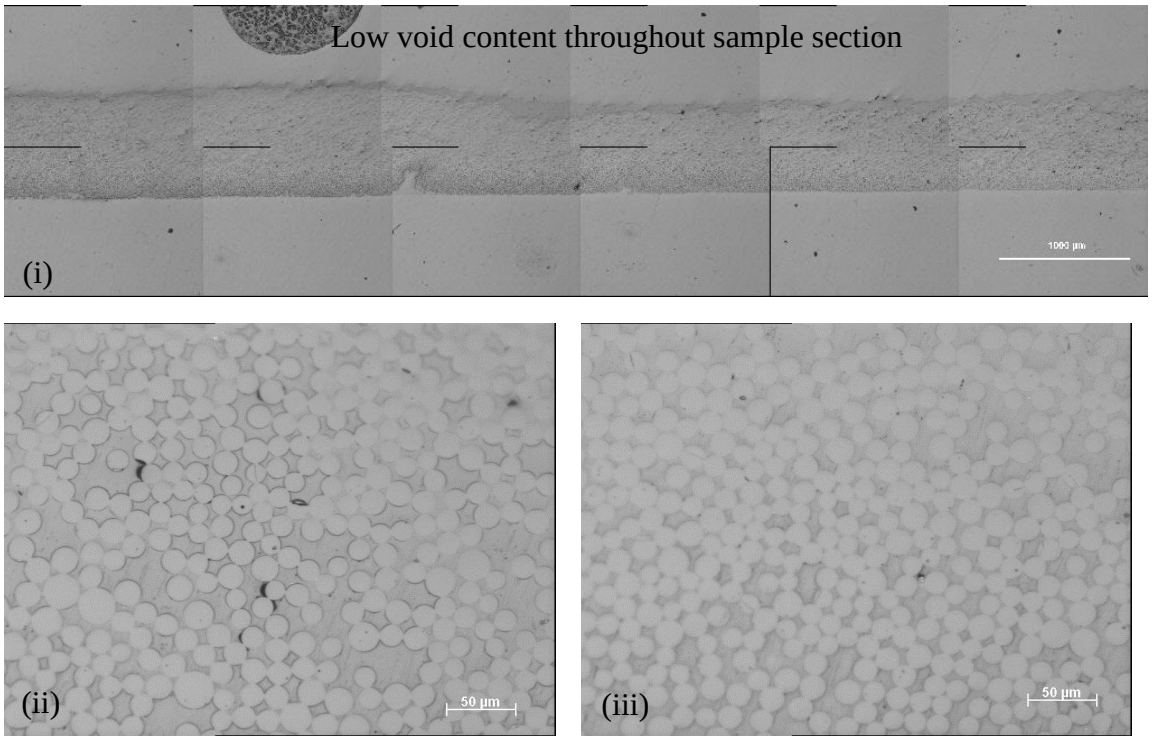

Figure 4.44 Micrographs (i), (ii) and (iii) showing tubes produced using Prototype-1 with polyester resin matrix at a 7 m/min winding speed.

Microstructural images show the polyester samples wound at 7 m/min are virtually void free, this can be seen in Figure 4.44. At this speed, the resin can easily penetrate the fibre bundle via pin impregnation which means there is a reduced chance of voids forming. This information is also in agreement with the void content results reported previously.

When looking at Figure 4.45 showing the tubes that were wound at 21 m/min. It is clear that there are areas of the sample where the resin has not penetrated the fibre bundles. As these voided areas are fairly isolated in regions within the sample, it suggests that there could be a difference with the fibre bundles at those areas. It was observed during processing that there were areas of the fibre which appeared heavily coated in the binder agent. These areas were held tightly and did not break up into loose filaments during the production process. It is therefore thought that this could also be contributing to the poor impregnation at certain sections (Figure 4.45 (i)) of the composite sample, rather than poor impregnation from the new process (these are termed void clusters and have been noted previously). This hypothesis is to be validated in Section 4.2.

In Figure 4.45 (ii) and (iii) it is possible to see damage that has occurred to the edges of the glass fibre filaments during either the cutting process (removing the samples from the tube) or the polishing process (too much pressure applied to the sample or polishing disk damaged). To reduce this, a larger sample was removed from the tube and excess was then removed to a greater extent by polishing. Also fewer samples were polished at the same time to reduce the risk of debris from one sample damaging other samples, and finally polishing disks were changed when polishing either epoxy or polyester samples to reduce damage through contamination of debris.

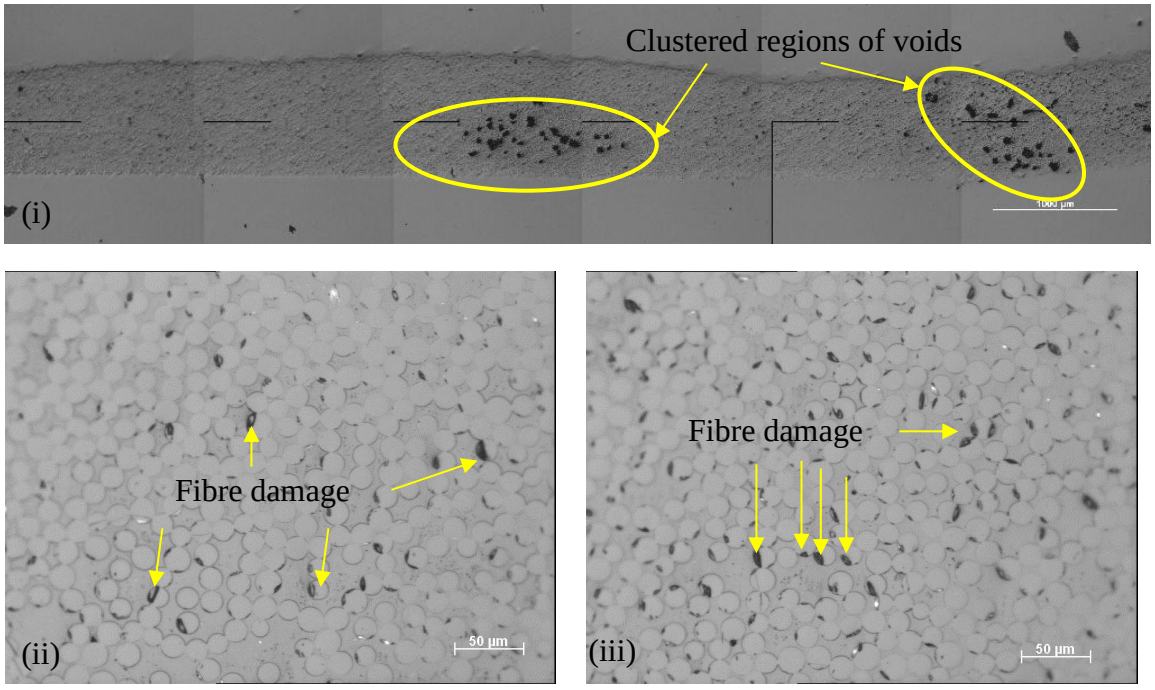

Figure 4.45 Micrographs (i), (ii), and (iii) showing tubes produced using Prototype-1 with a polyester resin matrix at a 21 m/min winding speed.

Figure 4.46 and Figure 4.47 show the hoop tensile strength of all the tubes wound using Prototype-1 with the comparative reference tube, both before and after normalisation to 55% fibre volume fraction.

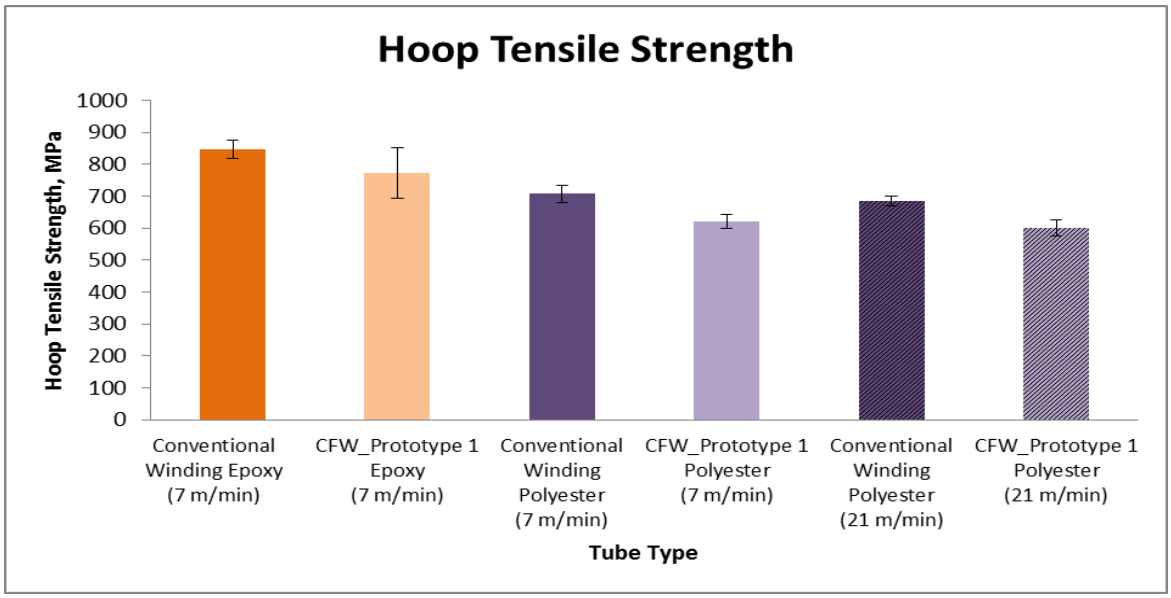

Figure 4.46 A graph showing the hoop tensile strength results comparing the reference tubes produced against the Prototype-1 tubes produced.

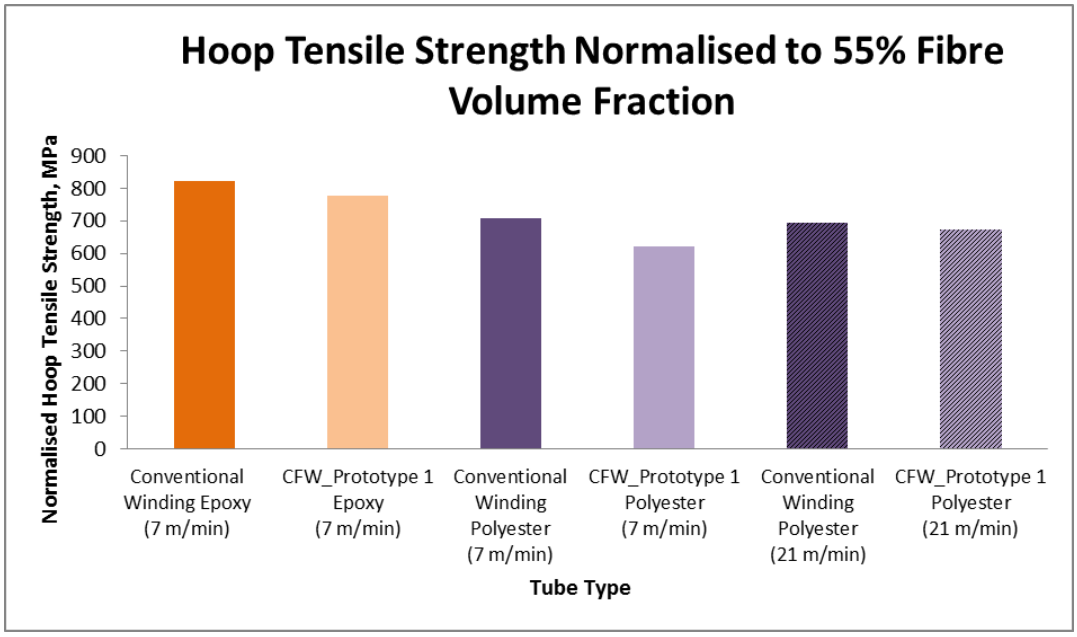

Figure 4.47 A graph showing the hoop tensile strength results comparing the reference tubes produced against the Prototype-1 tubes normalised to 55% fibre volume fraction.

From the results, it can be seen that the all the tubes produced using Prototype-1 have a comparable but slightly lower tensile strength than the conventionally wound composite tubes.

The slight decrease seen in the tensile strength here could be a result of manual intervention during conventional winding where the mandrel is painted with a layer of resin prior to winding. This aids with the impregnation process when the fibres are layered on the mandrel, as the excess resin is squeezed up through the layers (Figure 4.48 (i) and (ii)).

Figure 4.49 (i) and (ii) show clean filament wound samples which demonstrate the effect of not painting the mandrel prior to winding. Due to the fact the resin impregnator unit is not impregnating the fibre bundles 100%, there are dry filaments

reaching the mandrel. Without the resin layer painted onto the mandrel there is no resin to aid the impregnation of these under impregnated filaments so they remain dry and hence the voiding seen nearer the inner surface as seen in Figure 4.49 (i) and (ii). The aim of the new impregnator with the resin dispenser is to reduce the amount of manual input during the process and the waste resin generated.

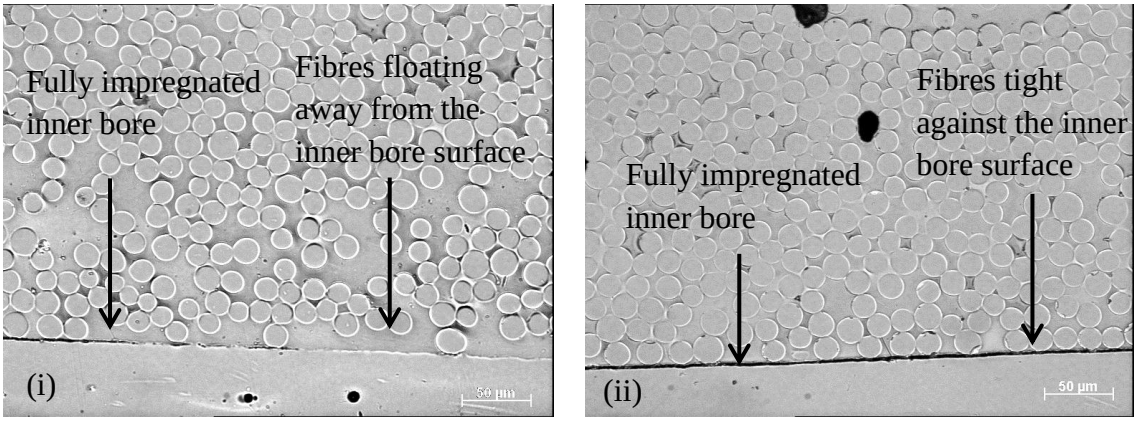

Figure 4.48 Micrographs (i) and (ii) showing polyester conventional wound samples (21 m/min) with the effect of manually painting the mandrel prior to winding.

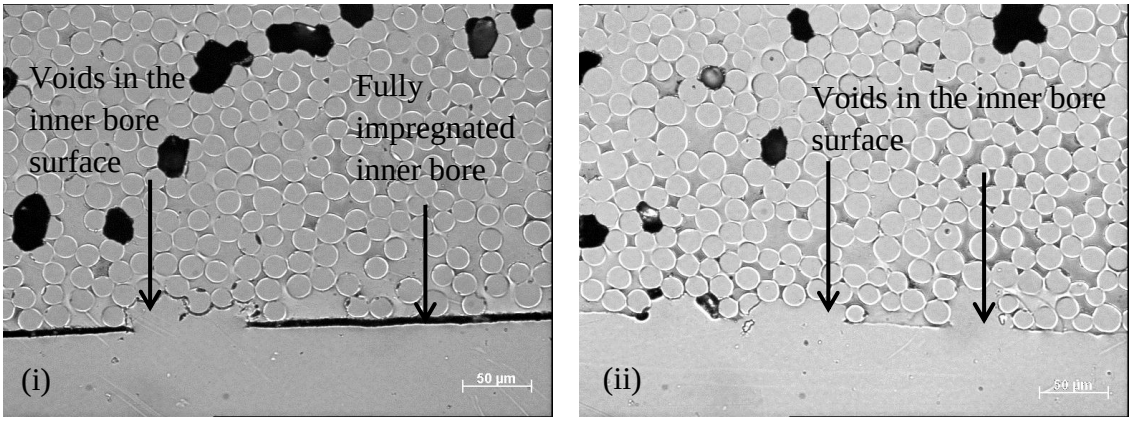

Figure 4.49 Micrographs (i) and (ii) showing Prototype-1 polyester clean filament wound samples (21 m/min) with the effect of an un-painted mandrel prior to winding which has resulted in the formation of voids on the inner bore.

In conclusion, it would appear at this stage that conventional winding is not significantly affected by the increase in speed from 7 to 21 m/min. However, it is

difficult to conclude if this is the case with the reference samples because during the conventional winding process the resin level is manually manipulated and the impregnation process is physically aided by the use of brushes to apply extra resin during processing. Although this was not completed by the operators during the clean filament winding trails this was thought to aid the impregnation significantly in the composite tube and therefore was considered for the proceeding trials.

4.1.2.3 Summary

When comparing Prototype-1 to conventional filament winding the following findings were noted:

(i) Samples produced using Prototype-1 was shown in these experiments to have similar physical properties to epoxy reference tubes and polyester reference tubes at specified speeds. However, for the polyester tubes wound at 7 m/min and 21 m/min, the hoop tensile properties are slightly lower than those of the corresponding reference tubes. This was thought mainly to be due to not painting the layer of resin on the tubes first (as completed during conventional winding). Therefore there is a greater risk of an under-impregnated inner tube, as the resin is squeezed to the top layers as more fibre is overwound.

(ii) When assessing Prototype-1, other features of this design make it impractical for use in an industrial filament winding facility. Due to the quantity of screws and bolts required to put Prototype-1 together there is a significant increase in the time to fit the unit to the transverse stage. This is also a problem at the end of winding when the unit needs to be removed for cleaning. This can become difficult with increase

screws and time consuming cleaning. This information was considered during the development of Prototype-1 to Prototype-2 which was developed in order to try and address the issues seen and described in the previous section.

4.1.2.4 Prototype-2

Prototype-2 was a redesign of Prototype-1, looking to reduce the issues seen during the production trials with Prototype-1 as well as address some of the further demands required of the system asked for by industry (covered in Section 3.1.3.1). In particular Prototype-2 focuses on maximising the degree of impregnation with the view to operations at higher winding speeds (up to 52 m/min as requested by the industrial partner). Using the design criteria mentioned in Section 3.1.3.1, Prototype-2 was designed and is shown in Figure 4.50 mounted onto the interface platform described in Section 4.1.2.1 on the industrial winding machine.

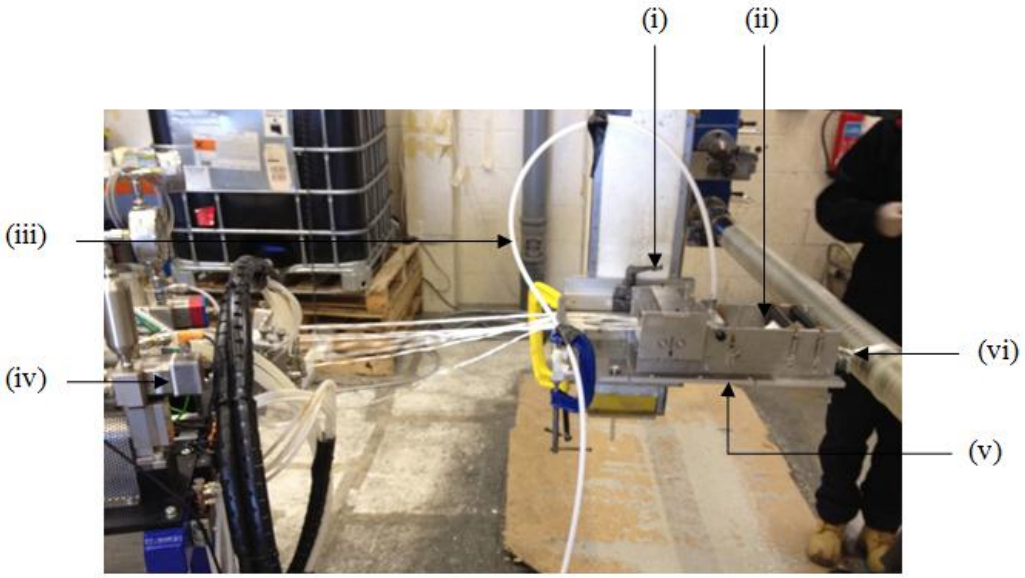

Figure 4.50 A photograph showing the dispenser connected to Prototype-2 which is mounted on the interface platform. Items labelled as (i) Spreading station, (ii) Prototype-2, (iii) Resin delivery pipe, (iv) Resin dispenser, (v) Interface platform, (vi) D-eye.

The tubing showing in Figure 4.50 at point (iii) is connected to the resin impregnator unit and is supplying the resin from the resin dispenser (epoxy) or pressure-pot (polyester). One of the improvements made from Prototype-1 was that the retrofitting took less than 10 minutes. All the individual components were designed to slot into the rig so they could be put in and removed without the use of screws. This then meant that during cleaning the components could be quickly removed and cleaned easily. This was one of the design criteria used for the design of Prototype-2.

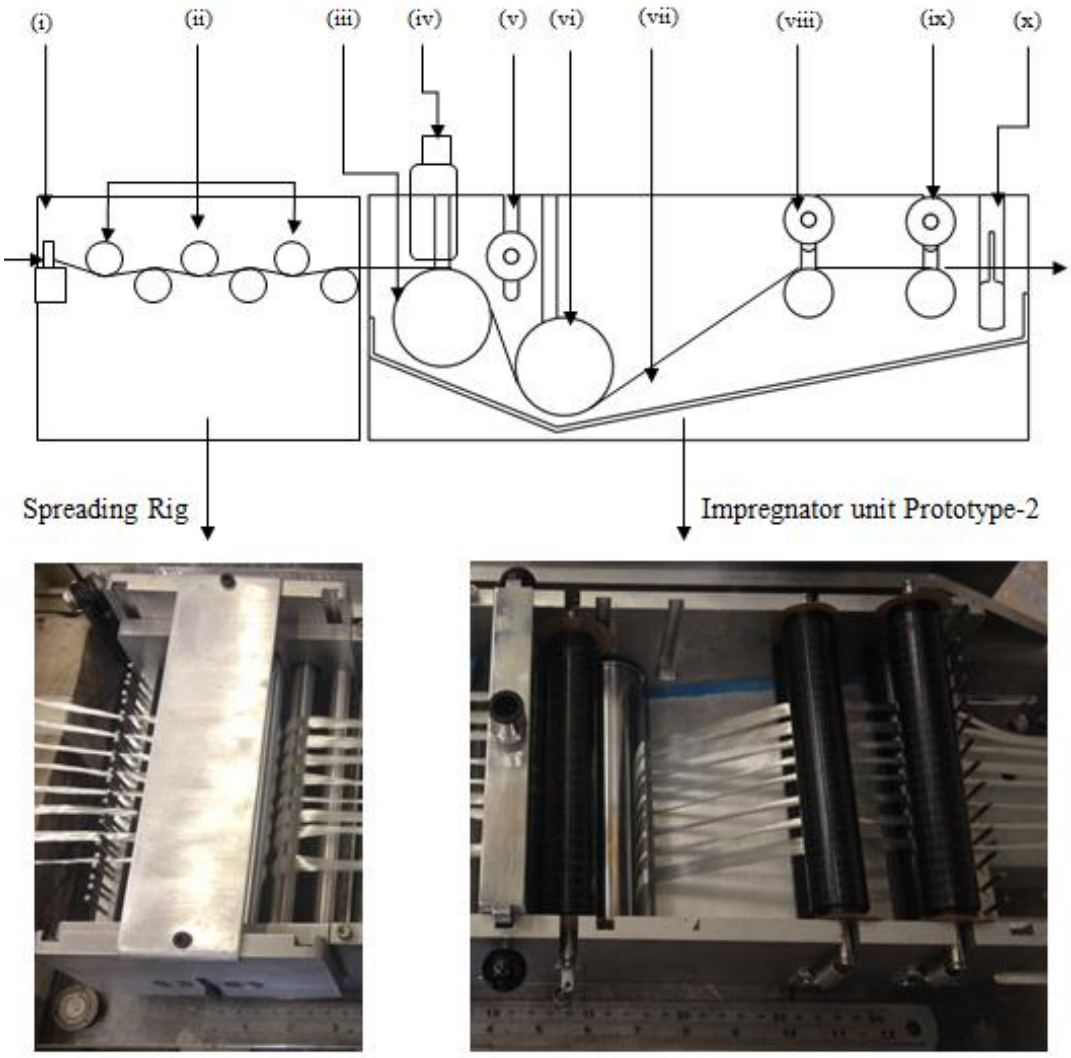

Figure 4.51 A schematic image of Prototype-2 and photographs to show manufactured components. The following components are labelled (i) Guide pins, (ii) 5 spreading rollers, (iii) 1st roller, (iv) Injector head, (v) Acetyl roller, (vi) Pin, (vii) Angled base plate, (viii) Pinch pins, (ix) Guide pins, (x) D-eye.

Figure 4.51 shows an enlarged image of the spreading station and Prototype-2 and the key components highlighted; these are discussed in detail in Section 3.1.3.2.2 of the Experimental.

4.1.2.4.1 Tube Production

Once Prototype-2 had been retrofitted to the interface plate and the winding angle defined to ensure a tight ribbon of fibres was achieved on the mandrel, the winding trial began. As discussed in Section 3.1.3.2.2, Figure 4.52 shows the positioning of the springs used during the winding of tubes to manipulate and squeeze the resin into the fibre bundles, whilst also squeezing the air bubbles out the composite. The pinch pins were used to introduce a wedge region where impregnation could be aided and allowed for better control over the fibre volume fraction.

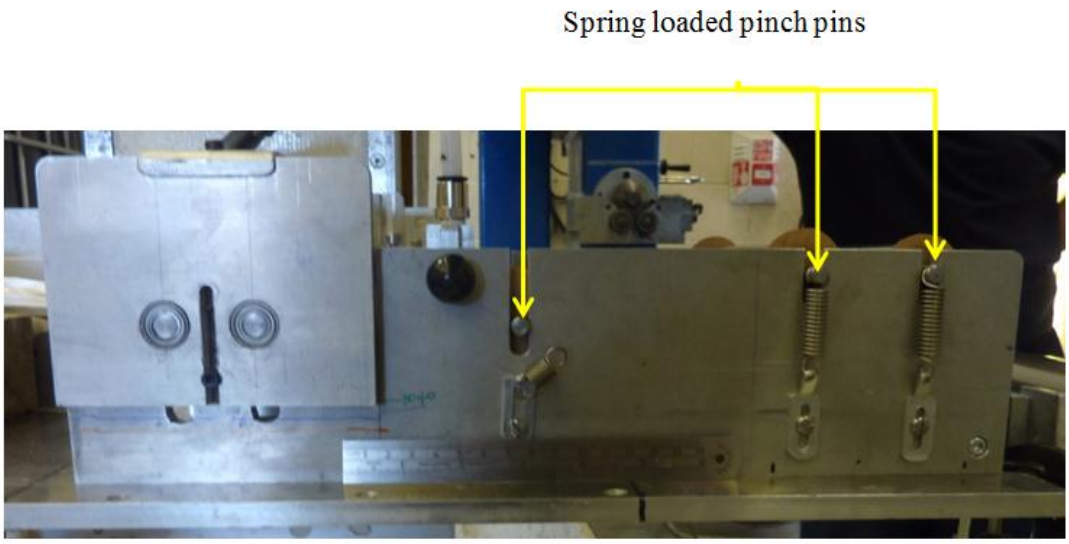

Figure 4.52 A Photograph showing the positioning of the springs used to introduce wedge impregnation.

Figure 4.53 (i) shows the guide pin before the spreading station and the spacing between the fibre bundle during winding which resulted in a gapped ribbon of fibres. To solve

this problem, the guide plate prior to the spreading station was narrowed, bringing the bundles of fibre together to form more of a ribbon at the impregnator this can be seen in Figure 4.54 (i) and (ii). This was done to make the injection more effective and reduce air entrapment caused by gaps between the fibre bundles. Tape was placed on injector so only width of ribbon was impregnated this reduced any excess resin waste at this point.

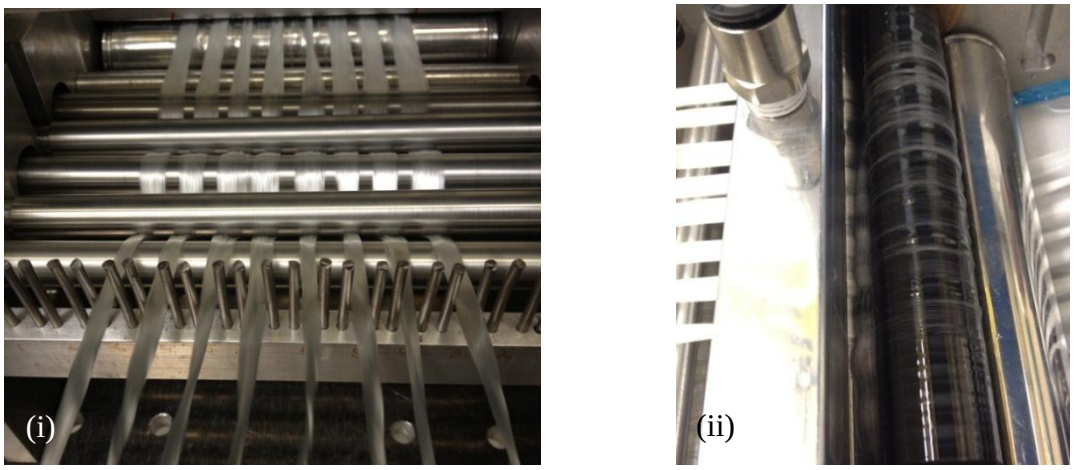

Figure 4.53 Photographs showing (i) the guide pins at the front end of the spreading unit and (ii) the impregnator unit and the acetal roller generating a resin wedge to help promote impregnation.

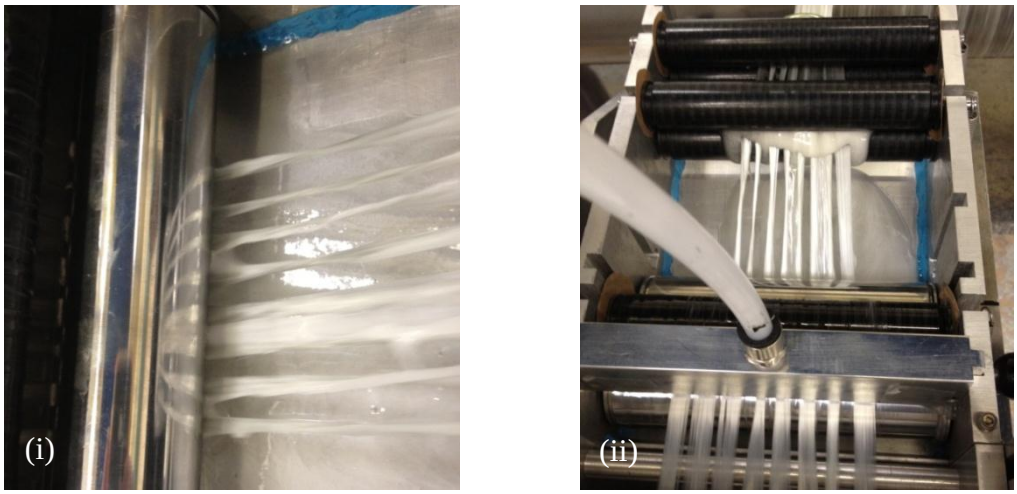

Figure 4.54 Photograph showing (i) fibres as they are pulled under the pin and coated from the base by the miniature reservoir and (ii) excess resin being removed at the first set of pinch rollers.

Trials were completed using epoxy resin and Prototype-2. Although there was a marked improvement over Prototype-1, it was thought that due to the information attained from conventional and clean filament winding trials that there was an issue with the compatibility of the fibres and the epoxy resin systems. It was therefore decided that Prototype-2 would concentrate on winding with polyester resin as there appeared to be better compatibility between the polyester and glass fibres. Section 4.2 investigates further the reasoning behind the observed incompatibility between the fibres and epoxy resin.

The results of clean filament winding are shown in the following section and compared to the corresponding reference tubes produced. The polyester tubes wound using Prototype-2 are shown in Table 4.6.

Winding	Resin System	Fibre	No. of Layers	Mandrel Diameter (mm)	Winding Speed (m/min)	Winding Angle	Fibre Tension (kg)	Density (kg/m^3)	Fibre Volume Fraction (FVF) (%)	Void Content (%)	Hoop Tensile Strength (MPa)	Hoop Tensile Strength Normalised to FVF
CFW_Prototype-2	CRYSTIC 397 PA Polyester	8 x 2400 tex (Type-II)	4	106	7	Hoop	15	1943.07 (±12.01)	54.38 (±0.89)	1.69 (±0.37)	715.33 (±48.33)	723.53
CFW_Prototype-2	CRYSTIC 397 PA Polyester	8 x 2400 tex (Type-II)	4	106	21	Hoop	15	1891.97 (±8.02)	50.88 (±0.51)	1.46 (±0.1)	725.49 (±46.21)	784.23

Table 4.6 Summary of the physical and mechanical properties of samples produced using Prototype-2 with the polyester resin system.

During filament winding with Prototype-2, a decision was made to coat the mandrel in resin prior to winding. This process was standard practice in conventional winding and was thought to potentially increase the hoop strength of the tube by improving the impregnated regions in the inner bore surface.

Figure 4.55 shows the density measurements of all the polyester tubes produced using Prototype-2 and conventional winding. It can be seen that the density values for all the tubes are similar. The slight decrease in density seen in the Prototype-2 tube wound at

21 m/min is due to the decrease in the fibre volume fraction, which can be seen in Figure 4.56. This decrease could be due to the increase in winding tension cause by the increase in winding speed (Henninger *et al.*, 2002). However, this differs to findings of Cohen, (1997) and Mertiny and Ellyin, (2002), who demonstrated that high winding tension, produced higher fibre volumes due to higher fibre motion and fibre compaction. This does not appear to be the case here. Higher resin volume fraction could be due to the addition of the resin on the mandrel prior to winding. This, as discussed previously, could increase the resin quantity on the sample and therefore results in a lower sample density and fibre volume fraction. Also gaps present in the ribbon of fibres as they are wound onto the mandrel could lead to resin rich areas in the composite or void entrapment, which would reduce the fibre volume in the sample and decrease the density.

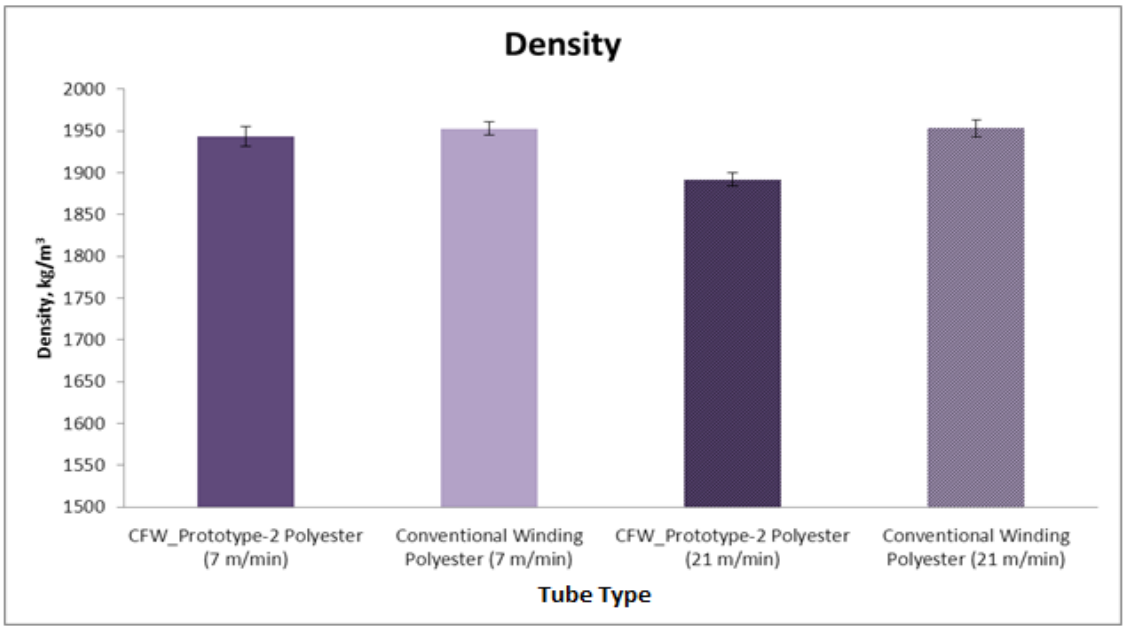

Figure 4.55 A graph comparing the density measurements obtained for the polyester reference tubes and the Prototype-2 polyester tubes.

Figure 4.56 shows the fibre volume fraction results for all the polyester tubes wound using Prototype-2 and the conventional winding process. The results show all the tubes wound have a similar fibre volume fraction (54%) with the exception of the higher speed Prototype-2 tube, which has previously been addressed. The 50-60% fibre volume fraction seen for Prototype-2 is a typical value obtained for all the reference tubes produced during this study, for epoxy and polyester at 7 and 21 m/min winding speeds.

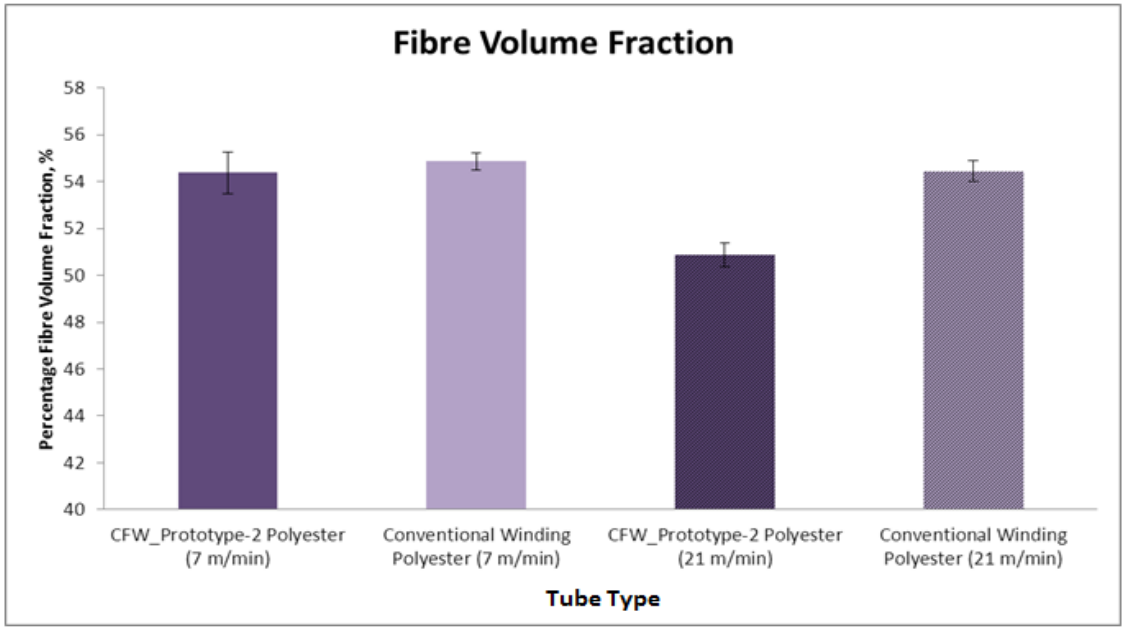

Figure 4.56 A graph comparing the fibre volume fraction measurements obtained for the polyester reference tubes and the Prototype-2 polyester tubes.

The void content measurements shown in Figure 4.57 demonstrates that the clean filament winding samples at 7 m/min has a higher measured average void content than the conventionally wound samples. This could be due to a couple of factors: (i) a different fibre manufacturer was used to supply fibres for the clean filament winding as opposed to the reference tubes. Therefore, the binder content and constituents on the

fibres may be different and therefore, have a different effect on impregnation, and (ii) sample size used in the measurements to represent the whole tube. This differs to the results seen at 21 m/min which have comparable void contents for clean and conventional tubes. When looking at Figures 4.58 and 4.59, which show the microstructural image of clean filament wound Prototype-2 polyester tubes wound at 7 and 21 m/min respectively, it can be seen that there are only limited areas of voids.

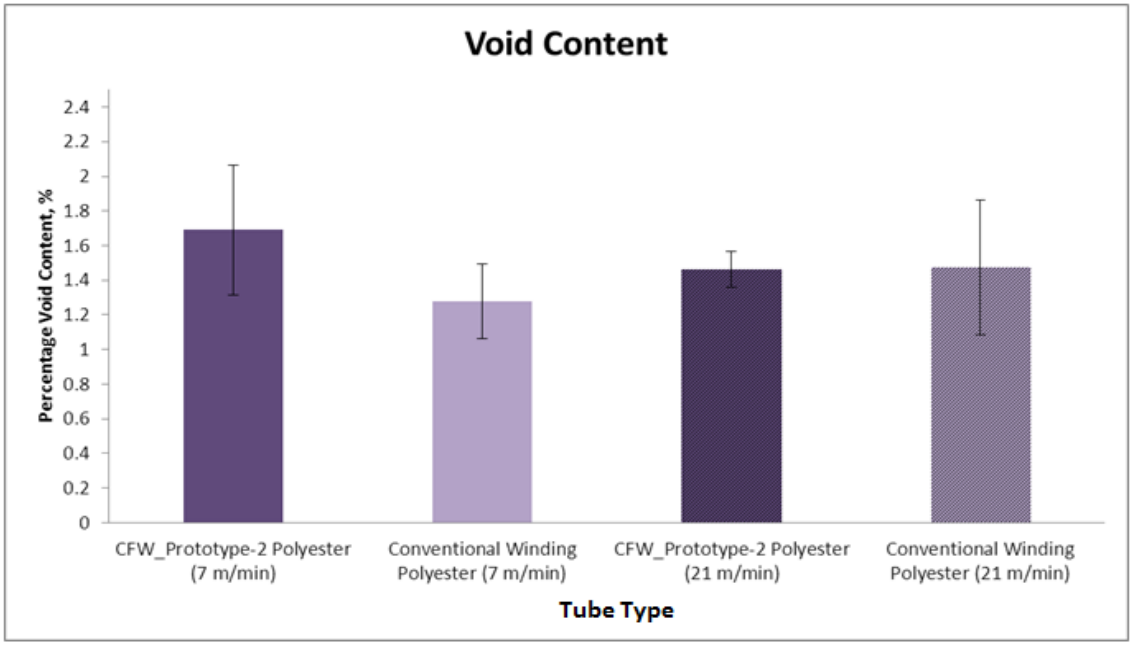

Figure 4.57 A graph comparing the void content measurements obtained for the polyester reference tubes and the Prototype-2 polyester tubes.

The small areas of voids could be due to variability in the binder content visually observed along the length of the fibre bundle. This was seen previously in Prototype-1 and reference polyester samples. These areas of fibre bundles not impregnated can cause weakness within the cured composite tube, resulting in premature failures due to the increased rate of crack propagation at these voids. However, there does not appear to be a clear correlation between the void contents and the normalised hoop tensile

strength shown in Figure 4.61. This being said the tubes produced were 4 layers thick and therefore a more noticeable effect may be seen if further layers are wound.

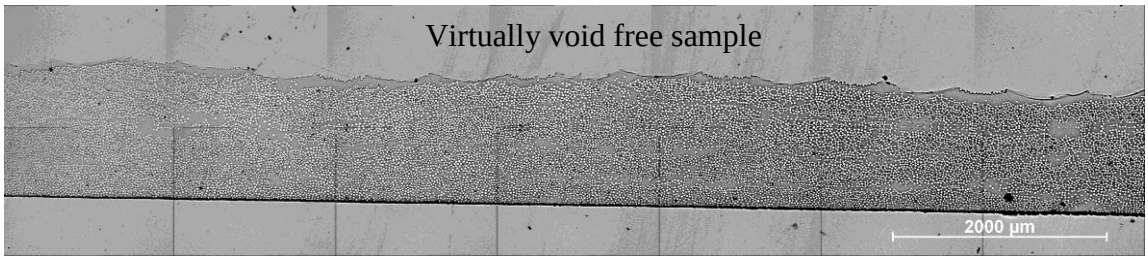

Figure 4.58 Micrographs showing polyester tubes produced using Prototype-2 at 7 m/min winding speed.

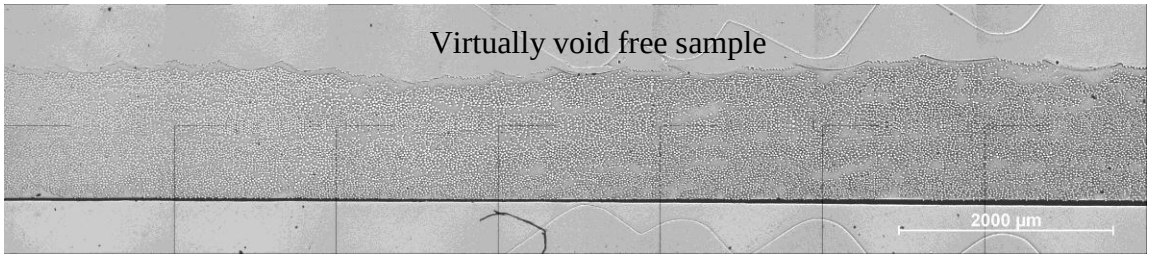

Figure 4.59 Micrographs showing polyester tubes produced using Prototype-2 at a 21 m/min winding speed.

The hoop tensile strength (shown in Figures 4.60 and 4.61) of the tubes wound using Prototype-2 are comparable and in the case of the 21m/min, tube exceeds the strength of the conventionally wound reference tubes. This demonstrates the effectiveness of Prototype-2 at impregnating the fibre bundles at low (7 m/min) and higher speeds (21 m/min). This also shows the improvement made in the clean filament winding process development from Prototype-1 to Prototype-2, where there has been an increase of over 100 MPa in the achievable hoop tensile strength of the composite rings. This can only be due to the better impregnation of the fibre bundles due to the increased area of pin impregnation in Prototype-2 compared to Prototype-1, as opposed to the capillary impregnation, which dominates conventional filament winding.

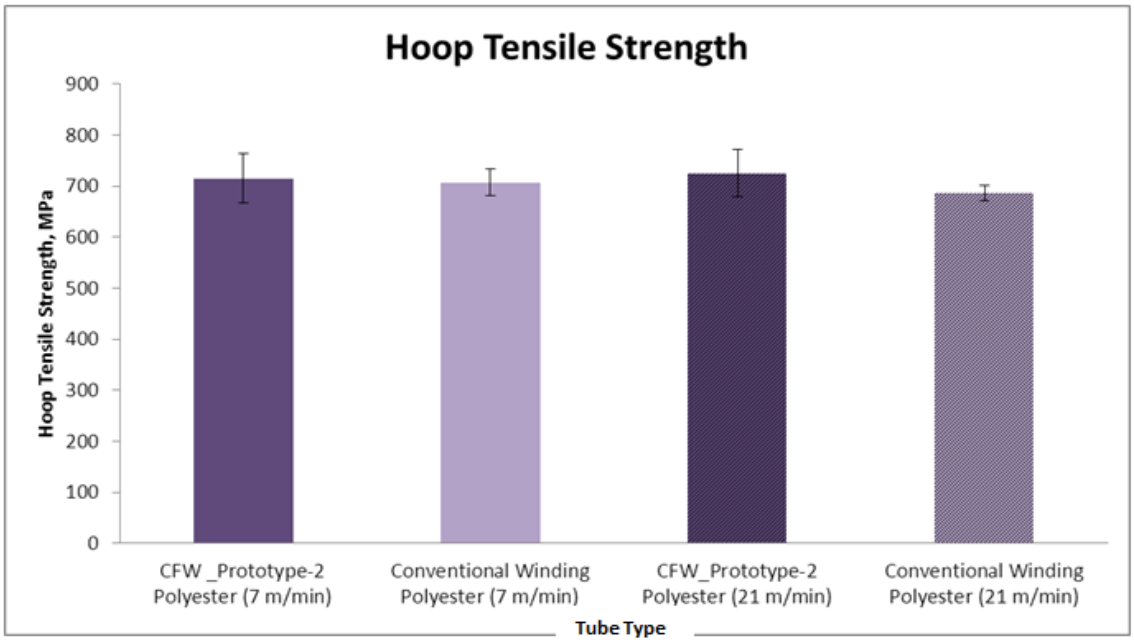

Figure 4.60 A graph comparing the hoop tensile strengths obtained for the polyester reference tubes and the Prototype-2 polyester tubes.

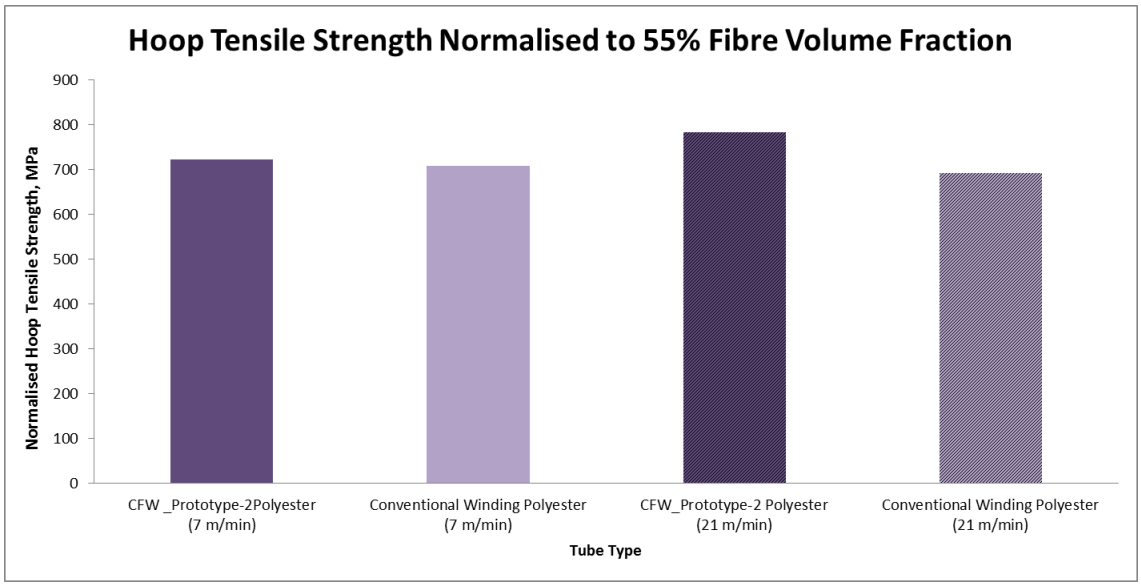

Figure 4.61 A graph comparing the hoop tensile strengths obtained for the polyester reference tubes and the Prototype-2 polyester tubes after normalisation to 55% fibre volume fraction.

From the micrographs shown in Figures 4.58 and 4.59 it can be seen that the inner bore of the tube surface is well impregnated and free from micro-pores. This could be one of the factors causing the improved performance seen between Prototype-1 tubes and

Prototype-2 tubes. The improved degree of impregnation seen in this region can be attributed to the resin layer added to the mandrel prior to winding. The addition of resin to the mandrel helps to impregnate the inner layers of the tube. Due to the compaction of the fibres as they are wound on top of each other the resin on the tube surface is squeezed through the layers coating any dry fibres in resin. The resin layer is likely to become more important the faster the winding speed used. This is due to the reduced time for the fibres to achieve 100% impregnation before the mandrel. The manual addition of resin to the mandrel surface appears to be the best method to achieve the higher tensile strengths seen in the tubes.

In addition to completing the trial at 21 m/min, the manufacturer requested that the clean filament winding system be used to wind at the highest speed used in their production process (52 m/min) in the factory. Therefore, in a subsequent trial and with minor modification to Prototype-2 winding trials were carried out to produce a 10 inch composite tube wound at 50 m/min. Micrographs of a conventionally wound and clean filament wound tubes are shown in Figures 4.62 and 4.63. Although outside the scope of this study, these images demonstrate the capability of the clean filament winding system to wind at much higher production speed and still be able to achieve similar physical properties to the conventionally wound process.

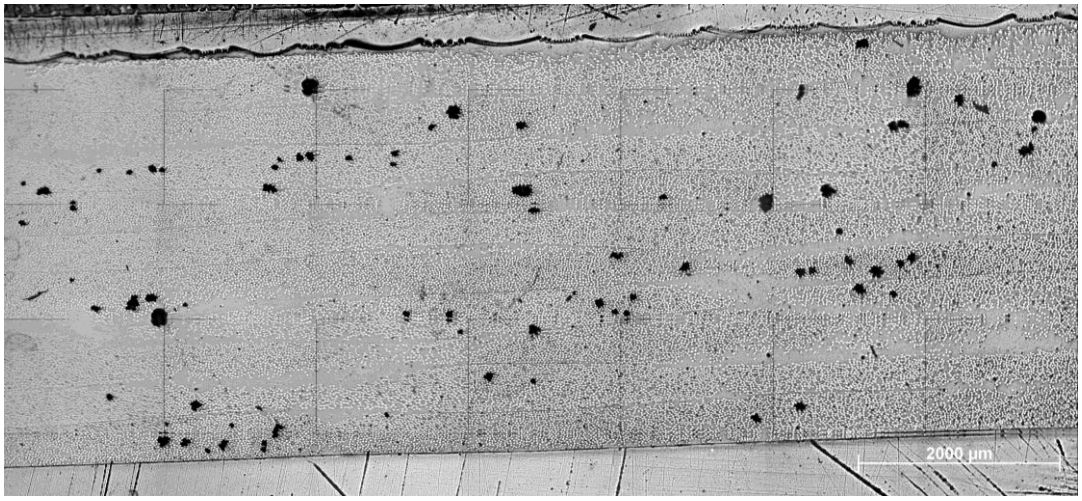

Figure 4.62 A micrograph showing a 10 inch tube wound using conventional filament winding at 50 m/min.

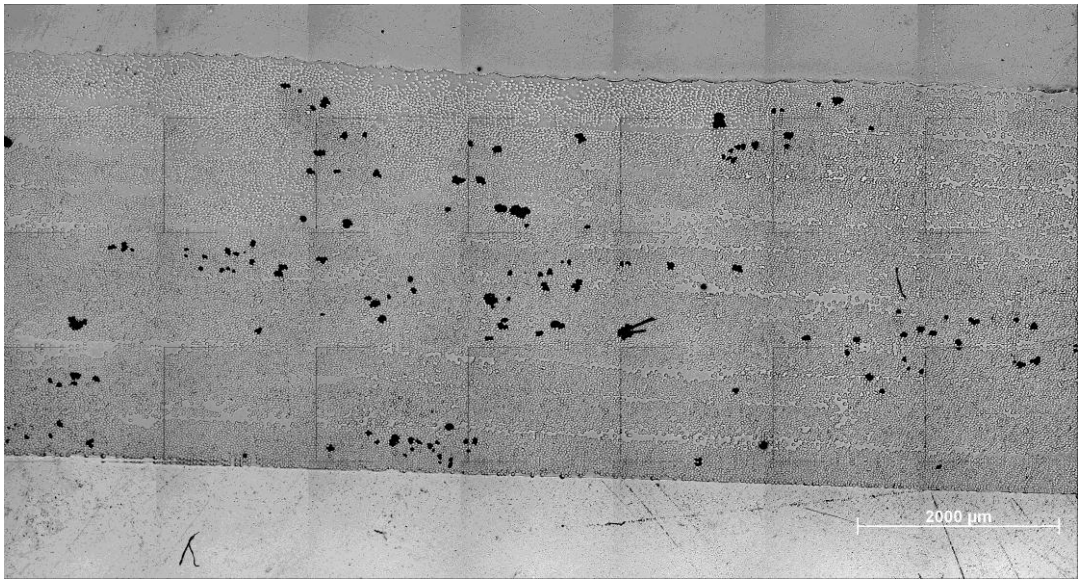

Figure 4.63 A micrograph showing a 10 inch tube wound using a modified version of Prototype-2 at 50 m/min to demonstrate process capability.

Having developed a clean filament winding impregnator unit (Prototype-2) that could produce filament wound tubes with the comparable and in some cases improved physical and mechanical properties, the next stage was to examine the advantages of using the clean filament winding process over the conventional process. Pandita *et al.*, (2007) showed that waste resin generation and solvent usage was reduced significantly

when compared with traditional wet-bath filament winding production. This being said a life cycle assessment of Prototype-2 was required to ensure that it still meets the clean filament winding philosophy by improving the environmental impact of the conventional winding system.

4.1.2.4.2 Life Cycle Assessment

Along with the overall physical and mechanical benefits seen in using Prototype-2 over conventional winding, there are more environmental and economic benefits that can be achieved. For Prototype-2 polyester resin tubes, an LCA was carried out to compare the advantages of the clean filament winding process compared to the conventional filament winding process. The following section looks at the results achieved from the LCA carried out on both processes.

Basic information was attained about the production process which remains unchanged between both processes with the exception of the dispenser power requirements. This information can be seen in Table 4.7.

Data Required	Data Acquired
Number of Tubes	4 (hoop winding)
Length of Tube	1.5 m
Winding Speed	7m/min
Mandrel Diameter	4.5 inch
Resin System	Epoxy / polyester
Roving/Layers	8 /4
Fibres	E-glass
Dispenser Power (max)	18.8 kW
Filament Winder Power (max)	3 kW
Oven Power	15 kW

Table 4.7 Data acquired in order to calculate the impact of clean and conventional filament winding.

Detailed information gathered for the LCA matrix is shown in Table 4.8. This information is process-specific and was measured for the clean filament winding process with Prototype-2 and for the conventional filament winding process. This information was then inputted into an LCA flow diagram which is seen in Figure 4.64 for conventional winding and Figure 4.65 for clean filament winding.

Tube	Speed (m/min)	Mass of Fibre Required (g)	Mass of Resin Required (g)	Mass of Resin Painted on the Mandrel (g)	Resin Wasted (g)	Resin Removed/Added at the Tube to Aid Impregnation (g)
Conventional Filament Winding	7	968	364	99	16	100 g removed from the tube
Clean Filament Winding	7	968	364	105	N/A	83

Table 4.8 Information gathered on-site for the LCA matrix.

It is important to note that the data reported here is dependent on the experience of the production team. The two operators concerned had over 10 years of practical experience with conventional filament winding and as such, have accumulated a wealth of knowledge and practical know-how. For example, they have become adept at estimating the volume of mixed resin that is required per set of mandrel diameters. Thus, minimising the volume of waste resin generated. With regard to the set-up and cleaning operations at the start and end of each shift, the two operators have developed an efficient sequence of activities to optimise the production of filament wound tubes in a time-efficient manner.

Gabi 5 (Thinkstep) was the computer software programme used to calculate the environmental impact of clean and conventional winding. An LCA can help manufacturers look at the following four aspects in order to improve processing:

(i) Design for environment: developing products that meet environmental regulations e.g. REACH, End of Life Vehicles.

(ii) Eco-efficiency: reducing material, energy and resource use in the most cost-effective way.

(iii) Eco-design: developing products with smaller environmental footprints such as fewer emissions, reduced water consumption and waste.

(iv) Efficient value chains: enhancing efficiency of value chains e.g. R&D, design, production, suppliers, distribution.

An LCA was carried out in this study on conventional and clean filament winding (taken using Prototype-2 impregnator unit). The data and information collected during the processing of the reference and clean filament wound tubes were used to produce flow diagrams shown in Figures 4.64 and 4.65. Reference information used to create the flow diagram consisted of manufacturing the raw materials (resins, fibres, solvents), the electrical power required to use the equipment in the process, transport and fuel, volumes of resin, fibres and solvent required for the process of the composite. In this case the end-of-life of the composite was not taken into account. With regards to the transport, the values calculated by the program normalised the transport process to the volume of the material used.

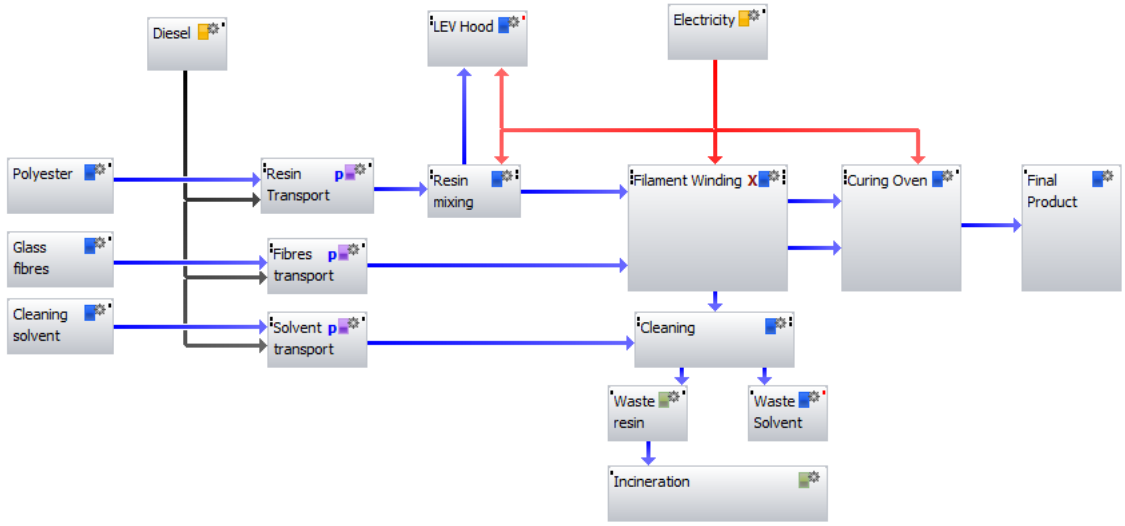

Figure 4.64 LCA flow diagram of the conventional filament winding process with a polyester resin system.

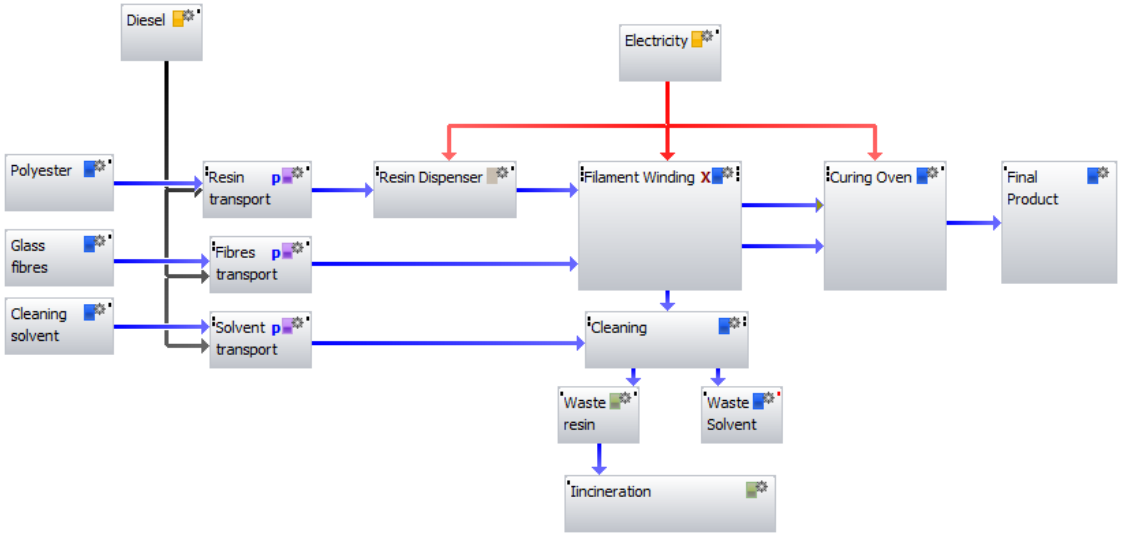

Figure 4.65 LCA flow diagram of the clean filament winding process with a polyester resin system.

From both the flow diagrams it becomes clear where the conventional process differs to the CFW process. One of the differences seen in conventional winding is the use of a local exhaust ventilation (LEV) hood (Figure 4.64). The LEV hood is required in conventional winding to extract airborne chemicals. This is not required in clean

filament winding as a resin dispenser is used to directly inject fibres (illustrated in Figure 4.65). Another area, which will have a larger environmental impact, is the quantities of waste resin and solvent (seen in Table 4.8) utilised in the clean filament winding tubes is much lower. This information is shown clearly in Figure 4.66 and Figure 4.67. It was assumed in clean and conventional winding that the waste resin generated from the process was cured and then incinerated. For the clean filament winding process the pressure-pot was connected to the resin dispenser and provided the power to the system to dispense the resin at given winding speeds.

Resin waste and solvent use are two of the biggest issues with conventional filament winding, and which clean filament winding aims to address. Figure Figure 4.66 presents clean filament winding as a percentage in relation to the conventional winding process. As can be seen in Figure 4.67 this aim has been achieved with the waste resin reducing by 88.1% and by 87.5% for solvent. The results demonstrate the reduction in the quantity of waste resin and solvent used when using clean instead of conventional filament winding. This was achieved via the direct resin impregnator unit, which is combined with dispenser system (pressure-pot) to impregnate the fibres directly at the resin impregnator unit. This then applies the correct resin quantities to achieve full impregnation of the fibre bundles at a given speed. The dispensing unit only delivers resin when the fibres are moving so there is no build-up of resin in Prototype-2 which needs to be disposed of. At the end of winding, the dispenser can be switched off and the static mixer thrown away, as opposed to the conventional winding process which has a resin bath with 2.5 litres of resin to dispose of. Also any excess resin removed

during the squeezing and manipulation of the fibres at the pinch pins and rollers flows back into the injector unit so is reused in Prototype-2.

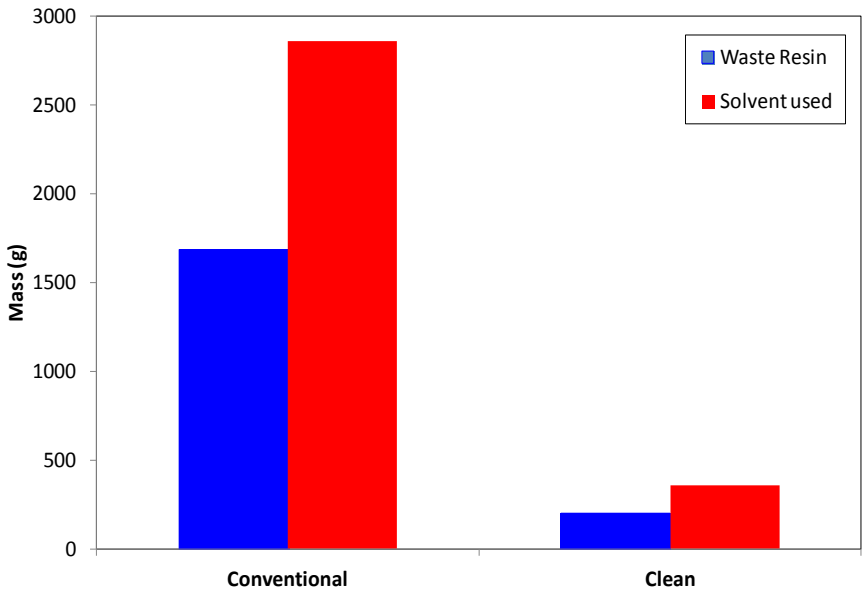

Figure 4.66 A graph showing a comparison of the waste resin (polyester) and solvent collected in grams during conventional and clean filament winding.

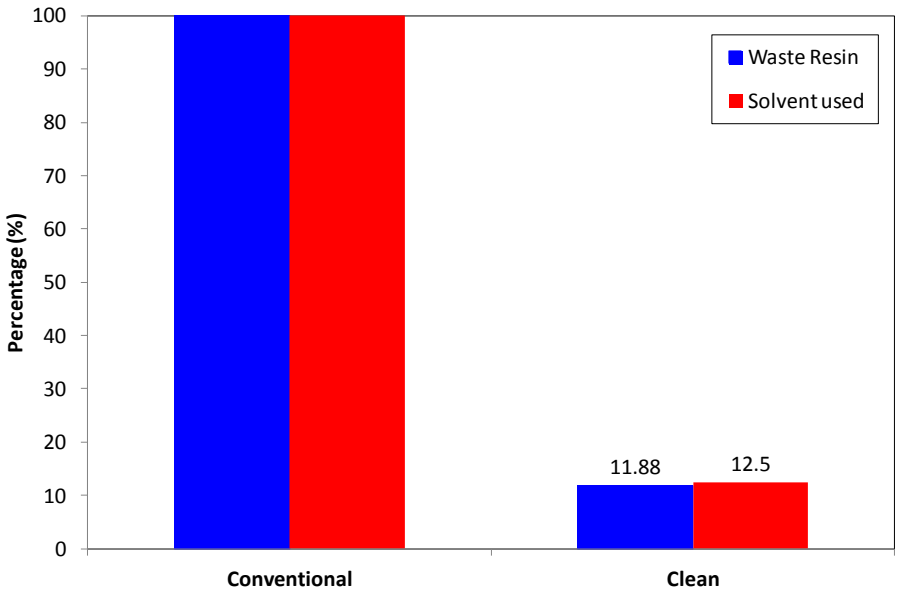

Figure 4.67 A graph showing a comparison of the waste resin (polyester) and solvent collected in during conventional and clean filament winding plotted as percentage against conventional winding.

The reduction in solvent used is 87.5% when using clean filament winding as opposed to conventional filament winding. This is due to the reduction in the amount of equipment requiring cleaning. For example, the items required for measuring out resin quantities, mixing resins, and catching drips, are reduced because the resin dispenser and disposable static mixer negates the need for them. Also, the area of the impregnator is much smaller than the large resin bath and so is much quicker and requires less solvent to clean. Although the solvent is recycled in the factory, if the volume required for winding could be reduced there would be significantly less exposure to solvents for a work force when cleaning and also sludge formed when combined with the polyester which requires disposal. These results are in agreement with previous findings by Shotton-Gale *et al.*, (2009), who suggested clean filament winding could significantly reduce the quantity of solvent required during the cleaning process, as well as significantly lowering the volume of waste resin generated.

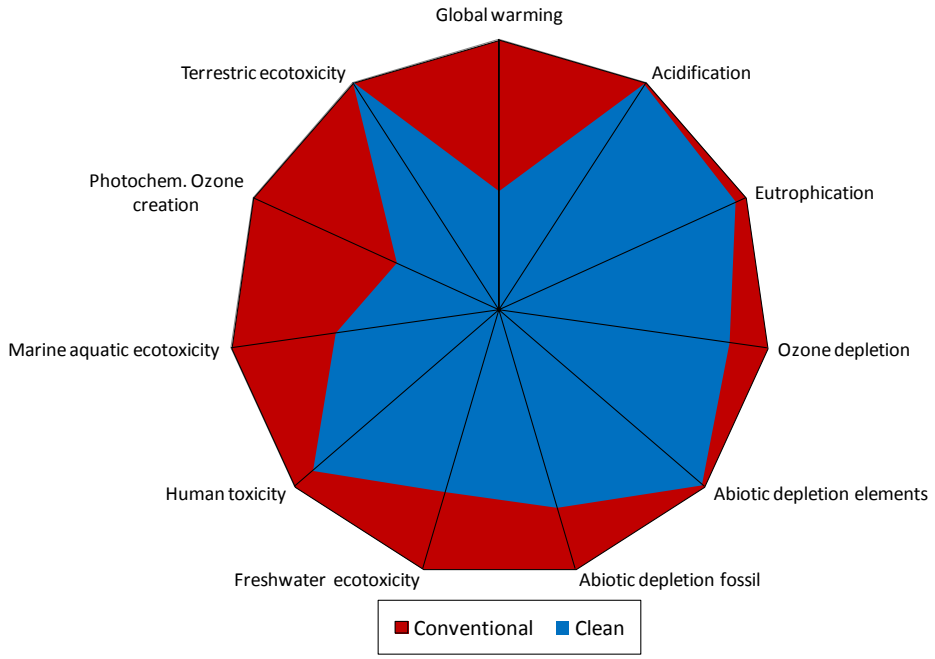

Figure 4.68 A spider-graph showing the environmental impact of a conventionally wound tube compared to a Clean filament wound tube produced using the polyester resin system.

The LCA data for the environmental impact of conventional and clean filament winding are shown in Figure 4.68. This figure shows the effect the conventional and clean filament winding tubes has on the environmental impacts derived by the Gabi 5 software. In the current study, CML 2001 (version Nov 2010) was used to compare the environmental impacts of the clean and conventional filament winding process. Each potential impact was measured against an equivalent emission; for example, acidification potential was measured in kilograms of SO_2 equivalent emitted (definitions of the other categories are defined in the Appendix Section D). From the graph it is clear that the clean filament winding process will reduce the environmental impact of a composite tube compared to a conventional filament wound tube.

In summary, the results obtained from the previous section indicate the advantages of clean filament winding over conventional filament winding with regards to the environmental impact of both processes. Due to the removal of the resin bath in favour of a resin impregnator unit, there is a reduction in the volume of waste resin and quantity of solvents required to clean it. The improvements seen in the reduction of environmental impact of the process can also lead to cost saving such as reduction in waste disposal as well as a less extensive LEV system installed to improve air quality.

4.1.2.4.3 Overall Summary

The improvements seen in clean filament winding are much greater when using Prototype-2 compared to Prototype-1. The composites produced were found to achieve much more comparable physical and mechanical properties. The key achievements are:

(i) The speed of retrofitting Prototype-2 was improved compared to Prototype-1 and took approximately 10 minutes before the set up was completed. This prototype met the design criteria and therefore, much more suitable for an industrial process.

(ii) Polyester resin systems can achieve a greater degree of impregnation compared to epoxy. Therefore, experiments focused on polyester resin matrix composites and further investigation was carried out into compatibility of the glass fibres to epoxy (Section 4.2 of Results and Discussion).

(iii) Physical and mechanical properties were comparable between tubes wound using Prototype-2 and conventional filament winding.

(iv) Coating the surface of the mandrel with resin prior to winding can improve impregnation levels at the inner bore region and therefore could potentially contribute to an increased hoop tensile strength.

(v) There is a significant reduction in the volume of waste resin and quantity of solvents required in the use of Prototype-2 over conventional filament winding.

(vi) The improvements seen in the reduction of environmental impact of the process can also lead to cost saving such as reduction in waste disposal as well as a less extensive LEV system installed to improve air quality.

4.2 GLASS FIBRE CHARACTERISATION

During the filament winding site trials that were undertaken in industry, there was a noticeable difference achieved with E-glass fibres and epoxy when compared to the polyester resin. A significantly improved degree of impregnation was seen in filament winding using polyester resin as opposed to epoxy. It was also noticed that using fibres from different manufactures had an effect on the degree of impregnation. As discussed

in the literature review the binder can have an effect on the impregnation seen in composites. It is important to understand any difference in the fibres surface characteristics and how this effects impregnation, as this has a knock on effect with the manufacturing process. This section characterises two fibre types: Type-I and Type-II with the aim of identifying differences between the as-received E-glass fibres which could affect composite processing and account for the void content that was observed during the site trials.

Type-I E-glass fibres used in this current study was single-ended fibre bundles specifically designed for use in filament winding and pultrusion applications in conjunction with polyester, vinyl ester and epoxy systems (See Table 3.1).

Type-II glass fibres were also single-end fibre bundle designed to reinforce polyester, vinyl ester, and epoxy resin systems in woven or multi-axial fabrics, pultrusion, and filament winding applications (See Table 3.1).

A comparison of mechanical properties of each fibre type is shown in Table 3.1. From the data sheets, it is difficult to make a direct comparison as the required information for both fibres is not always given. Furthermore, details of the experiments carried out to attain the results cited in Table 3.1 were given in some instances, but not in others.

The measurement used to describe the reinforcing fibres is tex. As mentioned previously, this is defined as the mass in grams of 1000 m of fibre. This means that the number of filaments within a fibre bundle can differ due to the filament diameter variations, whilst still being classed as the same glass fibre tex. The relationship between tex and the number of the individual filaments in a fibre bundle (N_F) is given by Equation 4.2:

$$N_F = \frac{100\ x\ tex}{(\pi r_F^2 \rho)}$$

Equation 4.2

Where radius r_F is the radius of the filament (μm) and ρ is the density of the fibre (g/cm^3) (Irfan *et al.,* 2011). The glass fibre density from both glass fibres was ascertained from the manufacturers. The density stated by the manufactures for Type-I and Type-II fibre types was 2620 kg/m^3. Therefore, 2620 kg/m^3 was used throughout this study in all calculations.

4.2.1 Fibre Features

When comparing both fibre types, there were visible differences between the two types of fibre supplied from the two manufacturers. The following section identifies the key characteristics that were observed in Type-I and Type-II fibre bundles.

(i) Striations

An example of striations is seen in Figure 4.69. These were most commonly seen in Type-II fibres and are a result of a crimping effect due to the continuous fibre bundle being over wound on top of itself to produce the fibre creels. A higher winding tension could be the cause for the excess crimping seen to be more prominent in Type-II fibres. Irfan *et al.,* (2014) commented on excessive tension as a possible reason for the crimp on the fibres after drying. Figure 4.69 demonstrates the high degree of crimping seen in Type-II fibres.

Figure 4.69 A photograph showing the high degree of fibre crimping seen in Type-II fibres.

(ii) Bundles Splitting/Segmentation

Segmentation of the bundle was common in both fibre types and is shown in Figure 4.70. This is not desirable because it could lead to resin rich areas in the composite due to a lack of reinforcing fibres. Furthermore, it can also result in the formation of voids due to air entrapment in these regions.

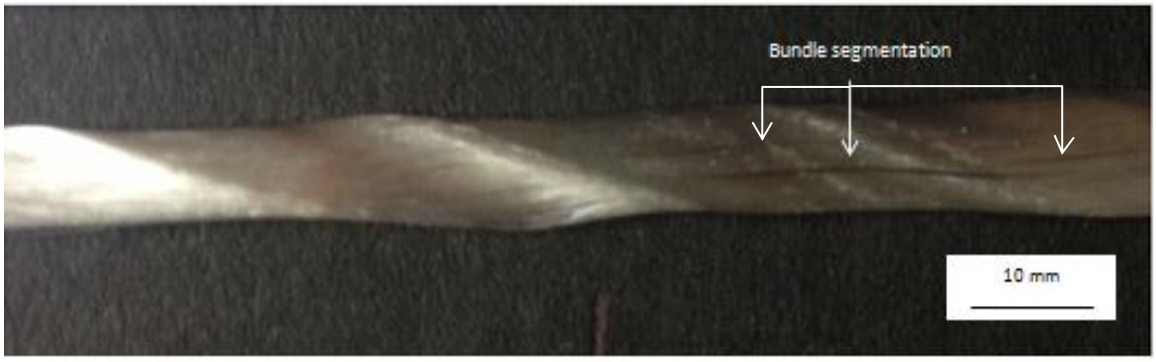

Figure 4.70 A photograph of Type-II fibres showing typical splitting/segmentation of the fibre bundle.

(iii) High Binder Content

On inspecting the surfaces of the Type-I and II fibres, it was observed that there were areas on the fibre surface where the relative concentration of the binder was significantly higher. These features were seen in small patches on Type-II fibres but

were observed to be excessive on the Type-I fibres. As well as areas of high binder content, there were areas with significantly lower visible binder content. Both high and low levels of binder content can be seen in Figure 4.71. With reference to Figure 4.71 (i) it was observed that the sections with lower binder content did not reflect the incident light as much as the regions with the higher binder content; as seen in Figure 4.71 (ii). At that stage in the study it was not known what the significance of the binder content was on the processability, impregnation rates, bundle coherence during processing and the strength of the fibre bundle. However, it was clear that there was a large variability in binder content in fibre Types-I and II.

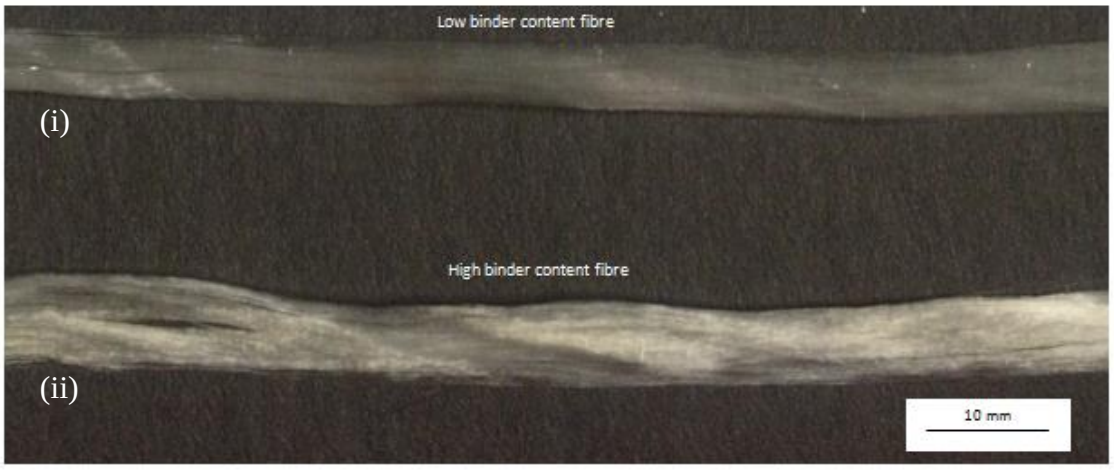

Figure 4.71 A photograph showing (i) low; and (ii) high binder content in Type-I fibres.

(iv) Fibre Bundle Twists

Twisting of the fibre bundle is observed during filament winding when drawing the bundles from the centre of the creel. The fibre bundle in a creel can be drawn out from the outer circumference (outside draw), seen in Figure 4.72 (ii), or from the bore (centre-pull), seen in Figure 4.72 (i).

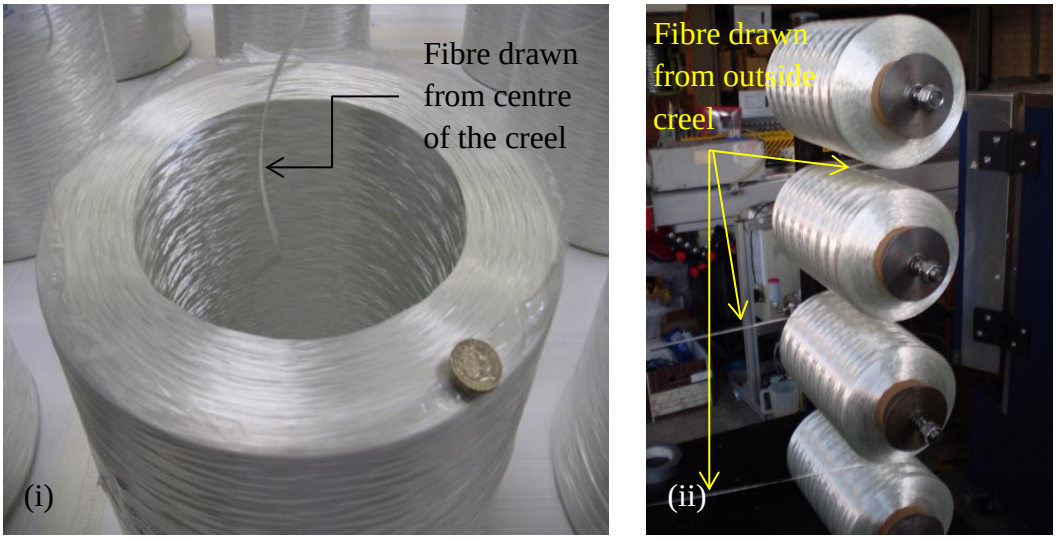

Figure 4.72 Photographs showing glass fibres being extracted by (i) centre-pull; and (ii) outside-draw.

Centre-pull is the predominate method of paying out the fibres in commodity high-volume filament winding products. This is because motorised spindles with tension control are not required. On the other hand outside-draw does require these items. Centre-pull creels are easier to store and stack. However, twisting of the bundle is inherent when centre-pull is used. This can influence the degree of achievable impregnation (Irfan *et al.,* 2014) at winding speeds used in industry.

Twists will also have an effect on the mechanical properties of the composites. Although some studies have demonstrated that a degree of twist in the fibre bundle can improve quasi-static tensile strength, a high degree of twist was found to damage the fibres and reduced the tensile strength of the yarn (Rao and Farris, 2000). However, twists have been found to influence the rate of impregnation, as they result in a greater fibre bundle thickness. This increases the compaction within the bundle and therefore increases the impregnation rate (Pandita *et al.,* 2012). During filament winding it was observed that the twist accumulates behind the tensioning device and then at some

period (random) the twisted region is hauled through the tensioning device. It is likely that this will lead to voiding and the resultant variability in the mechanical properties.

4.2.2 Visual Observations

4.2.2.1 As-Received Fibres

Figures 4.73 and 4.74 shows the fibre architecture of Type-I and Type-II fibres respectively, where the capillary impregnation process was used to impregnate fibres prior to mounting and polishing. Due care and attention was taken to ensure the fibre architectures were retained. From Figure 4.73, it can be seen that Type-I fibre appears to have an even cross-sectional thickness. This differs when compared to fibre Type-II which was observed to vary in cross-section; see Figure 4.74. It is also apparent in Figure 4.73 that Type-I fibres appear to be more uniformly dispersed without significant resin-rich areas. This was not observed in Type-II fibres.

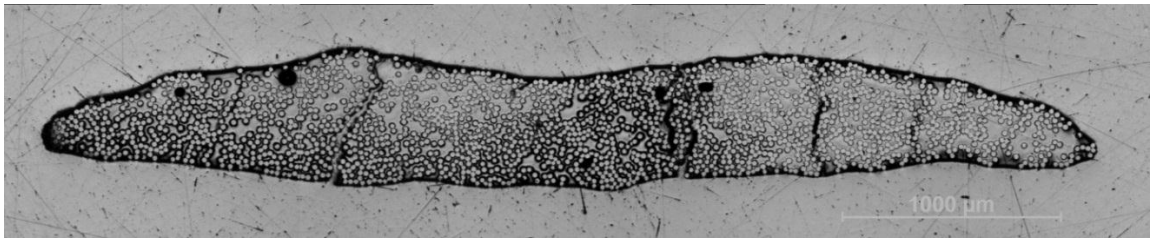

Figure 4.73 A micrograph of as-received Type-I fibre bundle showing the architecture.

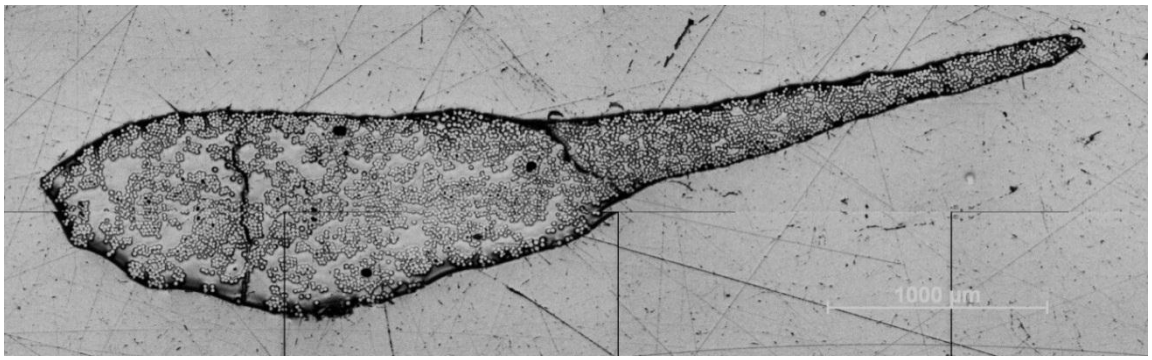

Figure 4.74 A micrograph of as-received Type-II fibre bundle showing the architecture.

The micrographs shown in Figure 4.75 and Figure 4.76, for Type-I and Type-II fibres respectively, were obtained from the impregnation-blocks described in Section 3.2.3.3. This experiment was undertaken to investigate the impregnation characteristics of as-received bundles without any imposed tension or manipulation as experienced during processing. Type-I fibres seen in Figure 4.75 shows that the filaments separate and spread out significantly upon contact with the mixed resin system. On the other hand, fibre Type-II, shown in Figure 4.76, displayed a completely different response when placed in the resin system. In this instance, the fibre bundle retained its architecture. However, the fibre distribution was not uniform with large areas of filament bunching, resin-rich regions and voids. It was noticed that the centre region of the bundle contained a higher void fraction.

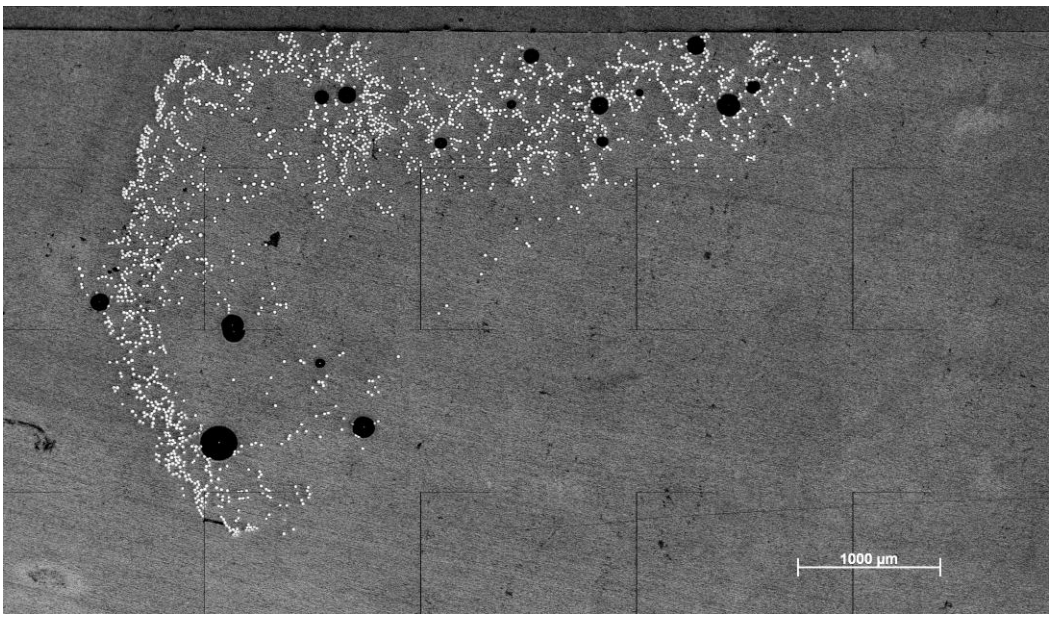

Figure 4.75 A 1micrograph showing a Type-I as-received fibre immersed and cured in the LY3505/XB3404 epoxy resin system.

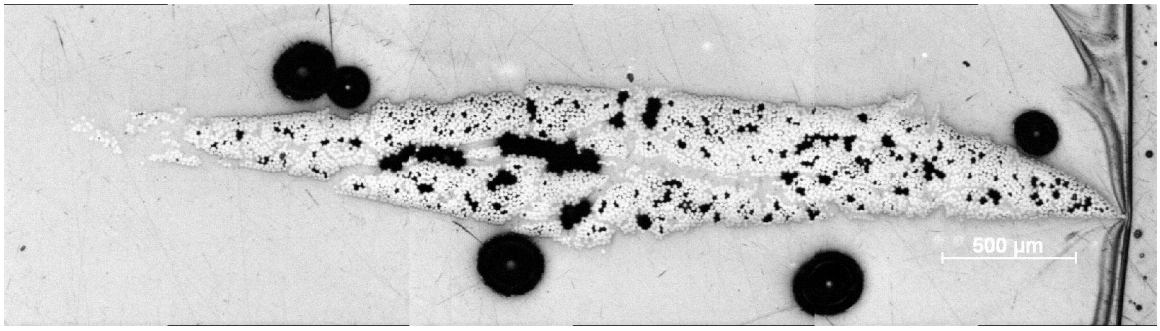

Figure 4.76 A m2icrograph showing a Type-II as-received fibre immersed in LY3505/XB3404 epoxy resin.

Although Type-I fibres had on average a lower binder content (0.31%) when compared to Type-II fibres (0.6%), the former had intermittent regions of higher binder content. Hence it does make it difficult to draw definitive conclusions on the significance of the binder content on the impregnation characteristics during production.

Figures 4.77 (i) and (ii) represent magnified regions of Figures 4.75 and 4.76, it can be seen that the average as-received filament diameters for Type-I and Type-II fibres are 25 and 17 µm respectively. This is due to differences in the production methods (Thomason *et al.*, 1999). Figure 4.77 (ii) also illustrates the voids which have formed in between the filament channels of the Type-II fibres.

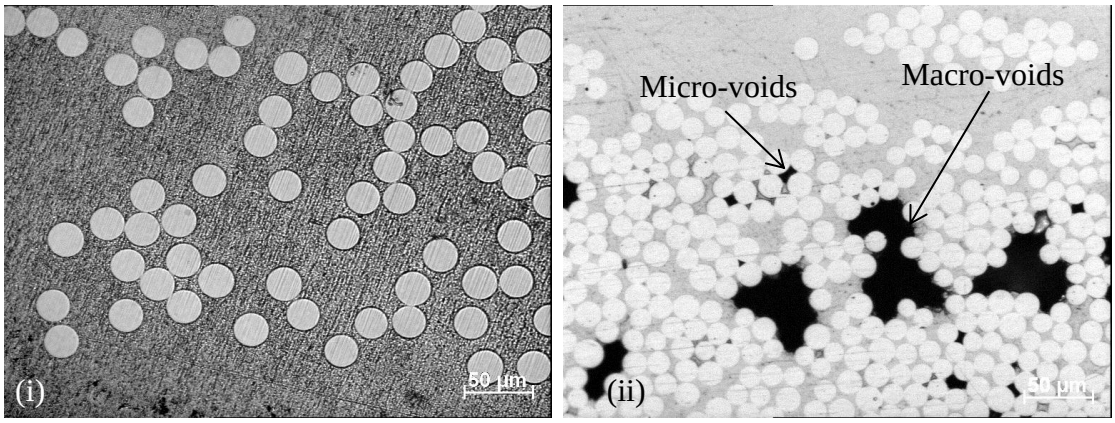

Figure 4.77 Micrographs showing as-received: (i) Type-I; and (ii) Type-II fibres that have been potted and polished.

Micro-pore voids as seen in Figure 4.77 (ii) may have been caused by capillary wicking (Park *et al.,* 2011). Capillary wicking is much slower than the viscous flow of the resin, leading to air entrapment as the resin moves over the filaments which have yet to be impregnated. Bayramli and Powell (1992) found similar results in carbon fibre/epoxy composites in their study of axial impregnation on single fibre bundles. They showed that the formation of voids can be a result of random fibre packing. As discussed previously, this was thought to be caused by the different rates of impregnation through different pore sizes, with the faster rates causing air to get trapped in the narrower channels. Micro-pore voids are expected more in the closely packed regions of the fibre bundle. One of the main causes for this filament bunching could be the level of binder remaining on the fibres after the manufacturing process. Fibres with a high level of binder were observed to be 'stiffer' during handling. The implication here is that sections of the bundle with a higher binder content result in the filaments being held together more effectively. This therefore suggests that some form of fibre manipulation during processing is required to disrupt the cohesion of the binder, thus improving the degree of impregnation.

4.2.2.2 SEM of As-Received Fibres

SEM images of as-received Type-I and Type-II glass fibres were obtained using the method described in Section 3.2.2.1. This gave a clear representation of the binder distribution. Figures 4.78 (i), (ii), (iii) and (iv) show that the binder distribution on Type-I glass fibres is uneven. As previously mentioned, the binder on the fibre surface can be dislodged/partially removed during subsequent manufacturing of the composite (filament winding, weaving etc.). Since the micrographs shown in Figures 4.78 (i) –

(iv) represent as-received bundles, that have not been subjected to any composite production, the origin of the residual binder can only be attributed to the production process of E-glass. Mallarino *et al.*, (2005) presented a similar SEM image of the uneven distribution of binder seen on as-received glass fibres (see literature review Figure 2.2 (ii)). Figure 4.78 (ii) represents debris that has been deposited on the surface of the fibre before SEM inspection. It was not possible to obtain any compositional information of the debris using energy dispersive X-ray spectography (EDX). Attempts to analyse the composition of the binder residues were unsuccessful, possibly because it was organic in nature or that the penetration depth of the beam was too great. Figures 4.78 (iii) and (iv) highlight the linking of two filaments by 'residual' binder; this is referred binder bridging.

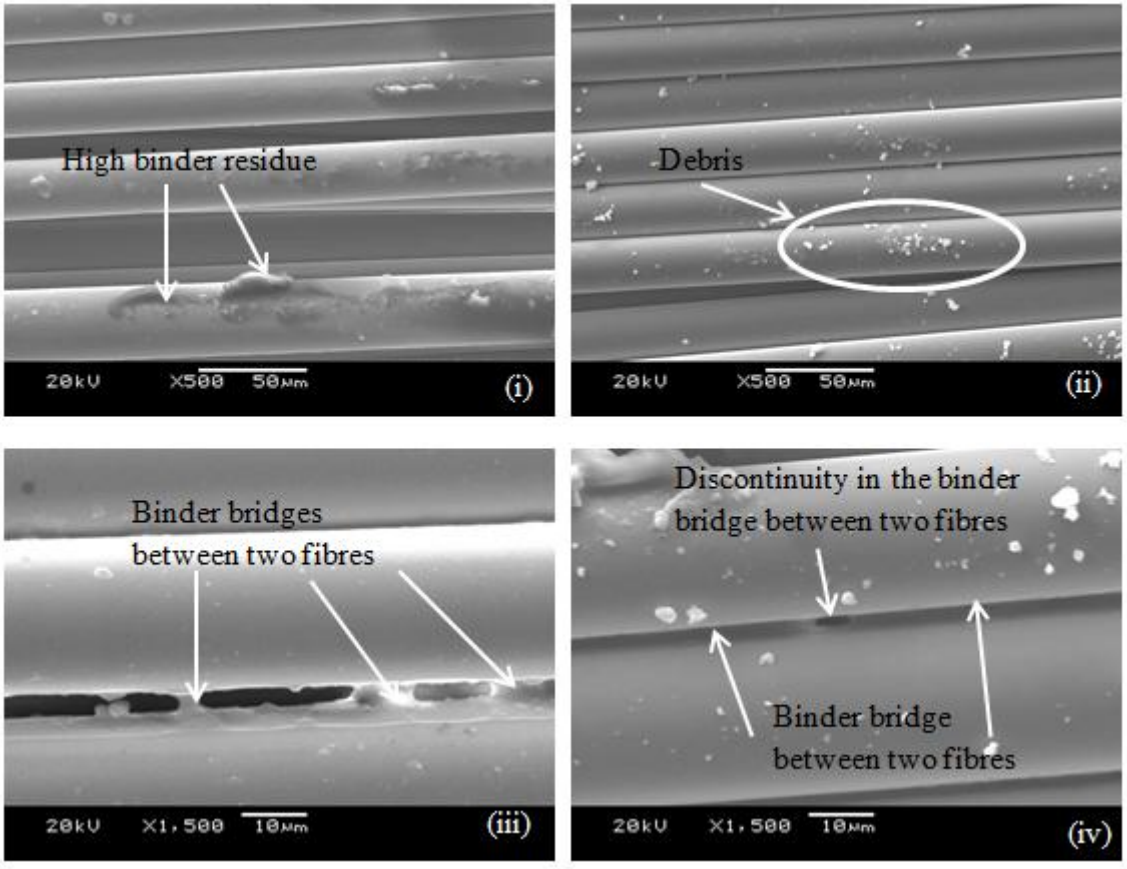

Figure 4.78 SEM images (i), (ii), (iii) and (iv) showing the distribution of binder on as-received Type-I fibres.

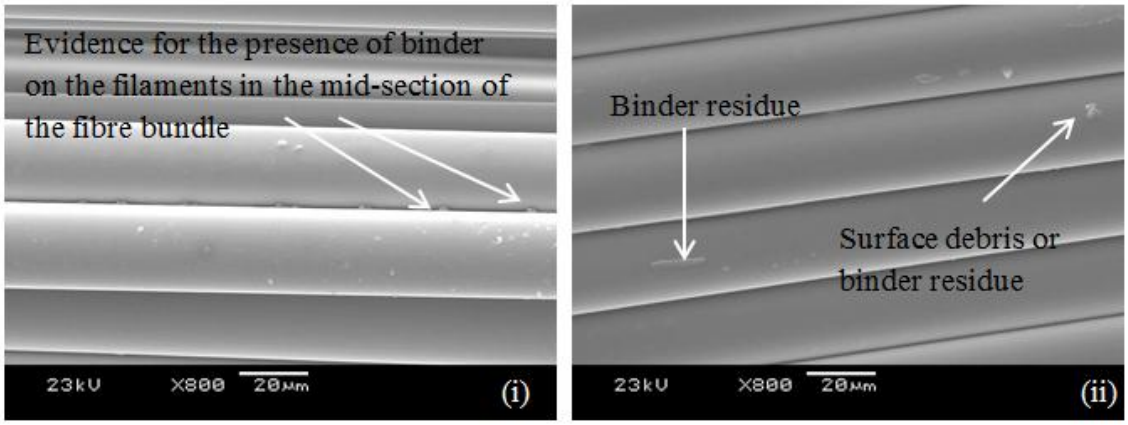

Figure 4.79 SEM images (i) and (ii) showing the distribution of binder on the mid-section filaments of an as-received Type-I.

Figure 4.79 shows a Type-I glass fibre which has had the top layers of filaments carefully removed so that the mid-section of the fibre bundle could be viewed. Figure 4.79 (i) and (ii) indicate the presence of the binder in the mid-section of the fibre bundle. However, the distribution in the excess binder in the mid-section of the fibre bundle was significantly lower when compared to the filament in the perimeter of the bundle (Thomason and Adzima, 2001).

As previously mentioned, within the creels there are often visibly higher concentrations of binder on sections of the fibre bundle. Figures 4.80 (i), (ii), (iii) and (iv) shows the SEM images taken of one of these high-binder content regions in Type-I fibres. It can be seen that there is a very large quantity of binder distributed in these regions. Moreover, the cohesion of the filaments within the binder appears to be high, thus possibley imparting ‘stiffness’ to the bundle as mentioned previously.

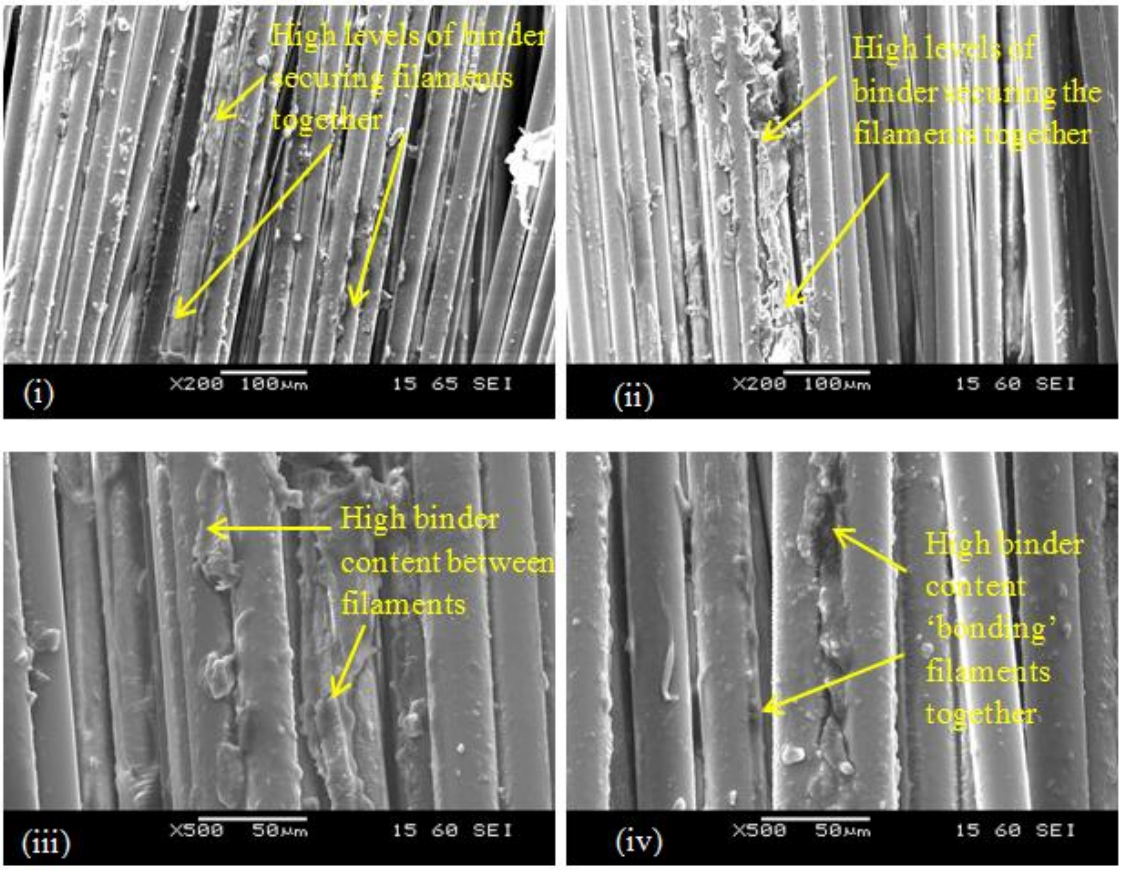

Figure 4.80 SEM images (i), (ii), (iii) and (iv) showing the high binder content regions seen in the as-received Type-I fibre bundle.

Figures 4.81 (i), (ii), (iii) and (iv) show the binder on the as-received Type-II glass fibre bundle. From these images, it can be seen that the degree of binder on the surface of the filaments appear higher than those seen in the micrographs of Type-I fibres (Figures 4.78 (i), (ii), (iii) and (iv)). In Figure 4.81 (ii) it can be seen that the binder residues are distributed in a particular direction. This is likely to be related to the winding angle of the fibre bundle within the creel.

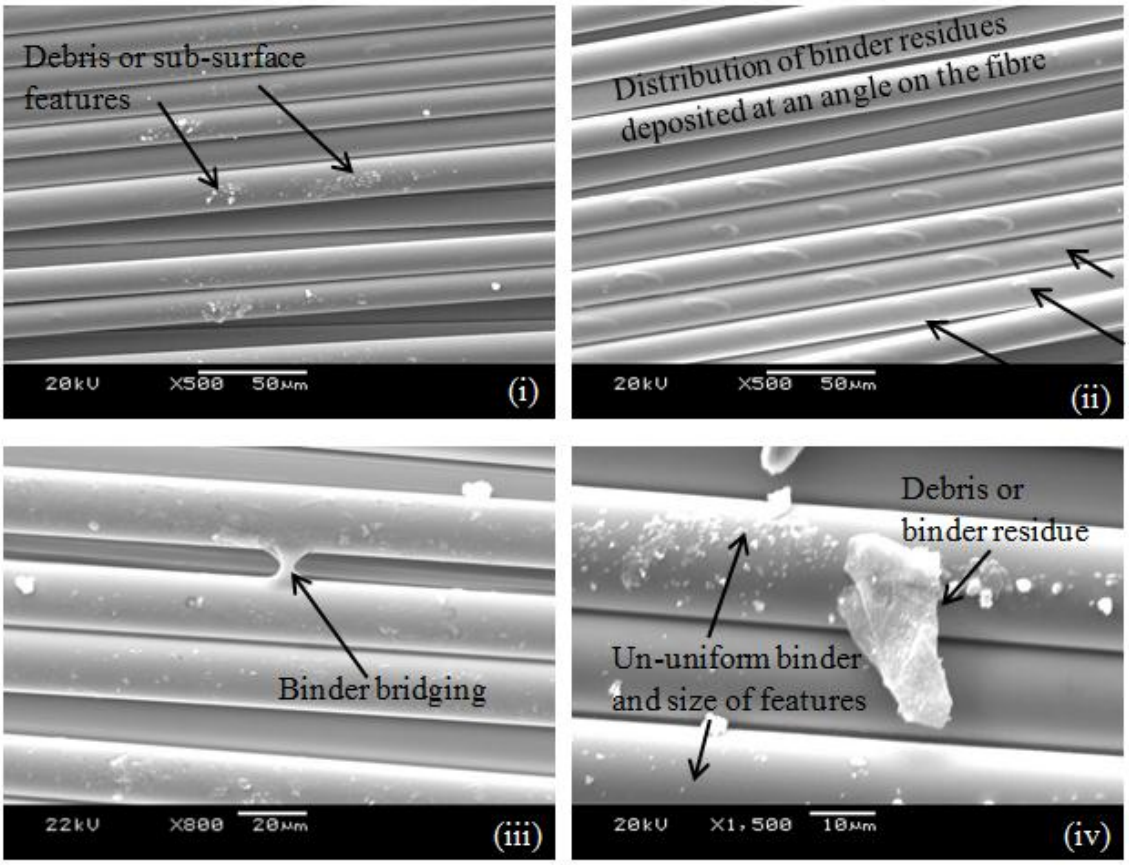

Figure 4.81 SEM images (i), (ii), (iii) and (iv) showing the high binder content regions seen in the as-received Type-II fibre bundle.

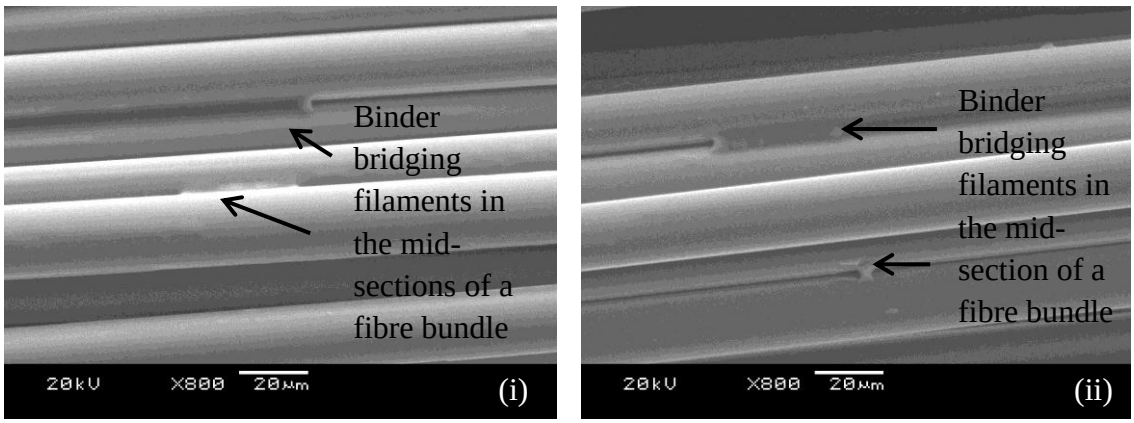

Figure 4.82 (i) and (ii) SEM images showing the distribution of the binder on the centre filaments of an as-received Type-II fibre.

As with the Type-I fibres, Figures 4.82 (i) and (ii) shows the Type-II fibre bundle with the top layer removed so the binder though fibre bundle can be observed. It appears that

there is a much larger distribution of binder on the filaments within the mid-section of the fibre bundle when compared to the Type-I fibres. This is consistent with the previous observation that the average binder content is higher in Type-II fibres.

In conclusion, it has been demonstrated that there are differences between Type-I and Type-II fibres in their as-received form with regard to the binder content and its distribution. Furthermore, the average fibre diameters for Type-I and II were 25 μm and 17 μm respectively.

4.2.3 Acetone extraction

Acetone extraction was used to remove the soluble components of the binder on the glass fibre bundles. Figure 4.83 shows the results of two experiments where Type-I and Type-II fibre bundles were immersed in acetone for 24 or 48-hours (detailed in Section 3.2.2.2).

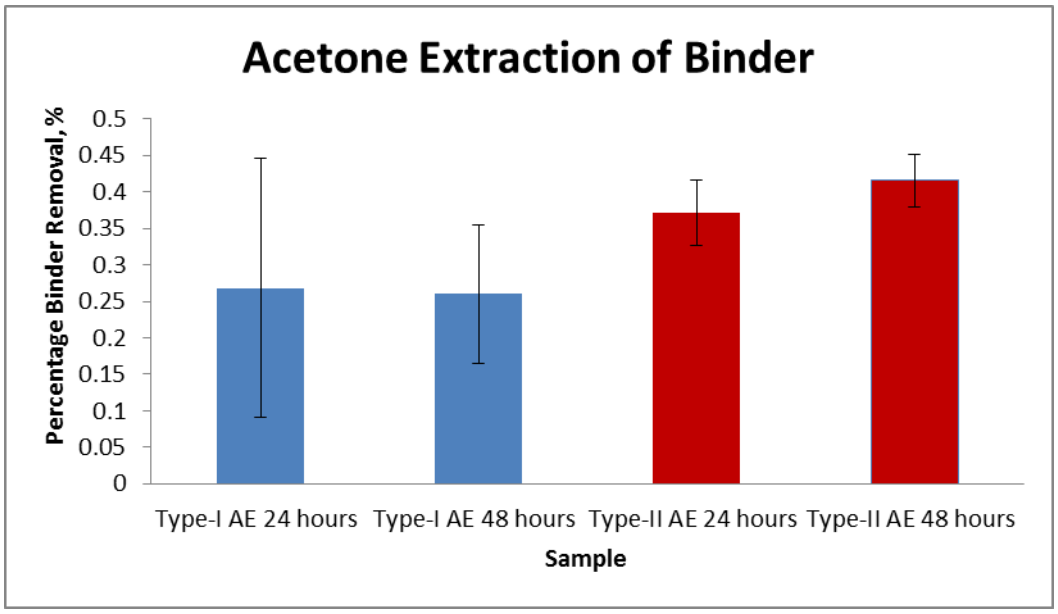

Figure 4.83 shows the results of two experiments where Type-I and Type-II were submerged in acetone for 24 or 48-hours.

With reference to Figure 4.83, it can be seen there is a higher mass of binder removed from Type-II fibre when compared to Type-1 (0.37% and 0.27% respectively). A further decrease of 0.4% was observed in Type-II fibres when the immersion time was increase from 24 to 48-hours. For Type-I fibre, there is a larger variability in the data and this could be due to the uneven binder distribution shown previously.

After acetone extraction for 24-hours of Type-I fibres, features that were attributed to debris previously can also be seen in Figure 4.84 (i). It can be seen from Figures 4.84 (ii) and (iii), that globule-like features are present. It is speculated this maybe components present in the binder that are insoluble in acetone. Areas indicating the depletion of the binder can be seen in Figure 4.84 (iv).

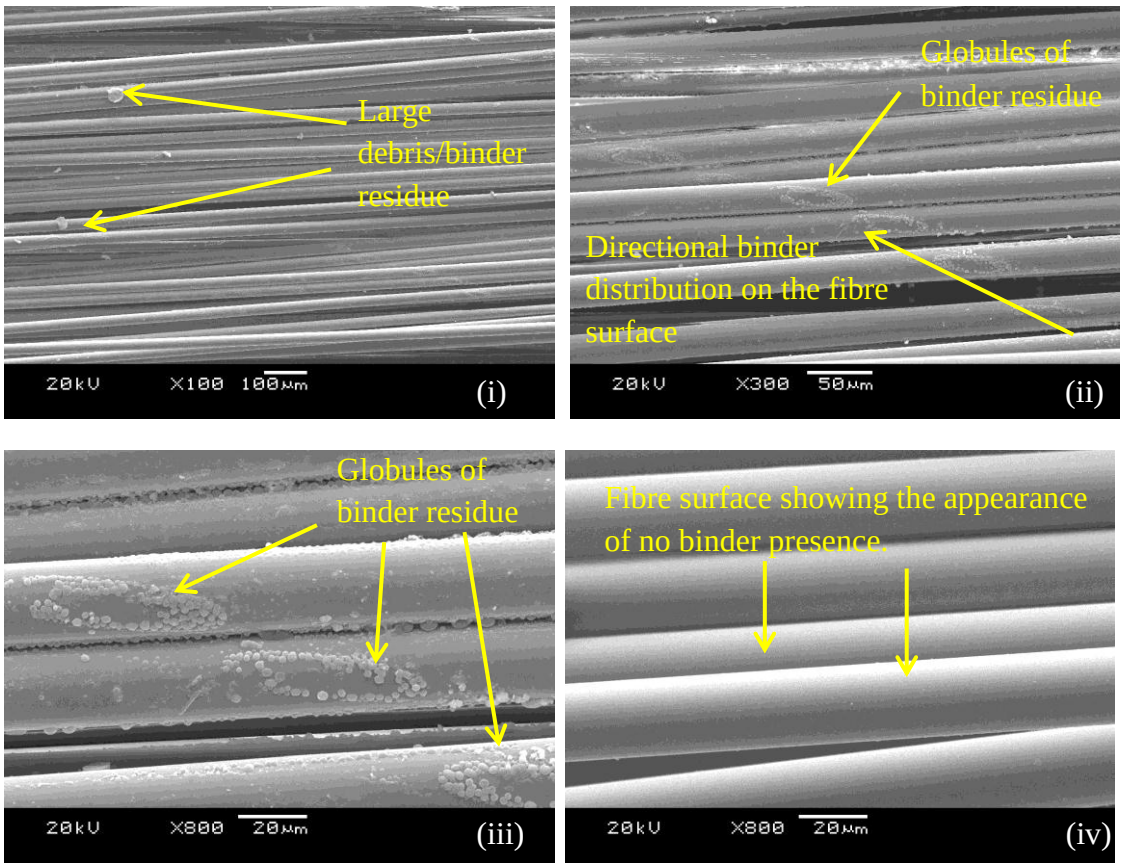

Figure 4.84 SEM images (i), (ii), (iii) and (iv) showing Type-I fibre bundle after 24-hour acetone extraction.

In the case of Type-II fibres, Figures 4.85 (i) and (ii), show lower levels of binder residue observed after 24-hours acetone extraction. Figure 4.85 (iii) shows the elliptical binder residue as observed previously in Figure 4.81 (ii). However the globule like features observed in Type-I fibres were not apparent in this instance. A significantly reduced binder residue is seen in Figure 4.85 (iv).

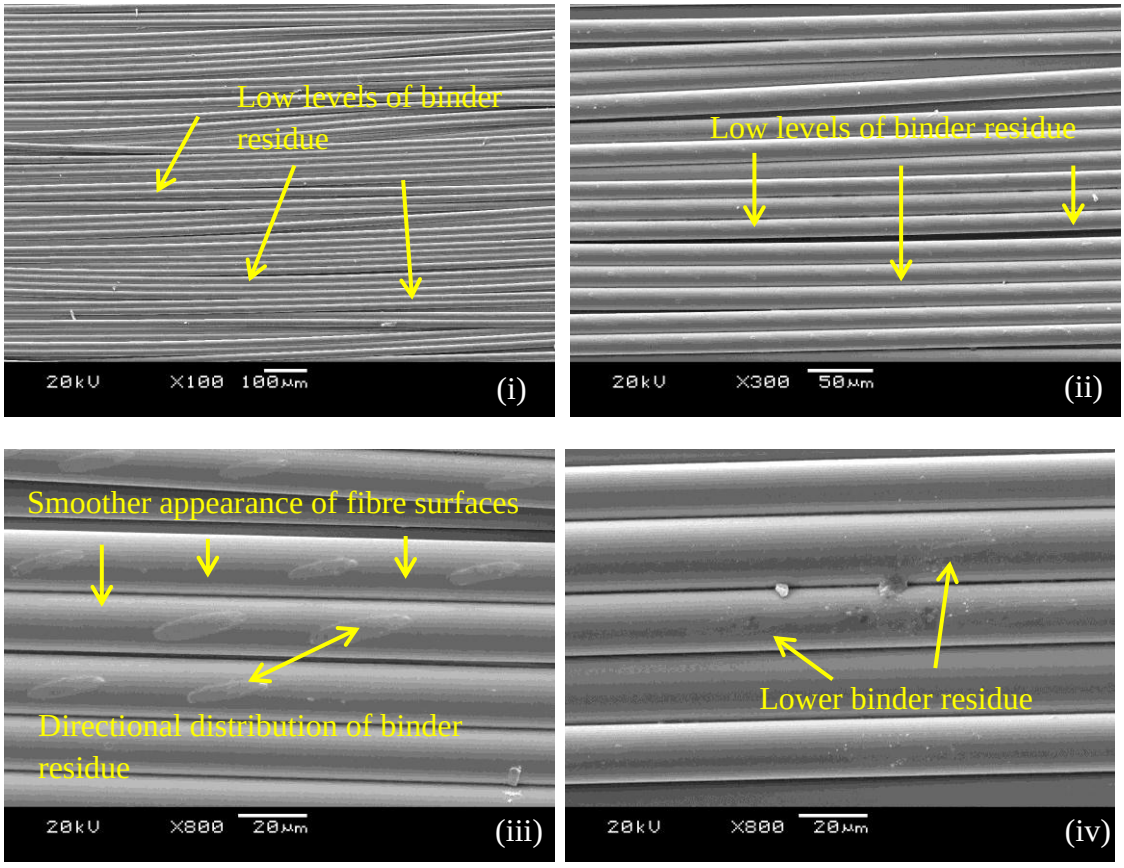

Figure 4.85 SEM images (i),(ii), (iii) and (iv) showing Type-II fibre bundle after 24-hour acetone extraction.

SEM images of Type-I bundles subjected to acetone extraction for 48-hours are shown in Figures 4.86 (i), (ii), (iii) and (iv). A large number of globules can be seen on the surface of the filaments. It is speculated that these could represent a redistribution/re-attachment of the globules that were observed previously in Figure 4.84 (iii). Since the

composition of the binder was not known, unfortunately it was not possible to investigate this aspect any further.

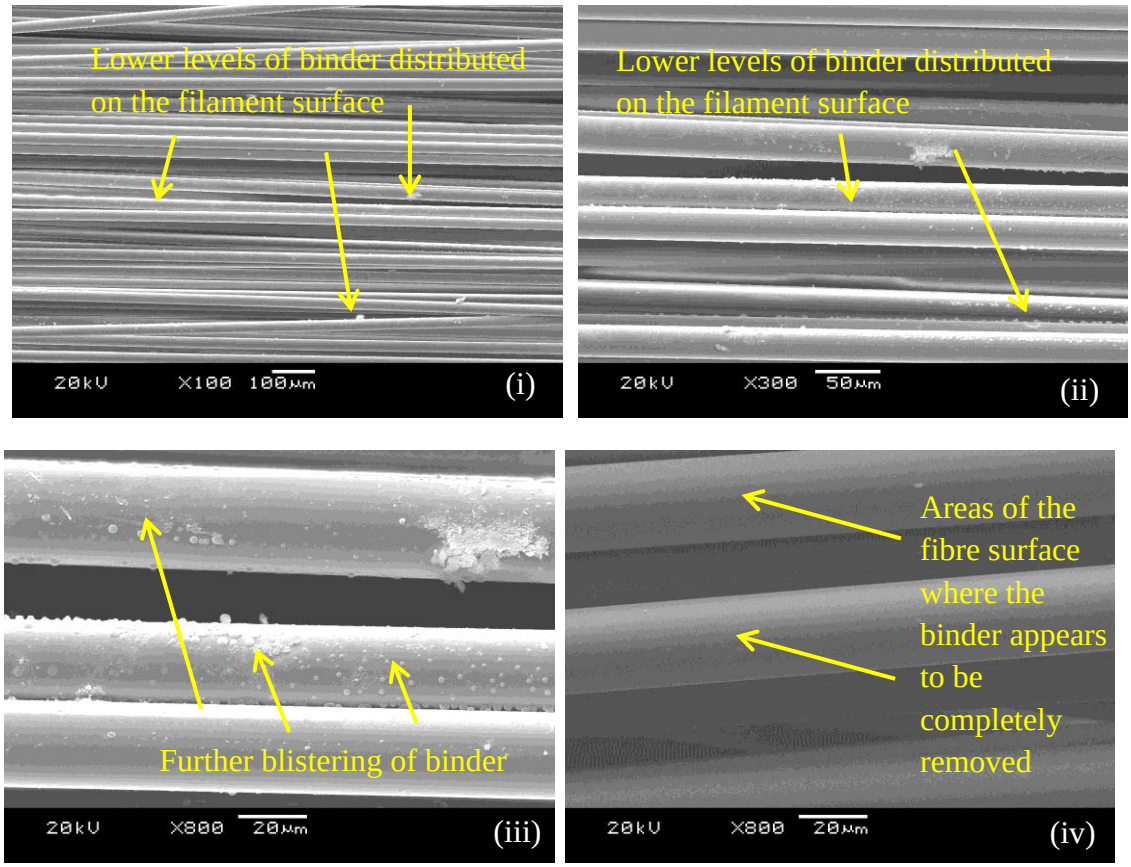

Figure 4.86 SEM images (i), (ii), (iii) and (iv) showing Type-I fibre bundle after 48-hour acetone extraction.

Figures 4.87 (i), (ii), (iii) and (iv) show the Type-II fibres after 48-hours of acetone extraction. In this instance, the binder residue on the surface of the filaments is reduced significantly. This observation is in agreement with the data presented in Figure 4.83.

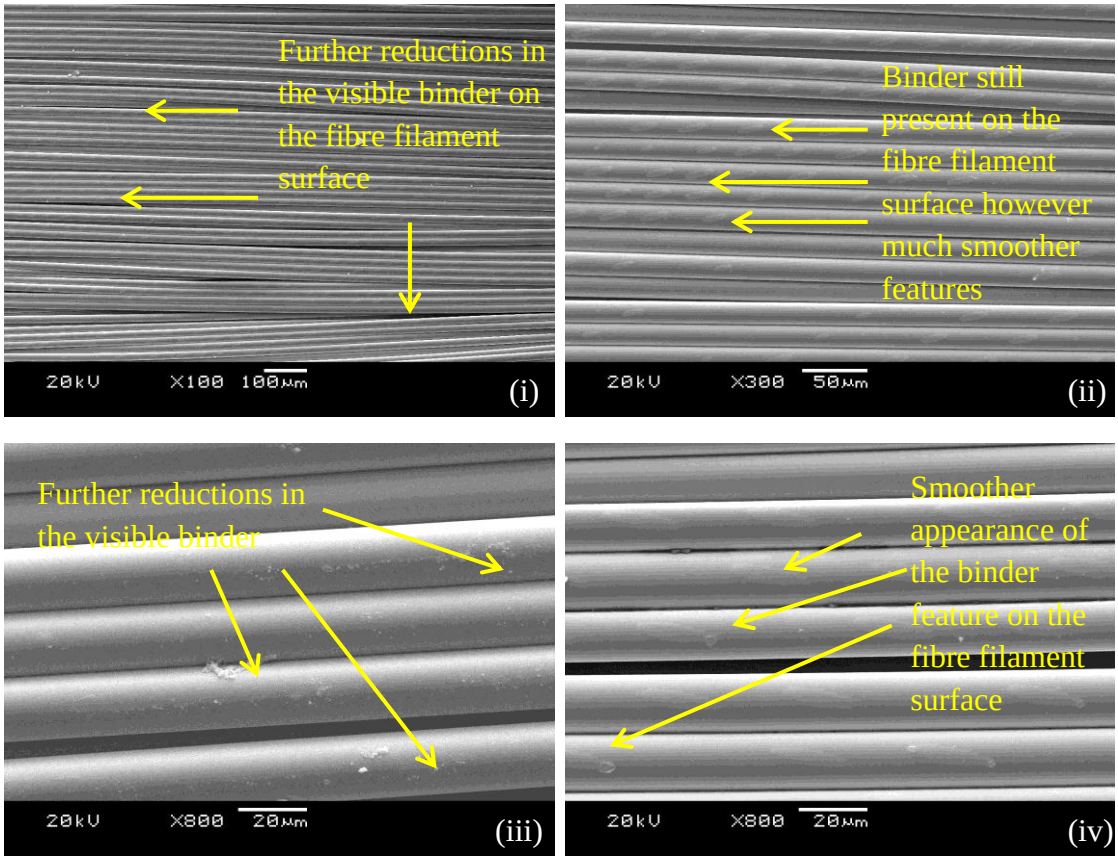

Figure 4.87 SEM images (i), (ii), (iii) and (iv) showing Type-I fibre bundle after 24-hour acetone extraction.

4.2.4 Loss-on-Ignition

The binder content on as-received fibre Types-I and II were determined using the loss-on-ignition (LOI) method, as described in Section 3.2.2.3. The samples were obtained from specified sections of the creels as illustrated in Figures 3.16. According to Mouritz and Gibson (2007), the mass loss of the fibres increases with temperature due to decomposition and volatilization of the organic binder. This occurs over the range 250-500 °C which is the decomposition temperature range for epoxy-based binders. In the LOI ASTM D4963/D4963M the temperature used is 625 °C to removal all organic compounds in the binder.

Figure 4.88 shows the percentage of binder found at specified locations of the Type-I fibre creel. It can be seen that there is a reduction in the binder content closer to the middle of the glass fibre creel. There are two possible reasons for this: (i) there is a redistribution of the binder content through the creel during the production process, where the binder is squeezed to the outer areas during the winding of the creel; and (ii) the migration of the binder towards the outer surface and inner bore during drying. A section of the fibre that was deemed to contain high binder content, as assessed visually was evaluated and is included in Figure 4.88. This proved conclusive evidence that these regions do contain an above average binder content.

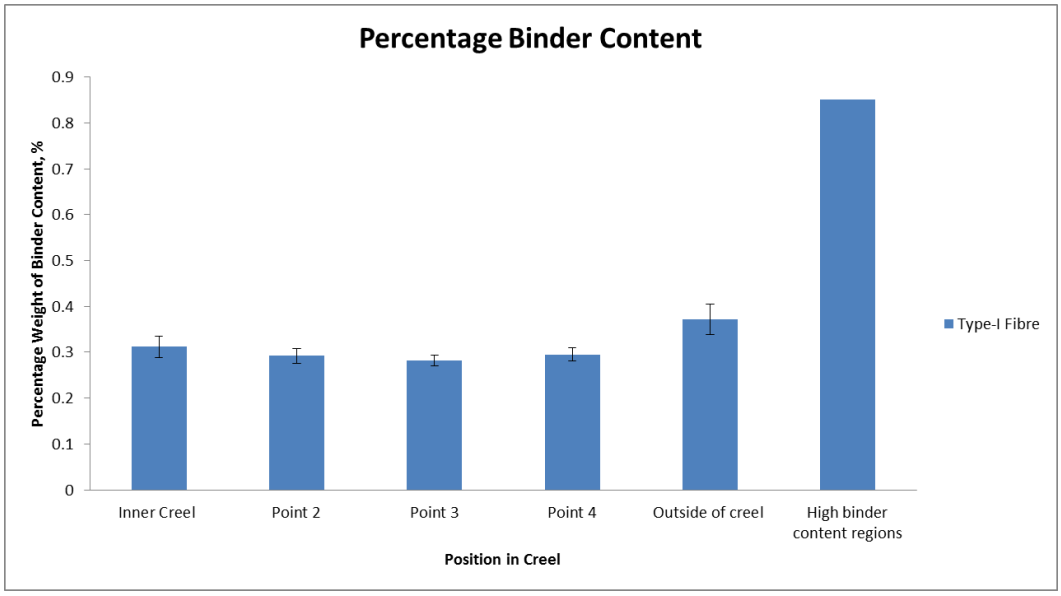

Figure 4.88 A graph showing the percentage binder content removed from Type-I fibres at five different points through a fibre creel. The far right bar shows a high binder content region seen in Figure 4.80.

A similar observation can be seen in Figure 4.89 for Type-II fibres but the binder content is relatively more uniform. It is noted that some manufactures remove a portion of the fibres from the bore and surface regions to ensure compliance with the specified binder content. The binder contents reported in Figures 4.88 and 4.89 are consistent with that reported in the literature (Britcher *et al.*, 1999 and Thomason, 2012)

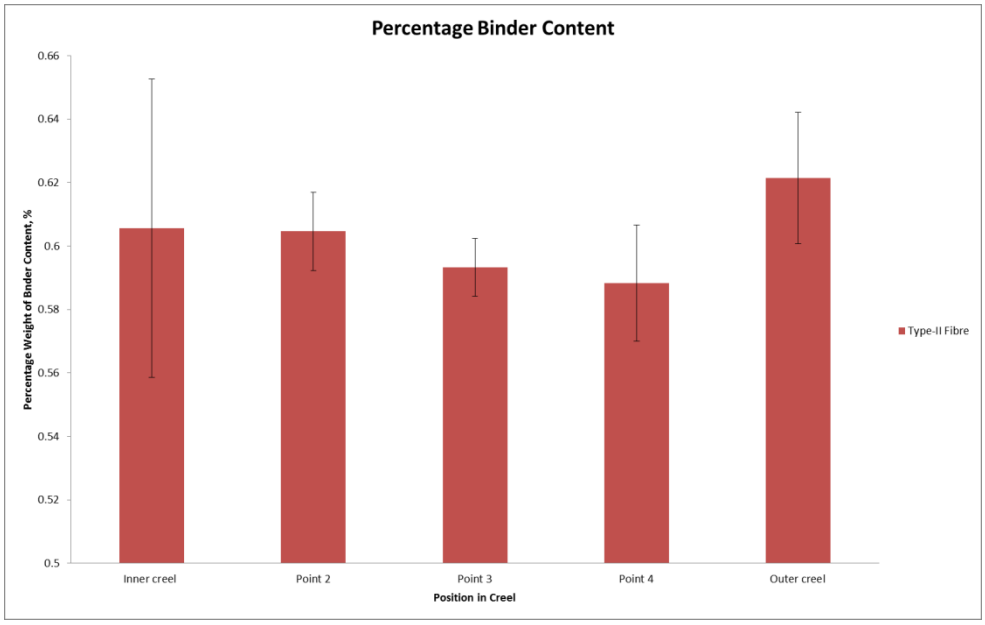

Figure 4.89 A graph showing the percentage binder content removed from Type-II fibres at five different points through a fibre creel.

The relative binder contents obtained from the acetone extraction and LOI for Type-I and II fibres are summarised in Figure 4.90.

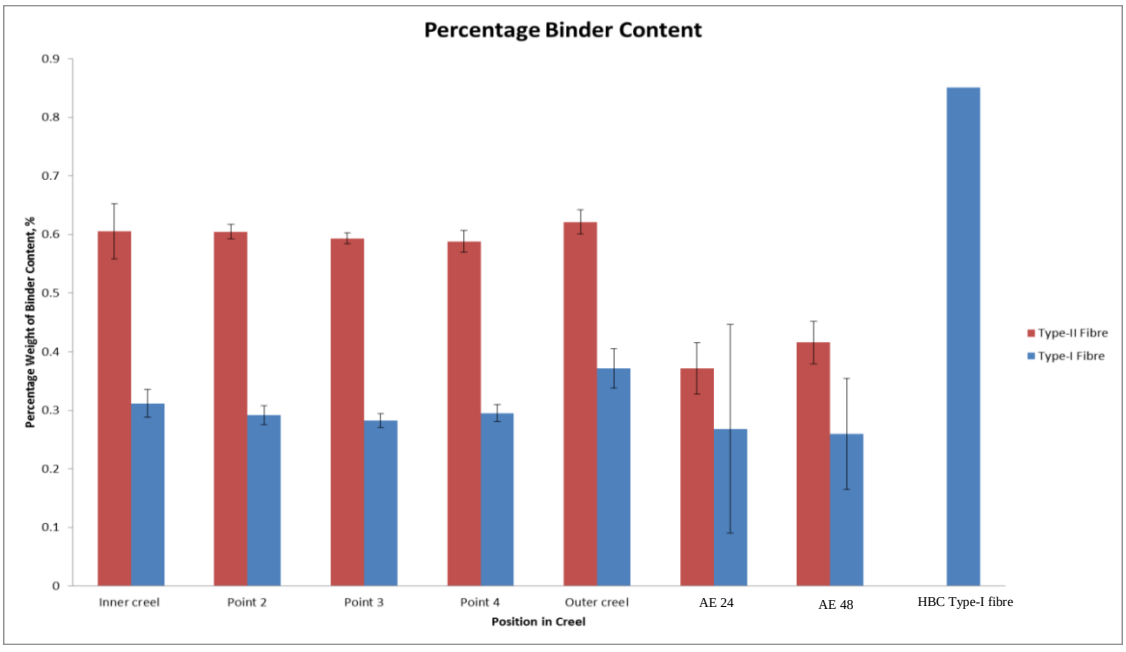

Figure 4.90 A graph showing a comparison in the percentage of binder present in Type-I and Type-II fibres heated at 625 °C for 30 minutes and subjected to 24 and 48-hours of acetone extraction.

SEM images of the Type-I fibres after the LOI procedure are shown in Figures 4.91 (i) and (ii). From the SEM images, it is apparent that the surface of the fibres is now devoid of binder residue. Figure 4.91 (i) shows blister-like features on the glass fibre surface. Lund and Yue (2010) reported similar features attributing them to the presence of defects in the melts before fibre drawing such as micro-bubbles, striae, and structural clusters. They stated these defects could become orientated along the fibre axis when drawing the melt in the glass fibre manufacturing process. Figure 4.91 (ii) shows possible contamination of dust particles (debris) from the oven during the LOI experiment.

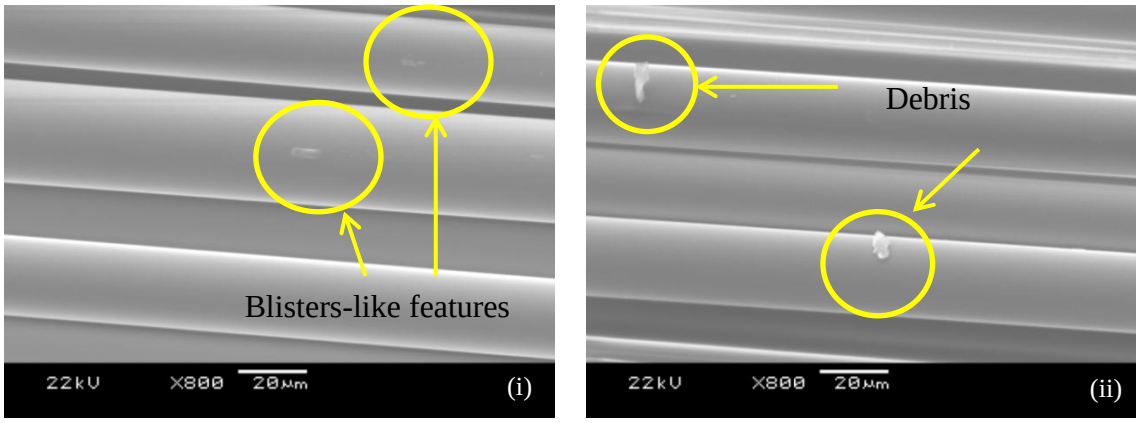

Figure 4.91 SEM images of Type-I fibre bundle after heating for 30 minutes at 625°C. (i) Highlighting blister-like features. (ii) Highlighting possible contamination caused during processing of sample or debris from the furnace.

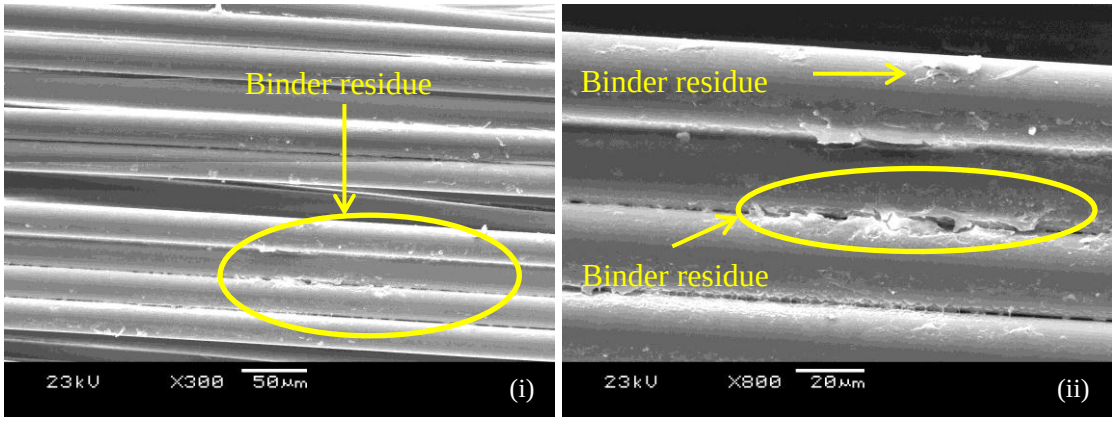

Figure 4.92 SEM images (i) and (ii) show the high binder content section of Type-I fibre bundle after heating for 30 minutes at 625 °C.

When a section of a fibre with high binder content (as assessed visually) was subjected to LOI, a significant binder residue was observed as shown in Figure 4.92. The reason for this was not established as the composition of the binder was not known. However, it is speculated that this may be inorganic in nature. Further work is needed to establish the origin of this residue.

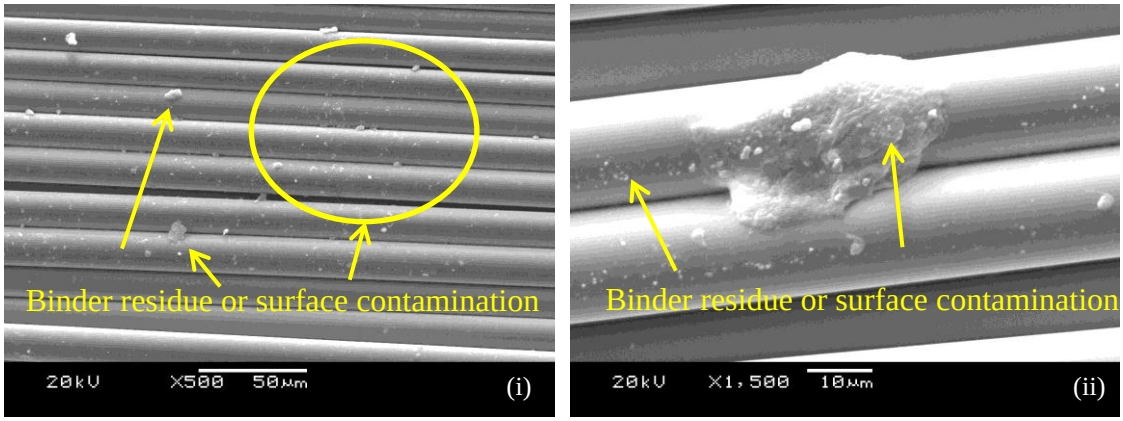

Figure 4.93 SEM images (i) and (ii) show Type-II fibre bundle after heating for 30 minutes at 625 °C.

The SEM images shown in Figure Figure 4.93 (i) and (ii) represent the fibre surface of the Type-II fibres after the 625 °C heat treatment for 30 minutes. The features observed have been attributed to the either the binder residue or the contamination from the furnace used during the LOI procedure. This residue observed in fibre Type-II was significantly lower than that seen in Type-I fibres.

4.2.5 Summary

(i) Type-II fibre bundle has a higher binder content on average when compared to Type-I fibres. In some instances, the profile of the binder reside was elliptical in both cases, possibly reflecting the winding pattern on the creel.

(ii) Type-I fibres possessed regions where the binder content was significantly high (0.85%). The cohesion of the filaments in these regions appeared to be high.

(iii) Both fibre types display a reduction in the binder content when subjected to 24 and 48-hour acetone extraction.

(iv) The binder residue, after acetone extraction, showed globule-like features on fibre Type-I. This was not observed in Type-II fibres.

(v) Type-I fibres displayed a higher visual residual binder content after LOI.

The consequence of the relative binder contents in fibre Types-I and II, on the impregnation characteristics, is discussed in the next section.

4.2.6 Impregnation Experiments

4.2.6.1 As-Received Fibres

The impregnation experiments described in Section 3.2.3.1 were carried out on Type-I and Type-II fibres to view the flow characteristics of resin as it penetrates through the thickness of the fibre bundle. The following fibre types were used in this series of experiments: as-received fibres, acetone extracted fibres; and fibres subjected to 625 °C for 30 minutes (LOI procedure). A schematic illustration of the terms used to describe the direction of through-thickness impregnation, was shown in Figure 2.21.

A photograph of the impregnation experiment is shown in Figure 3.19 (i) where a drop of the resin, with pigment was deposited via a micropipette on the centre of the bundle. Figure 3.19 (ii) illustrates the case where the drop of resin that has permeated through the bundle. A CCD camera and custom written software were used to identify when the resin was detected on the bottom surface of the bundle.

With reference to the variability in the fibre bundle as discussed previously (segmentation, undulations, high concentration of binder), 20 individual experiments were carried out on as-received Type-I and Type-II fibres. The results for as-received Type-I fibres are shown in Figure 4.94.

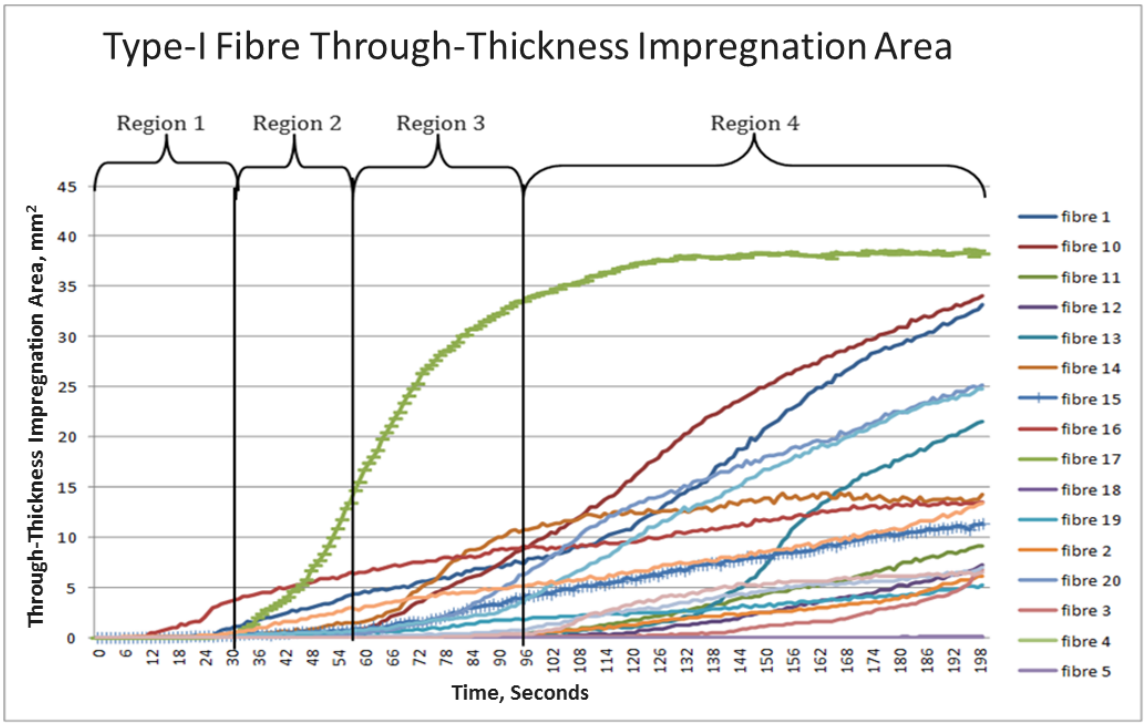

Figure 4.94 A graph showing the through-thickness impregnation area of the as-received Type-I glass fibre bundle.

The first experiments shown in Figures 4.94 and 4.95 demonstrate through-thickness impregnation time for as-received Type-I and Type-II fibres respectively. It is possible to see that on average Type-I fibres have a slower through-thickness impregnation time than that of the Type-II fibres. For Type-II fibres, the through-thickness impregnation time was between 3-80 seconds and for Type-I fibres this was between 10-132 seconds. The micrographs of the as-received bundles were shown in Figures 4.75 and 4.76 for Type-I and Type-II fibres respectively. The micrographs demonstrated Type-II fibres maintain the fibre architecture showing compact regions of filaments with macro-

channels running between them. The macro-channels are likely to have contributed to the observed decrease in through-thickness time seen in Type-II fibres. The resin block experiments demonstrated that Type-I fibres splay out during impregnation and therefore it was expected that the impregnation time for Type-I would have been faster than for Type-II fibres, but this was not the case. Since the viscosity of the resin was similar throughout this experimental series, the variability in the binder content and the surface energy (not addressed in the current study) may have contributed to the extended through-thickness time for the Type-I fibres.

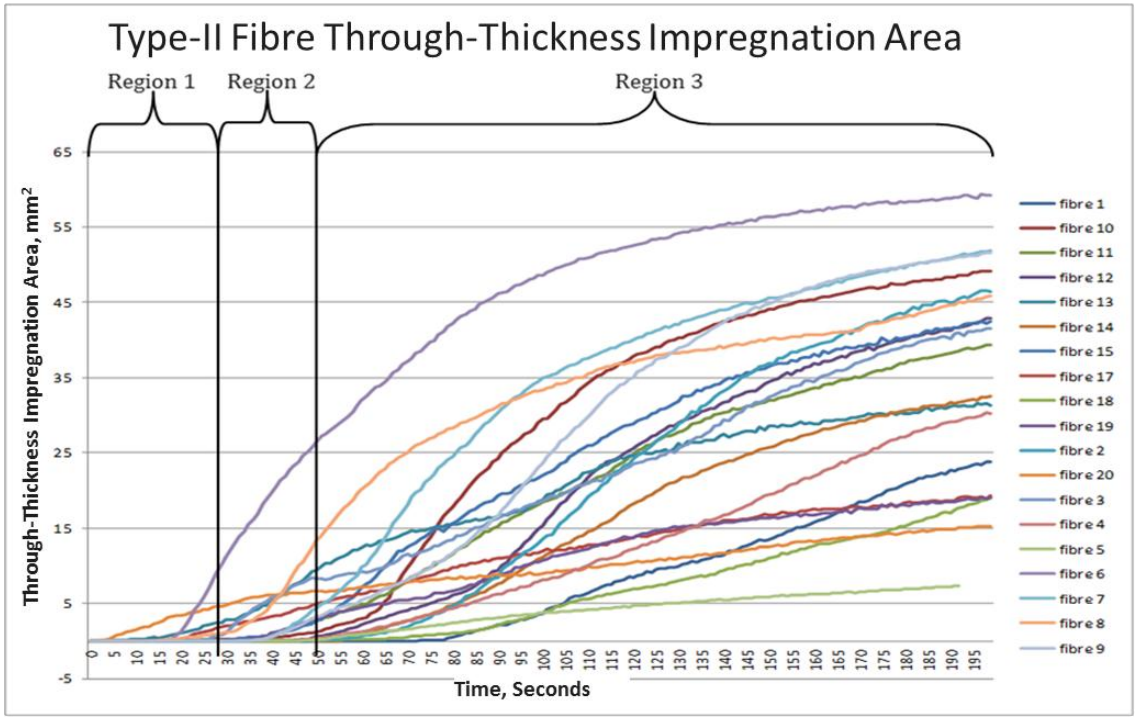

Figure 4.95 A graph showing the through-thickness impregnation area of the as-received Type-II glass fibre bundle.

Different regions which demonstrated a particular through-thickness characteristic are identified in Figures 4.94 and 4.95 for Type-I and Type-II fibre respectively. The graphs have been divided into four regions for Type-I and three regions for Type-II. Each region is described in the following section.

Region-1: This represents the situation when a fibre droplet was un-intentionally deposited on the edge of a fibre bundle. In this instance the droplet was detected as soon as the recording of the CCD camera began. Due to the shape of an as-received glass fibre bundle (see Figures 4.73 and 4.74), depositing a drop of resin on the edge of the glass fibre bundle will result in rapid through-thickness impregnation. Figure 4.96 (i) demonstrates a resin droplet that was deposited close to the edge of the as-received Type-I glass fibre bundle (Figure 4.94, trial 16). The image of the droplet captured from the bottom surface is shown in Figure 4.96 (ii).

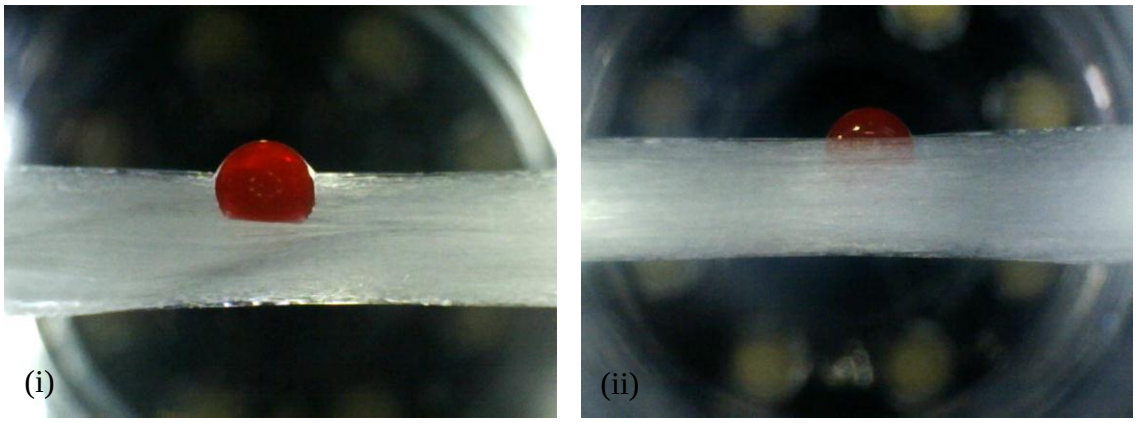

Figure 4.96 Photographs showing the resin droplet on the edge of the glass fibre bundle seen on fibre 16 of the as-received Type-I fibre impregnation trials. (i) Imaged from above the fibre droplet, and (ii) Imaged from below the fibre bundle.

Region-2: This describes the situation where the resin droplet was deposited off-centre (but not at the extreme edge as was the case of region-1) or there was segmentation in the fibre bundle. Segmentation of the fibre bundle is seen in Figure 4.97. It was also observed that the penetration characteristics in region-2 was influenced by the width of the as received fibre bundle. The as-received width of the E-glass fibres was not constant (Irfan *et al.*, 2013).

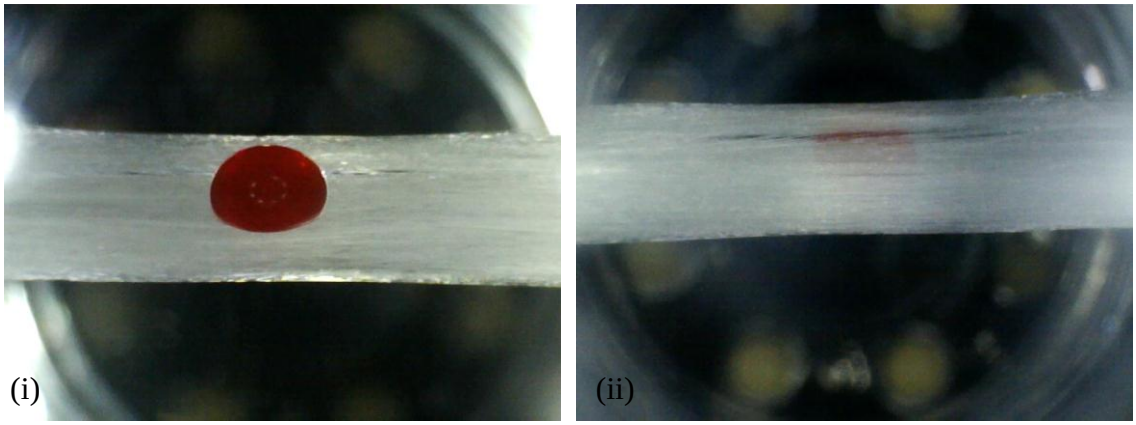

Figure 4.97 Photographs showing gaps in the glass fibre bundle seen on fibre 14 of the as-received Type-I fibre impregnation trials. (i) Imaged from above the fibre droplet (ii) imaged from below the fibre bundle.

Region-3: This region was characterised by the position of the droplet being in the centre of the glass fibre bundle. In this region, the filament within the fibre bundle tended to be more compacted. In situations like this, it was observed previously that the liquid usually 'wicked' faster along the fibre direction than flow in the transverse direction (Thomason and Adzima, 2001).

Region 4: This region is only representative for Type-I fibres and was normally characterised by a significantly lower compaction of the fibre architecture. This was observed to cause the resin drop to be retained on the upper surface of the bundle.

4.2.6.2 The Effect of Binder Content on Fibre Impregnation

4.2.6.2.1 Acetone Extraction

Figure 4.98 demonstrates that acetone extraction for 24-hours (samples coded as AE 24) increased the through-thickness impregnation time for Type-I fibres. 50% of the

samples did not show any appreciable through-thickness impregnation and the remainder displayed a range of 50-90 seconds. The as-received samples on the other hand, all with the exception of one fibre, demonstrated an onset of thought-thickness impregnation between 10-132 seconds.

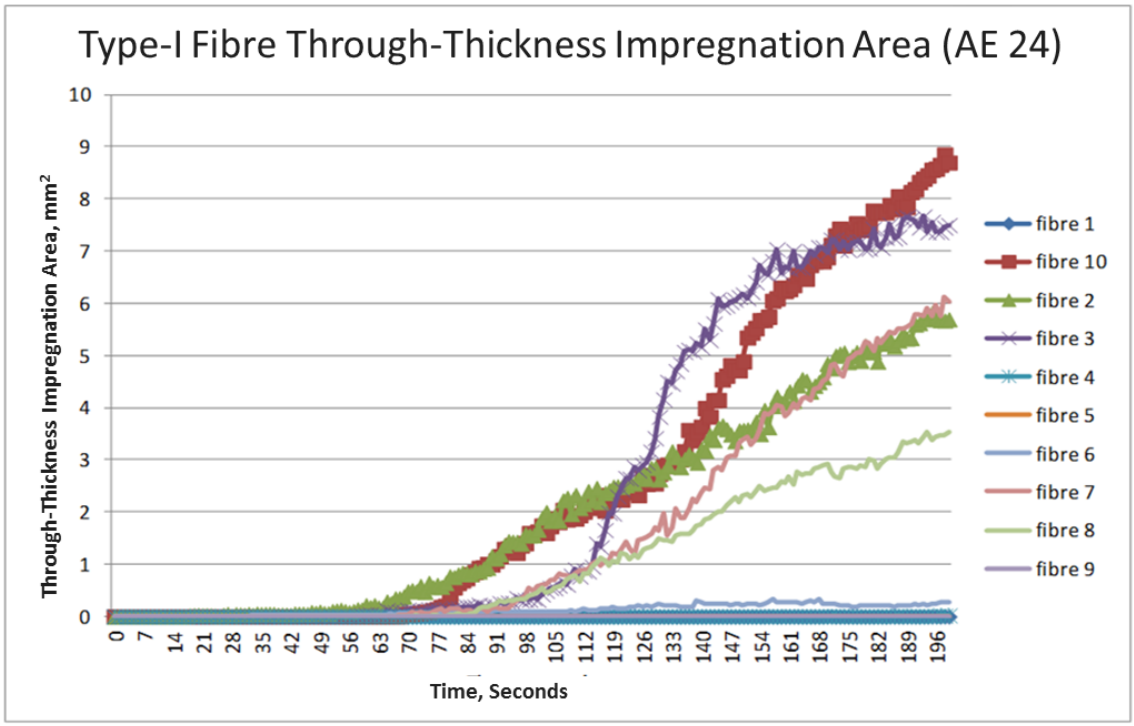

Figure 4.98 A graph showing through-thickness impregnation with Type-I fibres after 24-hours of acetone extraction.

Acetone extraction undertaken for 48-hours on Type-I fibres resulted in the fibres being too difficult to handle. In other words, the fibre architecture could not be maintained because the coherence of the bundle was lost and it was difficult to maintain the orientation of the fibres. Hence, impregnation experiments were not carried out for the samples that were treated for 48-hours on acetone.

Figure 4.99 and Figure 4.100 show the through-thickness impregnation characteristics of Type-II fibres after 24 (AE 24) and 48-hours acetone extraction (AE 48) respectively.

As with Type-I fibres, there is a significant increase in the time taken for the resin to penetrate through the fibre bundle after acetone extraction. As shown in Figure 4.95 for the as received Type-II fibres, the majority of the samples achieved through-thickness impregnation between 3-80 seconds. However in the case of AE 24 this range was 20-147 seconds. Within the data sets shown in Figure 4.99, seven out of the fifteen samples tested did not show any appreciable through-thickness impregnation. Increasing the acetone extraction time to 48-hours (Figure 101) resulted in four out of the fifteen samples that did not show any appreciable impregnation with an additional eleven showing a significantly reduced impregnation area.

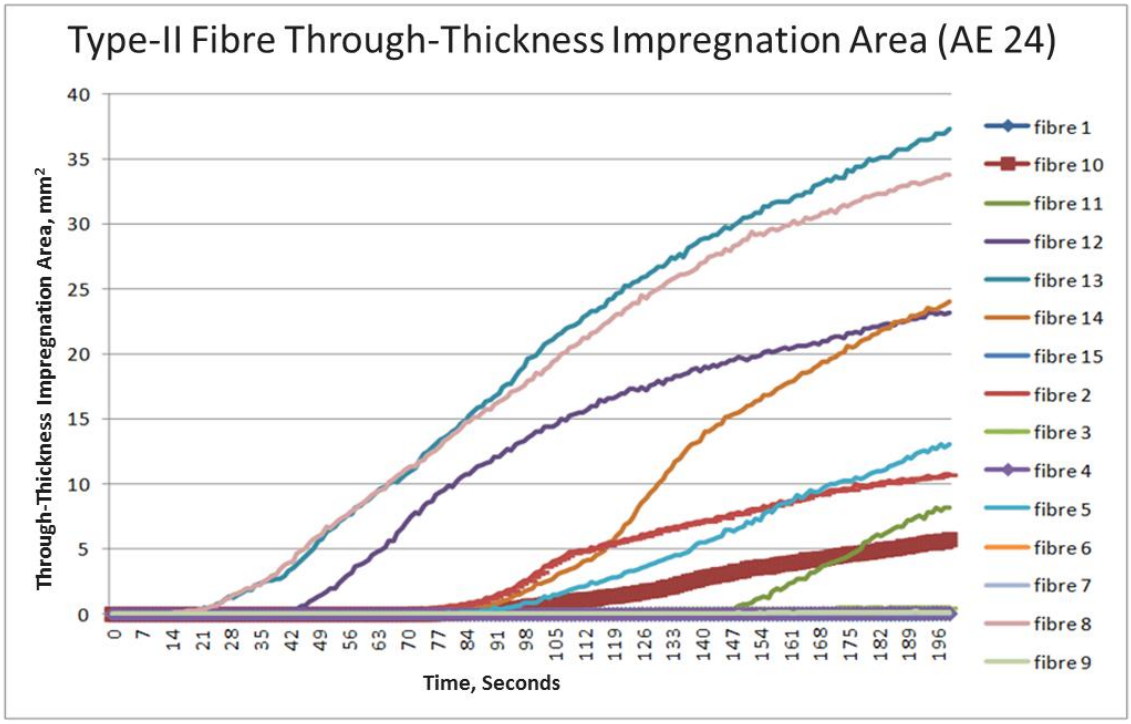

Figure 4.99 A graph showing through-thickness impregnation with Type-II fibres after 24-hours of acetone extraction.

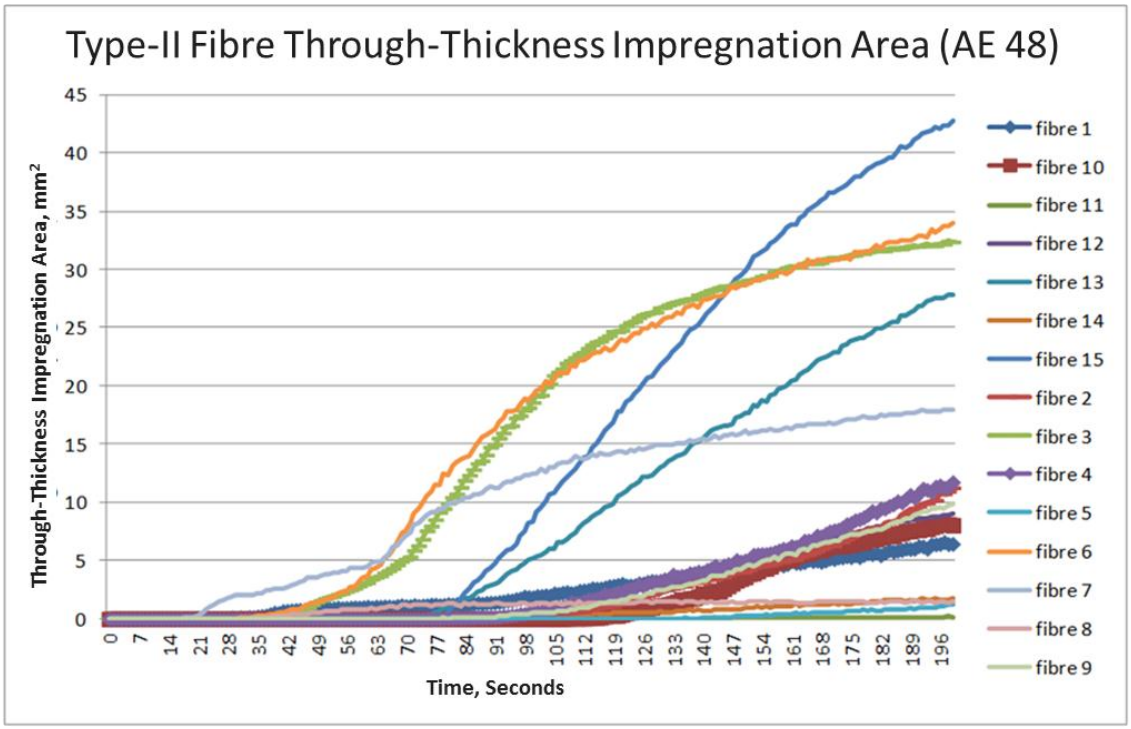

Figure 4.100 A graph showing through-thickness impregnation with Type-II fibres after 48-hours of acetone extraction.

4.2.6.2.2 Fibre Impregnation After Loss-on-Ignition

On inspecting Figure 4.101, it is clear that after Type-I fibres have been subjected to LOI, there is a dramatic reduction in the level of through-thickness impregnation. With the exception of fibre-5, where the resin was unintentionally deposited on the edge of the fibre bundle, 90% of the samples did not show any appreciable through-thickness impregnation.

In contrast to the results shown for Type-I fibres, the Type-II heat-treated fibres (see Figure 4.102) displayed variable through-thickness impregnation times. In other words, 50% of the samples showed similar characteristics as the as-received Type-II fibres with the remainder showing an extended time.

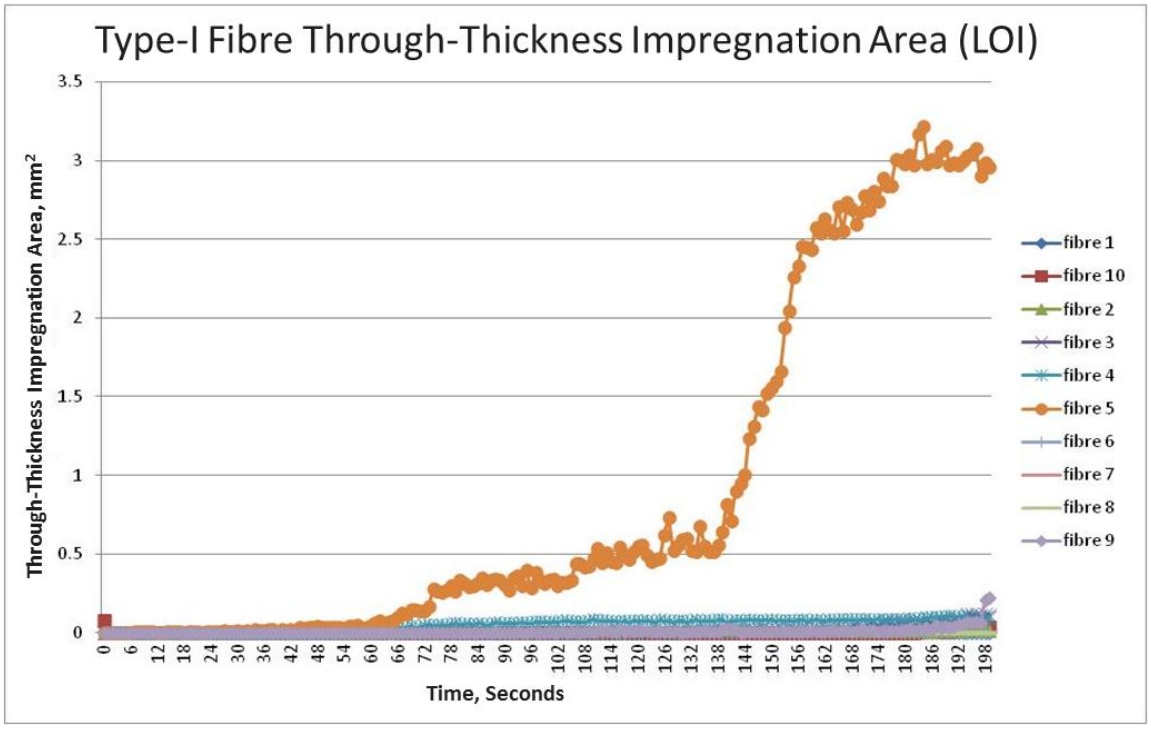

Figure 4.101 A graph showing the through-thickness impregnation area of Type-I fibres after burn-off at 625 °C.

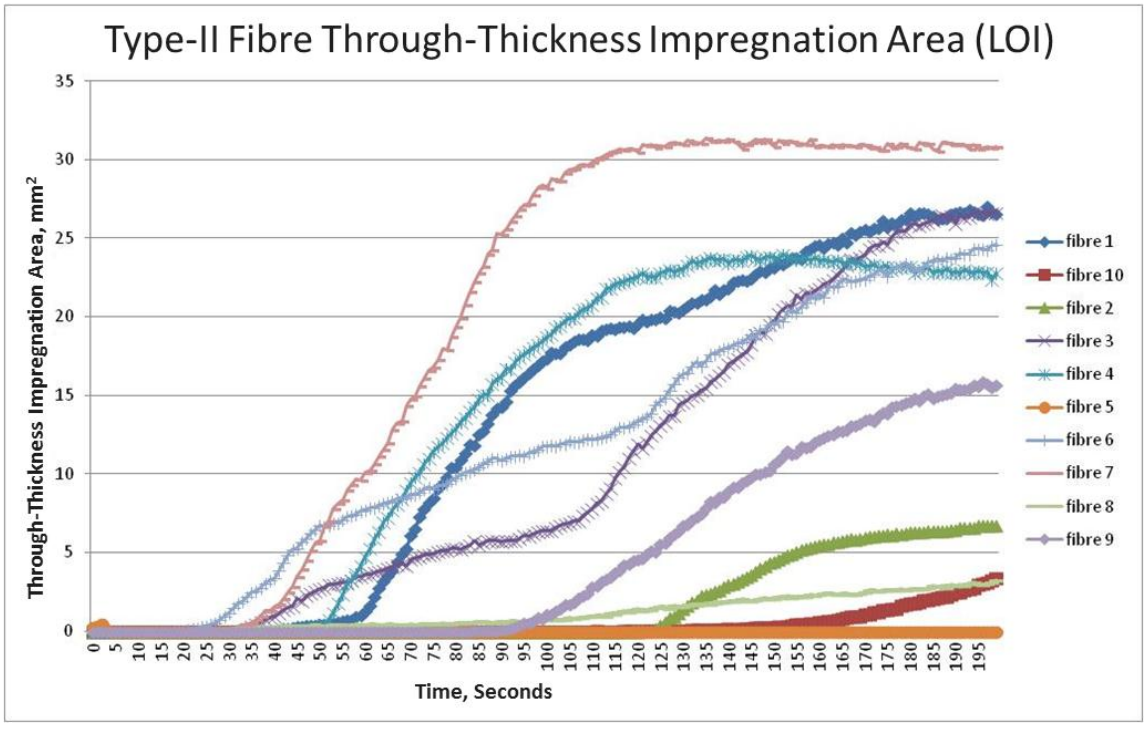

Figure 4.102 A graph showing the through-thickness impregnation area of Type-II fibres after burn-off at 625 °C.

4.2.6.2.3 Impregnation of Fibres with High Binder Content

The variability of the binder content was discussed in detail previously. Therefore, fibres with high binder content as detected visually were secured and the resin droplet experiments were undertaken. Figure 4.103 (i) and (ii) represents sections of a Type-I fibre with a high and low binder content respectively (assessed visually). Prior to the impregnation experiments, each fibre was marked on the intended area for the resin drop to be deposited.

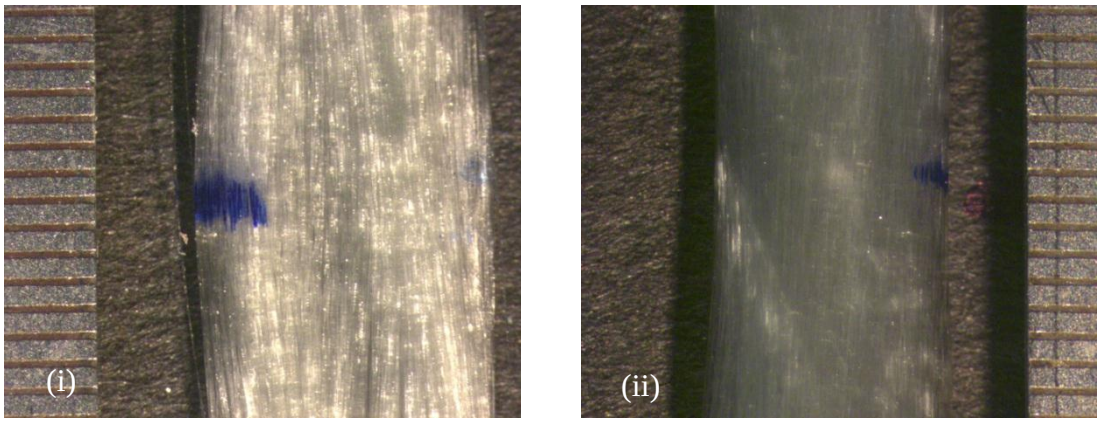

Figure 4.103 Photographs showing a Type-I fibre with a high and low binder content.

From Figure 4.104 it can be seen that compared to normal as-received Type-I fibres, higher binder content (HBC) resulted in a reduction in the through-thickness impregnation. With the exception of fibre-15 (deposited off-centre) Type-I as-received fibre show through-thickness impregnation on average before 114 seconds, whereas those with high binder contents show the average through-thickness impregnation onset after 114 seconds.

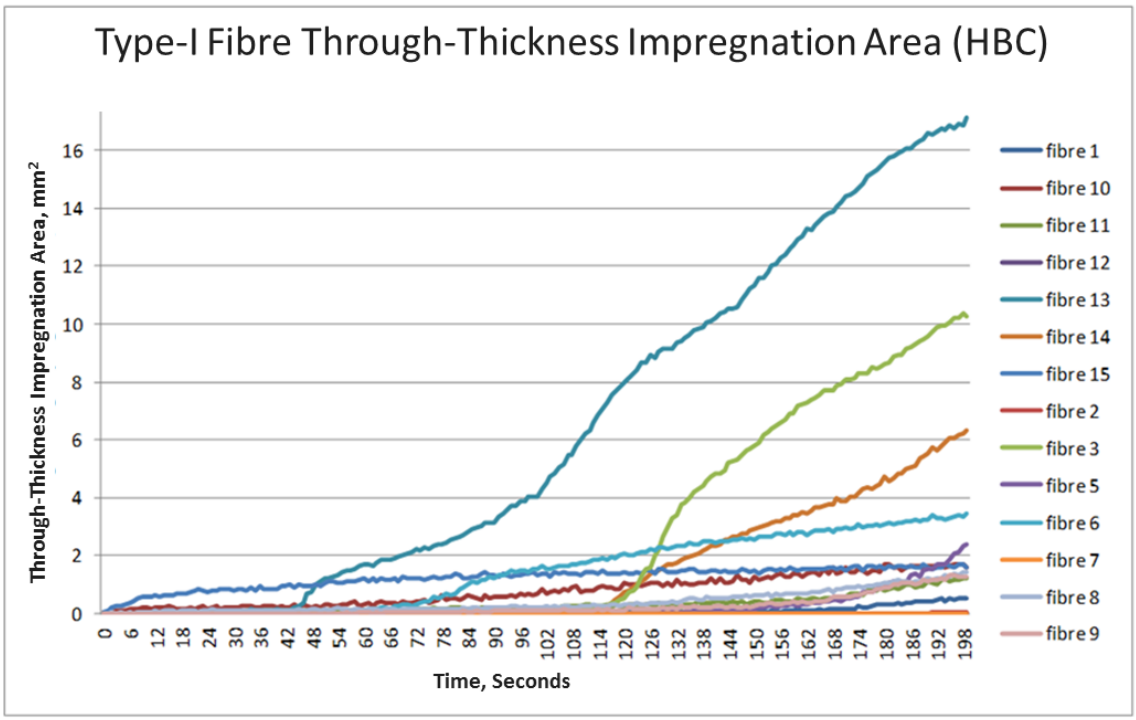

Figure 4.104 A graph showing the through thickness fibre bundle impregnation area of Type-I fibres with high binder content (HBC).

Although it is tempting to speculate on reasons to explain the data presented in Figures 4.94 – 4.104, there seem to be a large number of interrelated factors that could have affected the through-thickness characteristic seen in Type-I and Type-II fibres. For example:

(i) It was not possible to obtain identical specimens from within the creel. It was established that the binder content was variable as a function of position within the creel. Even within a specified position, regions of significantly high binder content were observed. Periodic segmentation was also observed frequently, but its position within the creel seemed random. In some instances, the imprint from the winding process was also imparted on the fibre bundles resulting in significant undulations.

(ii) It was also established that Type-I fibres splayed out when they were partially immersed in a silicon mould containing the resin system. On the other hand fibre Type-II retained the fibre architecture. However, when a drop of resin is placed on the surface of the bundle for Type-I fibres, the through-thickness impregnation was inferior to Type-II fibres. This was attributed previously to the macro-pores/channels present in Type-II fibres. However, the geometry and the relative position of the macro-pores were not consistent. A higher concentration of voids in Type-II fibres were observed when they were cast in silicon moulds. It is possible that these voids and macro-pores may have had an influence on the through-thickness impregnation of Type-II fibres.

(iii) Removing the binder via acetone extraction or LOI resulted in reduction of the through-thickness impregnation for both fibre types, with fibre Type-I being affected to a greater extent. It is speculated that removal of the binder may deplete polar components on the surface of the glass fibres. Likewise, LOI would then have a greater detrimental effect with regard to decreasing the polarity of glass fibres by the removal of hydroxyl groups. Unfortunately, it was not possible to investigate each one of these interrelated issues in detail. However, these findings demonstrate clearly the significance and importance of the binder and its distribution within the creel. Other factors which need to be considered are the variability in the fibre diameter, width and cohesion of the as-received fibre bundles. Sections of the bundle with a noticeably higher binder content showed reduced through-thickness impregnation. The higher binder contents were more prevalent in Type-I fibres.

4.2.7 Summary

(i) As-received Type-I fibres demonstrated a slower through-thickness impregnation time when compared to as-received Type-II fibres.

(ii) Acetone extracted Type-I fibres showed a significant reduction in the through-thickness impregnating time. Samples that were conditioned for 48-hours could not be tested due to loss of bundle integrity; caused by the removal of the binder. Type-II fibres exhibited a similar behaviour after 24-hours of acetone extraction. However no significant changes were observed after 48-hours of acetone extraction.

(iii) LOI was found to significantly reduce the through-thickness impregnation in Type-I fibres. However, this was not observed with the Type-II fibres.

4.2.8 Fibre Bundle Tensile Strength

A summary of the fibre bundle tensile strength for both fibre types in the as-received and acetone extracted states is presented in Figure 4.105. The Type-I and Type-II fibre bundles were obtained from random positions in the creel. It can be seen, in Figure 4.105, the average bundle tensile strength for Type-I and Type-II fibres were 960.1 and 1023.3 N respectively. The standard deviations were 83.4 and 93.8 N for Types-I and II fibres respectively. The individual test data is included in the Appendix E. This compares favourably to the information reported in the literature. R'Mili *et al.*, (2008) found the maximum load and the corresponding strain were reduced significantly in the dry bundle compared to light-oil lubrication (280 MPa to 230 MPa and 1.6% to 1.3% respectively).

With reference to Figure 4.105, 36.9 and 23.6% reductions in bundle strength were observed for Type-I and Type-II after 24-hours acetone extraction. The reduction in the

bundle tensile strength after 48-hours, with respect to the as-received states were 35 and 28.6% for Type-I and II respectively. This is reasonable because removing the binder will result in a significant increase in the inter-filament friction during tensile loading.

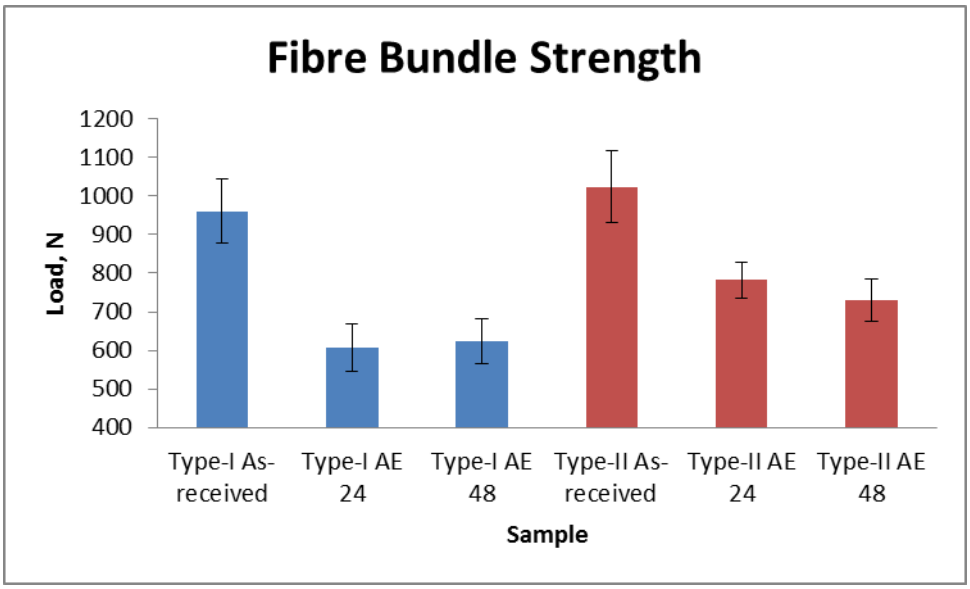

Figure 4.105 A graph showing the maximum tensile load a comparison between Type-I and Type-II fibres after being subjected to different treatments.

This is in agreement with the observations made previously by Hill and Okoroafor (1994), Feih *et al.*, (2008) and R'Mili *et al.*, (2008).

4.2.9 Summary

The previous section on impregnation characteristics of Type-I and Type-II fibres demonstrated the complexities involved in interpreting data due to the interrelated parameters influencing the results. In this section, the importance of the binder content has been reaffirmed. However, in this instance it is apparent that removing the binder has a detrimental effect on the tensile properties. It is accepted that the binder is not absent in any sections of the creel. However, it is important to emphasis the variability

not only on the binder content but also of the physical and geometric properties will have an influence on the final product.

5 CONCLUSION AND RECOMMENDATIONS FOR FUTURE RESEARCH

5.1 CONCLUSIONS

The following conclusions are drawn from the research reported in the previous chapters:

(i) Background: The clean filament winding concept was developed in the laboratory by Pandita *et al*., (2007). The focus of the current research was to demonstrate this technology in an industrial environment. This involved a pre-site visit to a filament winding factory to observe the procedures and protocols that were used to manufacture filament wound composite tubes using the conventional resin bath method. A prototype resin impregnator was designed and evaluated on site. On the basis of the observations made and the resultant properties of the tubes that were manufactured using the first prototype impregnator, a second one was designed to address some of the shortcomings.

(ii) Pre-site visit: The primary aim of the pre-site visit was to compile detailed notes on the procedures that were used on-site with conventional resin bath-based filament winding. Attention was also given to the desired location of the resin impregnator on the original resin bath or on the traversing arm of the filament winding machine. Detailed observations were also made to identify areas where resin drips occurred.

The decision was made to locate the resin impregnator on the traversing arm as it would eliminate the majority of the resin drip points observed with conventional wet-winding. However, it was appreciated at this point that the rate of axial, transverse and through-thickness had to be increased significantly as the distance between the point of

impregnation and the mandrel was of the order of 0.3 m. The corresponding distance for wet-filament winding was 2.5 m. It was also observed that a layer of resin was applied to the mandrel before conventional filament winding commenced. Moreover, additional resin was either applied or removed manually using a large paint brush.

The tension and the doctor-blade settings were also altered as required by the operators; this was based on the experience of the operators to obtain tubes of acceptable quality. Type-I fibres were used by the industrial concern. It was noted that the fibre bundles had randomly dispersed deposits of a yellow substance and that these regions resembles areas of higher binder distribution. The decision to locate the resin impregnator on the traversing arm of the filament winding machine meant that an interface plate had to be designed.

(ii) An interface plate was designed to enable quick assembly and disassembly. The time taken to remove the original interface plate (housing the fibre guides and the D-eye) and to fit the new one (to accommodate the resin impregnator) was 5 minutes.

(iii) Resin impregnator Prototype-1: This prototype was designed to investigate wedge, reservoir and injection-based impregnation. The reservoir was engineered to enable the excess resin on the fibres bundles to be channelled back to form a miniature reservoir thus enabling the bottom-face of the bundle to contact the resin. The remit was to control the resin volume fraction that is deposited on the mandrel, and to ensure thorough through-thickness impregnation. The key design requirements were to minimise fibre damage (by lowering the torturous trajectory of the fibre bundle and the applied tension). Prototype-1 was designed to enable maximum flexibility with regard to the position of the resin delivery-head (curtain-flow or injection), the volume of resin

to be retained on the impregnated bundle as it leaves the impregnator and the tension on the bundles.

The impregnator was modified to accommodate a compact fibre spreading unit prior to the impregnation station. A D-eye was also integrated on the resin impregnator along with a resin delivery system.

(iii) Resin delivery systems: The supply of resin to the impregnator was facilitated by a pressure-pot and a precision gear pump. The low viscosity of the components of the polyester resin meant that it could not be dispensed with the desired accuracy via a gear pump-based delivery system. Thus, it was necessary to use pre-mixed resin in a pressure-pot. In the case of the epoxy resin system, the precision gear pump system was used where the resin and hardener were stored separately and pumped on demand. In this instance, it was possible to synchronise the resin/hardener delivery rates to the fibre haul-off rate via an encoder. The pressure-pot was capable of delivering higher injection pressures and it did not suffer from any back-pressure build up as observed with the gear pump system. In the case of the pressure-pot, the resin was delivered directly to the impregnator. A static mixer was used to mix the resin and the hardener when the precision gear pump was used. Previous studies had established that a conventional Kenics® static mixer yielded a thoroughly mixed resin system.

(iv) Filament winding trials involving resin impregnator Prototype-1: The starting point of the on-site filament winding trials was the mounting of the interface plate on the traverse-arm of the filament winding machine.

The first series of experiments were undertaken to establish the appropriate level of tension that should be applied to the fibre bundles. These trials were undertaken using 8

bundles at combined tensions of 5, 10 15 and 18 kg. The physical and mechanical properties of these tubes suggest that 15 kg was an appropriate value as the void contents, fibre volume fraction and hoop tensile strengths were 1.5%, 54.85% and 971.13 MPa (normalised to 55% fibre volume fraction) respectively. The subsequent site trials were undertaken at 15 kg. The volume of resin that was applied or removed was not regulated as this was dictated by the operators of the filament winding machine.

A surprising finding was that the tubes manufactured with the polyester resin on average gave void fractions of 1.28% where those manufactured using the epoxy resin system yielded 3.5% (conventional wound tubes at 7 m/min). Similar findings were seen in the clean filament wound samples.

The relative higher viscosity of the epoxy resin system was thought to be a contributing factor along with its higher average binder content. The applied pressure from the two delivery systems was not investigated. Nevertheless, it led to three additional research elements: (i) quantification of the binder contents in the two classes of fibres; (ii) an investigation into the rate of through-thickness impregnation; and (iii) the design of a second resin impregnator (Prototype-2) that addressed some of the site requirements and the need to increase the impregnation efficiency. The normalised (55%) hoop tensile strengths for the conventional and clean filament wound tubes produced with the polyester resin at 7 and 21 m/min were 621.09 and 709.01, and 674.11 and 693.18 MPa respectively.

The conclusions reached from the first site trial were:

(a) The impregnation efficiency had to be increased to cater for the shorter distance between the impregnator and the mandrel;

(b) The tension on the fibre bundle had to be controlled as it had a major influence on the ultimate fibre volume fraction;

(c) The flexibility of the impregnator had to be reduced to reflect better the site requirements (time required for assembly and disassembly), without the adjustability required for a typical research programme.

(d) The time required for cleaning had to be comparable with that taken for conventional wet-winding.

(e) The physical and mechanical properties had to be equivalent for the two production techniques.

(v) Filament winding trials with resin impregnator Prototype-2: This device was designed and built to address the majority of the limitations of Prototype-1 including the time required for assembly and disassembly; pins/rollers that could be disassembled significantly quicker and effective resin fibre volume control as the impregnated fibres exited the resin impregnator. Epoxy-based tube results are not presented in this study as there were visible impregnation issues noted during the winding trials, therefore the focus for the site trials was placed on the polyester-based tubes and laboratory work was under taken to understand the potential causes of the high void contents seen in the epoxy-based tubes.

The void contents for the tubes manufactured using the polyester resin at 7 and 21 m/min were 1.69 and 1.46% respectively. The normalised hoop tensile strengths for the polyester resin at 7 and 21 m/min were 652.5 and 652.7 MPa respectively.

The Prototype-2 resin impregnator design was modified further in the final phase of this research project to demonstrate that the clean filament winding technology could compete with wet-filament winding at 52 m/min.

The time required to clean Prototype-2 at the end of production was 20 minutes. This corresponds well with that taken for the conventional process. It is worth noting that with the conventional filament winding process, the time taken by the operators at the start of the research programme was 55 minutes and this was reduced by them to 20 minutes with the advent of the clean filament winding programme.

The general conclusion that was reached with resin impregnator Prototype-2 was that the clean filament winding technology was capable of producing tubes of equivalent or marginally superior hoop tensile strengths. However, the LCA studies showed that the environmental and green credentials of the clean filament winding-based production method were superior.

(vi) LCA: The key conclusions reached from the LCA studies were that the environmental impact of the clean filament wound tubes compared to the conventional filament wound tubes was significantly lower. The data gathered on site for the LCA quantified the volumes of waste resin and solvents generated on site for the conventional and clean filament winding methods. For example, the conventional process required 2800 g of solvent for cleaning whereas the clean filament winding technique for Prototype-2 required 250 g. The volumes of waste resin generated for the conventional and clean techniques were 2616 and 83 g respectively.

(vii) Binder content: The higher void contents observed in the epoxy resin were unexpected, as previous laboratory trials resulted in void contents below 2%.

Therefore, a detailed study was undertaken to quantify the binder contents in the Type-I and II reinforcing fibres (from two suppliers). The average binder contents for Types-I and II were 0.31 and 0.6% respectively. However, the Type-I fibres had a significantly higher variability 0.22% compared to Type-II studies were 0.01% with areas of high binder content in Type-I fibres reaching 0.85%.

(viii) Through-thickness impregnation: An experimental method that was developed by a colleague was used to infer the through-thickness impregnation. Here, a drop of the epoxy resin with a dye was deposited on the surface of a bundle and the through-thickness impregnation rate was determined via a CCD camera and image analysis.

Type-I fibres demonstrated slower through-thickness impregnation when compared to Type-II fibres. Both fibre types demonstrated a reduction in their through-thickness impregnating rates when fibre bundles had been previously subjected to acetone extraction for 24-hours and heat treatment at 625 °C for 30 minutes. This reduction in through-thickness impregnation was seen to a greater extent in Type-I fibres.

Globular residues were observed to be present on the fibre surfaces after acetone extraction. This was greater for the Type-II fibres. It was not possible to identify the composition of these globules.

Unexpectedly, Type-I fibres showed regions with a high binder residue after heat treatment at 625 ºC for 30 minutes. In some instances, significant linking of the filaments by the residual binder was observed. Since sections of the fibre bundles with a higher distribution of binder were “stiffer”, bundle tensile tests were undertaken to assess the intrinsic strengths of the two classes of fibres.

(ix) Bundle tensile strength: The average tensile bundle strengths for the Type-I and II fibres 960.1 and 1023.3 N respectively. Both fibre types showed a subsequent reduction in tensile strength when subjected to acetone extraction for 24 and 48-hours. The reduction in fibre bundle strengths for the Type-I and II fibre bundles were 35 and 28.6%.

(x) General conclusion: This study has demonstrated that the clean filament winding technique is capable of producing tubes with equivalent physical and mechanical properties when compared with conventional wet-filament winding. The environmental benefits of the clean filament winding method are significantly superior. A number of parameters were shown to influence the void content and hoop tensile strength. For example, the applied tension, winding speed, binder content, resin content on the mandrel, the relative impregnation of the bundle, the factory temperature, stoichiometry, pressure of the resin delivery system and the vigilance of the operator. Given the magnitude of the interdependence, it is difficult to attribute a single parameter to the quality of filament wounds tubes. The output of this current study has been extended to demonstrate clean filament winding at 52 m/min.

5.2 RECOMMENDATIONS FOR FUTURE RESEARCH

In addition to the work presented in this thesis there is further research needed to address the knowledge gaps required to aid further process improvement. Future study should look to:

(i) Complete the analysis of tubes manufactured using the modified clean filament winding Prototype-2, which were wound at 50m/min. Due to dimensions of the

tubes wound at this was not possible during this study because a different method of mechanical strength would need to be used to compare the properties such as inter-laminar shear stress testing using 3-point bend tests.

(ii) Perform an in-depth study which investigates the reasons for the higher void content as seen in the tubes wounds using epoxy resin during conventional and clean filament winding. Modifications can then be made to the clean filament winding process in order to achieve the lower void content of epoxy tubes but maintain or improve the quality of the polyester tubes.

(iii) Investigate methods by which to improve impregnation during clean filament winding by looking at optimising the spreading of the fibres before they are impregnated with resin.

(iv) Complete a full feasibility trial using clean filament winding to considering manufacturing variability's such as increase number of fibre bundles or winding angles.

(v) Fully analyse the differences in both physical and mechanical properties for manufacturing tubes with either Type-I or Type-II fibres during clean filament winding.

(vi) Undertake further analysis on the effect of binder composition on fibre impregnation properties for Type-I and Type-II fibres.

(vii) Develop impregnation-monitoring equipment adapted to the clean filament winding process so that the resin volume fraction can be either increased or decreased based on the degree of impregnation of the fibre bundles.

6. LIST OF REFERENCES

Ahlstrom, C. and Gerard, J. (1995) The adhesion of elastomer-coated glass fibres to an epoxy matrix. Part I: The effect of the surface treatments on the tensile strength of the glass fibres. **Polymer Composites,** 16(4): 305-312.

Ahmadi, M. and Oskouei, A. (2009) Fracture Strength Distribution in E-Glass Fiber Using Acoustic Emission. **Journal of Composite Materials,** 44(6): 693–705

Ahmadi, Z., Ghaffarian, S. and Amiri, D. (2000) Continuous melt impregnation process: materials parameters. **Iranian Polymer Journal,** 9(2): 125–130

Ahn, K., Seferis, J. and Berg, J. (1991) Simultaneous measurements of permeability and capillary pressure of thermosetting matrices in woven fabric reinforcements. **Polymer Composites,** 12(3): 146–152

Aleong, C. and Munro, M., (1991). Effect of winding tension and cure schedule on residual stresses in radially-thick fiber composite rings. **Polymer Engineering and Science,** 31(18): 1344–1350

Amico, S.C. and Lekakou, C. (2002) Axial impregnation of a fiber bundle. Part 1: Capillary experiments. **Polymer Composites,** 23(2): 249–263

Amico, S. and Lekakou, C. (2002) Axial impregnation of a fiber bundle. Part 2: theoretical analysis. **Polymer composites,** 23(2): 263-273

ASTM D123 - 15 Standard Terminology Relating to Textiles

ASTM D578 / D578M - 05(2011) Standard Specification for Glass Fiber Strands

ASTM D792 (2013) Standard test method of density and specific gravity (Relative density) of plastic by displacement

ASTM D2290, (2004) 'Apparent tensile strength of ring or tubular plastics by split disk method'

ASTM D2584, (2002) 'Standard test methods for ignition loss of cured reinforced plastics'.

ASTM D2734, (2003) 'Standard test methods for void content of reinforced plastics'.

ASTM D3379 – 75 (1989) Standard test method for tensile strength and Young's modulus for high modulus single-filament materials (withdrawn 1998)

Azzarri, M., Cortizo, M. and Alessandrini, J. (2003) Effect of the curing conditions on the properties of an acrylic denture base resin microwave-polymerised. **Journal of Dentistry**, 31(7): 463–468

Azo Materials (2015) [online]. **Materials, A. to Z. of, E-glass fibre.** Available at: www.azom.com/article.aspx?ArticleID=764 [Accessed 22 January 2015]

Bates, P. and Charrier, J. (1999) Effect of process parameters on melt impregnation of glass roving. **Journal of Thermoplastic Composite,** 12(4): 276–296

Bates, P. and Charrier, J. (2000) Pulling tension monitoring during the melt impregnation of glass roving. **Polymer Composites,** 21(1): 104-113

Bates, P. J., Taylor, D., and Cunningham, M. F. (2001). Compaction and transverse permeability of glass rovings. **Applied Composite Materials,** *8*(3): 163-178.

Bates, P. Kendall, J., Taylor, D. *et al.,* (2002) Pressure build-up during melt impregnation. **Composites Science and Technology,** 62(3): 379–384

Bayramli, E. and Powell, R. (1991) Experimental investigation of the axial impregnation of oriented fiber bundles by capillary forces. **Colloids and Surfaces,** 56: 83–100

Bayramli, E. and Powell, R.L. (1992) Impregnation Dynamics of Carbon Fiber Tows. **Journal of Composite Materials,** 26(10): 1427–1442.

Bijsterbosch, H. and Gaymans, R.J. (1993) Impregnation of glass rovings with a polyamide melt. Part 1: Impregnation bath. **Composites Manufacturing,** 4(2): 85–92.

Binetruy, C., Hilaire, B. and Pabiot, J. (1998) Tow impregnation model and void formation mechanisms during RTM. **Journal of Composite Materials**, 32: 223-245.

Blok, H. and Rossum, J. (1953) The foil bearing—a new departure in hydrodynamic lubrication. **Lubrication Engineering,** (6): 316–320

Bogonez, F. (2014) **Fibre spreading and impregnation monitoring**. PhD thesis, University of Birmingham

Briard, R., Heitz, C. and Barthel, E. (2005) Crack bridging mechanism for glass strengthening by organosilane water-based coatings. **Journal of Non-Crystalline Solids,** 351(4): 323–330

Britcher, L., Kempson, S., Matisons, J. (1999) "Silanes on Glass Fibers - Adhesion Promoters for composite applications." In Mittal, K. and Pizzi, A. (eds.) **Adhesion promotion techniques: technological applications**. New York: CRC Press. pp. 347-386

Brydson. J. (1999) **Seventh Edition Plastic Materials**. Butterworth-Heinemann. Chapter 10, pp. 205-246.

Campbell, F. (2004) **Manufacturing processes for advanced composites.** Oxford: Elsevier Advanced Technology.

Chandler, H., Devlin, B. and Gibson, A. (1992) A model for the continuous impregnation of fibre tows in resin baths with pins. **Plastics rubber and composites processing and applications,** 18(4): 215-220

Chen, H. and Chiao, S. (1996) Fiber consolidation in the filament winding process: Modelling with undulating channels. **Composites science and technology,** 56(10): 1161-1169

Chung, T., Furst, H., Gurion, Z., Mcmahon, P., Orwoll, R. and Palangio, D., (1986). Process for preparing tapes from thermoplastic polymers and carbon fibres. US patent 4588538.

Cohen, D. (1997) Influence of filament winding parameters on composite vessel quality and strength. **Composites Part A: Applied Science and Manufacturing,** 28(12): 1035–1047

Composites UK (2015) [online]. Available from: www.compositesuk.co.uk/Information/FAQs/UKMarketValues.aspx [Accessed 22 May 2015]

Corrigendum to Regulation (EC) No 1907/2006 REACH

Dell'Anno, G. and Lees, R. (2012) Effect of water immersion on the interlaminar and flexural performance of low cost liquid resin infused carbon fabric composites. **Composites Part B: Engineering,** 43(3): 1368–1373

DiBenedetto, A. and Lex, P. (1989) Evaluation of surface treatments for glass fibres in composite materials. **Polymer Engineering and Science,** 29 (8): 543-555

Directive 1999/31/EC on Landfill of Waste

Directive 2000/53/EC on End of Life Vehicles.

Directive 2000/76/EC for Incineration of Waste

Ehrenstein, G. (2001) **Polymetric Materials : Structure - Properties – Application**. Munich: Hanser Gardener Publications Inc.

Everhart, M. C., Harris, D. L., Nickerson, D. M. and Hreha, R. D. (2006) High temperature reusable shape memory polymer mandrels. **SAMPE 2006: Creating New Opportunities for the World Economy**, Vol. 51: 245

Feih, S., Manatpon, K., Mathys, Z. *et al.*, (2008) Strength degradation of glass fibres at high temperatures. **Journal of Materials Science,** 44(2): 392–400

Feih, S., Boiocchi, G., Mathys, Z. *et al.*, (2011) Mechanical properties of thermally-treated and recycled glass fibres. **Composites Part B: Engineering,** 42(3): 350-358

Feuillade, V. *et al*., (2006) Relationships between the glass fibre sizing composition and the surface quality of sheet moulding compounds (SMC) body panels. **Composites Science and Technology,** 66(1): 115–127

Foley, M. and Gillespie, J. (2005) Modelling the Effect of Fiber Diameter and Fiber Bundle Count on Tow Impregnation during Liquid Molding Processes. **Journal of Composite Materials,** 39(12): 1045–1065

Fraser, W., Ancker, F., Dibenedetto, A., Elbirli, B. (1983) Evaluation of surface treatments for fibres in composite materials. **Polymer Composites,** 4(4):238–48

Gardiner, G. (2009) [online]. Composite world, **The making of glass fiber**. Available from: www.compositesworld.com/articles/the–making [Accessed 22 January 2015]

Gao, S., Mäder, E., Abdkader, A., and Offermann, P. (2003) Environmental resistance and mechanical performance of alkali-resistant glass fibres with surface sizings. **Journal of Non-Crystalline Solids,** 325(1): 230–241

Gaymans, R. and Wevers, E. (1998) Impregnation of a glass fibre roving with a polypropylene melt in a pin assisted process. **Composites Part A: Applied Science and Manufacturing,** 29(5-6): 663–670

Gebart, B. (1992) Permeability of Unidirectional Reinforcements for RTM. **Journal of Composite Materials,** 26(8): 1100–1133

Gomez, J. and Kilgour, J. (1993) The effect of temperature on silane coupling performance at the glass fiber/resin interface. In **SPI 48th Annual Conference**. Composites Institute. Cincinnati, OH: The Society of the Plastics Industry.

Gripps, D (2015) [online] Glass Fibre/Fiber. Available at: www.netcomposites.com/guide/glass-fibrefiber/32. [Accessed 15 January 2015]

Hatsuo, I. and Koenig, J. (1979) An investigation of the coupling agent/matrix interface of fiberglass reinforced plastics by Fourier transform infrared spectroscopy. **Journal of Polymer Science: Polymer Physics Edition,** 17(4): 615–626

Haupert, F. and Friedrich, K. (1995) Processing-related consolidation of high speed filament-wound continuous fibre/thermoplastic composite rings. **Composites Manufacturing,** 6: 201 – 204

Henninger, F. and Friedrich, K., (2002) Thermoplastic filament winding with online-impregnation. Part A: process technology and operating efficiency. **Composites Part A: Applied Science and Manufacturing**, 33(11), pp.1479–1486.

Henninger, F., Hoffmann, J., and Friedrich, K. (2002) Thermoplastic filament winding with online-impregnation. Part B. Experimental study of processing parameters. **Composites Part A: Applied Science and Manufacturing,** 33(12): 1684-1695

Hill, R. and Okoroafor, E. (1995) Weibull statistics of fibre bundle failure using mechanical and acoustic emission testing: the influence of interfibre friction. **Composites,** 26(10): 699–705

Hull, D. and Clyne, T. (1996) **An introduction to composite materials**. Cambridge: Cambridge University Press.

Iglesias, J., González-Benito, J., Aznar, A. *et al.,* (2002) Effect of glass fiber surface treatments on mechanical strength of epoxy based composite materials. **Journal of Colloid and Interface Science,** 250(1): 251–60

Industry Experts (2012) **Glass Fiber Reinforcements – A Global Market Overview** Available at: http://industry-experts.com/verticals/chemicals-and-materials/glass-fiber-reinforcements-a-global-market-overview [Accessed 24 February 2015]

Irfan, M., Machavaram, V., Mahendran, R. *et al.*, (2011) Lateral spreading of a fiber bundle via mechanical means. **Journal of Composite Materials,** 46(3): 311–330

Irfan, M. S. (2013) **Environmentally friendly pultrusion.** PhD thesis, University of Birmingham

Irfan, M, Machavaram, V., Murray, R., *et al.,* (2014) The design and optimisation of a rig to enable the lateral spreading of fibre bundles. **Journal of Composite Materials,** 48(15): 1813–1831

ISO 3341: 2000 Textile glass – yarns – Determination of breaking force and breaking elongation

Jarneteg, A. and Berglund, L. (1992) A simple Procedure for the Evaluation of fibre size effects on the properties of filament wound glass fibre composites. **Journal of Reinforced Plastics and Composites,** 11(1): 98–102

Jones, F. (1994) Handbook of Polymer-Fibre Composites F. Jones, ed., Longman Scientific and Technical.

Jones, F. (2007) The Chemical Aspects of Fibre Surfaces and Composite Interfaces and Interphases, and their Influence on the Mechanical Behaviour of Interfaces. In **Proceedings of the 28th Risø International Symposium on Material Science**: Interface Design of Polymer Matrix Composites – Mechanics, Chemistry, Modelling and Manufacturing. pp. 21–44. Denmark

Kinsella, M., Murray, D., Crane, D., Mancinelli, J., and Kranjc, M. (2001) Mechanical properties of polymeric composites reinforced with high strength glass fibres. In **International SAMPE Technical Conference** (Vol. 33, pp. 1644-1657). Chicago

Kliger, H. and Wilson, B. (1990) "Continuous fibre moulding processes A. Filament winding." In Mallick, P. and Newman, S (Eds.) **Composite Materials Technology: Processes and Properties**, USA: Hanser. pp. 179–210

Koran, P. and Kürschner, R. (2001) Effects of sequential versus continuous irradiation of a light cured resin composite on shrinkage, viscosity, adhesion, and degree of polymerization. **Journal of Esthetic and Restorative Dentistry,** 13(2): 140-141

Korotkov, V., Chekanov, Y. and Rozenberg, B. (1993) The simultaneous process of filament winding and curing for polymer composites. **Composites Science and Technology,** 47(4), pp.383–388.

Koussios, S., Bergsma, O. and Beukers, A. (2004a) Filament winding. Part 1: determination of the wound body related parameters. **Composites Part A: Applied Science and Manufacturing,** 35(2): 181–195

Koussios, S., Bergsma, O. and Beukers, A (2004b). Filament winding. Part 2: generic kinematic model and its solutions. **Composites Part A: Applied Science and Manufacturing,** 35(2): 197–212

Loewenstein K. (1983) “The manufacturing technology of continuous glass fibres.” In Loewenstein, K. (ed.) **Glass Science and Technology Vol. 6.** Oxford: Elsevier.

Lund, M. and Yue, Y. (2010) Impact of Drawing Stress on the Tensile Strength of Oxide Glass Fibers. **Journal of the American Ceramic Society,** 93(10): 3236–3243

Mallarino, S., Chailan, J. and Vernet, J. (2005) Glass fibre sizing effect on dynamic mechanical properties of cyanate ester composites I. Single frequency investigations. **European Polymer Journal,** 41(8): 1804–1811

Marissen, R., Van Der Drift, L. and Sterk, J. (2000) Technology for rapid impregnation of fibre bundles with a molten thermoplastic polymer. **Composites Science and Technology,** 60(10): 2029-2034

Market and Markets (March, 2014) **GFRP Composites Market by Raw Material, Manufacturing Process, Application (Transportation, Construction, Electrical and Electronics, and Others) and by Geography – Global Trends and Forecast to 2019** Available at: http://www.marketsandmarkets.com/Market-Reports/glass-fiber-reinforced-plastic-composites-market-142751329.html [Accessed 25 January 2015]

Meretz, S., Auersch, W., Marotzke, C., Schulz, E., and Hampe, A. (1993) Investigation of morphology-dependent fracture behaviour with the single-fibre pull-out test. **Composites Science and Technology**, 48(1), 285-290.

Mertiny, P. and Ellyin, F. (2002) Influence of the filament winding tension on physical and mechanical properties of reinforced composites. **Composites Part A: Applied Science and Manufacturing,** 33(12): 1615–1622n

Milewski, J. and Katz, H. (1987) **Handbook of Reinforcements for Plastics**. Van Nostrand Reinhold Co. University of Michigan. Available at: https://books.google.co.uk/books?id=nsNTAAAAMAAJ

Morgan, R. J. and Neal, J.E.O., (1977) “A review of the relation between the physical structure and mechanical response of Epoxies.” In Labana, S. (ed.) **Chemistry and Properties of Crosslinked Polymers**. New York: Academic Press. pp. 289–301

Morley, J. (1987) **High-performance fibre composites**. New York: Academic press.

Mouldlife. (2007). **Araldite ® LY 3505/ Hardeners XB 3403/ XB 3404 / Aradur ® 3405**. Available at: http://www.mouldlife.net/ekmps/shops/mouldlife/resources/Other/ly-3505-xb-3403-data-sheet.pdf.

Mouritz, A. and Gibson, A. (2007) **Fire properties of polymer composite materials**. Dordrecht: Springer.

Munro, M., (1988) Review of manufacturing of fiber composite components by filament winding. **Polymer Composites,** 9(5): 352–359

Nair, A., Machavaram, V., Mahendran, R., Pandita, S., Paget, C., Barrow, C. and Fernando, G. (2015) Process monitoring of fibre reinforced composites using a multi-measurand fibre-optic sensor. **Sensors and Actuators B: Chemical,** 212: 93-106

Net Composites (2012) [online]. **Clean Wet-Filament Winding Technology Developed by UK Consortium Showcased at JEC Europe**. Available at: www.netcomposites.com/news/clean-wet-filament-winding-technology-developed-by-uk-consortium-showcased-at-jec-europe/8038. [Accessed 24 January 2014]

Nishioka, G. (1990) Interaction of Organosilanes with Glass Fibers. **Journal of Non-Crystalline Solids,** 120(1): 102–107

Okoroafor, E. and Hill, R. (1995) Relating acoustic emission signal parameters to the strength of fibres used in the manufacture of polymeric composites. **Ultrasonics,** 33(2): 123–131

Olmos, D., López-Morón, R. and González-Benito, J. (2006) The nature of the glass fibre surface and its effect in the water absorption of glass fibre/epoxy composites. The use of fluorescence to obtain information at the interface. **Composites Science and Technology,** 66(15): 2758–2768.

Pandita, S., Irfan, M., Machavaram, V. *et al.,* (2012) Clean wet-filament winding - Part 1: design concept and simulations. **Journal of Composite Materials,** 47(3): 379–390

Pandita, S., Smith, S., Shotton-Gale, N., *et al.,* (2007) “Clean” Filament Winding: A New Manufacturing Process.

Pantano, C., Carman, L. and Warner, S. (1992) Glass fiber surface effects in silane coupling. **Journal of Adhesion Science and Technology,** 6(1): 49–60

Park, C., Lebel, A., Saouab, A., Bréard, J. and Lee, W. (2011) Modeling and simulation of voids and saturation in liquid composite molding processes. **Composites Part A: Applied Science and Manufacturing,** 42(6): 658–668

Park, S., and Jin, J. (2001) Effect of Silane Coupling Agent on Interphase and Performance of Glass Fibers/Unsaturated Polyester Composites. **Journal of Colloid and Interface Science,** 242(1): 174–179

Parratt, N. (1972) **Fibre reinforced materials technology.** USA: van Nostrand Reinhold.

Peltonen, P. and Järvelä, P. (1992) Methodology for determining the degree of impregnation from continuous glass fibre prepreg. **Polymer Testing**, 11: 215-224.

Peters, S. (2011) [online]. Composite Filament Winding S. T. Peters, ed., ASM international. Available at: http://books.google.com/books?hl=en&lr=&id=nciMwbQfymQC&oi=fnd&pg=PP2&dq=Composite+Filament+winding&ots=txqxgATYZM&sig=yuoGDUe9UbxoT-ky6eyevtWqPUI [Accessed September 25, 2013].

Polini, W. and Sorrentino, L. (2005) Estimation of the winding tension to manufacture full section parts with robotized filament winding technology. **Advanced Composite Materials,** 14(4): 305–318

Prnewswire.com (2015) [online]. Available from: www.prnewswire.com/news-releases/reportlinker-adds-global-glass-fiber-market-2010-2015-trends-forecasts-and-opportunity-analysis-83911817.html [Accessed 22 May 2015]

Rafiee, R. (2012) Apparent hoop tensile strength prediction of glass fiber-reinforced polyester pipes. **Journal of Composite Materials,** 47(11): 1377–1386

Rao, Y. and Farris, R. (2000) A modeling and experimental study of the influence of twist on the mechanical properties of high-performance fiber yarns. **Journal of Applied Polymer Science,** 77(9): 1938–1949

Rapra (2014) [online]. **Reinforcement types**. Available at: www.rapra.net/composites/material-selection/reinforcement-types.asp [Accessed 15 September 2013]

Ripert, H. and Charrier, J. M. (1992) **Compt-Rendus des 8e Journees Nationales sur les Composites,** Nov, 173

R'Mili, M., Moevus, M. and Godin, N. (2008) Statistical fracture of E-glass fibres using a bundle tensile test and acoustic emission monitoring. **Composites Science and Technology,** 68(7): 1800–1808

Roisum, D. (1993) The Mechanics of Web Spreading: Part 1. In **Proceedings of the Second International Conference on Web Handling**, Stillwater, OK, USA Tappi journal,76, 63-63

Saint-Gobain Vetrotex (2013) [online]. **S.-G., E, R and D glass properties.** Available at: http://glassproperties.com/glasses/E_R_and_D_glass_properties.pdf [Accessed 22 September 2013]

Scott Bader (2013) [online] **Crystic 397pa**. Available at: http://www.scottbader.com/uploads/files/934_crystic-397pa-resin-en-feb13.pdf.

Sever, K., Sarikanat, M., Seki, Y., Cecen, V., and Tavman, I. H. (2008) Effects of fiber surface treatments on mechanical properties of epoxy composites reinforced with glass fabric. **Journal of Materials Science,** 43(13): 4666-4672

Shelby, J. (2005) **Introduction to Glass science and Technology 2nd Edition Royal Society of Chemistry**. Cambridge: Royal Society of Chemistry.

Shen, F. C. (1995) A filament-wound structure technology overview. **Materials Chemistry and Physics** 42: 96-100

Shotton-Gale, N. E. (2013) **Clean filament winding: process optimisation**. PhD thesis, University of Birmingham

Shotton-gale. N, Harris. D., Pandita. S., Paget. M., and Fernando. G. (2009) Clean and Environmentally Friendly Wet-Filament Winding. In Goodship, V. (ed.) **Management, Recycling and Reuse of Waste Composites.** Cambridge: Woodhead Publishing Limited. pp. 329–368.

Shotton-Gale, N., Pandita, S.D., Paget, M., Wait, C., Allen, J.A., Harris, D. and Fernando, G.F. (2009), 'An environmentally friendly modified wet filament winding process', **ICCM Conference**.

Smith, I. (1961) The mechanism of the crosslinking of epoxide resins by amines. **Polymer 2,** 95-108

Thomason, J. (1995a) The interface region in glass fibre-reinforced epoxy resin composites : 1. Sample preparation, void content and interfacial strength. **Composites,** 26(7): 467–475

Thomason, J. (1995b). The interface region in glass fibre-reinforced epoxy resin composites : 2. Water absorption, voids and the interface. **Composites,** 26(7): 477–485

Thomason, J. (1999) The influence of fibre properties of the performance of glass-fibre-reinforced polyamide 6, 6. **Composites Science and Technology,** 59(16): 2315–2328

Thomason, J. (2012) Glass Fibre Sizings: A Review of the Scientific Literature. UK: Thomason, J. [Kindle Edition]

Thomason, J. and Adzima, L. (2001) Sizing up the interphase: an insider's guide to the science of sizing. **Composites Part A: Applied Science and Manufacturing,** 32(3): 313–321

Thomason, J. and Dwight, D. (1999) The use of XPS for characterisation of glass fibre coatings. **Composites Part A: Applied Science and Manufacturing,** 30(12): 1401–1413

Thomason, J. and Kalinka, G. (2001) A technique for the measurement of reinforcement fibre tensile strength at sub-millimetre gauge lengths. **Composites Part A: Applied Science and Manufacturing,** 32(1): 85–90

Tomlin, A. D. (2012) **Self-sensing composites: cure monitoring**. MRes thesis, University of Birmingham

Varna, J., Joffe, R., Berglund, L. and Lundström, T. (1995) Effect of voids on failure mechanisms in RTM laminates. **Composites Science and technology,** 53(2): 241-249

Vectroply (2014) [online]. **Reinforcement fibres**. Available at: http://vectorply.com/reinforcement-fibers/ [Accessed 15 September 2013]

Wait, C. F (2011) The reuse and recycling of glass fibre waste. MRes thesis, University of Birmingham

Wallenberger, F. T., Watson, J. C., Li, H., and PPG Industries, (2001) Glass Fibers.**ASM Handbook**, Vol. 21: Composites

Wang, L., Pandita, S., Machavaram, V. *et al.,* (2009) Characterisation of the cross-linking process in an E-glass fibre/epoxy composite using evanescent wave spectroscopy. **Composites Science and Technology,** 69(13): 2069–2074

Wang, T., Blum, F. and Dharani, L., (1999) Effect of interfacial mobility on flexural strength and fracture toughness of glass/epoxy laminates. **Journal of Materials Science,** 34(19): 4873–4882

Xiong, D. (2002). **An experimental and theoretical study of the cooling of a thin glass fiber during the formation process**. PhD thesis, Massachusetts Institute of Technology

Yue, Y., Von Der Ohe, R., and Jensen, S. (2004) Fictive temperature, cooling rate, and viscosity of glasses. **The Journal of Chemical Physics,** 120(17): 8053-8059

Zhu, Y., Wang, J., Tan, H. *et al.,* (2004) Capillary Micro-Flow Through a Fiber Bundle I. **Journal of Wuhan University of Technology Material Sciences,** 19(2): 94 – 97

7. APPENDICES

APPENDIX-A Impregnation modelling of Prototypes-1 and 2

The equation used to derive the degree of pin impregnation achievable in both prototypes is represented by Equation 7.1 (Gayman and Wevers, 1997):

$$Z = \sqrt{\frac{2k\ \Delta P\ ti}{\eta}}$$

Equation 7.1

Where:

Z is the fibre thickness;

ΔP is the change in pressure;

k is the transverse permeability;

η is the resin viscosity; and

ti is the impregnation time.

The fibre thickness, *Z* is calculated using Equation 7.2:

$$Z = \frac{A}{W}$$

$$Z = \frac{1\ mm^2}{8\ mm}$$

$$Z = 0.125\ mm$$

Equation 7.2

Where:

A is the area of fibre bundle (estimated to be 1 mm^2); and

W is the fibre bundle width (8 mm).

The transverse permeability, k can be calculated using Equation 7.3 for a hexagonal fibre array (Gebarts, 1992)

$$k_{y\ hexagonal} = \frac{16\ r_f^2}{9\pi\sqrt{6}}\left(\sqrt{\frac{V_A}{V_f} - 1}\right)^{5/2}$$

Equation 7.3

Where:

r_f is the measured fibre radius (8.5 μm);

V_A is the fibre arrangement (0.907 (Hull and Clyne, 1996, page 41)); and

V_f is the fibre volume fraction (0.6).

The fibre pressure, ΔP was calculated using Equation 7.4 (Bates and Charrier 1999):

$$\Delta P = \frac{T}{WR}$$

Equation 7.4

Where:

T is the tension;

W is the width of the roving; and

R is the radius of the pin (curved surface).

Therefore, the time required for 100% impregnation can be calculated using Equation 7.5:

$$\frac{\eta\,(125)^2}{2k\,\Delta P} = ti$$

Equation 7.5

To find the degree of impregnation at a given speed Equation 7.6 is used

$$Time_{available} = \frac{L}{V} = \frac{(m)}{(m/s)} = ???\,seconds$$

Equation 7.6

Where:

V is the velocity of fibre movement through the resin system;

L is derived using an equation from Chandler *et al*., (1992) for the impregnation length shown in Equation 7.7

$$L_1 = \frac{-Te_1 + \sqrt{Te_1^2 - \frac{\eta VAt}{3k\,H_0H_1}(H_1 - H_0)(2H_1 + H_0)}}{\eta V(2H_1 + H_0)/6H_0H_1}$$

Equation 7.7

Where:

Te_1 is the tension of the fibre tow/width of tow;

η is the resin viscosity;

V is the velocity of fibre movement through the resin system;

A is the radius of pin;

H_1 is the resin film thickness at the end (an estimation was made to the radius of a filament);

H_0 is the resin film thickness at the beginning;

K is the transverse permeability ; and

Te_1 is calculated by using Equation 7.8:

$$Te_1 - Te_0 = \frac{5\pi\eta V}{4}\sqrt{\frac{2A}{H_0}}$$

Equation 7.8

H_0 is derived using Equation 7.9:

$$H_0 = \left(\frac{\pi^2}{128}\right)^{1/3} R\left(\frac{6\eta V}{T_0}\right)^{2/3}$$

Equation 7.9

T_o is the tension of the fibre tow (neglecting any change) after the pin impregnation stage in Prototypes-1 and 2, there is no further addition of resin. Therefore the assumption is that the impregnation in this region is solely due to capillary impregnation, Pc.

To calculate capillary impregnation Equation **7**.10, taken from Ahn and Seferis (1991) was used.

$$P_c = \frac{F}{D_f} . \frac{(1-e)}{e} . \sigma cos\theta$$

Equation 7.10

Where;

F is the form factor (depends on fibre alignment and flow direction), F assumes the value of 2 for flow perpendicular to the fibre alignment;

D_f is the diameter of a single filament (m);

e is the porosity of the fibre reinforcement (0.4 is used and is taken as the required resin volume fraction);

σ is the surface tension of the wetting fluid (P_a –m) 23 x 10^{-3} N/m;

θ is the contact angle between the liquid and the solid (non-curing epoxy 57°); and

Values for σ and θ were taken from Amico and Lekuku (2002) and added into the equation.

Using Equations 7.1 and 7.10, the contributions from capillary, pin and the combined mechanisms were plotted as a function of the winding speeds. The results of these simulations are presented in Figure 1A and Figure 2A for Prototypes-1 and 2 respectively.

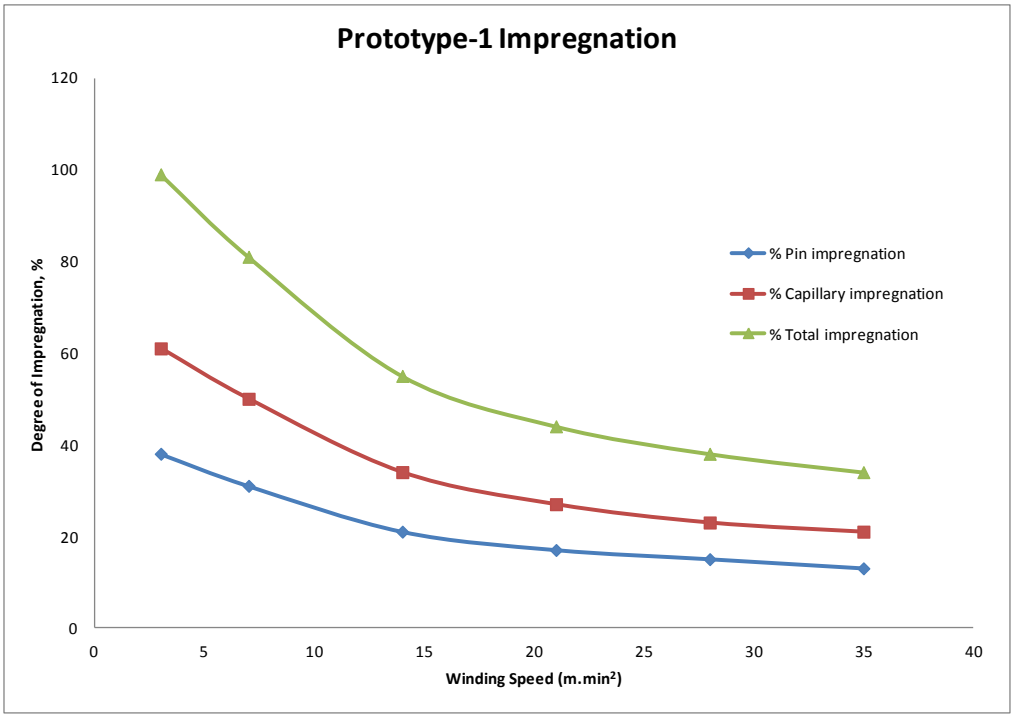

Figure 1A A graph showing the degree of impregnation achievable at different winding speed for resin impregnator Prototype-1.

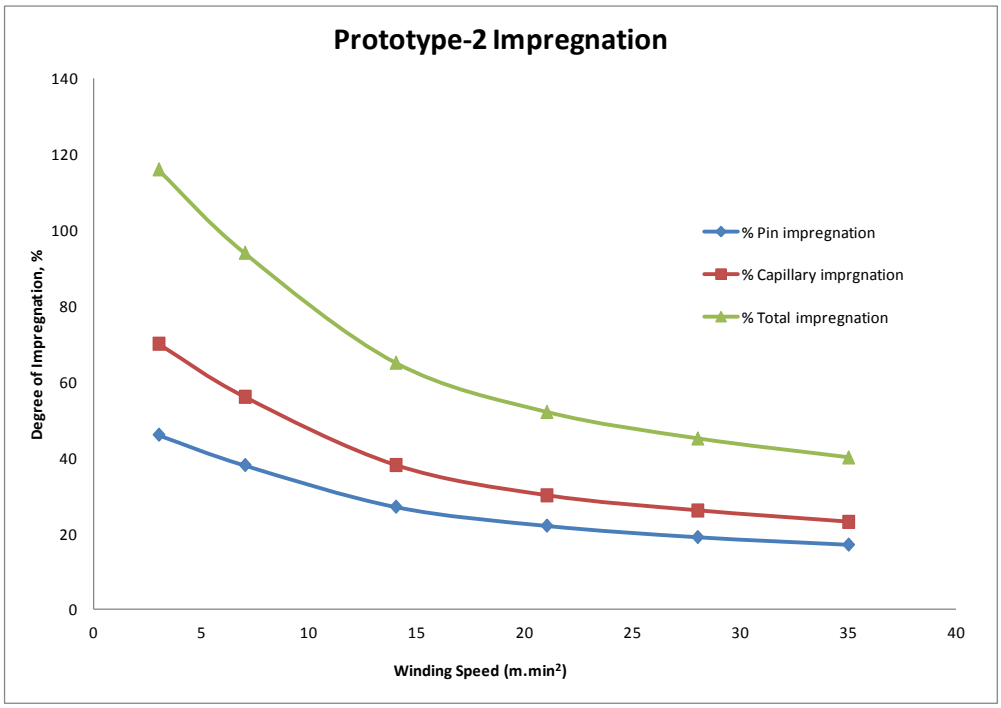

Figure 2A A graph showing the degree of impregnation achievable at different winding speed for resin impregnator prototype-2

The theoretical results from the above section were used to validate the designs of the clean filament winding Prototype-1 and Prototype-2 used in the subsequent filament winding site trials.

APPENDIX-B Calibration of Impregnation Monitoring Equipment

Calibrations were undertaken to verify the results obtained by the custom-written software. A thin film of the red pigmented NOA63 was cast and cured. 50 mm diameter disks were punched using a 50 mm leather hole punch. These disks with the known area/perimeter were used to check the output from the software. Firstly, the resin disk was placed on an as-received glass fibre and imaged using the USB cameras with the area calculated by the software. These results are shown in Table 1A. The resin disk was then imaged on the Lecia WILD M3C microscope with a 2 mm graticule. The area was then calculated using the ImageJ software; the results are included in Table 1A.

	Labview Calculated Area	Image J Calculated Area	Percentage Difference
Resin Disk 1	19.64	19.95	1.55
Resin Disk 2	20.37	19.95	-2.11
Resin Disk 3	20.52	19.79	-3.69
Resin Disk 4	19.98	20.55	2.77
Resin Disk 5	20.19	20.49	1.46
Resin Disk 6	19.91	19.93	0.10
Average	20.10	20.11	0.02

Table 1A Comparison between the areas calculated by the LabView software and that measured via image J for the 50 mm^2 cured red-pigmented resin disk.

The results show a good correlation between the Labview software calculation and image J measurements. This confirms the results by Bogonez that the acquired data is representative of the through thickness impregnation see in fibre bundles.

APPENDIX-C Data Set for Percentage Void Content of Tension Tubes

Figure 3A shows a scatter plot for the percentage void contents for composite tubes wound at different levels of fibre tension.

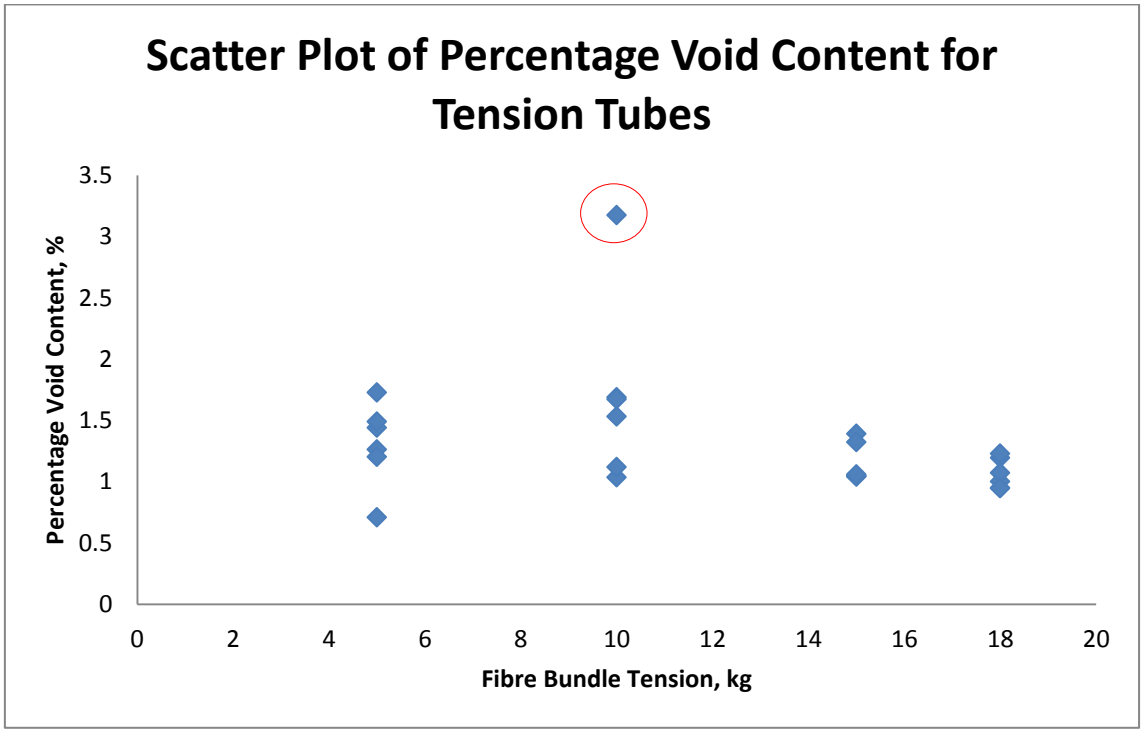

Figure 3A Scatter plot for the percentage void contents for composite tubes wound at different levels of fibre tension. The circled is the outlier for the 10 kg tube.

APPENDIX-D LCA Definition of Terms

Acidification potential - the decrease in pH of rain water caused by air pollutants.

Eutrophication potential - the enrichment of nutrients in a certain place caused by air pollutants, waste water and fertilization in agriculture**.**

Freshwater aquatic ecotoxicity potential – refers to the impact of toxic substances emitted to freshwater aquatic ecosystems.

Global warming potential – an index that attempts to integrate the overall climate impacts of a specific action. It relates the impact of emissions of a gas to that of an equivalent mas of CO2.

Human toxicity potential – potential harm of a unit of chemical released into the environment. This includes both inherent toxicity and generic source-to-dose relationships for pollutant emissions.

Marine aquatic ecotoxicity potential – refers to the impact of toxic substances emitted to marine aquatic ecosystems.

Ozone layer depletion potential – refers to the amount of ozone depletion caused by a substance. The ozone depletion potential is the ratio of the impact on ozone of a chemical compared to the impact of a similar mass of CFC-11.

Photochemical ozone creation potential – is an indicator of the ability of a volatile organic compound to contribute to photochemical ozone formation. A measure of the reactivity of an organic compound with hydroxyl radicals and subsequent formation of ozone.

Terrestric ecotoxicity potential – refers to the impact of toxic substances emitted to terrestrial ecosystems.

APPENDIX-E Fibre Bundle Tensile Strength

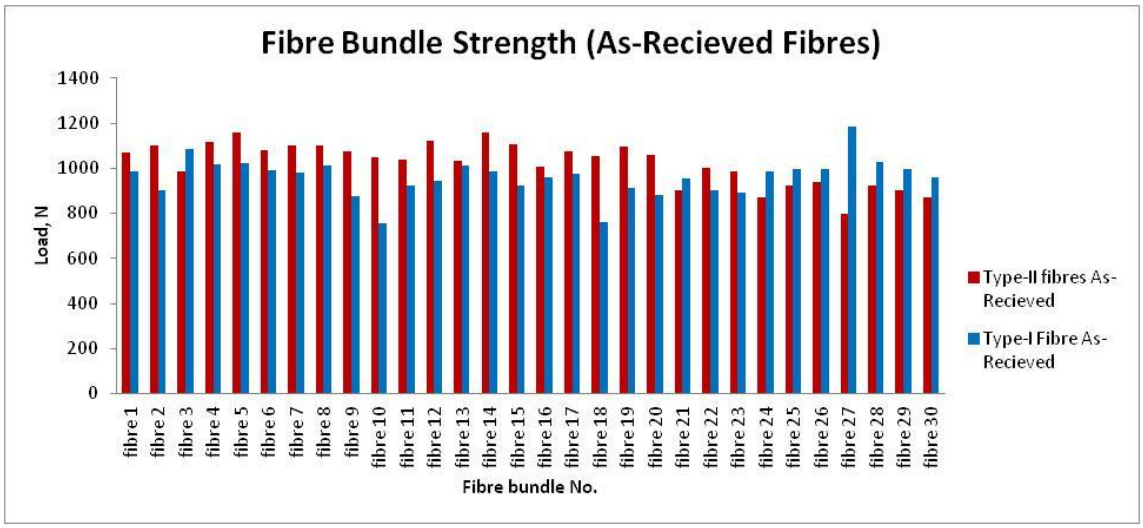

Figure 4A A graph showing the fibre bundle tensile strength of as-received Type-I and Type-II fibre bundles.

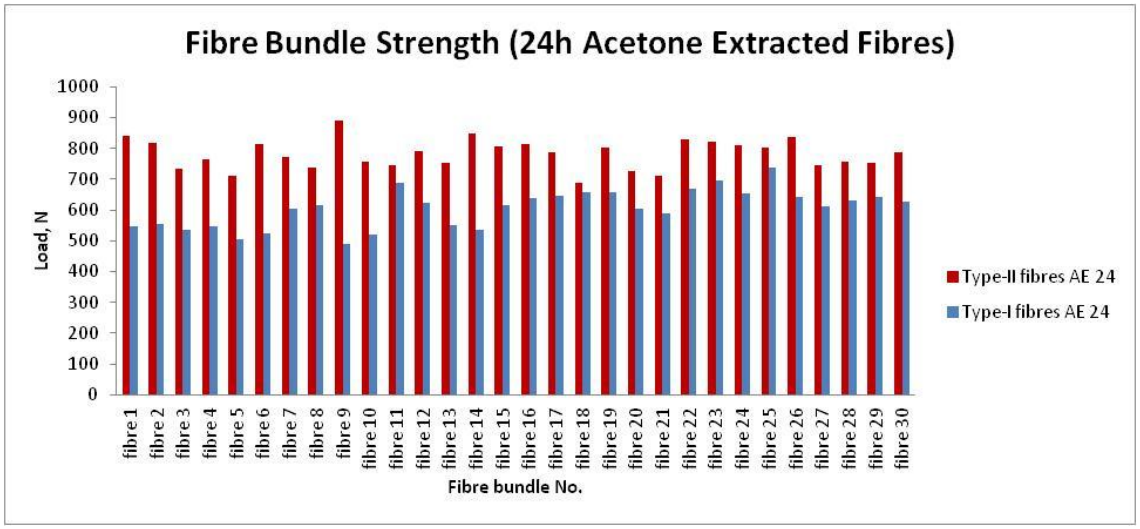

Figure 6A A graph showing the fibre bundle tensile strength of 24-hour acetone extracted Type-I and Type-II fibre bundles.

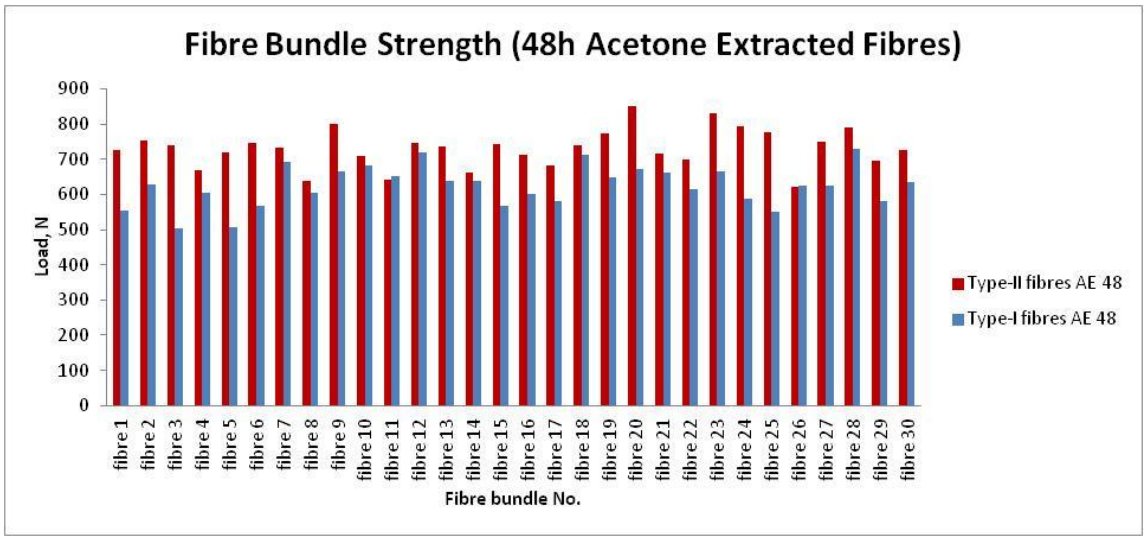

Figure 5A A graph showing the fibre bundle tensile strength of 48-hour acetone extracted Type-I and Type-II fibre bundles.